COMPREHENSIVE
FINAL PROJECT REPORT
(April 1, 2013-March 31, 2017)

MOLECULAR ASSESSMENT OF BACTERIAL COMMUNITY STRUCTURES OF LONG TERM OIL CONTAMINATED SOIL AND SCREENING OF LIPASE PRODUCERS FOR LIPASE PRODUCTION AND THEIR APPLICATION IN ESTER SYNTHESIS IN ORGANIC SOLVENTS

F.42-167/2013(SR)

Submitted to
UNIVERSITY GRANTS COMMISSION
NEW DELHI

Prof. Datta Madamwar
Principal Investigator
BRD School of Biosciences
Saradar Patel University
Vallabh Vidyanagar-388120
Gujarat

May-2017

ANNEXURE - III

UNIVERSITY GRANTS COMMISSION
BAHADUR SHAH ZAFAR MARG
NEW DELHI – 110 002

STATEMENT OF EXPENDITURE IN RESPECT OF MAJOR RESEARCH PROJECT

1.	**Name of Principal Investigator**	Prof. Datta Madamwar
2.	**Department of Principal Investigator**	BRD School of Biosciences
	University/College	Sardar Patel University, Vallabh Vidyanagar
3.	**UGC approval Letter No. and Date**	F. 42-167/2013(SR) 22-03-2013
4	**Title of the Research Project**	Molecular assessment of bacterial community structures of long term oil contaminated soil and screening of lipase producers for lipase production and their application in ester synthesis in organic solvents
5	**Effective date of starting the project**	April 01, 2013
6.	**a. Period of Expenditure**	April 01, 2013 to March 31, 2017
	b. Details of Expenditure	

Sr No.	Item	Amount Approved (Rs.)	Expenditure Incurred (Rs.) 2013-2014	Expenditure Incurred (Rs.) 2014-2015	Expenditure Incurred (Rs.) 2015-2016	Expenditure Incurred (Rs.) 2016-2017	Total Expenditure Incurred (Rs.) 2013-2016
i.	**Books & Journals**	0.00	0.00	0.00	0.00	0.00	0.00
ii.	**Equipment**	2,50,000.00	0.00	2,50,000.00	0.00	0.00	2,50,000.00
iii.	**Contingency**	1,20,000.00	44,454.00	52,738.00	22,808.00	0.00	1,20,000.00
iv.	**Field work/Travel (Give details in proforma at Annexure-IV)**	30,000.00	5,740.00	15,851.00	2450.00	5,081.00	29,122.00
v.	**Hiring Services**	30,000.00	11,910.00	NIL	6446.00	10,843.00	29,199.00
vi.	**Chemicals & Glasswares**	3,00,000.00	1,02,903.00	92,353.00	1,04,744.00	0.00	3,00,000.00
vii.	**Overhead**	97,800.00	0.00	97,800.00	0.00	0.00	97,800.00
viii.	**Any Other Item (Please specify)**	-		-	-	-	-

6. Staff Ms. Vrutika Patel

Date of Appointment June 17, 2013

No.	Items	From	To	Amount Approved Rs.	Expenditure Incurred Rs.
1.	Honorarium to PI (Retired Teachers) @ Rs. 18,000/- pm	NA	NA	0.00	0.00
2.	**Project Fellow:** **Non-GATE/Non-NET**- Rs. 14,000/- p.m. for initial two years and Rs. 16,000/- p.m. for the third year.	April 01, 2013 April 01, 2014 April 01, 2015 April 01 2016	March 31, 2014 March 31, 2015 March 31, 2016 June 16, 2017	5,28,000.00 For three years	1,18,533.00 1,68,000.00 2,00,866.00 40,533.00

1. It is certified that the appointment(s) have been made in accordance with the terms and conditions laid down by the Commission.

2. If as a result of check or audit objection some irregularly is noticed at later date, action will be taken to refund, adjust or regularized the objected amounts.

3. Payment @ revised rates shall be made with arrears on the availability of additional funds.

4. It is certified that the grant of **Rs. 12,18,520.00** (**Rupees twelve lakh eighteen thousand five hundred twenty only**) received from the University Grants Commission under the scheme of support for Major Research Project entitled "**Molecular assessment of bacterial community structures of long term oil contaminated soil and screening of lipase producers for lipase production and their application in ester synthesis in organic solvents"** vide UGC letter No. **F.42-167/2013(SR), dated 22-03-2013 and dated 24-05-2016.** Against this**,** an amount of **Rs. 13,54,053.00** (Rupees: Thirteen lakh fifty four thousand fifty three only) has been partly utilized for the purpose for which it was sanctioned and in accordance with the terms and conditions laid down by the University Grants Commission.

PRINCIPAL INVESTIGATOR **REGISTRAR**

ANNEXURE - IV

UNIVERSITY GRANTS COMMISSION
BAHADUR SHAH ZAFAR MARG
NEW DELHI – 110 002

STATEMENT OF EXPENDITURE INCURRED ON FIELD WORK

Name of Principal Investigator: Dr. Datta Madamwar

Name of the Place Visited	Duration of the Visit		Mode of Journey	Expenditure Incurred (Rs,)
	From	**To**		
Interview for the selection of Project Fellow by Dr. (Mrs.) Anuradha Nerurkar and Dr. Nilanjay Roy at Sardar Patel University, Anand	June 11, 2013	June 11, 2013	Private Travels (Taxi)	2700.00
Nanoparticles analysis at Central Salt & Marine Chemicals Research Institute (CSMCRI), Bhavnagar	August 08, 2013	August 08, 2013	Private Travels (Taxi)	770.00
Metagenomic sequencing at National Centre for Cell Science (NCCS), Pune	November 24, 2013	November 28, 2013	Railway	2270.00
Library work at Tamilnadu Agriculture University, Coimbatore	November 9, 2014	November 17, 2014	Railway	4160.00
Vatva, Ahmedabad	January 4, 2015	-	Private Vehicle (Taxi)	2310.00
Bioinformatics analysis at Department of Zoology, Delhi University, Delhi	January 15, 2015	January 31, 2015	Railway	9381.00
BARC, Water and Steam Chemistry Division, Kalpakkam, Tamil Nadu	September, 21, 2015	October 1, 2015	Air (Paid as per train)	2450.00
NIIST,Biotechnology Division, Trivandrum	November 20,2015	December 1,2015	Railway	5081.00
Total				29,122.00

Certified that above expenditure is in accordance with the UGC norms for Major Research Projects

Principal Investigator

Registrar
Sardar Patel University
Vallabh Vidyanagar

B R DOSHI SCHOOL OF BIOSCIENCES
Sardar Patel Maidan, Vadtal Road
Post Box No. 39
SARDAR PATEL UNIVERSITY
Vallabh Vidyanagar 388 120 (Gujarat) India
Tel. : +91-2692-234402 / 234412 / 231042
Fax : +91-2692-231041 / 236475
Website : www.spuvvn.edu/pgd/biosciences

ANNEXIUR -

PROFORMA FOR SUPPLYING THE INFORMATION IN RESPECT TO THE STAFF APPOINTED UNDER THE SCHEME OF MAJOR RESEARCH PROJECT

UGC FILE NO. F. 42-167/2013 (SR) YEAR OF COMMENCEMENT: 01-03-2013

TITLE OF THE PROJECT: "Molecular assessment of bacterial community structures of long term oil contaminated soil and screening of lipase producers for lipase production and their application for ester synthesis in organic solvents"

1.	Name of Principle Investigator	Prof. Datta Madamwar
2.	Name of University/College	Sardar Patel University
3.	Name of Research Personnel appointment	Miss. Vrutika. P. Patel
4.	Academic qualification	S. No. / Qualifications / Year / Marks / %age 1. / M.Sc. / 2011 / 1417 / 64.04 2. / M.Phil / - / - / - 3. / Ph.D. / - / - / -
5.	Date of Joining	17th June, 2013
6.	Date of Birth of Research Personnel	19th May, 1988
7.	Amount of HRA, if drawn	-
8.	Number of Candidate applied for the post	18 (16 appeared)

CERTIFICATE

This is to ceretify that all the rules and regulations of UGC Major Research Project outlined in the guidelines have been followed. Any lapse on the part of University will liable to terminate of said UGC project.

Principal Investigator
Dr. Datta Madamwar
Professor
BRD School of Biosciences
Sardar Patel Maidan, Vadtal Road
Satellite Campus, P. Box No.39
Sardar Patel University
V. V. Nagar-388120, Gujarat, India

Head of the Deptt.
HEAD
DEPARTMENT OF BIOSCIENCE
SARDAR PATEL UNIVERSITY
VALLABH VIDYANAGAR

Registrar/Principal
Sardar Patel University
Vallabh Vidyanagar

Annexure -VIII

BRD SCHOOL OF BIOSCIENCES
SARDAR PATEL UNIVERSITY
VALLABH VIDYANAGAR - 388 120, GUJARAT

Final Comprehensive Report of the work done on the Major Research Project.
(Report to be submitted within 6 weeks after completion of each year)

1. **Project report No. 1st/2nd/3rd/Final**: Final

2. **UGC Reference No.F**.: F. No. 42-167/2013(SR)

3. **Period of report:** From April 1st, 2013 to March 31st, 2017

4. **Title of research** "Molecular assessment of bacterial community structures of long term oil contaminated soil and screening of lipase producers for lipase production and their application in ester synthesis in organic solvents"

5. (a) Name of the Principal Investigator: Prof. Datta Madamwar

(b) Department: BRD School of Biosciences

(c) University/College where work has progressed: Sardar Patel University

6. Effective date of starting of the project: April 1st, 2013

7. Grant approved and expenditure incurred during the period of the report:

a. Total amount approved: (Total Grant Approved) **Rs. 13,55,800.00/-**

Rs. 8,51,800.00/- (1st Installment released)
Rs. 3,66,720/- (II nd Installment)

b. Total expenditure: **Rs. 13,54,053/-**

c. Report of the work done: (Please attach a separate sheet)

Introduction

Gauging the microbial community structures and functions become imperative to understand the ecological processes. Oil spills have been pivotal in delineating microbial diversity at the affected site in contrast to the pristine soil. Thus, it becomes important to understand how indigenous microbial communities respond to the stress in order to understand their role in degradation process. Cultivation independent analysis of the overall microbial community structure of such contaminated site using molecular profiling techniques have been instrumental in our understanding of the community dynamics, relative abundance, and distribution of microorganisms actively involved in restoration of such sites.

Interestingly, microbial community interacts with each other to adapt under extreme environmental changes via modulating genome architecture. The vast majority of these organisms have been characterized through culture-independent molecular surveys using conserved marker genes like the small subunit ribosomal RNA or more recently the shotgun sequencing. The ongoing development of next generation sequencing (NGS) methods can now be combined with advanced bioinformatics method to replace more traditional approach of metagenomic library screening.

Consequently, the intrinsic microbial community inhabiting stress conditions develop ability to degrader organic pollutants (fats and lipids). During this course of survival, they produce a wide range of enzyme and proteins in order to utilize the unusual nutrient sources and combat the stress conditions and hence, these microbes can be exploited for production of the biomolecules under artificially created conditions. The process of biodegradation mainly depends on microorganisms which enzymatically attack the pollutants and convert them into innocuous products. Major group of extracellular hydrolytic enzymes disrupt chemical bonds in the toxic molecules and results in the reduction of their toxicity.

In oil contaminated soils, one category of enzymes that are expected to be produced are lipases. Lipases (triacylglycerol ester hydrolases, EC 3.1.1.3) are ubiquitous enzymes that

catalyze the breakdown of fats and oils with subsequent release of free fatty acids, diacylglycerols, monoacylglycerols and glycerol. There has been a great input in lipase related research due to its myriad applications in areas such as in detergents, food, flavour industry, biocatalytic resolution of pharmaceuticals, esters and amino acid derivatives, synthesis of fine chemicals, agrochemicals, biosensor, bioremediation and cosmetics and perfumery to name a few. Special attention in research and development has been given to lipases as they are capable of complete replacement for conventional chemical synthesis of various fine and bulk chemicals along with reduced side products, lowered waste treatment costs and under conditions of mild temperature and pressure. This is because lipases are powerful tools for catalyzing not only hydrolysis, but also various reverse reactions, such as esterification, transesterification, and aminolysis, in organic solvents with the benefits of their specificity, regioselectivity and enantioselectivity.

Non-aqueous enzymology offers a platform for a kind of reactions wherein the enzymes are employed in absence or in presence of minute quantity of water. It has been well documented that, in addition to the properties of enzyme, the nature of organic solvent (logP) and water content in organic solvent (a_w) have important influence on enzyme activity in organic solvent. Chemical re-engineering of enzyme as biocatalyst has been constantly pursued to extent enzyme applications, particularly to reactions carried out under harsh conditions that often lead to enzyme denaturation. Efficient functioning of enzymes in organic solvents opens up new possibilities of application in biocatalysis [10]. However, customization of enzymes by chemical and physical modifications has more recently been attempted to improve their catalytic properties. Several strategies like solvent and protein engineering, chemical and surface modification of lipase, use of bipasic and reversed micellar systems, enzymes bioimprinting and enzyme immobilization have been employed to enhance lipase performance.

The most preferred method for protecting and stabilizing enzyme is immobilization. An important requirement for protein immobilization is that the matrix should provide a biocompatible and inert environment. Recent interest in nanotechnology has provided a wealth of diverse nanoscaffolds that could potentially support enzyme immobilization

due to their potential applications in biotechnology, immunosensing and biomedical areas. Discovery of nanoscale materials has paved a way for innumerable applications based on the extraordinary properties owing to size, mass transfer resistance and specific characteristics with respect to their composition. Processes such as silanisation, glutaraldehyde/carbodiimide activation, synthetic/natural polymers, aid in the binding of single/multi-enzyme systems to the nanomaterials. Various nanomaterials, such as nanoparticles, nanofibres, nanotubes, nanoporous, nanosheets and nanocomposites, have shown potential to revolutionise the preparation and the use of biocatalysts. Several bionano processes have been developed using fabricated nanoscale structures with biomolecules as nanoblocks. Thus, in this study we intend to explore the potential of nanomaterials for lipase immobilization.

In this work, we report production, partial purification and characterization of solvent tolerant lipase produced from solvent stable *Pseudomonas* sp. DMVR46 isolated from oil contaminated soil. There are scanty reports for the production of pentyl valerate ester immobilized in MBGs from purified lipase. Thus, we intend to use this lipase for esterification of pentanol and valeric acid to produce pentyl valerate, a compound with fruity aroma used in industries. The main purpose for the study was exploitation of DMVR46 lipase in non-aqueous environment and its reusability.

Also we intended to develop sustainable nanocomposite using different types of nanoparticles for immobilization of *Candida rugosa* lipase. One of nanoparticles used was exfoliated graphene oxide (EGO) as a host to increase the stability of enzyme by immobilization. These nanobioconjugate of lipase and EGO were further applied for the synthesis of flavor ester ethyl caprylate. The effects of some major influential factors, such as reaction temperature, enzyme concentration, the substrates molar ratio conditions and solvent on the esterification reaction were also scrutinized. Furthermore, the operational stability of immobilized lipase was also examined in order to explore its potential in organic solvents.

In another aspect we aimed to emphasize the use of functionalized quantum dots nanoparticles viz: cadmiuim sulphide and zinc oxide for lipase immobilization as a recyclable catalyst for ester production. Enzymatic esterification with the use of lipase

immobilized on to carriers for synthesis of short chain esters is limited. Zinc oxide nanoparticles were used for transesterification of geranyl acetate and optimization of various parameters for enhanced ester synthesis. Furthermore, these nanocomposites were entrapped into microemulsion based organogels (MBGs).

(i) **Brief objectives of the project**

1. To isolate and screen indigenous lipase producing microbial strains from oil-contaminated soil sites. Physico-chemical analysis of the oil contaminated soil mainly soil texture, moisture, pH, nutrients, total organic carbon, heavy metals etc.
2. Development of method for the extraction of metagenome from oil contaminated soil which is suitable for further molecular analysis work such as PCR amplification, restriction digestion etc.
3. To assess bacterial community structure of oil contaminated soil using cultivation dependant and cultivation independent analyses.
4. To study the community structure of lipase producers following 16S rRNA gene analysis of oil contaminated sites.
5. Optimization of important parameters effecting lipase production for obtaining high yields, purification and physicochemical characterization of lipases.
6. Exploitation of lipases following various immobilization techniques including microemulsion based organogels to improve esterification in organic solvents.

(ii) **Work done so far**

(a) Methodology, Research results and Achievement

Methodology: Experimental approach

(1) Molecular assessment of microbial community inhabiting oil perturbed soil: Tracking taxonomic and functional behavior using shotgun sequencing approach

1.1 Sampling site and physicochemical analysis of soil samples

To study the shift in microbial community structure across the oil polluted sites we collected bulk soil samples from the depots of long term oil contamination located near industrial area of Kadi, Ahmedabad. Different sampling sites (i.e. P1, P2, P3) of soil were

selected that represents accumulated edible cotton seed oil contamination since last 20 years, resulted from oil spillage in ginning mills (GPS location for polluted site 23º 17' 46.2624"N 72º 20' 37.2840"E). Another sampling site was located near the industrial estate about 500 meters away from oil contaminated site and was considered as control soil sample (C1, C2, C3) as a reference to demonstrate changes in microbial community under oil stress (GPS location for control site 23º 17' 17.1780"N 72º 21' 36.6048"E). At each site sampling was performed in replicates and collected soil was archived at 4°C until further use. Physicochemical analysis of soil samples such as soil moisture, soil texture, organic carbon content, soil carbon/nitrogen ratio (C:N) were determined.

1.2 Screening of bacterial strains having oil degrading ability

Soil obtained from polluted sample was serially diluted and spread on Nutrient agar, Luria agar, Plate count agar and Tributyrin agar plate supplemented with tributyrin oil as a carbon source and incubated for 2 days at 37ºC. Bacterial strains were selected on the bases of their ability to hydrolyze tributyrin oil by producing a clear zone around bacterial colonies. A total of 40-50 strains were isolated based on their distinct morphological characteristics of the colonies and hydrolysis of trybutyrin oil. Further, all the bacterial strains were checked for their purity and maintained as pure culture at 4ºC. All the isolated cultures on plates were observed for 48h and sub cultured once in every month.

1.3 Identification of isolates by 16S rRNA gene sequencing analysis

Genomic DNA from all the isolated bacterial strains was extracted using protocol of phenel:chloroform as described by Asubel et al., 1997. After extraction, the amplification of 16S rRNA gene from genomic DNA was carried out using 20pmoles of universal primer 8F (5'-AGAGTTTGATCCTGGCTCAG-3') and 1492R (5'-GGTTACCTTGTTACGACTT-3'). Amplification program consist of initial denaturation step at 94°C for 5min; followed by 35 cycles of 1min denaturation step at 94°C, 1min annealing step at 55°C and 1min elongation step at 72°C and a final extension step at 72°C for 15min using Bio-Rad iCycler version 4006 (Bio-Rad, USA). Amplified DNA product was processed for Amplified rDNA restriction analysis (ARDRA) in order to remove similar bacterial species based on their unique banding pattern. Bacterial cultures

showing discrete banding profile was selected from all isolates and sequenced using BigDye terminator cycle sequencing ready reaction v 3.1 in an automated 3500xl DNA analyzer (Applied Biosystems Inc, USA) to analyze bacterial community structure.

1.4 Metagenomic DNA extraction and sequencing

Metagenomic DNA from each soil samples i.e. polluted and control (P1, P2, P3, C1, C2 and C3) was extracted and pre-standardized by Desai and Madamwar; 2006. Finally, 50µL MilliQ water was used to dissolve DNA at the final step.

Briefly, soil sample (5g) was pre-washed with double distilled water before DNA extraction according to the method of Zhou et al., 1996. Briefly, after adding 5g glass beads (d = 3mm) and 20mL DNA extraction buffer (100mM Tris, 100mM EDTA, 1.5M NaCl, 10% Sucrose, 1% CTAB, 100mM sodium phosphate buffer pH = 8.0) to the pretreated soil, the sample was vortexed for 5min followed by addition of ProteinaseK (100 µg/mL) and Lysozyme (10 mg/mL) and was agitated at 200 rpm for 30 min at 37°Con environmental shaker. Subsequently, the homogenate was heated at 65ºC and lysed in presence of 10 % SDS for 1h. Further, 0.5g of powdered activated charcoal (PAC) was added to crude cell lysate and incubated for 30min under same condition. After centrifugation at 12000 rpm for 15min at room temperature, DNA was extracted with an equal volume of phenol and chloroform-isoamyl alcohol (24:1 v/v), precipitated with isopropanol and the DNA pellet was washed twice with 70% chilled ethanol. The air dried DNA was resuspended in appropriate volume of milli-Q grade water and resolved on 0.8% agarose gel and viewed by staining with ethidium bromide upon exposure to UV light (Alpha Innotech, USA).

Equal concentration of environmental metagenomic DNA (obtained by Qubit reading) from each subsequent sites were mixed to form a composite genetic pool (i.e. P1+P2+P3=P and C1+C2+C3=C) representing total DNA composition for each site. Isolated DNA was sheared and sized to produce DNA library according to the manufacturer's protocol from Ion Xpress™ Plus gDNA Fragment Library Preparation Kit. DNA Sequencing was performed on Ion Torrent PGM platform using sequencing chip 318 to generate short reads with an average insert size of 300bp. Metagenomic DNA sequencing was done by outsourcing at Xcelris Lab Pvt Ltd, Ahmedabad, India.

1.5 Taxonomic analysis for sequencing data

The taxonomic positions of sequenced reads was analysed and studied using Ribosomal Database Project (RDP) classifier: classification based on 16S rRNA gene sequences. The 16S rRNA sequences were extracted from the results of BLASTN analysis against the nt/nr database and submitted to the RDP classifier with E value < 1X10-1 and 80% confidence level. The RDP classifier predicted the taxonomic origin of 16S rRNA up to the rank of genus.

1.6 Rarefaction analysis

Rarefaction curve was generated for all reads, except unassigned reads. Species richness was plotted according to the data obtained from RDP dataset, whereas, additional species likely to be discovered was addressed by plotting the discovery rate of dataset, which is obtained by repeatedly selecting random subsample of the dataset at 10, 20, upto- 90 % of the original size and then plotting the number of leaves predicted by LCA algorithm using MEGAN.

1.7 Functional characterization and classification of genes

Functional characterization of reads was done on the basis of assembled data obtained from polluted sample. Gene calling was performed on the contigs using FragGeneScan in order to predict operon reading frame (ORF). The ORFs were functionally annotated and assigned to the Clusters of Orthologous Groups of proteins (COG) with an E value cut-off 10-5.

1.8 Data availability

The sequence data for both soil samples i.e. polluted and control obtained from Ion Torrent PGM platform has been deposited at MGRAST server (version 3). MGRAST IDs for the datasets are 4508969.3 and 4516462.3 for polluted soil and control soil, respectively. MGRAST IDs for the contig obtained from both the samples are 4515485.3 and 4512472.3, respectively. The sequences obtained from the culturable diversity study have been submitted to GenBank, NCBI and their accession numbers are from KR140170 to KR140186 (polluted soil) and KR140187 to KR140201 (control soil).

(2) Solvent tolerant Pseudomonas sp. lipase: Characterization and application in nanobiocatalysis

2.1 Screening of organic solvent tolerant lipolytic micro-organisms from oil contaminated soil

Soil samples were obtained from oil spilling sites near industrial area of Kadi, Ahmedabad, Gujarat, India (as described in section 1.2). The enrichment for lipase producing organisms were carried out in 250mL Erlenmeyer flask containing 100mL BHM (Bushnell Hass Medium) amended with different substrates i.e. tributyrin oil, olive oil and cotton oil. Solvent tolerance was determined by plate overlay method as described by *Ogino et al.,* 2000. Five microliters of overnight grown cultures was transferred to tributyrin agar plates (1% (v/v) tributyrin oil, 0.3% (w/v) yeast extract and 0.5% (w/v) peptone extract, 1.5% (w/v) agar-agar). The plates were kept for 20min until the drop gets dry and thereafter flooded with 18mL of different solvents like iso-octane, cyclohexane, toluene, isopropanol, methanol, DMSO. Colonies were examined for solvent tolerance after incubation at 37°C for 24 h. The ability of the cultures to grow and produce lipase in presence of solvents was monitored.

2.2 Identification of isolated DMVR46 bacterium using 16S rRNA approach

Bacterial strain designated as DMVR46 was selected on the basis of its solvent tolerance and was identified using 16S rRNA gene sequencing. The genomic DNA of DMVR46 was used as template of PCR reaction (30µL) using universal primers 8F (5'AGAGTTTGATCCTGGCTCAG-3') and 1492R (5'-GGTTACCTTGTTACGACTT-3'). The amplification of 16S rRNA gene was done in BioRad PCR cycler (BioRad iCycler version 4.006, BioRad, U.S.A.). Each PCR cycle (total 35 cycles) consisted of 1min denaturation step at 94°C, followed by 1 min annealing step at 55°C and 1 min elongation step at 72°C, with an initial denaturation step at 94°C for 5 min and a final extension step at 72°C for 15 min. PCR products were resolved on 1.2% low melting agarose gel in 1X TAE buffer and was visualized with ethidium bromide staining in Gel Documentation (Alpha-Inotech, USA.). The amplified PCR product was subjected to sequencing by automated DNA Analyzer 3500 using ABI PRISM® BigDye™ cycle sequencing kit (Applied Biosystems, USA). The nearly complete sequence (>95%) was

submitted to Genbank at NCBI. BLAST (n) program at NCBI server was used to identify and download nearest neighbour sequence from BLAST database [Ausubel et al., 1997].

2.3 Optimization of process parameters for maximum lipase production

Optimization of process parameters for lipase production from isolate DMVR46 was aimed to evaluate the effect of a single parameter at a time, and later manifesting it as standardized condition before optimizing the next parameter. The isolate DMVR46 was cultured in 100ml medium containing 0.5% (w/v) peptone, 0.3% (w/v) yeast extract and 1% (v/v) tributyrin oil. The parameters scrutinized are as follows:

i. pH: 6, 7, 8, 9, 10 and 11
ii. Temperature: 30, 37, 40, 45, 50°C
iii. Inducers: cotton seed oil, soybean oil, sunflower oil, trybutyrin oil, maize oil, olive oil and groundnut oil (each at initial concentration of 1% (v/v).
iv. Nitrogen sources: peptone, yeast extract, tryptone, casein, urea, ammonium sulphate and ammonium nitrate were used to observe the influence of nitrogen sources (1% w/v) on lipase production.
v. Carbon sources media were supplemented with dextrose, lactose and sucrose at 1% (w/v).

The best carbon, nitrogen and inducer sources achieved were further tested for varied concentration of 0.2%, 0.5%, 1%, 1.5% and 2%. All experiments were performed in triplicates and the results shown are the average of three independent experiments. Data are represented as mean with standard deviation.

2.4 Growth profile for lipase production

A Erlenmeyer flask of 500mL capacity containing 200mL of production medium (0.3% (w/v) yeast extract, 0.5% (w/v) peptone as a basal medium and 1.5% (w/v) tryptone, 0.5% (w/v) dextrose and 1% (w/v) cotton seed oil) was inoculated with an overnight grown culture of DMVR46 to obtain an initial culture density (A_{600}) 0.05 and incubated at 37°C in an orbital shaker (150rpm). The samples were withdrawn at regular intervals of 24 h and analysed for cell growth and enzyme activity. The enzyme activity was

estimated from supernatant (crude lipase) obtained upon centrifugation and cell growth was observed by suspending pellet in distilled water.

2.5 Partial purification of solvent tolerant DMVR46 lipase

Solvent tolerant lipase from DMVR46 was purified in two sequential steps. *Step 1:* The culture supernatant was obtained by centrifugation at 10,000x *g* (Kubota, Model 6500 Japan) for 20 min followed by precipitation using acetone as solvent. Chilled acetone was added slowly to the culture supernatant of strain DMVR46 upto 60% (v/v) concentration with continuous stirring and kept at -20°C for O/N to allow protein precipitation. The precipitates were harvested by centrifugation at 10,000x *g* for 20min at 4°C and resuspended in 50 mM sodium phosphate buffer (pH 8.0). *Step 2:* The enzyme containing solution was applied to a DEAE-Cellulose column previously equilibrated with 50mM sodium phosphate buffer (pH 8.0). The flow rate was adjusted to 15mL/h (approx) having the fraction volume of 1 mL and each fraction was further assayed for enzyme activity and protein content. The lipase preparations (crude and purified fractions) were electrophoresed on SDS-PAGE as described by Laemmli et al., 1970. Protein bands on the gel were visualized upon silver staining.

2.6 Characterization of purified lipase DMVR46

Optimum pH of the solvent tolerant lipase was determined by measuring the enzyme activity over a pH value ranging from 6.0-10.0 at 37°C for 30 min. Different buffers used for determination of lipase activity were: pH 6.0-8.5 sodium phosphate buffer, pH 9.0-10.0 Glycine-NaOH buffer. The effect of temperature on the lipase was studied by carrying out the enzymatic reactions at different temperature in the range of 30-50°C at pH 8.5 (50mM sodium phosphate buffer). The reactions were carried out for 0 to 30 min and proceed for enzyme activity. The thermal-stability of the lipase was assayed at various temperatures ranging from 30-50°C for different time interval from 0 to 4 h. At each time interval, 1 mL sample was pipette out and then assayed for residual activity, which was expressed as percentage of initial activity. The effects of different metal ions (Ca^{+2}, Mg^{+2}, Fe^{+2}, Co^{+2}, Zn^{+2} and Ba^{+2}) and inhibitors (EDTA and β-mercaptoethanol)

were investigated by pre incubating the purified lipase with 10 mM solutions of these ions or inhibitors at pH 8.5 for 30 min at 37°C. Similarly, the effects of surfactants (SDS, CTAB, Triton X-100, Tween 20 and Tween 80) at the concentration of 0.5% were examined. The effects of various organic solvents on the activity and the stability of the purified lipase were investigated following method defined by Ogino et al., 2000. The stability of lipase in organic solvents was examined by integrating 3mL of purified enzyme and 1mL of solvent in crew cap vials to attain a final solvent concentration of 25% (v/v). The solution was incubated in shaker (150rpm) at 37°C for 0 to 4 h and lipase activity was assayed in the aqueous phase. The substrates, p-nitrophenyl fatty acid esters, of varying chain length (C2, C4, C8, C12, C16 and C18) were used at the final concentration of 0.3mg/mL and the lipase activity was gauged according to the pNPP method.

2.7 Application of purified solvent stable DMVR46 lipase for synthesis of ethyl butyrate in non-aqueous medium

2.7.1 Carboxylation of multiwalled carbon nanotubes (MWCNTs)

At first in order to build up functional groups, pristine MWCNTs were suspended in a blend of concentrated sulfuric acid: nitric acid (3:1 v/v) and sonicated for 6h. The suspension was centrifuged at 15,000 x *g* for 30 min at 4°C and continuous water washes were given to eliminate acid. Finally, semi-solid residue was collected and vacuum dried at 37°C for 1h to obtain acid functionalized MWCNTs abbreviated as f-MWCNTs.

2.7.2 Adsorption of lipase onto functionalized nanotubes

Ten mg of f-MWCNTs in 9mL of phosphate buffer (50mM, pH 8.5) were sonicated for 10 mins. Then 1mL of prepared enzyme solution (50mg/mL in 50mM phosphate buffer pH 8.5) was added in the mixture of f-MWCNTs, stirred overnight at 37°C for immobilization of lipase. Finally, the nanobioconjugate were separated by centrifugation at 13,000 x *g* for 20 min at 4°C from supernatant and washed twice with buffer solution in order to eliminate loosely bound enzyme. After centrifugation, the supernatant was pulled together (for activity measurements) and the resulting solid was vacuum dried for 1h at 37°C.

2.7.3 Studies on the applications of immobilized lipase for biocatalysis

Immobilized lipase was further supplemented for synthesis of short chain ester ethyl butyrate. The reaction system consists of 20mL n-heptane with equimolar (0.1M) concentrations of 1-ethanol and butyric acid in 100mL stopper flask, instigated by addition of immobilized lipase (50mg including the weight of f-MWCNTs) and f-MWCNT without lipase (as a negative control) kept on orbital shaker at 37°C and 150rpm. Esterification reaction using free enzyme equivalent to the amount immobilized on MWCNTs was also executed. Process parameters such as effect of organic solvents, solvent stability, temperature, agitation and substrate molar ratio were scrutinized in order to get superior ester production. At every 24h interval 100µL of the reaction mixture was withdrawn and analyzed by gas chromatograph.

2.8 Reusability study for immobilized lipase

After completion of one reaction cycle (48h), immobilized lipase was recovered by centrifugation (10000 x *g* for 15 mins) and washed 2-3 times with fresh n-hexane for complete removal of residual substrates and products followed by air drying. The next reaction cycle was commenced by addition of new substrates where the residual activity determined after each cycle was analyzed using Gas Chromatograph under standard condition. The conversion achieved in the initial batch was set to be 100%.

2.9 Analytical procedures

2.9.1 Determination of lipase activity and protein content

p-Nitrophenyl palmitate was used as a substrate with a final concentration of 0.3mg/mL dissolved in 1mL of isopropanol and mixed with 9mL of 50mM sodium phosphate buffer (pH 8.5) containing gum arabic (0.1%) and Triton X-100 (0.6%). The reaction mixture comprised of 240µL substrate solution and 10µL of appropriately diluted enzyme solution, and incubated at 40°C for 10 min. The amount of immobilized enzyme was measured by calculating the difference between the activity of enzyme before immobilization and after immobilization (from supernatant). One unit of enzyme activity was defined as the amount of enzyme liberating 1µmol *p*-nitrophenol/min under standard

assay conditions. Amount of protein in the supernatant was determined using bovine serum albulin (BSA) as standard.

2.9.2 Characterization studies for immobilization

The size and morphologies of MWCNTs before and after lipase immobilization was assayed by Transmission Electron Microscopy (TEM) (Philips-Technai 20, Holland). The KBr pellet technique was used for determining FTIR (Fourier Transform Infrared Spectroscopy) spectra for free and immobilized lipase using Spectrochem GX-IR, Perkin Elmer, USA.

2.9.3 Quantification of ester production

Samples (100µL) were withdrawn at regular intervals and ester accumulation was monitored by Gas Chromatograph (Perkin Elmer, Clarus-500, USA) equipped with flame ionization detector in order to establish the product formation profile. The column was 30m Rtx-®-20 (Crossbond 80% dimethyl-20% diphenyl polysiloxane) capillary column. The temperature of the injector and detector were maintained at 250°C. The carrier gas served as nitrogen with the split flow rate of 30mL/min. The column temperature was programmed to increase from 70-190°C at the rate of 15°C/min. Ester identification and quantification were done by comparing the retention time and peak area of the sample with the standard. All the experiments were repeated thrice at each operating condition and the relative standard deviation.

(3) Conjugation of Candida rugosa lipase on exfoliated graphene oxide for catalysis in organic solvent

3.1 Covalent functionalization of exfoliated graphene oxide using 3-aminopropyltriethoxysilane (APTES) as a cross linker

10 mg of EGO was suspended in 10% APTES (diluted in ethanol) and sonicated for 4h followed by overnight stirring at room temperature. The modified EGO was recovered by centrifugation at 13,000 × *g* for 20 min at 4°C. The obtained pellet was washed thoroughly with ethanol and deionized water in order to remove excess APTES and

vacuum dried. Modified EGO's were centrifuged and vacuum dried for 1h at 37ºC resulting into a dark glossy product.

3.2 Conjugation of lipase on APTES functionalized exfoliated graphene oxide (EGO)

Silane functionalized EGO was dispersed into 9mL of 50mM phosphate buffer (pH 8.5) containing 1mL of 40mg/mL *Candida rugosa* lipase. The mixture was stirred at 37°C overnight followed by centrifugation (13,000 x *g* for 20min) and vacuum dried. The EGO was then washed thrice with phosphate buffer (50mM) to eliminate unbound lipase. The amount of immobilized lipase adsorbed on nanoparticles was determined by measuring the initial concentration and its final concentration in supernatant after immobilization using lipase assay. The schematic representation for immobilization of lipase onto EGO is described in Figure 25.

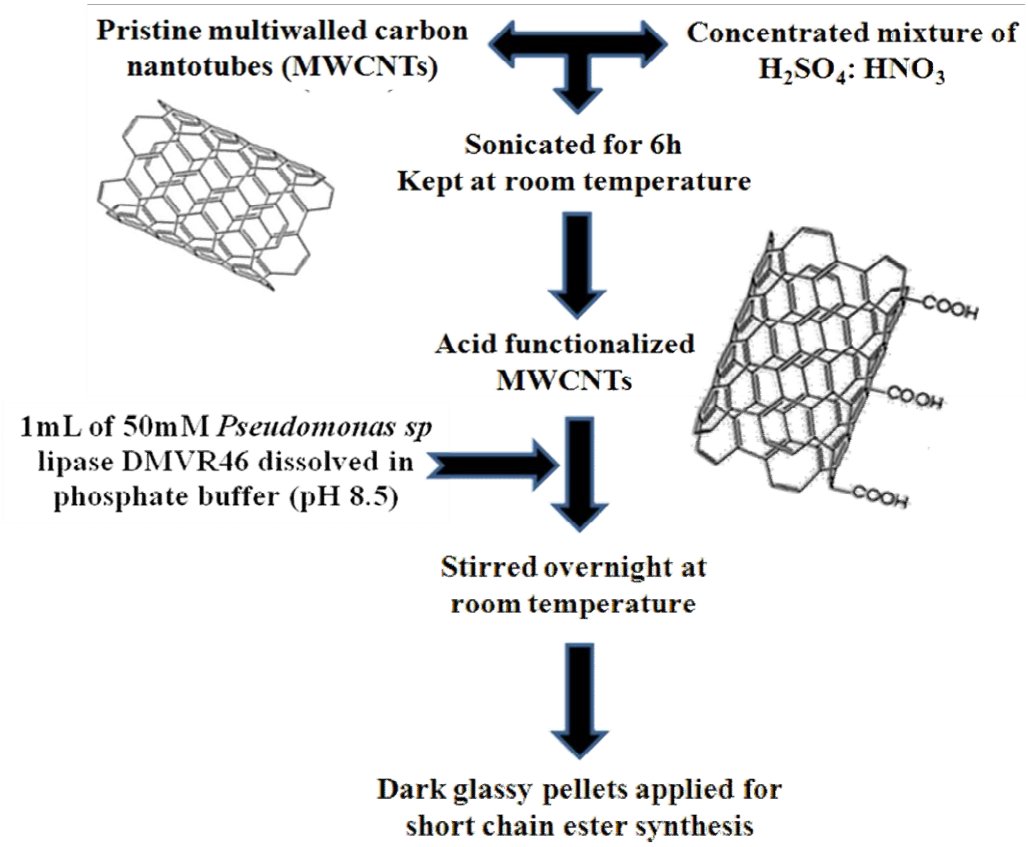

Figure 25: Conjugation of *Candida rugosa* lipase to functionalized EGO in presence of APTES as cross linking agent

3.3 Lipase activity and Protein content determination

The reaction solution was prepared by addition of free or immobilized lipase to p-NPP solution (0.4mM in 100mM phosphate buffer pH 8) and incubated for 10min at 40°C, 150rpm followed by measuring absorbance at 410nm using UV-Vis spectrophotometer (add details). One unit of enzyme activity is defined as the amount of enzyme that liberates p-nitrophenol at the rate of 1µmol per min under specified conditions.

Percentage Protein loading, specific activity and activity yield was determined by following equations:

% protein loading = amount of protein immobilized ÷ initial amount of protein loaded X 100

3.4 Application of immobilized CRL for synthesis of ethyl caprylate

The immobilized lipase preparation was applied for synthesis of flavored ester ethyl caprylate in cyclo-octane as reaction medium. The reaction system consisted of equimolar concentration of ethanol (0.1M) and caprylic acid (0.1M) as a substrate and mixed with 20mL of cyclo-octane in 100mL stopper flask. The reaction was initiated after addition of enzyme to the substrate where equivalent amount of native lipase and EGO-lipase were used separately for catalysis. Negative controls using APTES treated EGO was kept for monitoring catalysis (if any) in absence of enzyme. The experiment was carried out at 37°C and continuously stirred at 150rpm to ensure all the enzyme particles were homogeneously dispersed by modulating the operative variables. The operative variables used for the experiment were:

i) Effect of enzyme concentration: ranging from 5mg to 40mg/mL.

ii) Effect of temperature: different temperatures measured were 20, 30, 37, 40, 50 and 60°C.

iii) Effect of substrate concentration: substrate concentration ranges from 0.05M to 0.25M.

iv) Effect of organic solvents: different solvents used were n-hexane, cyclohexane, n-octane, and cyclo-octane.

Samples (100μL) were withdrawn periodically to study the time course of reaction and analyzed by Gas Chromatograph (GC, Perkin Elmer, USA)) in order to establish the product formation profile. No reaction was detected in absence of the enzyme. All the experiments were repeated thrice at each operative condition and the relative deviation was within ±1%.

3.5 Reusability studies

For reusability studies, after completion of each cycle for esterification, the immobilized lipase was recovered by centrifugation at 10,000 x *g* for 25 min. The recovered enzyme was then washed with anhydrous n-hexane twice in order to remove any remaining substrate or product accumulated on EGO, air dried and subsequently used for next cycle

3.6 Quantification of ester using Gas chromatograph

The time course of reaction was determined by a Gas Chromatograph (PerkinElmer, Model Clarus 500, Germany) equipped with a flame-ionization detector (FID). The column was 30 m Rtx-®-20 (Crossbond 80% dimethyl-20% diphenyl polysiloxane) capillary column. The temperature of injector and detector were maintained at 250°C. The carrier gas served as nitrogen with the split flow rate of 90mL/min. The column temperature was programmed to increase from 40-120°C at the rate of 3°C/min, from 120-200°C at the rate of 10°C/min and from 200-220°C at the rate of 2°C/min. Ester identification and quantification were done by comparing the retention time and peak area of the sample with the standard. Pure ethyl caprylate (≥98%) was used as external standard.

3.7 Characterization studies

3.7.1 Electron Microscopy

The morphologies of EGO before and after functionalization of each step were studied by TEM (Philips-Technai 20, Holland) and SEM (Hitachi S-3000N). For TEM analysis, the specifications used were W-emitter as electron source, LaB6, accelerating voltage (200kv), objective lens (S-TWIN), point resolution (0.27nm or better), line resolution

(2.0nm), magnification (25X to 75,00,200X or higher) and a single tilt holder with LCD camera. The samples were dispersed into isopropanol and a drop was placed on a copper grid. The samples were observed after drying under vacuum. While, for SEM analysis the samples were directly placed on carbon tapes.

3.7.2 Fourier transformation infrared spectroscopy (FTIR)

The chemical modifications arise on surface of EGO after each step of functionalization was studied by Fourier Transform Infrared (FT-IR) spectroscopic analysis using Spectrochem GX-IR, Perkin-Elmer, USA.

3.7.3 Thermal gravimetric analysis (TGA)

Thermal analysis of EGO was carried out in order to study decomposition of oxygen functional groups by TGA-SDTA 851 and DSC 822 (Mettler Toledo) with heating rate of 20°C/min under N_2 atmosphere. The system was employed with PtRh furnace capable of operating from 25 to 1500C, the temperature being measured using type R thermocouple. The system is vacuum tight, allowing measurements to be conducted under controlled atmosphere. The sample size range from 5-7mg and the mass was recorded as a function of temperature.

3.7.4 Raman spectroscopy

The Raman scattering was performed at room temperature with a Renishaw Raman microscope using laser excitation at 514nm with 50x objective where the laser beam was focused in an area of ~1μ (micron).

(4) Enzyme-Quantum dot conjugates: Attachment of CdS nanoparticles to lipase

4.1 Surface functionalization of CdS nanoparticles using organic silanes

Ten mg CdS nanoparticles were suspended in 10mL of isopropanol followed by addition of 4.5μL chilled ammonia with 3.05 μL water and kept on stirring for 30 mins at 37°C. Nanoparticles were further treated with 0.48 mmol APTES and 0.32 mmol TEOS followed by overnight stirring at 37°C for functionalization. The modified CdS

nanoparticles were recovered by centrifugation at 13,000 × *g* for 20 min at 4°C. The pellet was washed thoroughly with isopropanol and water to remove excess APTES and TEOS respectively and vacuum dried.

4.2 Immobilization of Candida rugosa lipase on modified CdS nanoparticles

Functionalized CdS nanoparticles (10mg) were dispersed into 9mL of phosphate buffer (50mM, pH 8.5) followed by sonication for 5min. to this mixture 1mL of lipase solution (50mg/mL suspended in 50mM phosphate buffer (pH 8.5)) was added. The mixture was stirred at 37°C overnight, centrifuged (13000 x *g* for 20min) and vacuum dried. The nanoparticles were then washed thrice with 50mM phosphate buffer (pH 8.5) to eliminate unbound lipase. The amount of immobilized lipase adsorbed on nanoparticles was determined by measuring the initial concentration and its final concentration in supernatant after immobilization following lipase assay.

4.3 Characterization studies

The morphologies of CdS before and after functionalization of each step were studied by TEM (Philips-Technai 20, Holland). For analysis, samples were dispersed into isopropanol and a drop was placed on a copper grid. The samples were observed after drying under vacuum.

A JEOL JEM-2100 high-resolution transmission electron microscopy (HRTEM) equipped with an energy dispersive X-ray (EDAX) spectrometer was used to characterize the internal structures of samples and to analyze their elemental composition.

The fluorescence microscopy images of CdS and CdS+Lipase were recorded on a fluorescence microscope (Olympus U-CMAD3) using an excitation filter of 460-495 nm and a band absorbance filter covering wavelengths below 505 nm. The samples were excited with a 50 W mercury arc lamp. Fluorescent microscopy images of several randomly selected sites were captured with a digital camera connected to the microscope.

The measurement of mass change during modification was analysed using TGA/DTA-7200 thermal analyser (Seiko SII-EXSTAR). The system was employed with PtRh furnace capable of operating from 25°C to 1500°C, the temperature being measured using type R thermocouple. The measurements are conducted under controlled atmosphere as

the system is vacum tight. TGA-DSC analysis was performed using 10mg of samples in alumina crucible without lid, in argon atmosphere. The temperature range was varied from 30-1000°C and with heating rate of 20°C/min.

The chemical modification on the surface of nanoparticles before and after functionalization was studied by Fourier transform infrared (FT-IR) spectroscopic analysis using Spectrochem GX-IR (Perkin Elmer, USA) in order to confirm binding of lipase on nanoparticles. The circular dichroism study was done using Jasco 815 spectropolarimeter using a quartz cell of path-length 10 mm.

4.4 Optimization of various parameters for enhanced enzymatic ester synthesis

The immobilized lipase was applied for esterification of pentyl valerate (mimic of pineapple flavor). The reaction mixture for ester synthesis consists of 20mL cyclohexane with equimolar concentration (0.1M) of each valeric acid and pentanol in 100mL stopper flask. The reaction initiated after addition of enzyme (50mg) to the substrate where native lipase and CdS-lipase were used separately for catalysis. The experiment was carried out at 37°C and continuously stirred at 150rpm to ensure all the enzyme particles were homogeneously dispersed. Reaction mixture of 100µL was withdrawn at every hour and was analyzed by Gas Chromatograph (Clarus-500) for accumulation of pentyl valerate.

Activities of free and immobilized lipase were optimized by running the enzymatic reaction according to an experimental design

i) Different pH viz: 5 to 9.5 with an increment of 0.5 and temperature 20, 30, 37, 40, 50, 60°C.

ii) Different molar ratio of various valeric acid and pentanol were used keeping the concentration of one substrate as constant while the other was varied.

iii) Reaction medium (n-hexane, n-heptane, iso-octane, cyclo-octane and cyclohexane)

iv) Effect of various chain length of fatty acids and alcohols

Samples (100µL) were periodically withdrawn in order to study the time course of reaction and analyzed by Gas Chromatograph (GC, Perkin Elmer, USA)) to establish the product formation profile. No activity was detected in the absence of the enzyme. All the

experiments were repeated thrice at each operative condition and the standard deviation was within ±2%.

4.5 Reusability studies for ester synthesis using immobilized lipase

For reusability studies, after completion of each cycle for esterification, the immobilized lipase was recovered by centrifugation at 10,000 x *g* for 5 min. The recovered enzyme was then washed with anhydrous cyclohexane twice in order to remove any remaining substrate or product accumulated and subsequently used for next cycle.

4.6 ***Analytical techniques***

4.6.1 Lipase assay

The activity for free and immobilized lipases was determined by measuring the initial hydrolysis rate of p-nitrophelyl palmitate (p-NPP) at the desired temperature on spectrophotometer. One unit of lipase activity was defined as the amount of enzyme releasing 1µmol p-nitrophenol/minute at pH 7.5 and 40°C. Soluble protein was estimated using bovine serum albumin (BSA) as standard.

4.6.2 Quantification of ester formation using GC

Quantification of accumulated ester was done by Gas Chromatograph using FID detector as described by Raghvendra et al., 2010. Samples (100µL) were withdrawn periodically after initiation of reaction and analysed by gas chromatograph (PerkinElmer, Model Clarus 500, USA) equipped with flame ionization detector and 30 m Rtx-®-20 (Crossbond 80% dimethyl-20%diphenyl polysiloxane) capillary column. The carrier gas was nitrogen at split flow rate of 90mL/min. The injector and detector temperatures were 250 and 280°C respectively and oven temperature was programmed to increase from 100 to 160°C at the rate of 20°C/min, from 160 to 280°C at the rate of 2°C/min and from 165 to 175°C at the rate of 1°C/min. Ester identification and quantification were done by comparing the retention time and peak area of the sample with the standard. Pure pentyl valerate (≥98%) was used as external standard.

(5) Zinc oxide nanoparticles supported lipase immobilization for biotransformation in organic solvents: A facile synthesis of geranyl acetate, effect of operative variables and kinetic study

5.1 PEI coating of ZnO nanoparticles and its modification with SAA

The grafting of PEI onto the surface of naked ZnO nanoparticles was carried out in two steps. In first step, PEI (1.5mL) was suspended in a solution containing 10% APTES (1mL in 9mL ethanol). To this mixture 10mg of ZnO nanoparticles were added and stirred vigorously to react for 24h. The composite obtained was isolated by centrifugation (10000X*g* for 15min) and repeatedly washed with ethanol and milliQ in order to remove excess PEI. Secondly, to introduce amide and acid groups onto the surface of nanoparticles, 10mg of PEI-coated ZnO nanoparticles was suspended in 10mL solution of SAA (10mg/mL) followed by stirring of the mixture at room temperature for 4h. The prepared succinated nanocomposites (ZnO-PEI-SAA) were separated by centrifugation and washed thrice with deionized water to remove excess SAA and by product.

5.2 Characterization of prepared nanocomposites

The chemical modification on the surface of nanoparticles before and after functionalization was studied by Fourier transform infrared (FT-IR) spectroscopic analysis using Spectrochem GX-IR (Perkin Elmer, USA) in order to confirm binding of lipase on nanoparticles. The surface morphologies for each ZnO samples before and after functionalization were studied by TEM (Philips-Technai 20, Holland) and SEM. Samples were prepared by placing a droplet of sample (dispersed into isopropanol) on a copper grid covered by Formvar foil (200 mesh). The samples were then dried and analyzed. The fluorescence microscopy images of ZnO and ZnO+Lipase were recorded on a fluorescence microscope (Olympus U-CMAD3) using an excitation filter of 460-495 nm and a band absorbance filter covering wavelengths below 505 nm. The samples were excited with a 50 W mercury arc lamp. Fluorescent microscopy images of several randomly selected sites were captured with a digital camera connected to the microscope. The measurement of mass change during modification was analysed using TGA/DTA-7200 thermal analyser (Seiko SII-EXSTAR). The system was employed with PtRh furnace capable of operating from 25°C to 1500°C, the temperature being measured using type R thermocouple. The measurements are conducted under controlled atmosphere as

the system is vacum tight. TGA-DSC analysis was performed using 10mg of samples in alumina crucible without lid, in argon atmosphere. The temperature range was varied from 30-1000°C and with heating rate of 20°C/min.

5.3 Immobilization of lipase on modified ZnO nanoparticles

Immobilization of lipase on ZnO was done by two different methods. i) Adsorption of lipase on PEI- and succinated PEI- grafted ZnO nanoparticles: ZnO-PEI and ZnO-PEI-SAA (10mg each) were suspended in 10mL phosphate buffer (50mM, pH 7) containing 1mL *Candida rugosa* lipase (50mg/mL). The mixture was incubated at 4ºC for 16h followed by centrifugation and then vacuum dried at 37ºC for 1h. ii) Covalent immobilization using glutraldehyde (GLU) as cross linker: The covalent immobilization procedure was developed using GLU as cross-linking agents between the lipase and the amino groups located on the surface of the ZnO-PEI. In a typical procedure, 10mg of ZnO-PEI was incubated in 10mL phosphate buffer solution (50mM, pH 7.0) containing 1%(w/v) GLU and allowed to react for 10min. Then, 1mL of lipase solution (50mg/mL) was incorporated into the mixture and stirred for overnight. The resultant nanobioconjugant obtained from both the procedures (physical adsorption and covalent attachment) were dried under vacuum (37ºC for 1h) and further preceded for transesterification of geranyl acetate in organic solvents. The amount of enzyme immobilized is calculated based on the residual enzyme remaining in the supernatant.

5.4 Enzyme activity and protein assay

The enzymatic activity of free and immobilized lipase was measured using the lipase assisted hydrolysis of *p*-nitrophenyl palmitate (*p*-NPP)as the substrate and the spectrophtometric determination of liberated *p*-nitrophenol (*p*-NP).

5.5 Enzymatic synthesis of geranyl acetate catalyzed by free CRL as well as immobilized lipase preparations

Synthesis of geranyl acetate as industrially important ester was studied using free as well as immobilized biocatalyst in presence of organic solvent as reaction medium. In 10ML

screw cap glass vials, equimolar concentration of Geraniol (0.1M) and vinyl acetate (0.1M) were used as a substrate and mixed with 3mL of n-hexane. Later on, the reaction was initiated after addition of enzyme to the substrate where native lipase and immobilized lipases were used separately for catalysis. The experiment was carried out at 37°C and continuously stirred at 150rpm to ensure all the enzyme particles were homogeneously dispersed. Reaction sample of 100µL was withdrawn periodically and analyzed using Perkin Elmer, Clarus-500 Gas Chromatograph equipped with flame ionization detector and 30m Rtx-®-20 capillary column. The carrier gas was nitrogen at split flow rate of 90mL/min. The temperature of the detector and injector was maintained at 250ºC. The oven temperature was programmed to increase from 40 to 180ºC at the rate of 3ºC/min up to 180-230ºC (20ºC/min) and maintained at 230ºC for 20min. Ester identification and quantification were done by comparing the retention time and peak area of the sample with the standard.

5.6 Effect of operative variables on enzymatic production of geranyl acetate

In order to obtain enhanced geranyl acetate synthesis different operative variables were used for the experiment. The operative variables used in the study were (i) Effect of temperature: 30, 37, 40 and 50°C. (ii) Effect of organic solvents: different solvents used were tetrahydrofuran, 1,4-dioxane, acetone, chloroform, benzene, toluene and n-hexane. (iii) Effect of substrate concentration: Substrate concentration ranges from 0.1M to 0.5M. The concentrations of geraniol and vinyl acetate were varied one at a time keeping the other constant. (iv) Effect of acyl donor: acetic acid, ethyl acetate and vinyl acetate were used as acyl donor.

Samples (100µL) were periodically withdrawn to study the time course of reaction and analyzed by Gas Chromatograph (GC, Perkin Elmer, USA)) in order to establish the product formation profile. No reaction was detected in the absence of the enzyme. All the experiments were repeated thrice at each operating condition and the relative deviation was within ±1%.

5.7 Reusability studies for immobilized lipase preparations

After establishing the conditions for maximum geranyl acetate production, the reusability study for all the immobilized lipase nanocomposites was carried out. After the first run of lipase activity determination the immobilized lipase was collected using centrifugation and washed three times with n-hexane in order to removed excess substrate and product. The activity during the first run was defined as 100% and that during the succeeding runs was regarded as relative activity. All the experiments were performed in triplicate and data were shown as relative deviation within ±1%. Also, after every 3-4 cycles of reusability dehydration treatment was given in order to remove accumulated water formed as byproduct. The nanocomposites were treated with molecular sieves (30mg) for overnight in 2mL n-hexane solution.

(6) Increasing esterification efficiency by double immobilization of lipase-ZnO bioconjugate into AOT-reverse micelles and microemulsion based organogels

6.1 Fabrication of lipase on ZnO functionalized with PEI

Fabrication of lipase on functionalized ZnO nanoparticles were carried out in two steps. Firstly, Branched polyethyleneimine (1.5mL) was suspended in a solution containing 10% APTES in ethanol. To this mixture 10mg of ZnO nanoparticles were added and stirred vigorously to react for 24h. The obtained composite was purified by centrifugation (10000X*g* for 15min) and repeatedly washed with ethanol and milliQ in order to remove excess silane and PEI. Secondly, 10mg of ZnO-PEI was incubated in 10mL phosphate buffer solution (50mM, pH 7.0) containing 1% (w/v) GLU and allowed to react for 10 min. Then, 1mL of lipase solution (50mg/mL) was incorporated into the mixture and stirred for overnight. The mixture was centrifuged and washed with phosphate buffer (50mM) in order to eliminate unbound lipase.The amount of immobilized lipase adsorbed on nanoparticles was determined by measuring the initial concentration and its final concentration in supernatant after immobilization using lipase activity.

6.2 Entrapment of ZnO doped lipase into AOT/Iso-octane microemulsion and PVA gels

(i) Preparing microemulsions: In 10mL screw cap vials, 0.1M sodium bis (2-ethylhexyl) sulfosuccinate (AOT) with W_o=60, 2mL isooctane and 50mM phosphate buffer (pH-8.0) were taken to attain the corresponding z([co-surfactant]/[surfactant]) and W_o([water]/[surfactant]) value, respectively. The mixture was vigorously vortex for 5 min to obtain a clear homogeneous solution of 0.1M AOT/iso-octane/buffer reverse micelle. Following the similar protocol, suspensions of previously prepared ZnO-E nanocomposite (108µL) was doped to AOT reverse miceller mixture instead of phosphate buffer to obtain the corresponding W_o value. The enzyme entrapped into reverse micelles was designated as ZnO-E@RM. (ii) Preparing gelling matrix: The MBGs were prepared by introducing AOT microemulsion containing ZnO-E to a second solution of 2% PVA dissolved in water. Typically 2mL of prepared microemulsions were introduced into 2% polymer solution and then moderately stirred to obtain homogenous mixture. Finally, immobilized matrix with entrapped lipase was carefully poured in a Teflon dish and allowed to dry at 40-45°C for 40h. A thin film of immobilized lipase was formed, which was then cut into small pieces (1 X 1cm with 110±10µm thickness) and stored at 4°C. Microemulsions prepared with AOT-reverse micelles were designated as ZnO-E-RM@PVA and further characterized.

6.3 Lipase activity, Protein content and Immobilization Yield (%) determination

The reaction solution was prepared by addition of free or immobilized lipase to p-NPP solution (0.4mM in 100mM phosphate buffer pH 8) and incubated for 10min at 40°C, 150rpm followed by measuring absorbance at 410nm using UV-Vis spectrophotometer. One unit of enzyme activity is defined as the amount of enzyme that liberates p-nitrophenol at the rate of 1µmol per min under specified conditions.

The amount of protein was determined by Folin-Lowry method at 595nm [Lowry et al.] using bovine serum albumin as standard. Percentage Protein loading, specific activity and activity yield was determined by following equations:

% protein loading = amount of protein immobilized ÷ initial amount of protein loaded X 100

% activity yield = immobilized lipase activity ÷ crude lipase activity X 100

Specific activity = lipase activity ÷ total protein

6.4 Characterization of immobilized enzymes

6.4.1 Effect of pH on enzyme stability

The effect of pH on enzyme stability was determined after introduction of free as well as immobilized lipases in buffers of citrate (100mM, pH 5-6), phosphate (100mM, pH 7-8) and Tris-HCl (100mM, pH 9-10) for 1h at 37°C followed by measuring the relative activity of enzyme. At each time interval 1 mL sample was pipette out and then assayed for residual activity, which was expressed as percentage of initial activity (taken as 100%). All the experiments were repeated thrice at each operating condition and the relative standard deviation was within ±2%.

6.4.2 Effect of temperature on enzyme stability

The thermal stability of free or immobilized lipases was determined by incubating the enzyme in water bath for 1h at the temperature ranging from 20-50°C followed by measuring the relative activity of enzyme. At each time interval 1 mL sample was pipette out and then assayed for residual activity, which was expressed as percentage of initial activity (taken as 100%). All the experiments were repeated thrice at each operating condition and the relative standard deviation was within ±2%.

6.4.3 Effect of storage on enzyme stability

The storage stability was determined by relative activity measurements of free and immobilized lipase for 20 days at 4°C. At each time interval 1 mL sample was pipette out and then assayed for residual activity, which was expressed as percentage of initial activity (taken as 100%). All the experiments were repeated thrice at each operating condition and the relative standard deviation was within ±2%.

6.5 Biocatalytic transformation of ethyl and pentyl valerate by free and immobilized lipase

Synthesis of ethyl and pentyl valerate as industrially important esters was studied using free and lipase immobilized on ZnO-E-RM@PVA in n-hexane. The reaction was initiated by addition of free and immobilized lipase in solution consisting of n-hexane (2mL), with acid/alcohol molar ratios of 2:1. 1:1, 1:2, 1:3, 1:4 and 1:5) followed by incubation at different temperatures (30, 37, 40 and 50°C), 150 rpm for 0, 2, 4, 6, 8 and 12h. In parallel, the reaction in presence of prepared support ZnO-RM@PVA without lipase was designed for control. The amount of ester produced was analyzed by Gas chromatograph. (PerkinElmer, Model Clarus 500, Germany) equipped with a flame-ionization detector (FID). The column was 30 m Rtx-®-20 (Crossbond 80% dimethyl-20% diphenyl polysiloxane) capillary column. The temperature of injector and detector were maintained at 250°C. The carrier gas served as nitrogen with the split flow rate of 90mL/min. The column temperature was programmed to increase from 40-120°C at the rate of 3°C/min, from 120-200°C at the rate of 10°C/min and from 200-220°C at the rate of 2°C/min. All the aforementioned experiments were done in triplicates and the mean of data obtained was reported. In order to investigate reusability, the immobilized biocatalyst was recovered from the reaction mixture using centrifugation, followed by washing with anhydrous n-hexane after each run. Further immobilized lipase matrix was dried for overnight and implemented with fresh substrates for determination of the esterification percentage. All the experiments were repeated thrice at each operating condition and the relative standard deviation was within ±2%.

6.6 Characterization study

The chemical modifications was studied by Fourier transform infrared (FT-IR) spectroscopic analysis using Spectrochem GX-IR (Perkin Elmer, USA) in order to confirm binding of lipase on nanoparticles. The vacuum dried samples were mixed with IR grade KBr and finely ground to form homogenous powder under dry conditions for preventing adsorption of water vapour. This mixture was made into pellet and placed inside vacuum concentrator for ensuring total dry conditions. The dried pellets were then

fixed in sample holder and analysis was performed in the mid IR region of 400-4,000cm^{-1}. The measurement of mass change during was analysed using TGA/DTA-7200 thermal analyser (Seiko SII-EXSTAR). The system was employed with PtRh furnace capable of operating from 25°C to 1500°C, the temperature being measured using type R thermocouple. The measurements are conducted under controlled atmosphere as the system is vacuum tight. TGA-DSC analysis was performed using 10mg of samples in alumina crucible without lid, in argon atmosphere. The temperature range was varied from 30-1000°C and with heating rate of 20°C/min.

6.7 Kinetic parameters

The kinetic parameters for both free and immobilized lipase (ZnO-E-RM@PVA) system were determined by varying substrate molar ratio concentration. The effects of concentrations of valeric acid and pentanol o the initial rate of pentyl valerate synthesis were studied using free and immobilized lipase keeping the initial concentration of one of the substrates, that is, pentanol/valeric acid constant (1 mM), and varying the initial concentration of the other (1µmM, 2µmM, 3µmM, 4µmM, and 5µmM). One unit of enzyme activity was defined as amount of lipase required for synthesis of 1µmole of pentyl valerate. The K_m and V_{max} values were obtained from Lineweaver–Burk plots.

Results and Discussion

(1) Molecular assessment of microbial community inhabiting oil perturbed soil: Tracking taxonomic and functional behavior using shotgun sequencing approach

1.1 Physico-chemical analysis of soils

The physicochemical analysis of soil samples from both (control and polluted) sites are tabulated in Table 1.1 showing considerable difference (*P-value* <0.05) in all the corresponding parameters. Soil with oil stress revealed higher nitrogen (1.5 times) and potassium (1.3 times) content as compared to that of control soil sample. This difference could be ascribed to the characteristic feature of soil ecosystems with inherent bioremediation potential. Total organic carbon was found to be 1.05% and 0.71% for polluted and pristine soil, respectively.

Table 1.1: Physico-chemical analysis of soil samples

Sr. No	Parameters tested	Polluted soil	Control soil
1	Texture of soil	Fine loamy soil	Fine loamy soil
2	Temperature (°C)	37	37
2	pH	8.10	8.26
3	Organic carbon (%)	1.05	0.71
4	Total Nitrogen ($Kgha^{-1}$)	2070	1371
5	Available P_2O_5 ($Kgha^{-1}$)	37.75	26.78
6	Available K_2O ($Kgha^{-1}$)	170.45	122.21
7	EC (dSm^{-1})	0.33	0.19

1.2 Enumeration of total bacterial count achieved from collected soil sample

Bacterial colonies from polluted as well as control samples were isolated on nutrient agar, Luria agar, plate count agar and trybutyrin agar supplemented with tributyrin oil as carbon source at the dilutions of 10^{-5} which is tabulated in Table 1.2. The isolated colonies were further purified by repetitive streaking. As shown in Table 1.2, total bacterial counts were found to be highest in nutrient agar for both the samples in comparison to other media used. Also as the source of bacteria, organisms were also isolated on medium present with trybutyrin oil. Total number of lipolytic bacteria was found to be 1.8×10^3 in polluted soil. Whereas, addition of tributyrin oil in tributyrin agar decreased total bacterial count i.e. less than 30 in pristine soil sample. Since the contaminated site of the study is oil perturbed soil effort was made to isolate organisms on tributyrin agar plates containing tributyrin oil as carbon source. Total bacterial counts of $1.8X10^3$ CFU/mL were obtained from oil contaminated soil whereas <30 bacterial counts were attained from control sample when screened on tributyrin agar plates. The probable reason for this could be production of

extracellular enzymes by particular microorganisms to combat these stressed condition in such contaminated environment.

Table 1.2: Total bacterial counts from the soil samples

Sr. No	Media	Polluted CFU/ml	Control CFU/mL
1.	Nutrient Agar	2.03 X 10^3	3.67 X 10^3
2.	Luria Agar	1.83 X 10^3	3.02 X 10^3
3.	Plate count Agar	1.57 X 10^3	2.65 X 10^3
4.	Trybutyrin Agar	1.8 X 10^2	<30

1.3 Bacterial community structure using culture dependent approach

Biodegradation by intrinsic microbial populations is the key and reliable system through which thousands of organic contaminants are eradicated from the environment. Using culturable approach higher number of total bacterial count was observed in presence of tributyrin from polluted environment in comparison to that of pristine. Result evidently indicates the adaption of organism toward oil stress. Genomic DNA having good yield and purity was extracted from isolated bacterial strains. The purity ratio i.e. 260/280 for extracted genomic DNA was found to be on an average 1.85 specifying lack of protein impurities. The 16S rRNA gene was amplified from all the isolated genomic DNA of bacterial strains using universal primers (8F and 1492R). Fig 1(a) and Fig 1(b) flaunts high molecular weight genomic DNA extracted from bacterial strains and amplification of 1.5kb 16S rRNA gene from genomic DNA, respectively.

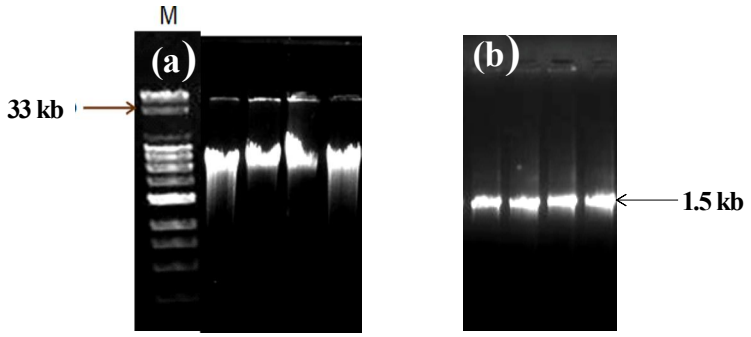

Figure 1: (a) Genomic DNA electrophoresed on 0.8% agarose gel. (b) PCR amplified product of 16S rRNA gene electrophoresed on 1.2% agarose gel

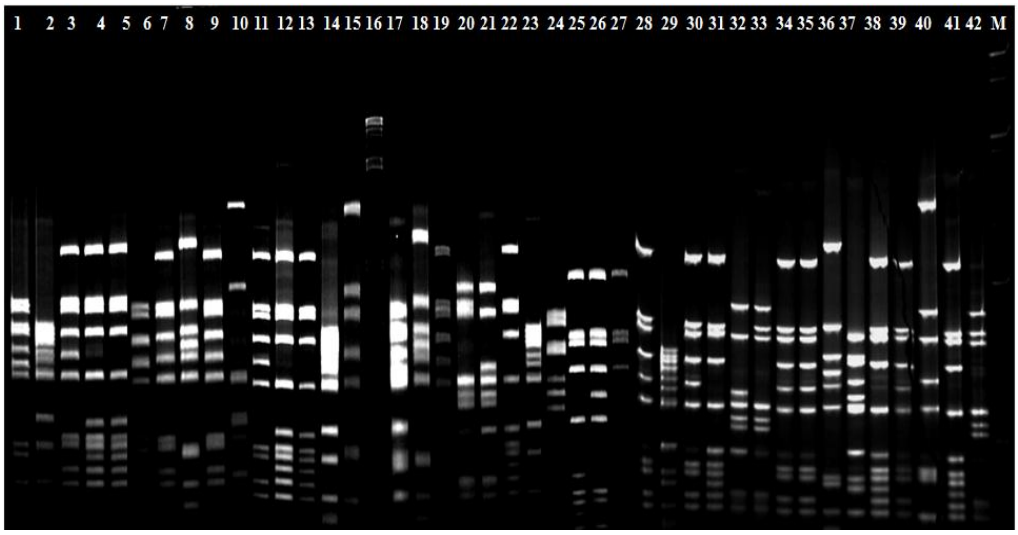

Figure 2: Restriction digestion pattern of amplified 16S rRNA gene product using *HhaI, HaeIII* and *MspI*. Analysis of digest product on 6% denaturing polyacrylamide gel from Lane 1-42

Amplified ribosomal DNA restriction analysis (ARDRA) is recognized method for diversity analysis which is fairly cheaper and easier to execute in comparison to other molecular techniques used for biodiversity analysis. All the isolated bacterial strains obtained during study were morphologically different but still shows similar banding pattern (Fig. 2) Bacterial cultures showing discrete banding profile was selected from all isolates and sequenced to analyze bacterial community structure. Total 50 different cultures were isolated on the bases of their banding pattern and processed for 16S rRNA sequencing.

1.4 Metagenomic DNA extraction and analysis

Soil collected from the industrial area was used for metagenomic DNA extraction. The obtained DNA was of high molecular weight and pure enough for further sequencing studies (Fig 3). Details about purity ratio and quality of metagenomic DNA (after pooling up DNA for each respective site i.e. P=P1+P2+P3 and C=C1+C2+C3) with reverence to humic acid is described in Table 1.3.

Sequencing of two DNA libraries (viz. polluted soil and control soil) was performed and data from the experiments are condensed in Table 1.3. The sequencing run resulted in 17, 06,040 reads (an average read length of 339bp) for polluted sample and 39,98,015 reads (an average

read length of 356bp) for control sample. In total 31,284,971 numbers of bases were assembled into 201,285 contigs for polluted soil and 58,039,898 number of bases were assembled into 262,608 contigs for control soil sample using MetaVelvet assembler.

Table 2.3: Summary of sequencing result

	Polluted	Control
DNA concentration (ng/μL)	404	358
Number of reads	17,06,040	39,98,015
Average read length	339	356
Total number of contigs	201,285	262,608
Max contig length	1347	1258
Number of bases in contigs	31,284,971	58,039,898
N50	157	221

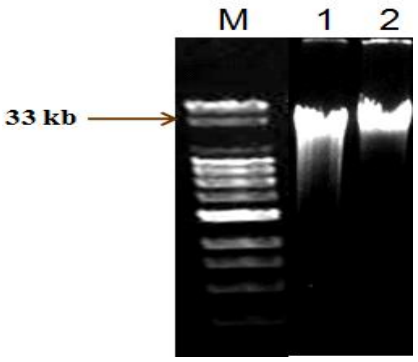

Figure 2.3: Metagenomic DNA extracted from polluted as well as control soil sample and electrophoresed on 0.8% agarosa gel. Lane M is of marker, Lane 1 is for polluted soil sample (representing polled metagenomic DNA for P1+P2+P3=P) and Lane 2 is for control soil sample (representing polled metagenomic DNA for C1+C2+C3=C).

1.5 Bacterial diversity analysis

According to RDP classifier, Bacteria is the dominant domain for both polluted (95.7%) and control (97.6%) as indicated in Fig 4**(a).** Eukaroyta was found to be 2.3% for polluted site and 1.2% for control site which was followed by Unassigned proteins with 1.8% for polluted and 2.4% for control samples. As shown in Fig 4(b), the polluted sample includes eight phyla, where *Proteobacteria* (60.9%) is found to be most abundant phylum followed by *Bacteroidetes* (5.6%), *Verrucomicrobia* (2.4%) representing 68% of total sequences. Where as, phylum for control sample was mainly dominated by *Proteobacteria* (30%) followed by *Bacteroidetes* (7.4%) and *Verrucomicrobia* (4.3%).

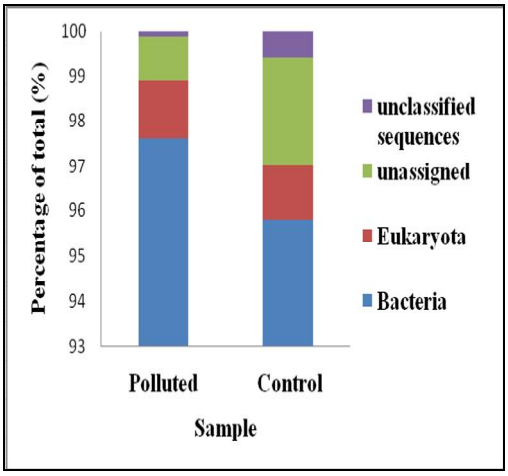

Fig 4(a)

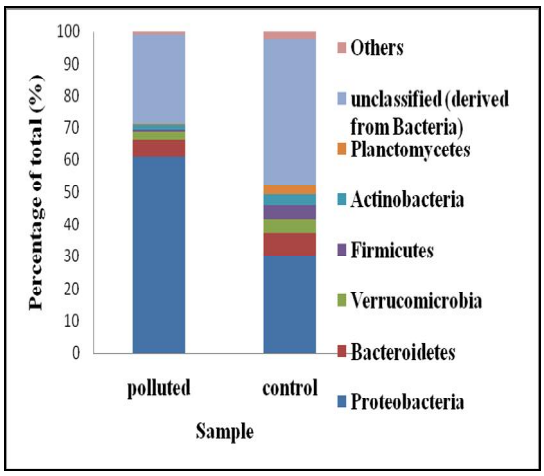

Fig 4(b)

Fig 4(c) exhibits the classification of bacteria at class level for both the soils. It can be clearly seen from the graph that there is vast community shift in in polluled samples. *Betaproteobacteria* (56%) is found in abundance at class level followed by Gammaproteobacteria (2.2%), *Actinoproteobacteria* (1.3%) and *Alphaproteobacteria* (1.1%) in polluted soil. Control soil comprise of *Gammaproteobacteria* (14%) in abundance followed by *Betaproteobacteria* (6%), *Alphaprotebacteria* (5%) and *Actinobacteria* (3%).

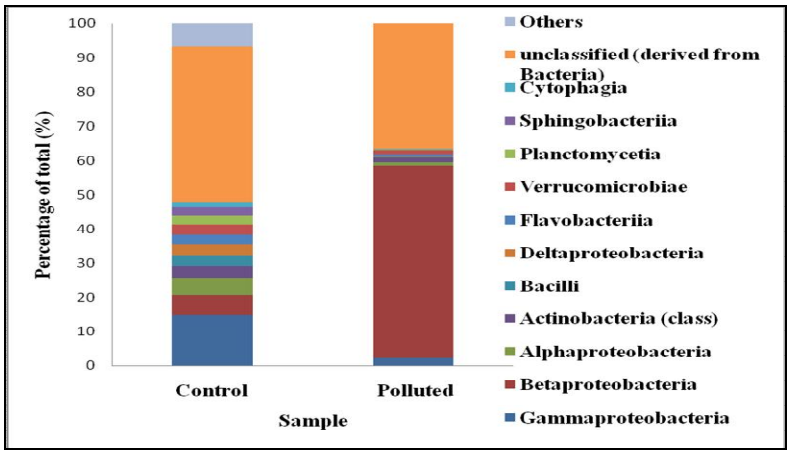

Fig 4(c)

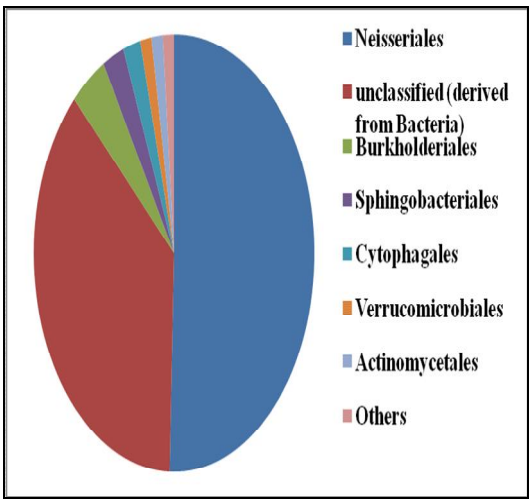

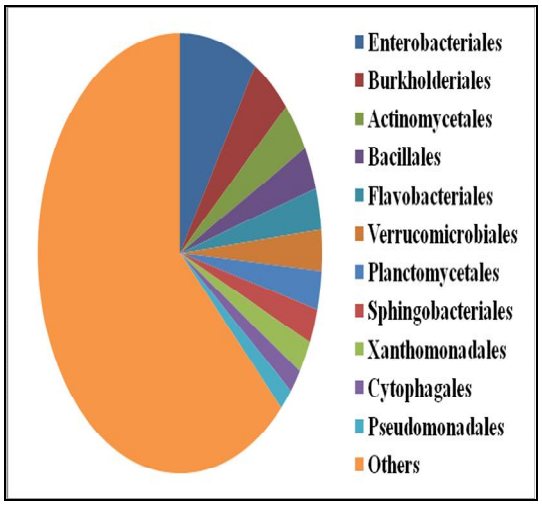

Fig 4(d) **Fig 4(e)**

Fig 4: Qualitative analysis of bacterial community structure of poluted and control site at (a) Domain level comparision (b) Phylum level comparision (c) Class level comparision and (d) Order level comparision for polluted soil (e) Order level comparision for control soil classified according to RDP classifier

In polluted soil at order level *Neisseriales* (50%) was present in abundance followed by *Burkholderiales* (4%) and *Sphingobacteriales* (2%). For control soil, *Enterobacteriales* (8%) was found to be dominant rather than Neisseriales **(Fig 4(d)).** This indicates the shifting in community for polluted soil where certain microbes adapt themselves to survive under harsh conditions.

1.6 Rarefaction analysis

Statistical analysis of biodiversity provides interesting insights as reflected in rarefaction curves. Rarefaction analysis was carried out in order to assess species richness of the system. Using RDP, we analyzed the microbial richness, based on sequence reads, between libraries of polluted and control soil samples (Fig 5(a)). Whereas, plotting the number of leaves predicted by LCA algorithm revealed that the number of taxonomic leaves or clades of control soil are all higher than those of polluted ones. Also, control and polluted soil contains 629 and 396 leaves for all assigned taxa, respectively (Fig 5b). Our results suggest that the current sampling depth is not yet close to the natural status for bacteria.

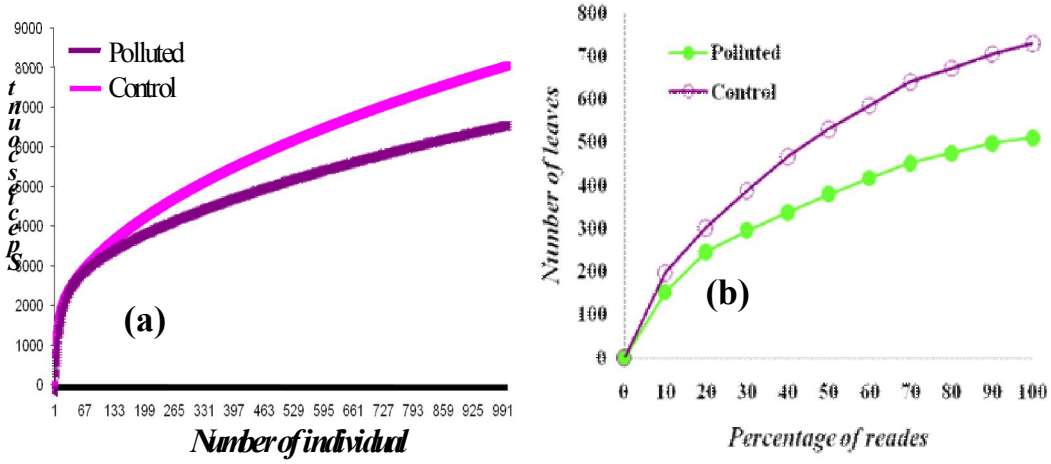

Figure 5: Statistical comparative analysis for the reads assigned between control as well as polluted soil sample (a) Rarefaction curves on species counts using RDP dataset and (b) percentage of reads

1.7 Gene function annotation and classification

Understanding the factors that influence microbial community structure is an important goal in microbial ecology. Our analysis results indicate that oil has a significant impact on soil microbial functional communities in contaminated soil. On one hand oil contamination could be toxic to many microbial populations reducing microbial diversity and on the other hand, the vast range on carbon substrates and subsequent metabolites present in oil-contaminated soil could facilitate the development of rather complex microbial communities. In this study, microbial functional genes encoded for lipid metabolism was analyzed annotated using COG database. Assembled contigs were analyzed by assigning predicted functions to genes based on COG. In total 22 classes based on functional categories were identified by COG database (Fig 6). In the category "metabolism" large amount of reads are distributed among "amino acid transport and metabolism (E)", "energy production and conversion (C)", "carbohydrate transport and metabolism (G)", and "lipid transport and metabolism (I)". The class "lipid transport and metabolism (I)" was further characterized for various kinds of enzymes responsible for fatty acid metabolism under stress conditions. Classes such as "inorganic ion transport and metabolism (P)" and "coenzyme metabolism (H)," "secondary metabolites biosynthesis, transport, and catabolism (Q)," and "signal transduction mechanisms (T)" are

associated with transport of ions/compounds and other metabolic processes (Fig 6). COG categories/accessions important in lipid metabolism are described in Table 1.4.

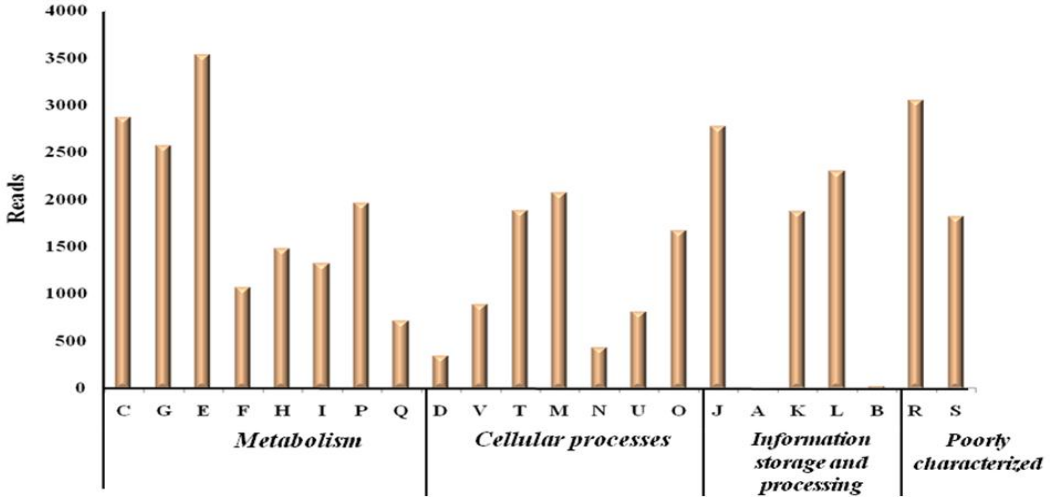

Figure 6: Characterization of metagenomic sequencing reads of contaminated soil sample according to the Cluster of Orthologous Groups of protein (COGs)

Table 1.4 : COG categories as discovered from the metagenomic reads for lipid metabolism

COG No.	*Name of the protein*
COG3425	3-hydroxy-3-methylglutaryl CoA synthase
COG0304	3-oxoacyl-(acyl-carrier-protein) synthase
COG0332	3-oxoacyl-[acyl-carrier-protein] synthase III
COG4247	3-phytase (myo-inositol-hexaphosphate 3-phosphohydrolase)
COG1211	4-diphosphocytidyl-2-methyl-D-erithritol synthase
COG0439	Biotin carboxylase
COG2272	Carboxylesterase type B
COG4589	CDP-diglyceride synthetase
COG1024	Enoyl-CoA hydratase/carnithine racemase
COG0821	Enzyme involved in the deoxyxylulose pathway of isoprenoid biosynthesis
COG0657	Esterase/lipase
COG1398	Fatty-acid desaturase

COG1022	Long-chain acyl-CoA synthetases (AMP-forming)
COG3127	Lysophospholipase
COG1443	Isopentenyldiphosphate isomerase
COG2185	Methylmalonyl-CoA mutase, C-terminal domain/subunit (cobalamin-binding)
COG1260	Myo-inositol-1-phosphate synthase
COG2867	Oligoketide cyclase/lipid transport protein
COG0558	Phosphatidylglycerophosphate synthase
COG1562	Phytoene/squalene synthetase
COG3243	Poly(3-hydroxyalkanoate) synthetase
COG4553	Poly-beta-hydroxyalkanoate depolymerase
COG1657	Squalene cyclase
COG0020	Undecaprenyl pyrophosphate synthase

1.8 Metabolic pathway analysis for fatty acid biosynthesis

Fatty acid biosynthesis in almost all the organisms culminates in formation of saturated fatty acids. All organisms produce fatty acids via a repeated cycle of reactions involving the condensation, reduction, dehydration and reduction of carbon-carbon bonds. First step in fatty acid biosynthesis (Fig 7) is the ATP dependent formation of malonyl-CoA from acetyl-CoA and bicarbonate by acetyl-CoA carboxylase (*acc*, EC 6.4.1.2) enzyme. All bacterial organisms contain a type II synthase (FAS II) for which each reaction is catalyzed by a discrete protein and reaction intermediates are carried in the cytosol as thioesters of the small acyl carrier protein (ACP). Malonyl CoA:ACP transferase encoded by *fabD* gene (EC 2.3.1.39) undergoes transacylation of malonyl from CoA to ACP. The chain elongation step in fatty acid biosynthesis consists of the condensation of acyl groups, which are derived from acyl- CoA or acyl-ACP, with malonyl-ACP by two types of 3-ketoacyl-ACP synthases. The first class of 3-ketoacyl-ACP synthase III (*fabH*, EC 2.3.1.180) is responsible for the initiation of fatty acid elongation and utilizes acyl-CoA primers. The second class of enzymes (*fabF* EC 2.3.1.179 and *fabB,* EC 2.3.1.41) is responsible for the subsequent rounds of fatty acid. Thus, produced acyl-ACP is catalyzed by three enzymes [NADPH-dependent

3-ketoacyl-ACP reductase (*fabG*, EC 1.1.1.100), 3-hydroxyacyl-ACP dehydratase (*fabZ,* EC 4.2.1.59) and NAD(P)H-dependent enoyl-ACP reductase (*fabI,* EC 1.3.1.9, 1.3.1.10)] for reduction, dehydration and reduction of carbon-carbon bonds ,respectively. Further, additional cycles are initiated by *fabF* and *fabB*. The *fad*R_{Ec} protein is a global regulator of fatty acid degradation, is a transcriptional activator that binds to the *fabA* promoter region.

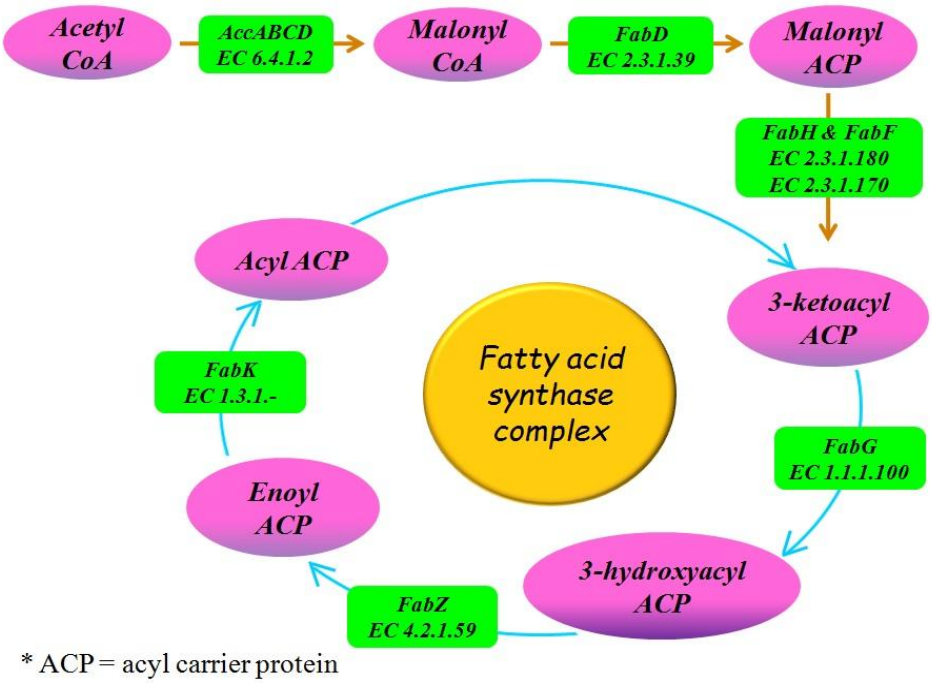

Figure 7: Fatty acid synthesis and metabolism pathway predicted in polluted soil sample based on KEEG analysis. Pink colors indicate formation of compounds within the reactions and green labels indicates presence of genes detected in metagenomic reads

Finally, input to fatty acid synthesis is acetyl CoA and the output is free fatty acid synthesis. The *fab* and *fad* proteins are highly conserved in many grampositive bacteria including *Bacillus*, *Clostridium*, *Streptomyces* and other related genera. Moreover, its orthologues are unexpectedly present in more diverse genera, such as *Metanosarcina* (*Archaea*), and *Bordetella*, *Burkholderia* and *Chromobacteria* (*β*-proteobacteria). Also, genome analysis indicated that only the α-, β and γ-proteobacteria have the proteins of this pathway.

Any given soil possess a unique reservoir of (microbial) genes involved in (bio) transformation of complex organic/inorganic mixtures into simpler elemental form, through

interlinking pathways. Depending upon the soil ecosystem, the gene pools changes and acclimatize the environmental need. Analyzing these gene pools, one can predict the existing scenario and future response can be predicted. Looking at the array of results obtained though shotgun method functional metagenomic approach was successfully applied to understand the functional repository of oil perturbed soil.

(2) Solvent tolerant Pseudomonas sp. lipase: Characterization and application in nanobiocatalysis

2.1. Isolation and identification of solvent tolerant lipase producing bacteria

Out of all isolates showing clearance zone on tributyrin agar plate, the isolate DMVR46 (Fig. 8) showed the highest lipase activity (9.47 U/mL), and hence was used for further studies. Organic solvent tolerant lipase produced by strain DMVR46 was identified as *Pseudomonas sp.* on the basis of 16S rRNA gene sequencing followed by BLAST analysis which showed sequence homology (100%) with the complete 16S rRNA gene sequence of *Pseudomonas sp*. The sequence of strain DMVR46 was deposited in NCBI with an Accession number KF636492. Phylogenetic affiliation of isolate DMVR46 with related *Pseudomonas sp*. is shown in Fig. 8.

Table 2.1: Profiling of lipase producers isolated from oil contaminated sites by spectrophotometric method

Culture	Lipase activity [units/mL]	Protein activity mg/mL	Specific activity [units/mg]
DMVR46	**9.477**	3.968	2.388
DMVR63	0.327	3.158	0.103
DMVR22	0.581	7.211	0.080
DMVR20	0.414	4.896	0.085
DMVR9	0.837	5.455	0.153
DMVR18	1.132	2.932	0.386
DMVR12	3.236	5.211	0.620
DMVR2	0.951	4.634	0.205
DMVR37	0.269	3.212	0.058
DMVR15	1.183	4.185	0.282
DMVR24	4.752	6.453	0.732

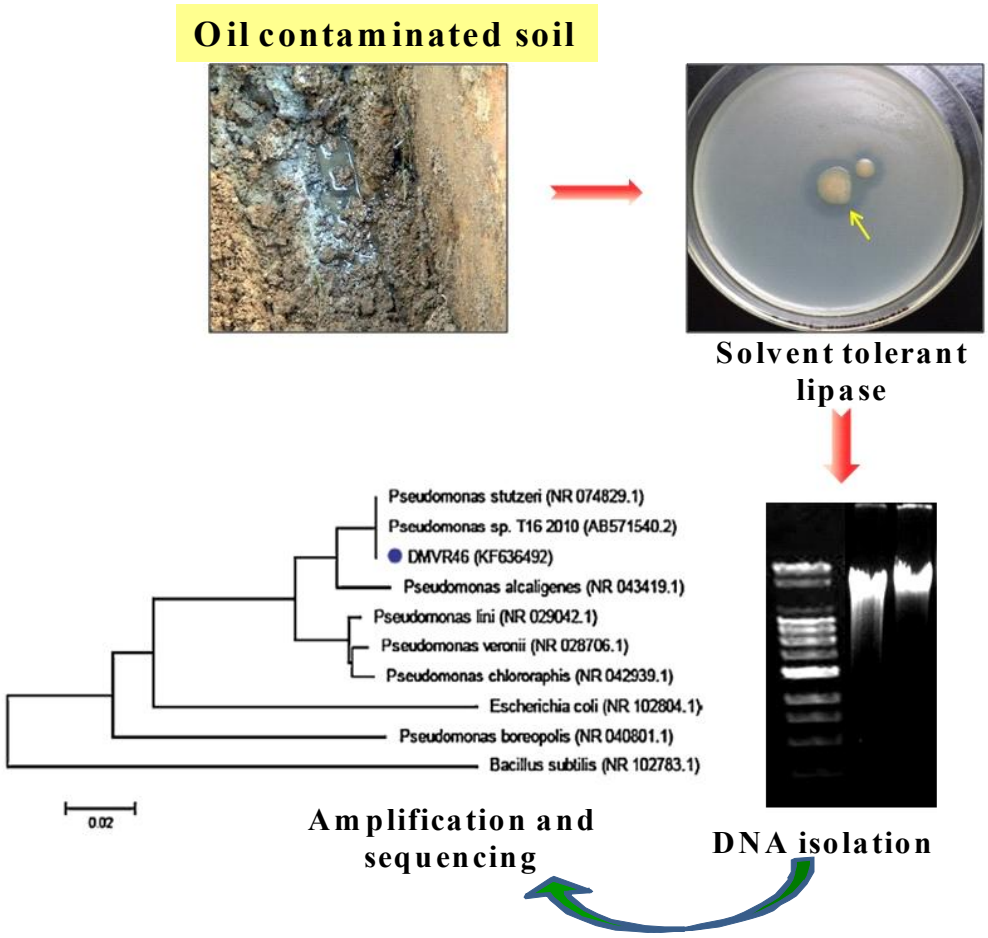

Figure 8: Pictorial representation for isolation of solvent tolerant lipase producing bacterial strain from oil contaminated site and Extraction of DNA. Phylogenetic tree based on 16S rRNA gene sequence of *Pseudomonas* sp. DMVR46. (GenBank accession No. KF636492) and sequence of closest phylogenetic neighbours obtained by NCBI BLAST (n) analysis, numbers in the parenthesis indicate accession numbers of corresponding sequence. The tree was constructed using MEGA 5.0 software. *Bacillus subtilis* strain NR 102783 has been taken as an out-group

2.2. Growth profile for lipase production

Various physico-chemical parameters were scrutinized for maximum lipase production. The optimum temperature and pH for initial lipase activity was found to be 37°C and pH 8.0 [Fig. 9(a), 9(b)]. Among various inducers tested for lipase production, cotton seed oil (1% (v/v)) with an activity of 48 U/mL [Fig. 9(c)] was the best inducer followed by soya bean and maize oil. The best lipase production (75.54 U/mL lipase activity) was obtained with 1.5% tryptone [Fig. 9(d)] as organic nitrogen supplement. However, all the inorganic nitrogen sources resulted in the reduction of bacterial growth as well as lipase

production. Also, as shown in Fig. 9(e) cotton oil used at the concentration of 1% (v/v) and tryptone with concentration of 1.5% (w/v) stimulated lipase activity. Using optimized conditions the maximum lipase activity of 79.54 U/ml was observed on 2nd day with cell mass of 16.571 (including dilution factor) absorbance at 600 nm (assay done using pH STAT method. On 3rd day decline in lipase activity as well as growth was observed (Fig. 10). The decrease of lipase production and growth of the bacterial cells at the later stage could be possibly due to pH inactivation, proteolysis, or both.

2.3. Purification of solvent tolerant lipase DMVR46

The extracellular lipase secreted by DMVR46 was purified by acetone precipitation and DEAE-Cellulose anion-exchange chromatography. About 28.95 fold purification with 29.74% yield was achieved (Table 2.2). Silver staining and activity staining of the partially purified lipase fraction revealed that lipase migrated as a single high molecular weight single band on SDS-PAGE (Fig. 11). The purified lipase was homogenous and its molecular mass was estimated to be ~32.0kDa.

Table 2.2: Purification of lipase produced by *Pseudomonas* sp. DMVR46

Purification Steps	Total activity (Units)	Total protein (mg)	Specific activity (U/mg)	Fold purification	Yield (%)
Crude enzyme	3951	1764.5	2.23	1	100
Acetone precipitation	2780.4	112.5	24.71	11.08	70.37
DEAE - Cellulose	1175.3	18.2	64.57	28.95	29.74

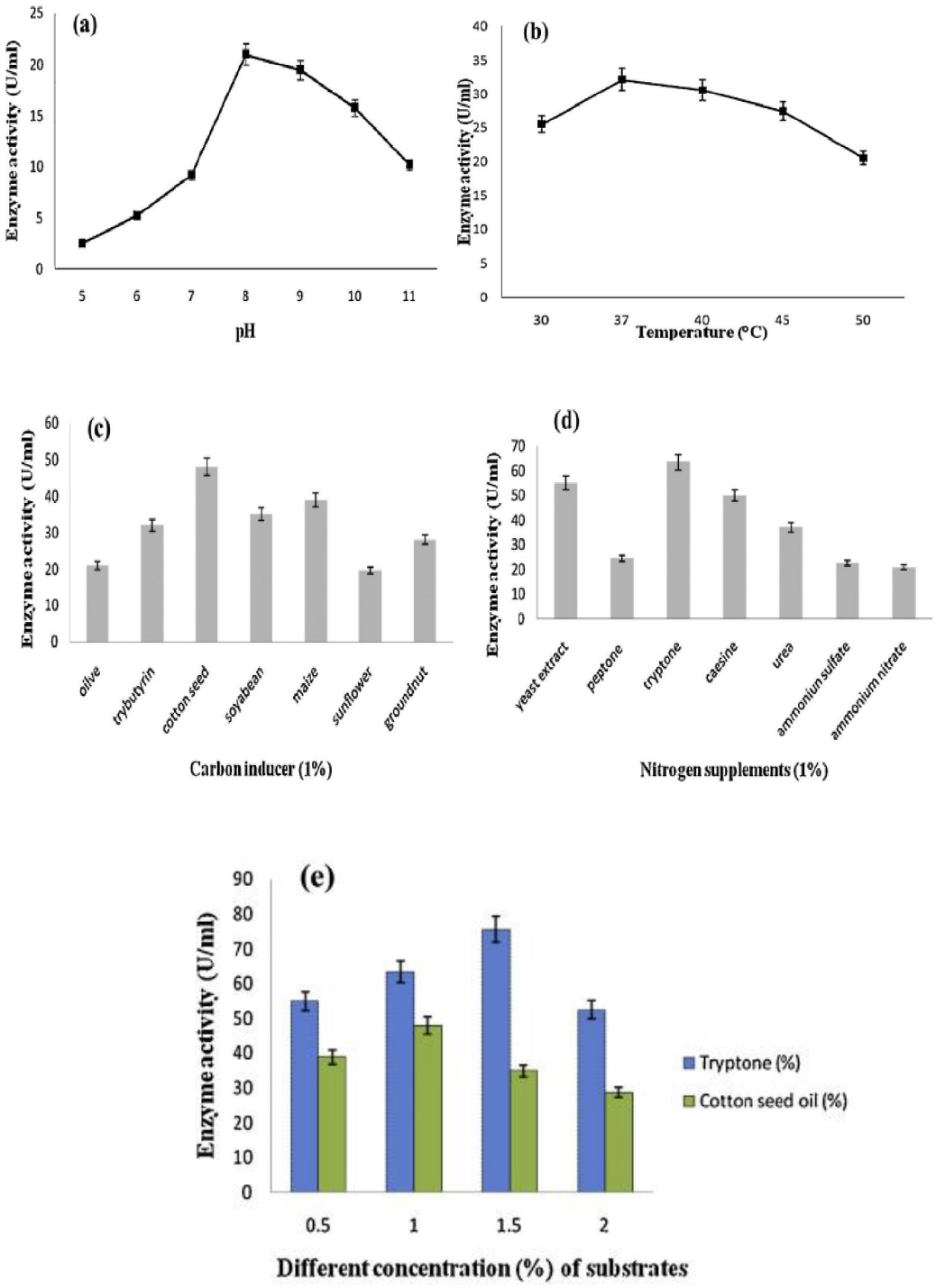

Figure 9: Effect of (a) pH, (b) temperature, (c) carbon inducer, (d) nitrogen supplements, (e) different substrate i.e. tryptone (%) and cotton seed oil (%) concentration on lipase production by DMVR46

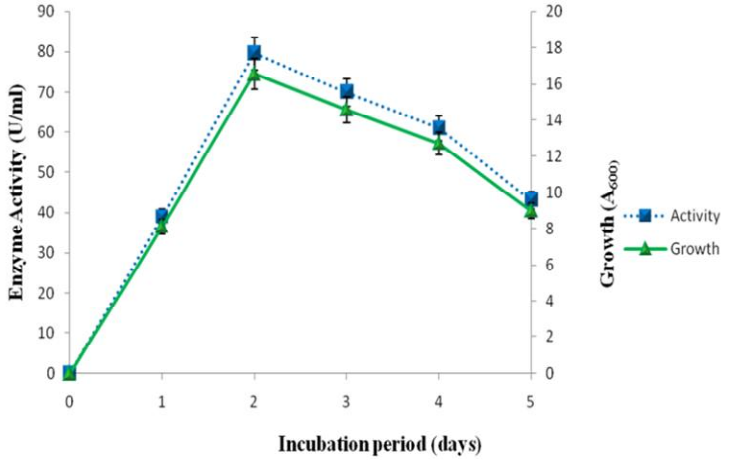

Figure 10: Profile of lipase produced by *Pseudomonas* sp. DMVR46. The production was carried out at 37°C under shaking condition (150rpm) in presence of cotton seed oil with pH 8

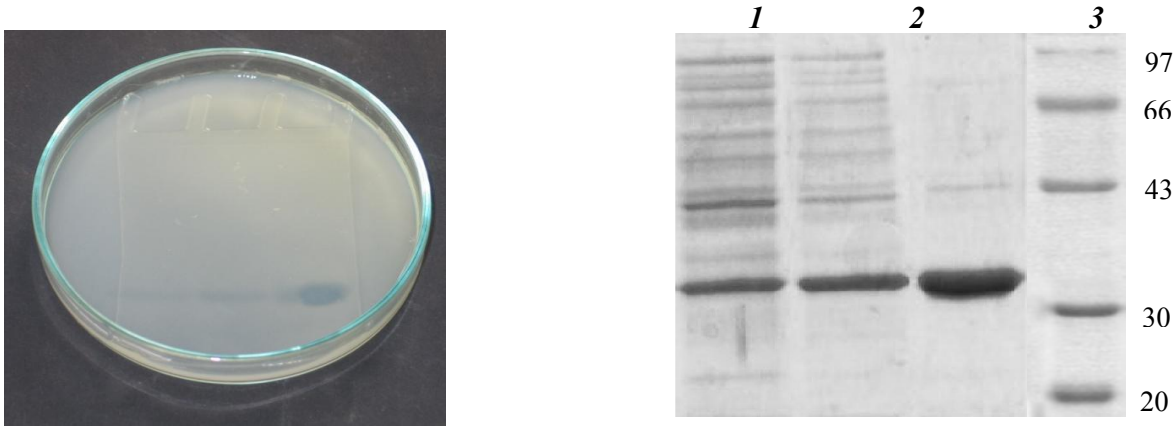

Figure 11: SDS-PAGE of lipase DMVR46 at different stages of purification. Lane M: protein marker; Lane 1: Supernatant; Lane 2: Lipase concentrated by acetone precipitation; Lane 3: Lipase purified by DEAE-Cellulose

2.4 Characterization of purified lipase

The optimum pH for purified lipase was found to be 8.5 (Fig. 12) and it retained 100% of its maximum activity, while remarkable drop was obtained below pH 8.0 and above pH 9.0 indicating alkaline nature of enzyme. The optimum temperature for lipase activity was observed to be 37°C as indicated in Fig. 13(a). The trend for thermal stability of purified lipase on different temperature is shown in Fig. 13(b). Lipase DMVR46 retained approximately 68% of its initial activity at 37°C when incubated for 4h. With increase in

temperature, at 40°C enzyme retained only 28% of initial activity, while at 50°C enzyme was drastically inactivated as shown in Fig. 13(b).

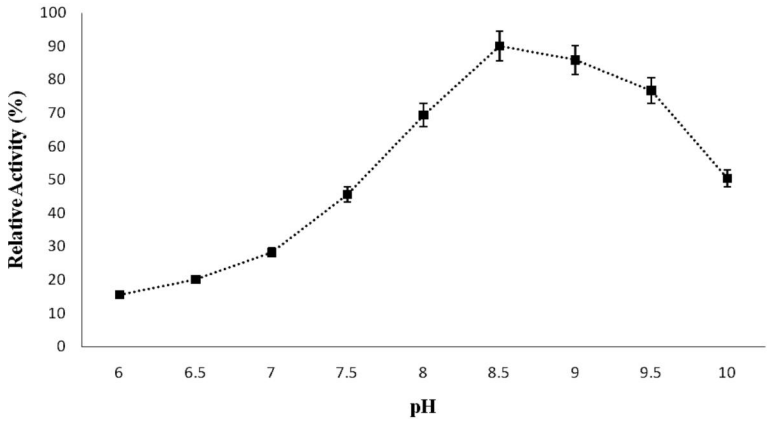

Figure 12: Effect of pH on activity of lipase obtained from purified *Pseudomonas* sp. DMVR46. The enzyme was added to various buffer systems (pH 6.0 to 10.0) of 50mM at 37°C for 30min. The buffer systems used were pH 6.0-8.5 sodium phosphate buffer and pH 9.0-10.0 Glycine–NaOH buffer

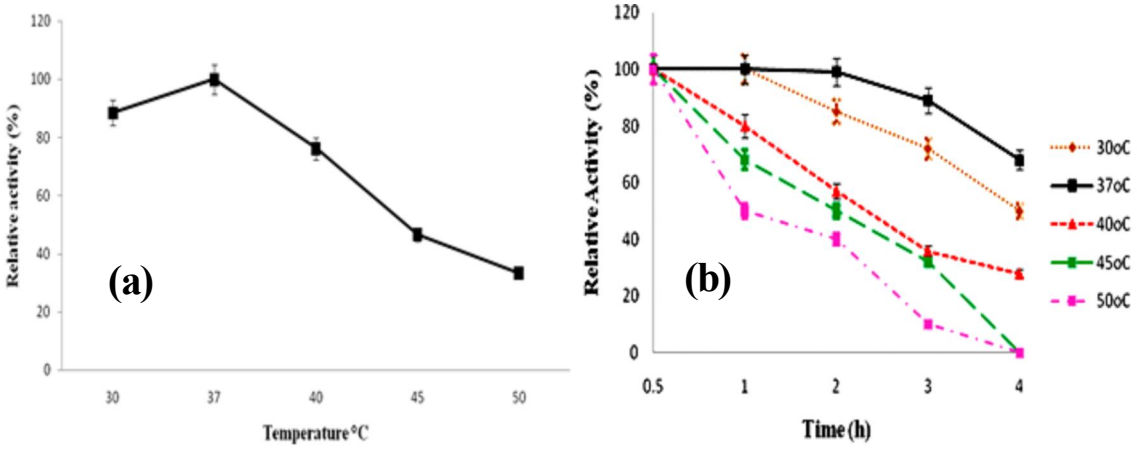

Figure 13: (a) Temperature profile of purified DMVR46 lipase. The effect of temperature on lipase activity was studied by carrying out the enzyme reaction at different temperature in the range of 30-50°C at pH 8.5 using sodium phosphate buffer (50mM).The reaction was carried out for 4h. (b) Thermal stability of purified lipase was measured by incubating the lipase in 50mM sodium phosphate buffer (pH 8.5) at 30°C, 37°C, 40°C, 45°C and 50°C for 4 h. Residual lipase activity (%) was calculated relative to the initial activity

The substrate specificity of purified lipase was resolved by testing the lipolytic activities against p-nitrophenyl fatty acid esters according to the spectrophotometric method. The affinity for hydrolytic activity of enzyme towards substrate is evident from Fig. 14. The result signifies higher hydrolytic activity for long chain substrate (p-nitrophenyl

palmitate) p-NPP; this can be clarified in the terms of lipase structure. Lipases exist in two forms, closed (inactive) and open (active) forms. *Pseudomonas sp.* lipase has been characterized of lacking interfacial activation and 'lid' in contrast to most of other lipases. The CMC (critical micelle concentration) values for different substrates were found to be (p-nitrophenyl butyrate) p-NPB 200µM, (p-nitrophenyl caprylate) p-NPC 5µM, (p-nitrophenyl laurate) p-NPL 100µM, p-NPP 50µM and (p-nitrophenyl stearate) p-NPS 20µM. Thus, from the results it can be concluded that i) no interfacial activation was noted with short and moderate chain substrates, while activation was observed at point using substrate of long chain (p-NPP) and ii) the lack of interfacial activation of lipases could be caused not only by the structural features of the enzyme but also by very low CMC values of the substrate.

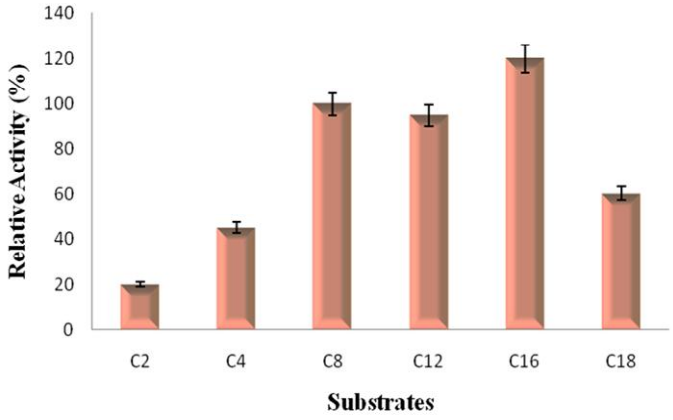

Figure 14: Substrate specificity of purified DMVR46 lipase against various fatty acid esters. The activity of lipase towards different p-nitrophenyl esters were determined and calculated relative to the maximum activity measured towards p-nitrophenyl caprylate (taken as 100%)

Among the tested metal ions Ca^{+2}, Mg^{+2} and Ba^{+2} significantly stimulate activity while Zn^{+2} and Co^{+2} sturdily inhibit lipase activity (Table 2.3). Many lipases have been found to display enhanced activity in the presence of Ca^{+2}. The presence of Ca^{+2}, Ba^{+2} and Mg^{+2} boost up lipase activity owing to binding of metal complex to the active site of the enzyme which leads to the conformational changes in protein. Alternatively, Ca^{+2} might complex with fatty acids produced during catalysis eliminating the possibility of product inhibition.

The chelating agent EDTA drastically reduces lipase activity signifying that purified lipase may be a metalloenzyme, whereas in presence of disulphide reducing agent β-mercaptoethanol minor decrease in activity was observed (Table 2.3). PMSF, a serine inhibitor has a marginal effect on DMVR46 lipase at 10mM concentration exhibiting 95% of relative lipase activity. This may be ascribed to the fact that the catalytic serine residue is inaccessible owing to the presence of lid covering the active site which is a characteristic feature for most of the lipases.

Table 2.3: Effect of various metal ions, inhibitors and surfactants on DMVR46[a] lipase activity at pH 8.5 and 37°C

Metal ions	Relative lipase activity (%)
Control [b]	100
Ca^{+2}	135.1
Mg^{+2}	119.4
Fe^{+2}	98.3
Co^{+2}	7.7
Zn^{+2}	3.6
Ba^{+2}	110.3
EDTA	40.44
2- mercaptoethanol	98.89
PMSF	95.7
Iodoacetate	36.12
SDS*	80.65
Triton X-100*	137.5
Tween 20*	92.49
Tween 80*	96.39
CTAB*	12.5

[a] Lipase DMVR46 was incubated with various metals, inhibitors (10mM) and detergents (0.5%) with the superscript * in 50mM sodium phosphate buffer (pH 8.5) at 37°C for 30 min.
[b] Lipase activity is shown as value relative to the initial activity without addition of effectors (Control).

Surfactants facilitate access of substrate to the enzyme by reducing the interfacial tension between oil and water increasing the lipid-water interfacial area where catalytic reactions takes place. Non-ionic detergent Triton X-100 enthused lipase activity (Table 2.3). Whereas, Tween 80 has modest influence on lipase activity by reducing it, while anionic surfactant sodium dodecyl sulphate (SDS) showed 20% decrease in activity. Cationic

surfactant (CTAB) completely inactivated the enzyme, as CTAB has been thought to destroy the conformation of lipase.

Table 2.4: Organic solvent stability of *Pseudomonas* sp. DMVR46 lipase at pH 8.5 and 37°C

Organic solvents (25%)	Log P	Relative lipase activity (%)
Control	-	100
Methanol	-0.76	8.90
Ethanol	-0.24	30.5
Butanol	0.89	0
Iso-propanol	0.28	40.8
Toluene	2.64	0
Acetone	-0.23	45.23
Iso-octane	4.7	120.41
Cyclohexane	3.2	80.52
n-Hexane	3.5	78.98
Chloroform	2.0	0

`Note: Data are means of triplicate determinations. The purified enzyme and organic solvents were mixed in a 3:1 ratio, and the mixture was incubated at 37°C with shaking at 150rpm for 4h and assayed for lipase activity. Activities of DMVR46 in presence of various organic solvents are shown as a value relative to those in the absence of organic solvent (Control).

High activity and stability of lipases in organic solvents is considered as novel attributes. Effects of different organic solvents (25%) on the stability of *Pseudomonas* sp. DMVR46 lipase are revealed in Table 2.4. The enzyme was found to be quite stable and active in most of the organic solvents. The highest stability was achieved in isooctane, cyclohexane and n-hexane with the relative lipase activity of 120%, 80% and 78% respectively after 4 hour. The activation of lipase could be elucidated by the interaction of organic solvents with hydrophobic amino residues present in the lid that covers the catalytic site of the enzyme, thereby maintaining the lipase in its open conformation. When organic solvents such as toluene, butanol and chloroform was added to purified lipase solution and incubated for 1 hour, the enzyme got drastically inactivated. The probable cause for this can be ascribed to the incubation of enzyme in polar solvents (Log P values < 3.0), removing water molecules essential for its catalytic function which leads to diminish in activity of enzyme. The results suggested DMVR46 lipase exhibited fairly good stability, retaining more than 70% of its activity in presence of organic solvents

with Log P value of 3.00 or higher. The reasonably elevated stability of DMVR46 lipase in organic solvents makes it potentially useful for practical application in many synthetic reactions in non-conventional media.

2.5 Adsorption of purified lipase DMVR46 onto functionalized multiwalled carbon nanotubes: Characterization and application in non-aqueous biocatalysis

Immobilization of the enzyme has been granted as an imperative cornerstone to cover the way for enzyme technology from lab curiosity to industrially viable process. In principle, the carriers for enzyme immobilization should be chemically stable and inert to microbiological contamination.

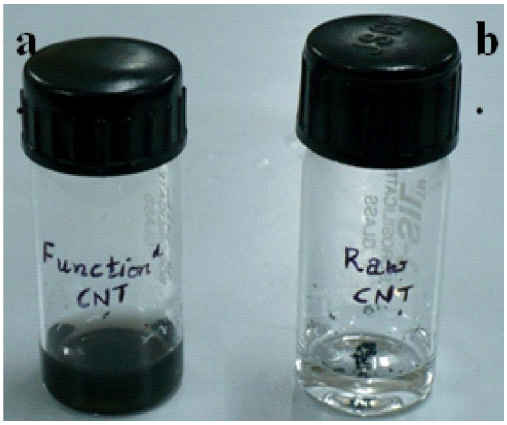

Figure 15: (a) Functionalized carbon nanotubes (b) pristine carbon nanotubes

In the present work, -COOH functional groups were introduced onto the surface of MWCNTs through carboxylation (Fig. 15). The resulting surface functionalized MWCNTs were employed for lipase immobilization with *Pseudomonas sp.* lipase DMVR46 having molecular weight of close to 32kDa, employed as a model enzyme and assessed for immobilization efficiency, specific activity, ester synthesis and stability studies (Fig. 16) Immobilization yield (%) calculated from the protein content in free lipase against protein in supernatant after immobilization was about 81% with equivalent binding efficiency of enzyme. Moreover, recovered enzyme activity and specific activity for immobilized lipase was also calculated and found to be 2.145 U/mL (recovered enzyme activity) and 9.53 U/mg MWCNTs (specific activity), respectively. The surface-

functionalization was confirmed and characterized by FTIR and TEM analysis where the corresponding details are described in the following sections.

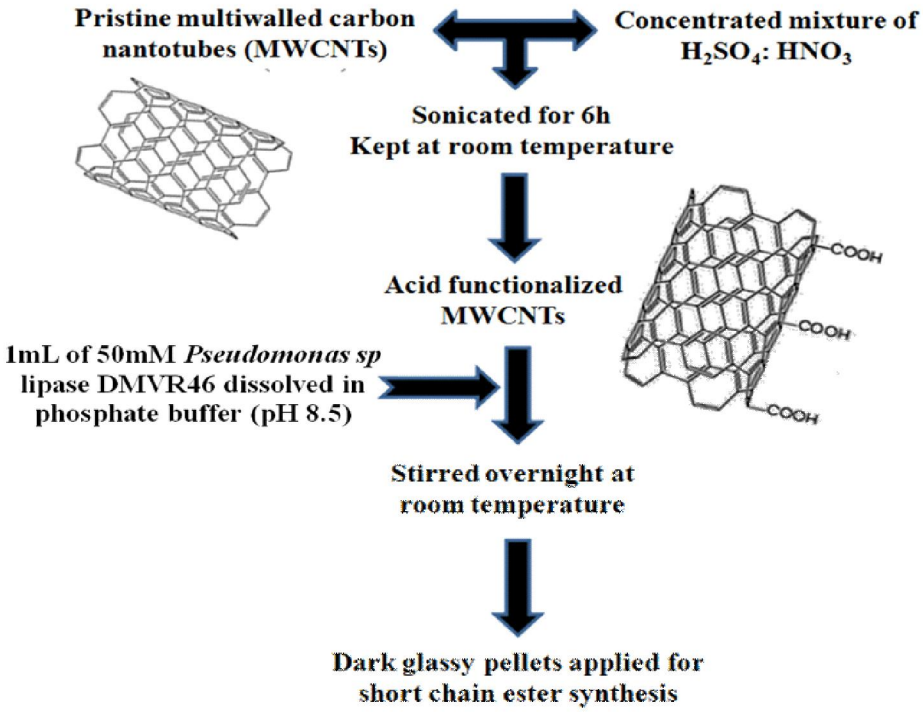

Figure 16: General scheme for acid functionalization of multi-walled carbon nanotubes (f-MWCNTs) and immobilization for solvent tolerant lipase

2.5.1 Characterization of functionalized MWCNTs: Morphological and chemical properties

FTIR characterization

To confirm the occurrence and alterations of functional groups on the surface of MWCNTs due to carboxylation, FTIR analysis was employed and the related spectrums are demonstrated in Fig. 17. As it can be seen from Fig. 17, the IR spectrum of raw MWCNT (Fig. 17(A)) showed weak absorption at ~3430 cm^{-1} (possibly due to adsorbed water), additionally no other peak was observed in the spectra indicating the absence of functional groups. The spectrum of f-MWCNT (Fig. 17(B)) showed weak absorption at around 2926 cm^{-1} which can be attributed to stretching vibrations of alkyl groups [Ma et al., 2006]. Moreover, peak at 3435cm^{-1} traced to OH stretching and a significant absorption at 1634 cm^{-1} assigned to C=O stretching suggest the carboxylation of MWCNTs. In spectra Fig. 17(C), as lipase is a protein, the adsorption at 1638cm^{-1} is

possibly due to C=O stretching of the amide moieties present in protein. Additionally, the peak at 1122cm^{-1} in lipase may be assigned to C-N stretching. Interestingly, the spectrum of carboxylated MWCNTs with immobilized lipase (Fig. 17(D)) showed all the prominent peaks of lipase and carboxyl group. The absorption at 3385cm^{-1} became stronger, possibly due to the contribution from both OH and NH groups. The stretching of CO at 1638cm^{-1} is shifted to 1643cm^{-1} indicates the interaction with 'N' of the amide group increasing the CO stretching frequency. The peaks of 1563 cm^{-1} and 1413 cm^{-1} in spectrum D may be due to trace of asymmetric and symmetric stretching of C=O moieties. Also, it is important to notice that some functional groups such as NH and OH groups may overlap. Furthermore, the broad absorption band at 3434 cm^{-1} is due to O-H stretching, vibration and presence of carboxylic groups. While, the same adsorption band is shifted to 3385 cm^{-1} in immobilized lipase. The simultaneous shifting and peak broadening at 1643 cm^{-1} in the spectrum of immobilized lipase clearly shows the utilization of the intermediate groups for the stable bond formation.

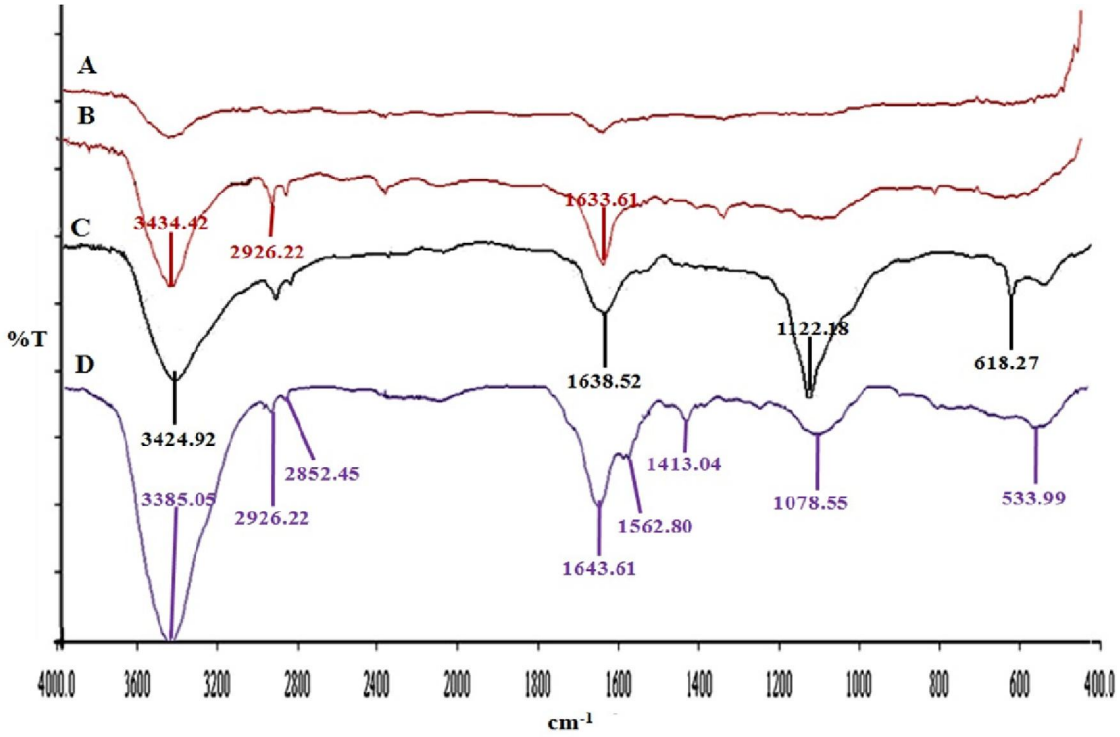

Figure 17: FTIR overlay for (A) pristine MWCNTs (absence of functional groups) (B) carboxylation of MWCNTs (f-MWCNT) (C) *Pseudomonas* sp. lipase and (D) lipase immobilized on functionalized MWCNTs

Imaging analysis of immobilized lipase on functionalized MWCNTs by TEM

In this work, the size and morphology of functionalized MWCNTs with and without immobilized lipase were scrutinized by Transmission Electron Microscopy (TEM) (Fig. 18a and 18b). Carboxylation of nanotubes resulted in highly jagged surface with the diameter of 28nm. Prolonged exposure to concentrated acid resulted in oxidation of carbon atoms rendering the surface accessible for chemical and biological reactions. A slight increment in the diameter of f-MWCNT was observed after immobilization of lipase. A higher roughness with the immobilization of lipase and the presence of visible bud-like projections might be the adsorbed enzymes.

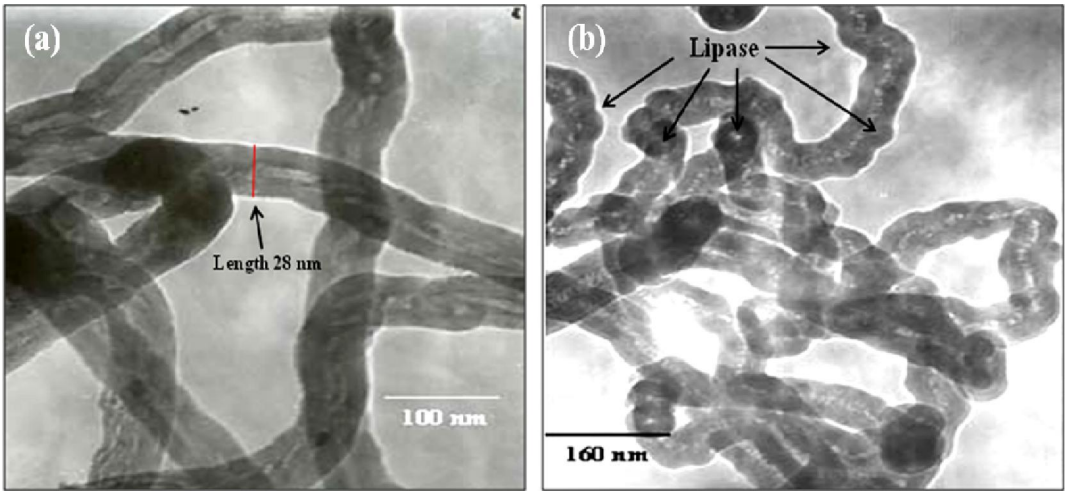

Figure 18: TEM analysis of (a) functionalized MWCNTs and (b) lipase immobilized with bud like projections on surface of f-MWCNT

2.5.2 Optimization of experimental parameters for enhanced ester synthesis

Effect of organic solvents and its stability on immobilized lipase

Organic solvent plays key role for any enzymatic transformation which significantly influence the catalytic power of enzyme. The most important criteria for solvent selection in biocatalysis are a high substrate and product recovery, biocompatibility, chemical and thermal stability, non-biodegradability, non-hazardous nature and low cost. The most commonly used parameter to classify solvents in terms of biocompatibility is the Log*P* value, which is defined as the partition coefficient of a given compound in a two-phase *n*-octanol and water system. In current study, a series of organic solvents

covering a wide range of Log*P* values was selected and results are revealed in Fig. 19(a). The results proposed that non-polar solvents have good compatibility with enzyme molecule in contrast to that of polar solvents. Higher rate of esterification was noticed with n-heptane and n-hexane where immobilized lipase illustrated 74% and 68% ester synthesis while free lipase exhibited only 52% and 48% ester formation, respectively. The higher rate of esterification could be attributed to the effect of solvent on the enzyme performance influenced by the bulkiness and hydrophobicity of solvent.

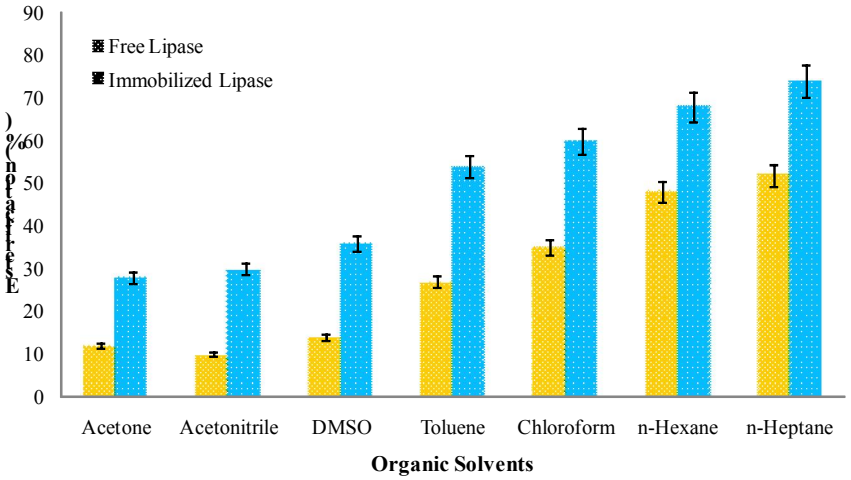

Figure 19(a): Effect of different organic solvents on synthesis of ethyl butyrate. Reaction conditions: ethanol (0.1M), butyric acid (0.1M), 150rpm, pH 8.5, temperature (37ºC), time (24h)

Polar solvents like acetonitrile and DMSO were too sluggish to give only 36% of conversion with immobilized lipase. The hydrophilic solvent may deactivate the enzyme in the way of disrupting the functional structure of enzyme or stripping off the essential water from the enzyme. This alters the native conformation of lipase by disturbing hydrogen bonding and hydrophobic interactions. As a consequence, the catalytic activity of enzyme was decreased due to the lack of bound water to preserve the enzyme conformation flexibility. This structural mobility is necessary for its catalytic action.

The stability of immobilized lipase was studied in different organic solvent by measuring the residual activity versus time as demonstrated in Fig. 19(b). The solvent stability study explained that immobilized lipase have improved stability in the non-polar solvents such

as n-heptane, n-hexane and toluene which gave the almost 95%, 93% and 68% of residual activity after the 96h at 40ºC, respectively. While in case of the polar solvents such as DMSO, acetonitrile and acetone activity was reduced to almost 50%, 45% and 30%, respectively. The results clearly specify that non-polar solvents have good compatibility with enzymes in comparison to that of polar ones, as stripping of water layer around the enzyme is not possible in case of non-polar solvents. These results are in good agreement with many reports where non-polar organic solvents illustrated enhanced stability for the enzymes.

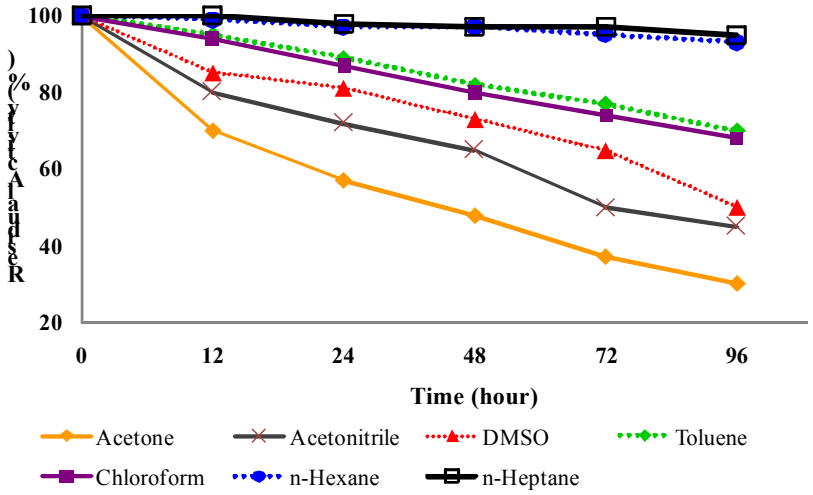

Figure 19(b): Effect of organic solvent on the stability of immobilized lipase. Reaction conditions: ethanol (0.1M), butyric acid (0.1M), 150rpm, pH 8.5, temperature (37ºC), time (96h)

Effect of temperature

The reaction temperature is a crucial factor which helps to augment the catalytic interaction with the substrate, diminish the viscosity of reaction medium and improves the solubility of reactant/substrate in reaction media. The effect of reaction temperature on the enzymatic synthesis of ethyl butyrate was investigated over a range from 20°C to 50°C. As shown in Fig. 20 it was examined that initial rate of synthesis increases linearly with the increase in temperature from 20°C to 40°C. The activity of lipase reached the maximum of 78% for immobilized lipase and 58% for free lipase at 40°C in 72h. However, further rise in temperature beyond 40°C resulted in a rapid loss of enzyme stability pulling down the reaction yield. Indeed, above a certain temperature, enzyme

inactivation occurs, and the stability decreases. This is due to (i) the partial inactivation of the enzyme in organic solvent at high temperature for a long time because protein undergoes partial unfolding by heat-induced destruction of non-covalent interactions (ii) increase in temperature may alter confirmation of lipase resulting in decreased activity and stability. The results clearly showed that immobilized enzyme possesses better stability up to 40°C. Thus, 40°C was considered to be optimum temperature for the corresponding biotransformation and used for further experiments.

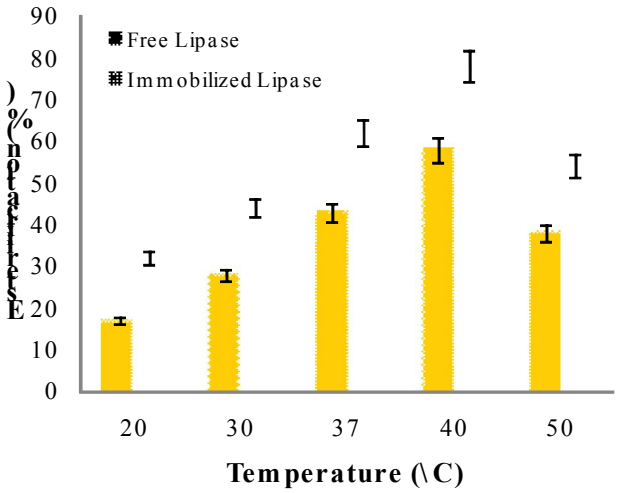

Figure 20: Effect of temperature on ester synthesis. Reaction conditions: ethanol (0.1M), butyric acid (0.1M), n-heptane (20mL), 150rpm, pH 8.5, time (24h)

Effect of agitation

In immobilized catalysts, reactants have to pass from the bulk liquid phase to the enzyme particle's surface, and then diffuse from the external surface to the enzyme active site. The external mass transfer resistance and intraparticle diffusion rate play significant roles during the reaction. Thus, it is essential to ensure the effect of mass transfer in the solid liquid system where both substrates are in liquid phase while the polymer supported biocatalyst is in the solid form. Several experiments were performed in the range of 50 to 200 rpm by taking 0.1 M ethanol and butyric acid each at 40°C using n-heptane as solvent. It can be clearly seen from the results flaunted in Fig. 21 at increase in speed of agitation exerted ester production upto 78% from 0 to 150 rpm and later remains almost constant with increase in agitation speed from 150 to 200 rpm. The result conveys that, for this system, shaking at 150 rpm is optimum for transporting the substrates to the

enzyme at the same time sufficient enough for moving out the product from the site as well. This clearly indicates that there was no significant effect of external mass transfer diffusion when rotation speed increased from 150 to 200 rpm for corresponding system in an orbital shaker.

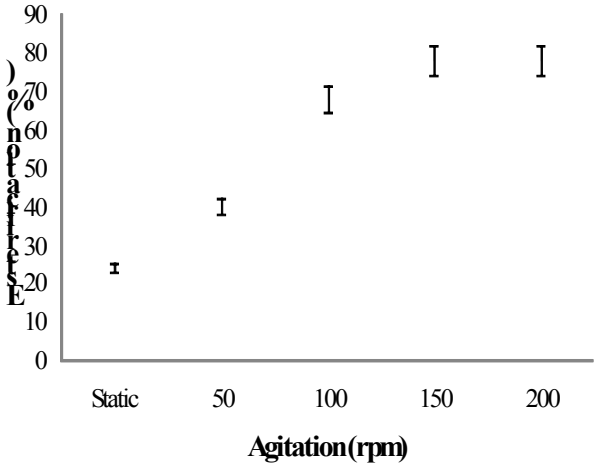

Figure 21: Influence of agitation on esterification. Reaction conditions: ethanol (0.1M), butyric acid (0.1M), n-heptane (20mL), 150rpm, pH 8.5, temperature (40°C), time (24h)

Substrate molar ratio

In order to determine the optimum ratio of the substrates, the concentrations of ethanol and butyric acid were varied one at a time keeping the other constant and carrying out esterification reaction. In one set of experiment the ethanol concentration was kept constant at 0.1M varying butyric acid concentration. The utmost amount of ester (80%) was produced with 0.2M of butyric acid at 40°C, pH 8.5 in 48h (Fig 22). Also, when concentration of acid was further increased beyond 0.2M, the ester production was adversely influenced. When the same experiment was replicated keeping butyric acid concentration constant at 0.2M (obtained from the previous study) and varying ethanol concentration from 0.1-0.25M highest yield was attained at 0.15M concentration with 81% of product formation in 48h (Fig. 22)). The reactions proceeded very quickly at low alcohol content (up to 0.15M) and reached a maximum in 48h while higher concentrations of alcohol exhibited an inhibitory consequence on reaction slowing it down drastically. Thus, the molar ratio of butyric acid to ethanol was found to be

0.2:0.15M corresponding to maximum esterification of 81% with absolute utilization of both substrates.

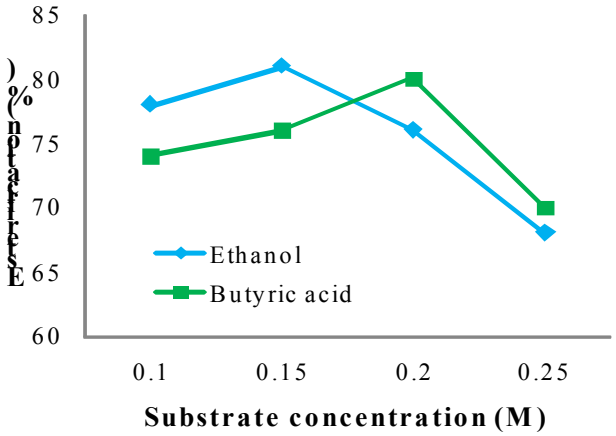

Figure 22: Influence of substrate molar ratio concentration on ester production. Reaction conditions: ethanol (0.1-0.25M), butyric acid (0.1-0.25M), n-heptane (20mL), 150rpm, pH 8.5, temperature (40°C), time (24h), 150 rpm

2.5.3 Synthesis of ethyl butyrate

Short chain esters are volatile compounds in flavor and fragrance applications in food, beverages, pharmaceuticals and personal care industries. Among them ethyl butyrate has been widely used in the food industry due to its pleasant fruity flavor similar to that of pineapple. The purified lipase immobilized on f-MWCNT was subjected for the synthesis of ethyl butyrate in the presence of n-heptane under optimized condition. It is evident from the results (Fig. 23) that free enzyme catalyzes reaction at a very slow rate, revealing only 47% of conversion in 48h. While, immobilized lipase showed higher ester synthesis (80% in 48h) and remains stable upto 72h under the same condition. This conveys that ample amount of enzyme has been adsorbed on the surface of f-MWCNT, which can be clarified by binding of enzyme molecules on surface of f-MWCNT involving hydrophobic interactions engrossed with active sites leading to conformational change which alters the substrate specificity of the enzyme.

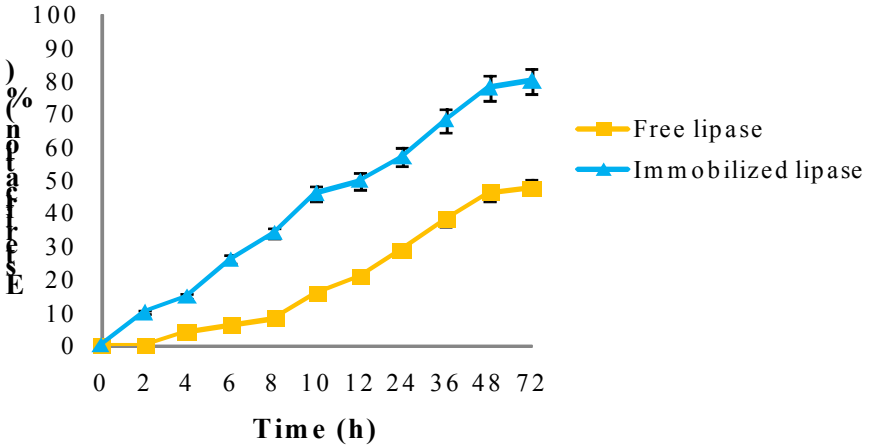

Figure 23: Synthesis of short chain ester ethyl butyrate using free lipase (■) and immobilized lipase (●). Reaction conditions: ethanol (0.15M), butyric acid (0.2M), n-heptane (20mL), 150rpm, pH 8.5, temperature (40°C)

2.5.4 Reusability study

In the present study, immobilized lipase was subjected to reusability examination for determining the efficiency of immobilization. After 48h reaction of each cycle, the immobilized lipase was recovered by centrifugation and regenerated by n-hexane washing and air drying and then subjected to the next reaction cycle by supplementing with fresh substrates. Interestingly, the results existing in Fig. 24 showed that ester synthesis by immobilized lipase was not significantly affected up to 3 cycles retaining 100% of its initial activity. This could be attributed to the better absorption and dispersion of immobilized lipase on surface of f-MWCNT increasing the availability of substrates to the enzyme's active site. Also, the immobilization of lipase has been reported to improve the catalytic activity of enzyme by providing protection against the inhibitory effect of organic solvents. Furthermore, the results in Fig. 24 also depicted that the activity of immobilized lipase starts declining slowly after 3rd cycle. The decrease in the activity of the biocatalyst after 3 consecutive cycles may be due to: (i) accumulation of water formed as a byproduct during the esterification reaction, (ii) inactivation of enzyme molecules by the influence of solvent and (iii) desorption of lipase from the support surface during repeated use. Even though the results showed that lipase immobilized on f-MWCNT can be used successfully in industrial applications requiring long-term reaction stability.

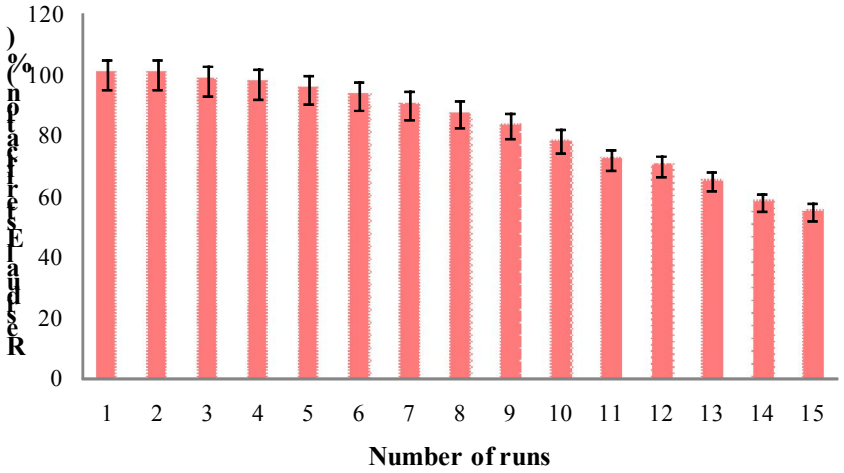

Figure 24: Reusability study for the immobilized lipase. Reaction conditions: ethanol (0.15M), butyric acid (0.2M), n-heptane (20mL), 150rpm, pH 8.5, temperature (40°C), time (48h)

(3) Conjugation of Candida rugosa lipase on exfoliated graphene oxide for catalysis in organic solvent

Present study details the immobilization of *Candida rugosa lipase* onto APTES functionalized exfoliated graphene oxide (EGO) and its application for the synthesis of the flavor ester ethyl caprylate using organic solvent as reaction medium. The schematic representation for functionalization of pristine EGO and immobilization of lipase on functionalized EGO followed by condensation of ethanol and caprylic acid to ethyl caprylate is represented in Fig 25. The study mainly focuses on the effects of immobilization and reaction parameters (enzyme concentration, temperature, substrate molar ratio, organic solvents and its stability, reusability studies) at individual level.

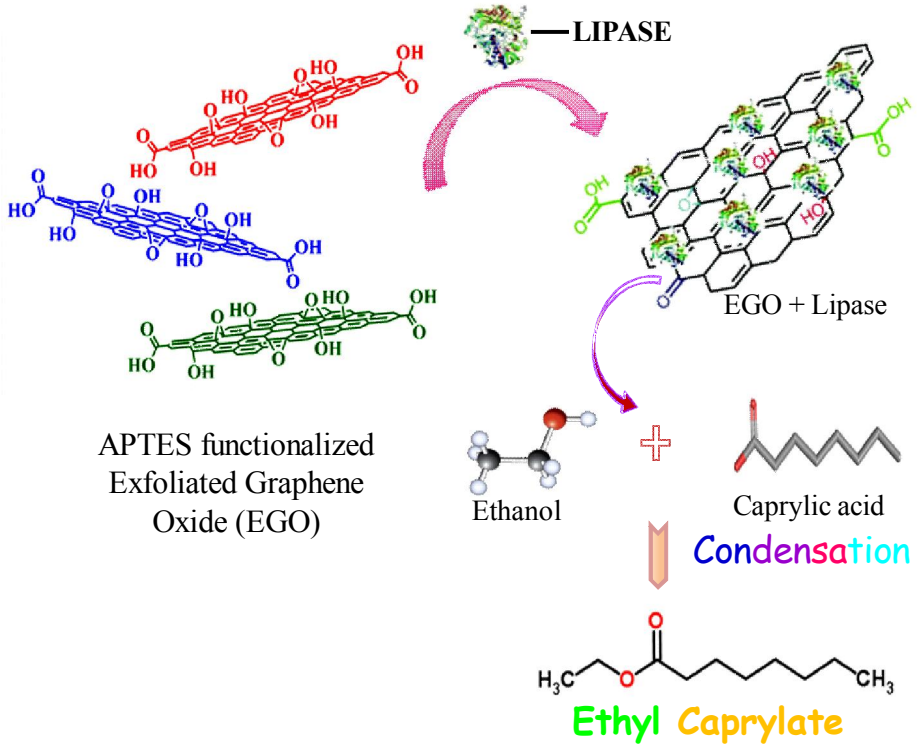

Figure 25: Schematic representation for functionalization of exfoliated graphene oxide followed by immobilization of lipase. Further the prepared nanobioconjugant was utilized for synthesis of ethyl caprylate

3.1 Characterization of functionalized exfoliated graphene oxide (EGO)

3.1.1 Electron microscopy of surface modified exfoliated graphene oxide (EGO)

Figs 26A and 26C exhibit TEM and SEM micrographs of pristine EGO. The distortion seen on the surface is caused by the oxygen groups and extremely small thickness of EGO (less than 3nm) leading to wrinkled topology, with folded features. Oh and his colleagues reported similar folding features of graphene oxide paper prepared from amine functionalized poly(glycidyl methacrylate)/ graphene oxide core shell microspheres. Fig 26B and 26D display TEM and SEM images of APTES functionalized EGO. It can be clearly seen from the figure that EGO gets highly agglomerated due to presence of silane moieties. Contrast of SEM micrographs in Fig 26B and 26D shows crumpled sheet like structure which confirms the covalent functionalization of graphene oxide via APTES. The surface area of modified EGO was found to be in the range of 1100-1200m^2/g.

Immobilization of lipase on functionalized EGO is seen in Fig 26E. The figure demonstrates crystal like agglomerated structure of enzyme (when compared to enzyme as control in Fig 26F) overlapped between the sheets of functionalized EGO. Fig 26E also suggests binding of lipase on the surface of functionalized EGO.

3.1.2 Fourier transform infrared spectroscopy (FTIR) studies of chemically modified exfoliated graphene oxide (EGO)

The FTIR spectra of pristine EGO, APTES-functionalized EGO and lipase immobilized EGO is shown in Fig 27. All the functionalized samples i.e. EGO, EGO+APTES and EGO+APTES+LIPASE showed three weak peaks at 2963.11 cm^{-1}, 2924.76 cm^{-1} and 2852.45 cm^{-1} which can be attributed to C-H stretching vibrations of methylene groups. The second peak is at 1632.68 cm^{-1} which is associated with asymmetric vibrations of C=C. The characteristic band at 573.88 cm^{-1} confirms the presence of epoxy groups complying with deformation vibrations. Furthermore, the broad absorption band at 3434.03 cm^{-1} is due to O-H stretching vibration and presence of carboxylic groups in all the three samples.

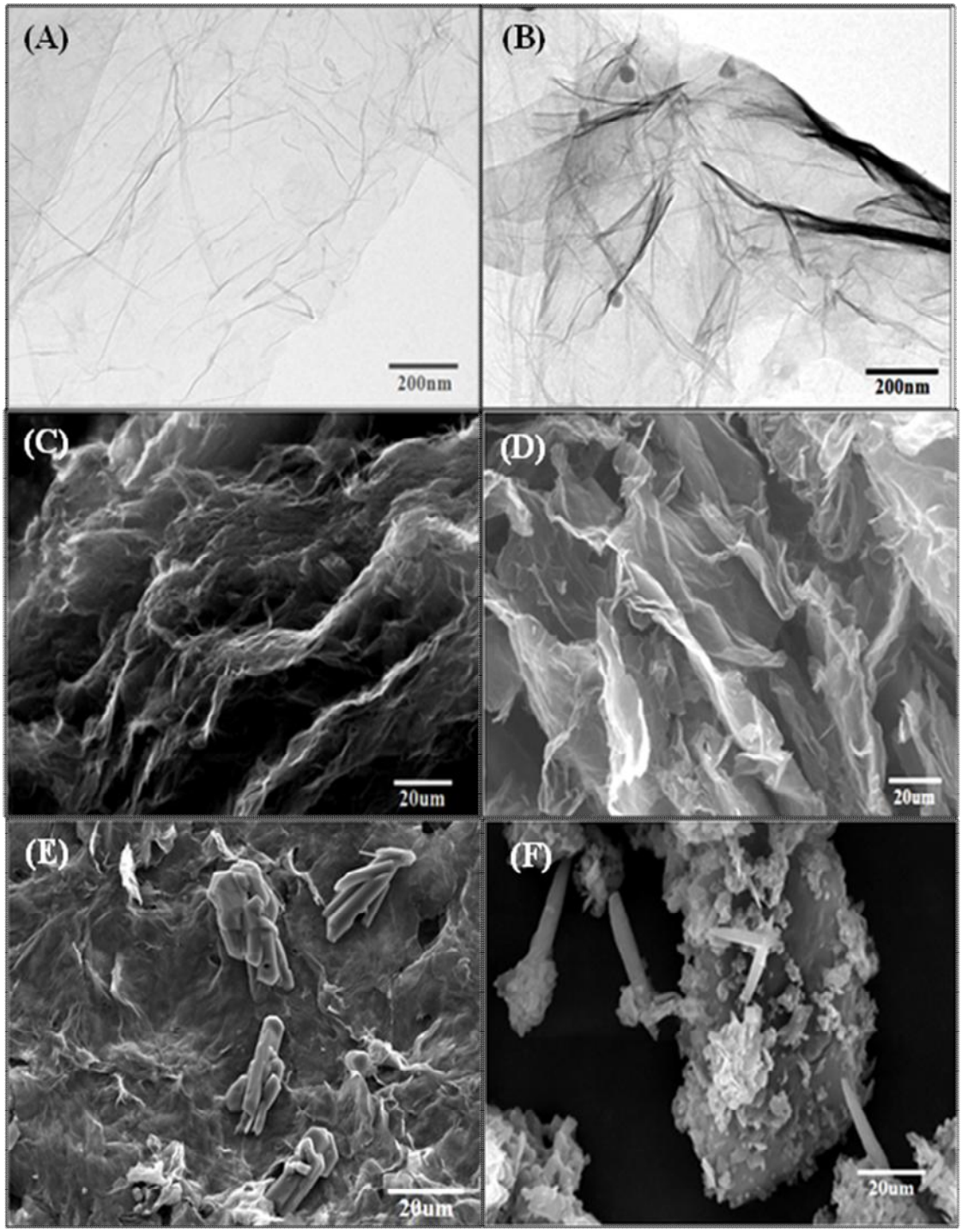

Figure 26: Images of SEM (C, D, E, F) and TEM (A, B). Figure A and C display pristine exfoliated graphene oxide, B and D exhibits APTES treated exfoliated graphene oxide and E demonstrates lipase immobilized on exfoliated graphene oxide while F is control for lipase

In spectra for APTES functionalized EGO, the additional strong and broad absorption peak is observed at 1118.45 cm^{-1} assigning to the formation of Si-O and $SiO-C_2H_5$ groups due to presence of APTES. The appearance of peak 1118.45 cm^{-1} provides more evidence for successful chemical functionalization. The peaks at 1562.80 cm^{-1} and 1413.53 cm^{-1} are attributed to aromatic C=C bond stretching and C-H bending vibration frequencies, respectively. The NH_2 bending mode is distributed amongst two adsorption peaks at 1626.05 cm^{-1} and 1562.80 cm^{-1}. While in lipase immobilized spectra it can be observed that split peak at 1562.80 cm^{-1} and 1626.05 cm^{-1} was replaced by a single peak shifted to 1633.61 cm^{-1}. The peak at 1413.04 cm^{-1} indicates C-N stretching of amide bond. This is supported by peak at 1243 cm^{-1} which is due to the interaction of N-H bending and C-N stretching of amide bond. The spectrum of immobilized lipase in Fig 27 shows successful binding of lipase to functionalized EGO with the disappearance/reduction in intensity of the activating groups, peaks and peak broadening.

3.1.3 Raman spectroscopic studies

In present work, Raman spectroscopy was used in order to collect changes in vibration information occurred during functionalization and enzyme immobilization. Fig 28 shows Raman spectra of exfoliated graphene oxide at each phase of chemical modifications/reactions. A laser excitation of 514 nm was used, and the powdered samples were directly deposited on wafers in the absent of solvent. A Raman spectrum, in Fig 28 refers to (a) pristine exfoliated graphene oxide (EGO), (b) silane functionalized EGO (EGO+APTES), (c) lipase immobilized EGO (EGO+APTES+LIPASE).

In spectrum of EGO the G band peaks at 1597.2 cm^{-1} (Fig 28a) corresponds to the first order scattering of tangential C-C. The second, D peak appears at approximately 1358.95 cm^{-1} (Fig 28a) originating from the disorder in the planar sp^2-hybridized carbon network, which is characteristic of the lattice distortion in the graphene sheets. The strength of this peak is related to the amount of disordered graphite and the degree of conjugation disruption in the graphene sheets. After silanization, both G band and D band were observed to shift at lower frequency (Fig 28b). After APTES treatment G band appears at 1598.33 cm^{-1} while the D band appeared at 1360.60 cm^{-1} (Fig 28b). Ratios of intensities

of the D band/G band have been used as an indicator of the amount of disorder within the sheets. There was no significant change on the intensities of bands after chemical treatment of EGO. The I_D/I_G ratio for EGO was found to be 0.73 indicating mid-order graphitic nature, while the value remained same (0.75) in the case of APTES treatment. For lipase immobilized spectra, in addition to D band and G band a strong peak was observed at 948cm^{-1} (Fig 28c). Raman feature for such spectra often indicates presence of inorganic sulfate compounds.

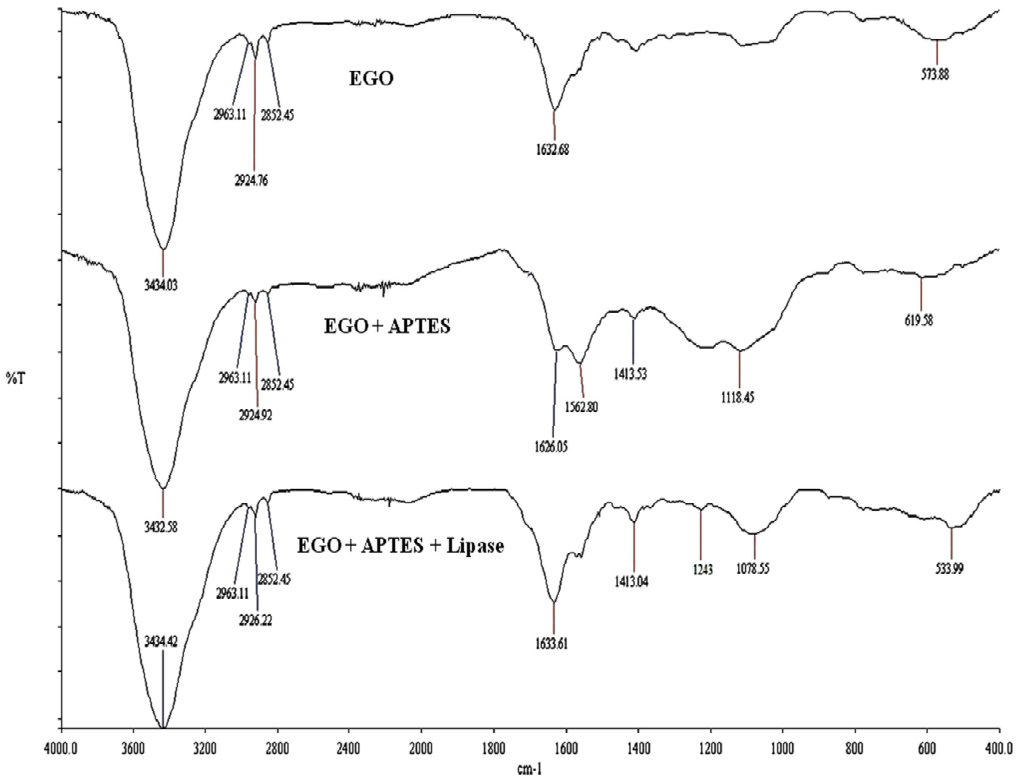

Figure 27: FTIR overlay spectra of pristine EGO, Silane functionalized EGO and lipase immobilized EGO

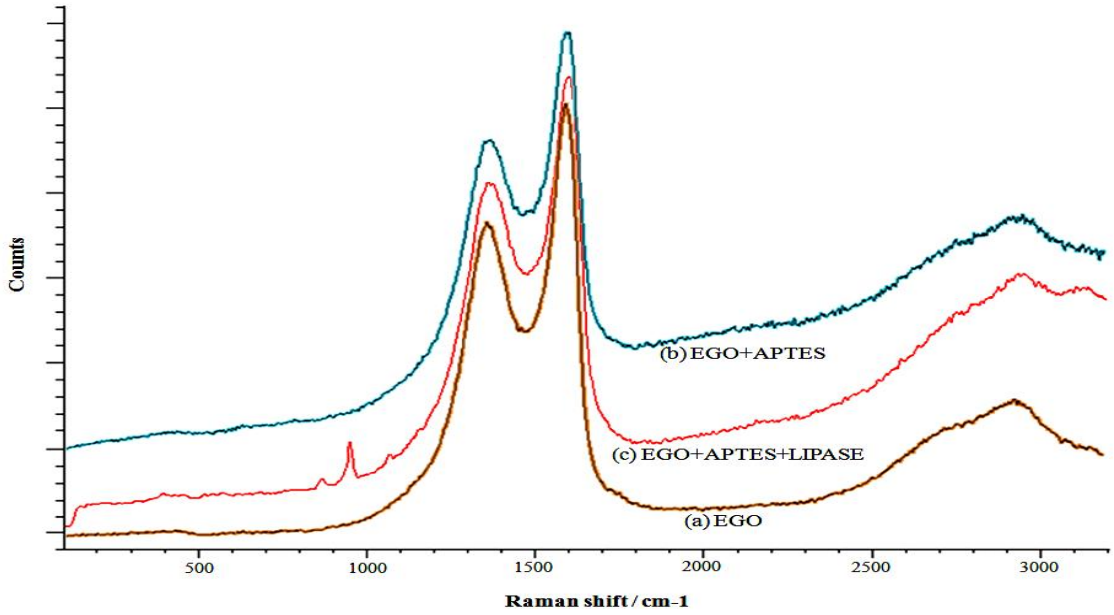

Figure 28: Raman spectra of (a) pristine EGO (b) Silane functionalized EGO and (c) lipase immobilized EGO

3.1.4 Thermo gravimetric analysis

The successful functionalization was also reflected in TGA curves. TGA analysis was performed on as such exfoliated graphene oxide and lipase immobilized EGO using *Mettler Toledo*. Fig 29 shows TGA curves in nitrogen upto 700°C at heating rate of 20°C min^{-1}. It can be observed from the curve that EGO shows very small weight loss below 100°C, but significant weight loss occurs after 400°C due to decomposition of oxygen groups on EGO.

In case of lipase immobilized EGO, nearly 10% of weight loss was observed at around 100°C and steeply decreasing thereafter with much faster rate. This is much obvious due to loss of bound water molecule. This attributes to thermo-decomposition of lipase indicating successful enzyme immobilization on exfoliated graphene oxide.

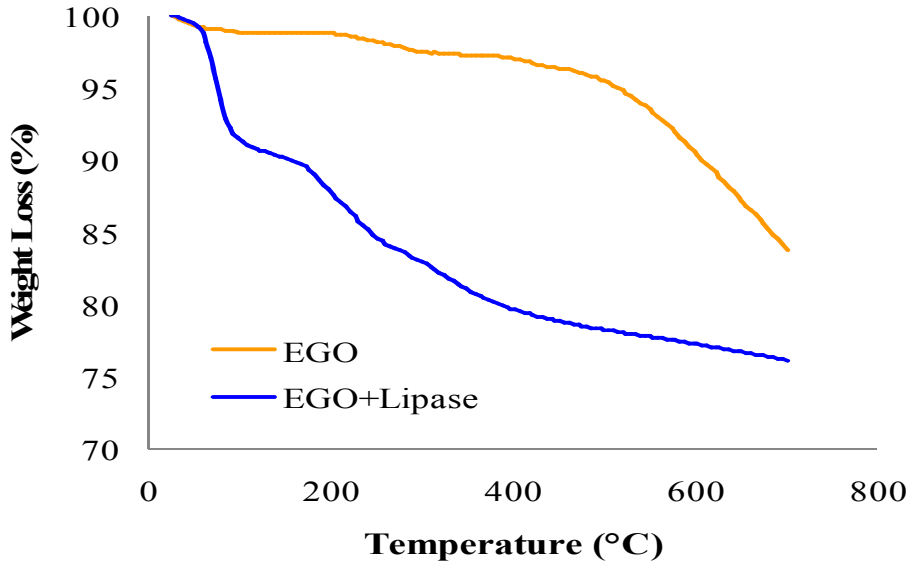

Figure 29: TGA weight loss curves of (a) pristine EGO and (b) lipase immobilized functionalized EGO

3.2 Enzymatic esterification experiments

3.2.1 Effect of enzyme concentration

The amount of enzyme in the biocatalytic reaction system directly affects the product yield. The influence of biocatalyst loading on production of ethyl caprylate was examined by varying enzyme concentration from 5-50mg/mL. As shown in Fig 30, the conversion of the product increased gradually from 12% to 75% when the amount of biocatalyst increases from 5mg/mL to 40mg/mL. However, the conversion of ethyl caprylate decreased slightly when the enzyme concentration was increased up to 50mg/mL. This indicated that for immobilized system, the ester production increases linearly with increase in concentration upto a certain level. Beyond this optimum concentration, further increment in concentration does not contribute to any significant addition in ester production.

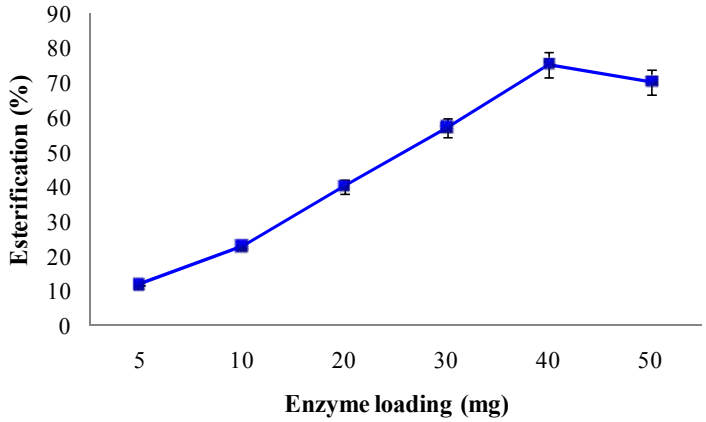

Figure 30: Effect of enzyme concentration on ester synthesis using 2mg of EGO as immobilizing matrix. Reaction condition: 20mL of 0.1M substrate (ethanol and caprylic acid), 0.1M cyclo-octane, 37°C, 150rpm

3.2.2 Effect of temperature

In the present study, the effect of temperature on free and immobilized lipase was carried out at 20, 30, 37, 40, 50 and 60°C which exhibited more or less similar trend for ester production as shown in Fig 31. The activity of lipase (both immobilized and free) significantly increased with increase in temperature from 20 to 40°C, reaching the maximum of 80% for immobilized lipase and 58% for free lipase at 40°C on second day. Further increase in temperature beyond 40°C marginally reduces product formation. This is due to the partial inactivation of the enzyme in organic solvent at high temperature for a long time because enzyme undergoes partial unfolding by heat-induced destruction of non-covalent interactions. For lower temperatures (20°C), immobilized lipase showed low conversions of only 25% and free lipase used as control showed 27% of ester production (Fig 4.9). This suggests that at lower temperatures, the reaction rate is limited by mass transport phenomena. The results acquired in the study present very important aspects for immobilized enzymes: (i) The increment in temperature to 60°C did not exhibited drastic decrease in activity which provides a great deal of option in choosing high temperatures for conversions required for solid/semi solid substrates. (ii) Activity at lower temperatures can be useful aspect while dealing with highly volatile substrates and products having very low boiling point. Thus, the prepared nanobioconjugant of EGO-lipase have an added advantage due to the carrier i.e EGO being highly thermostable at

higher temperature provides robust environment for enzyme linkages. The effect of temperature on affinity of free and immobilized enzyme can be seen in Arrhenius plot (Fig 32).

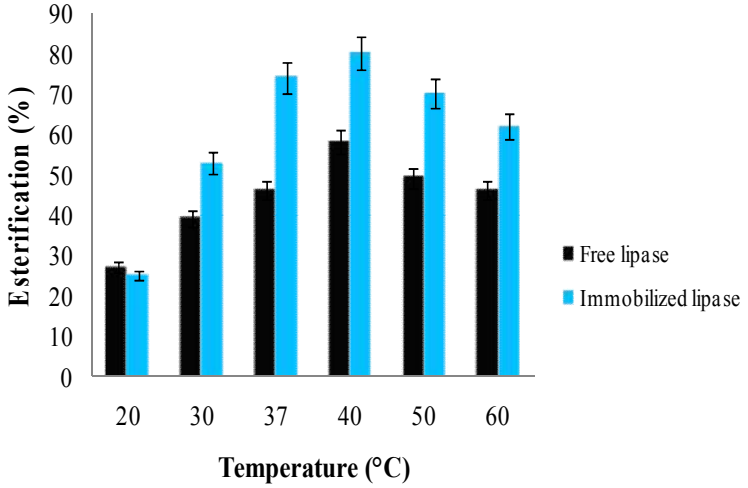

Figure 31: Effect of temperature on free lipase and immobilized lipase at pH 8.5. Reaction conditions: Reaction condition: 40mg/mL of enzyme, 20mL of each 0.1M ethanol and caprylic acid, 0.1M cyclo-octane, 150rpm

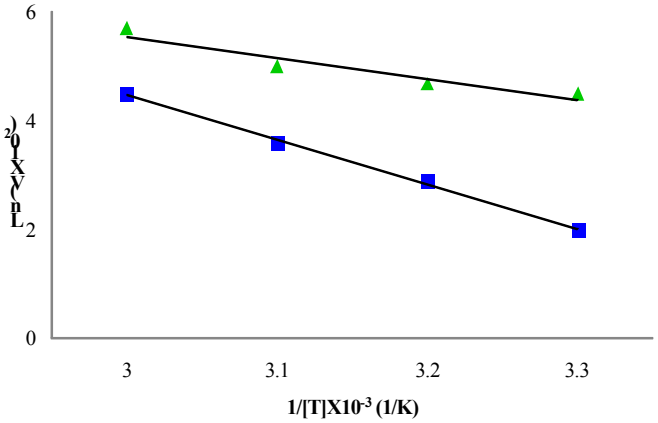

Figure 32: Arrhenius plot for free and immobilized lipase. Activation energies for free lipase (▲) and immobilized lipase (■) were calculated to be 7.2 and 1.48 KJ/mol, respectively

3.2.3 Effect of substrate molar ratio

In order to determine the optimum ratio of the substrates, the concentrations of ethanol and caprylic acid were varied one at a time keeping the other constant and carrying out esterification reaction. In one set of experiment the ethanol concentration was kept

constant at 0.1 M varying caprylic acid concentration. As shown in Fig 33 the maximum amount of ester (83%) was produced with 0.15M of caprylic acid at 40°C, pH 8.5 in 48h. Also, when concentration of caprylic acid was further increased beyond 0.15M, the ester production was adversely affected. When the same experiment was repeated keeping caprylic acid concentration constant at 0.15 M (obtained from the previous study) and varying ethanol concentration from 0.05-0.25M highest yield was obtained at 0.1M concentration with 85% of product formation in 48h. The reactions proceeded very quickly at low alcohol content (up to 0.1 M) and the yield reached maximum in 48h while higher concentrations of alcohol exhibited an inhibitory effect on reaction slowing it down drastically. Maximum esterification rates were observed at a molar ratio ethanol/acid of 0.1/0.15M this is probably the situation where maximum acyl transfer occurs. At higher molar ratios, the large increase in alcohol concentration may promote the binding of alcohol molecules to the lipase, during the first reaction step, competing with the acid. These leads to decrease in the reaction rate, since the reaction will be restricted by the amount of acid in the vicinity of the enzyme. Thus, the molar ratio of caprylic acid to ethanol was found to be 0.15:0.1M corresponding to maximum esterification of 85% with complete utilization of both substrates.

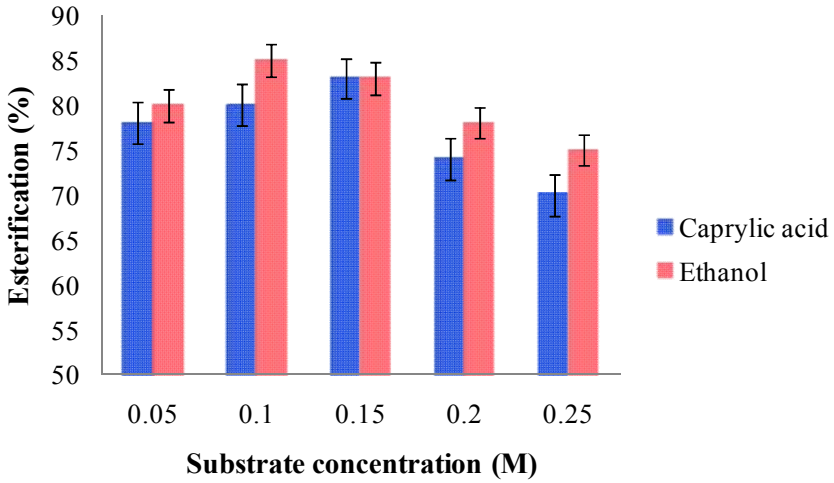

Figure 33: Influence of substrate concentration on the efficiency of ester synthesis where caprylic acid and ethanol concentration was varied from 0.05M-0.25M. Reaction condition: 40mg/mL of enzyme, 20mL of each 0.1M ethanol and caprylic acid, 0.1M cyclo-octane, 40°C, 150rpm.

3.2.4 Effect of organic solvents

Solvents (straight chain and cyclic) such as n-hexane, cyclohexane, n-octane and cyclo-octane were used as reaction medium for synthesis of ethyl caprylate. Among them, the cyclic alkanes were found to be better solvents as reaction medium when compared to straight chain alkanes. Fig 34 shows the effect of different organic solvents on esterification reaction. In this study free and immobilized lipase exhibited highest esterification of 56% and 82%, respectively in the presence of cyclo-octane, followed by cyclohexane showing 46% and 78%, whereas n-hexane and n-octane showed less efficiency. Hence, cyclo-octane was chosen as reaction medium as it fulfills the following important criteria necessary for biocatalytic reaction: (i) is inert or least reactive towards the reaction, (ii) is inert towards the enzyme, conserving enzyme structure and prevent stripping off the essential water molecule from enzyme's vicinity, and (iii) able to efficiently transport the substrates to the active site of enzyme and at the same time carry product away from it. Also it can be clearly seen from Fig 34 that cyclic alkanes were found to be better solvents as reaction medium when compared to that of straight chain alkanes.

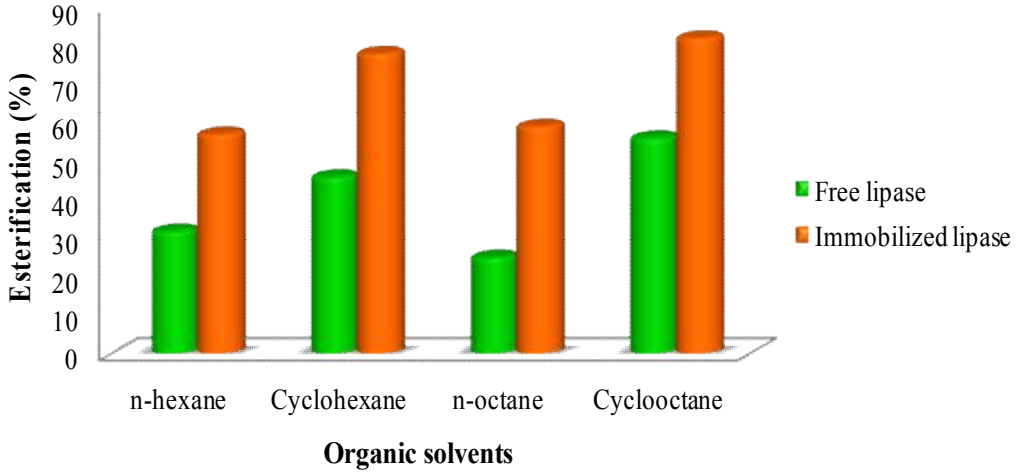

Figure 34: Effects of different organic solvents (n-hexane, cyclohexane n-octane and cyclo-octane as reaction medium on the synthesis of ethyl caprylate. Reaction condition: 40mg/mL of enzyme, 20mL of each 0.1M ethanol and caprylic acid, 40°C, 150rpm and substrate concentration ethanol/caprylic acid: 0.1M/0.15M

3.3 Time course for ester synthesis

The synthesis of ethyl caprylate by free and immobilized lipase was studied using cyclooctane as reaction medium. The experiment was carried out at 0.15:0.1M acid/alcohol molar ratio under optimized conditions. There was no product formation in negative control i.e EGO without lipase. The utmost esterification yield of 85% was observed within 48h when lipase was immobilized on EGO. In contrast to this free lipase exhibited only 62% of ester formation under same condition (Fig 35). The increased esterification of the immobilizing system could be attributed to the "lid" structure of the lipase. It is well known that *Candida rugosa* lipase (CRL) has a lid consisting of 26 amino acids. This lid is pulled back at the interfaces exposing the active site making CRL a highly surface active enzyme. In this work therefore, at the oil-water interface, opening of the lid of CRL must have resulted in a self-catalytic bond formation with the carboxylic groups of EGOs leading to an enhanced immobilization of enzyme compared with that of free. Another possible reason for enhanced ester synthesis in immobilized system is dispersion of enzyme on large surface area of EGOs in a proper orientation where aggregation of the enzyme is prevented leading to high activities as compared to that of free enzyme in organic synthesis.

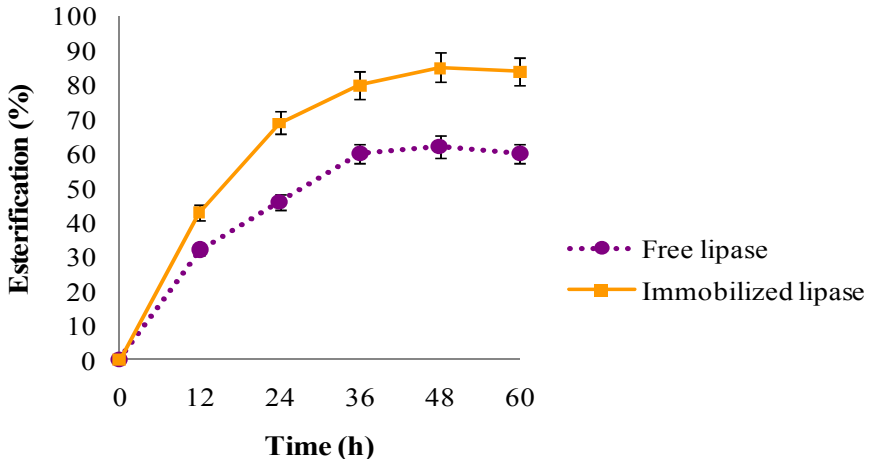

Figure 35: Time course for the synthesis of ethyl caprylate using free as well as immobilized lipase using cyclo-octane as reaction medium. Reaction condition: 40mg/mL of enzyme, 20mL of each 0.1M ethanol and caprylic acid, 40°C, 150rpm and substrate concentration ethanol/caprylic acid: 0.1M/0.15M

The kinetic parameters of immobilized lipase were compared to that of free lipase derived from a series of experimental determinations. As observed from Table 3.1, immobilized lipase showed low K_m value (0.83mM) and higher V_{max} (0.204mM/min) value as compared to that of free lipase. These alterations suggest that lipase after immobilization resulted in increased affinity for substrates and enhanced accessibility of active sites. The K_{cat}/K_m ratio is a measure of the catalytic efficiency of enzyme and was used to compare the apparent kinetic parameters of immobilized lipase. Compared to native lipase, a higher K_{cat}/K_m ($0.386 mM^{-1}\ min^{-1}$) value was observed for immobilized lipase which supports observations from Fig 35, confirming that immobilized lipase shows increased catalytic specificity in non-aqueous system.

Table 3.1: Kinetic constants of esterification reaction catalyzed by the free and immobilized lipase

Sample	V_{max} (mM/min)	K_m (mM)	K_{cat} (min^{-1})	K_{cat}/K_m ($mM^{-1}\ min^{-1}$)
Free	0.025	1.512	0.238	0.157
Immobilized	0.204	0.83	0.321	0.386

3.4 Reusability studies

To further examine the potential of immobilized lipase for ethyl caprylate production, its operational stability was investigated. The enzyme preparation was given solvent washes after every cycle (48 h for each cycle) in order to remove any substrate or product absorbed onto EGO and reused in fresh medium supplemented with substrates. It was observed that immobilized lipase catalyze reaction appreciably upto 10 cycle retaining 92% (Fig 36) of its activity, after which lipase activity started declining slowly. The initial rates of higher esterification rates can be attributed to the distance of enzyme molecules from the surface of EGO provided by APTES resulting in more flexible environment for the enzyme. However, the steep fall in esterification activity was

observed after 20 runs. This may be attributed to the washing of immobilized biocatalyst which leads to enzyme leaching that limits mass transport and decrease in the exposure of the active sites to substrates. In present work, reusability of immobilized lipase was studied upto 30 consecutive cycles which demonstrate stability of enzyme with meager loss of activity. Also, immobilized lipase exhibited good storage stability without significant decrease in activity after being stored for 68 days under refrigeration. These results further prove that this is promising technique for immobilization and production of ethyl caprylate for industrial purpose.

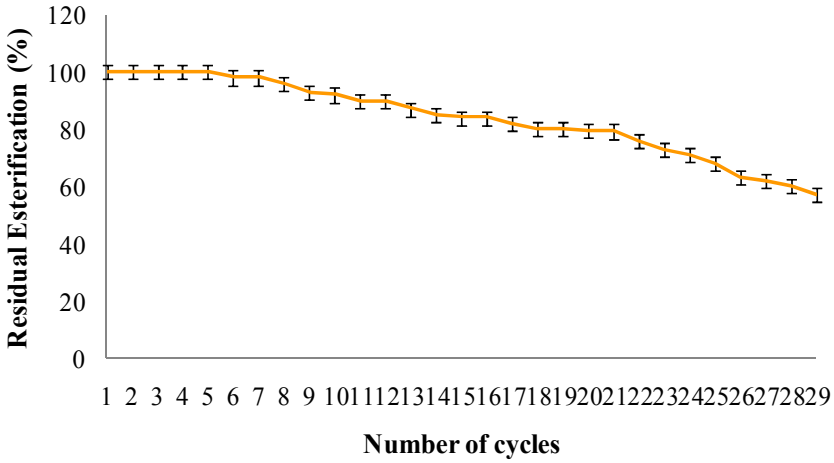

Figure 36: Reusability study for the synthesis of ethyl caprylate using lipase immobilized on EGO at pH 8.5 and 40°C

(4) Enzyme-Quantum dot conjugates: Attachment of CdS nanoparticles to lipase

4.1 Characterization studies for functionalized CdS nanoparticles

4.1.1. Microscopy studies

The microstructure investigation of functionalized and pristine nanoparticles was carried out using transmission electron microscopy (TEM) to reveal the morphology of nanoparticles. Fig 37(a) illustrates the electron micrograph of CdS NP's modified with APTES recorded at the accelerating voltage of 200keV. CdS NP's were almost spherical in shape showing agglomeration. The average diameters of CdS NP's were manually calculated and are displayed in Fig 37(b). The particle size was obtained in the range of 20-28nm (as observed from mean dispersion graph in Fig 37(b) with the average particle size of 24nm. CdS functionalized with APTES in the micrograph reveals that small

particles aggregate into secondary particles due to cross linker APTES and exhibits and large surface area. This is generally attributed to a certain degree of compactness existing between the nanoparticles. However, there was no clear difference found with lipase immobilized nanoparticles. Thus in order to check whether immobilization has taken place fluorescence microscopy study was carried out.

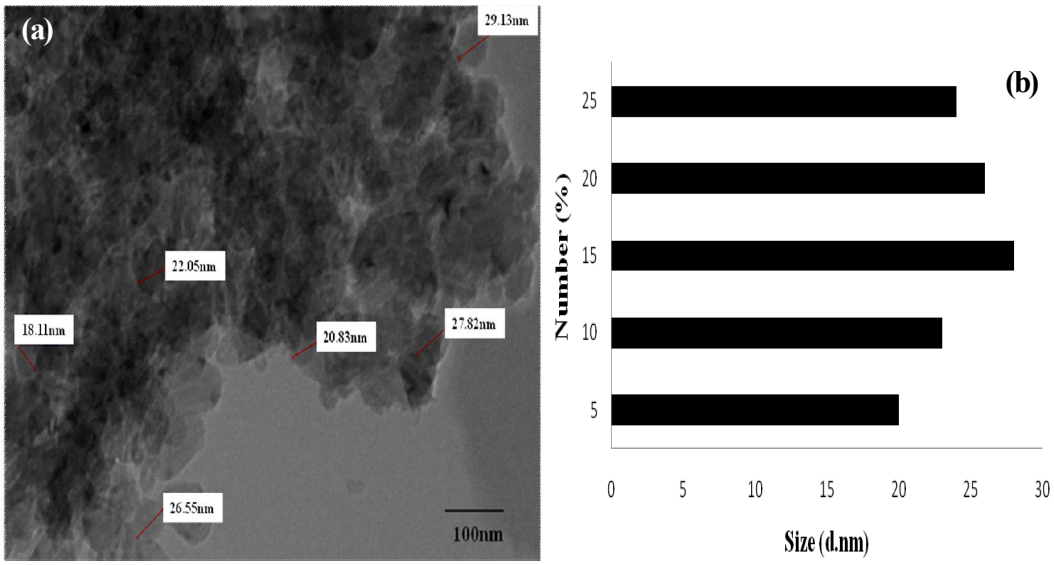

Figure 37: (a) TEM image for highly agglomerated CdS nanoparticles at 100nm exhibiting quasi spherical morphology. The agglomeration is formed due to cross linking after modification (b) Mean dispersion graph for size distribution of CdS nanoparticles showing size variability from 20 to 30nm

The luminescence properties of functionalized CdS nanoparticles were recorded by fluorescence microscopy. CdS NP's (Fig 38(a)) have adsorption maximum at about 380nm, however lipase immobilized CdS NP's (Fig 38(b)) was excited at 460nm to overcome the strong background fluorescence. The bright green colour under fluorescence microscopy further confirmed aggregation of CdS NP's with lipase. These results therefore clearly demonstrated binding of lipase on CdS nanoparticles employing simple functionalization techniques. These results were also justified from the protein content of immobilized lipase (0.225mg/mL) as well as the specific activity (1.08 U/mg of CdS). Moreover, Immobilization yield (%) calculated from the protein content in free

lipase against protein in supernatant after immobilization was about 75% with equivalent binding efficiency of enzyme.

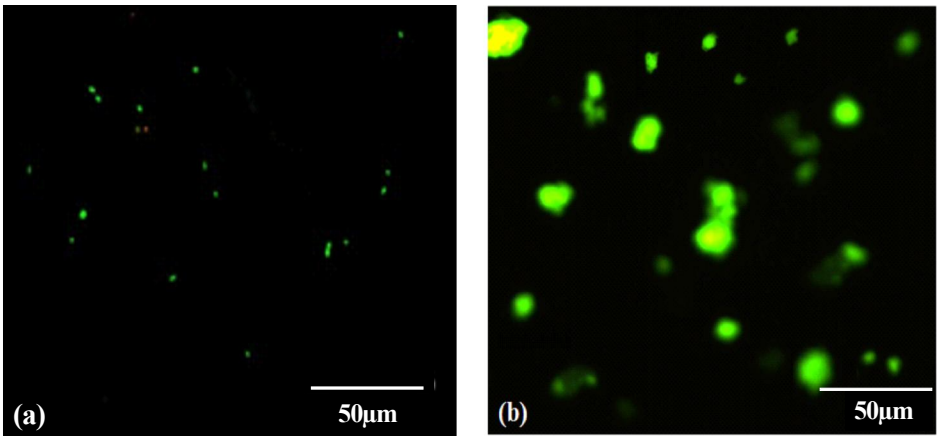

Figure 38: (a) Fluorescence micrograph for pristine CdS nanoparticles, (b) Fluorescence micrograph for lipase immobilized CdS nanoparticles

To further verify the crystalline phase of CdS nanoparticles, SAED (Selected area electron diffraction) patterns were obtained using HR-TEM analysis which exhibits polycrystalline nature of the nanoparticles as shown in Fig 39. This diffraction pattern was indexed on the basis of cubic system and the three diffraction lines corresponding to (111), (400), (511) planes indicates that Bravais lattice is face centered cubic (fcc). We also calculated lattice parameter from this diffraction pattern which comes out to be 5.47A° slightly lower in comparison to the reported value i.e. 5.81A°. [JCPDS file no. 10-0454].

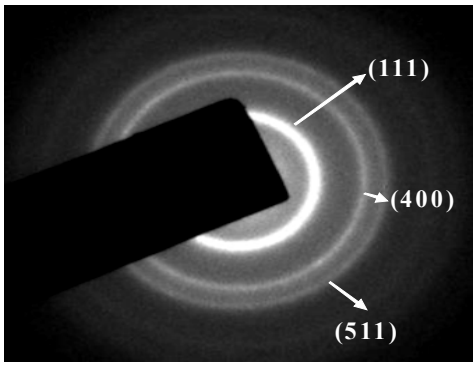

Figure 39: Selected area electron diffraction (SAED) pattern showing polycrystalline nature of CdS nanoparticles

The elemental composition of the CdS-CRL conjugates was examined using an EDAX spectrometer attached to TEM operated at 200kV. A typical EDAX spectrum (Fig 40) from the conjugates confirmed the presence of C, O, Cd, and S. The Cd:S atomic ratio of 2:1 is consistent with our experimental stoichiometric CdS within experimental error.

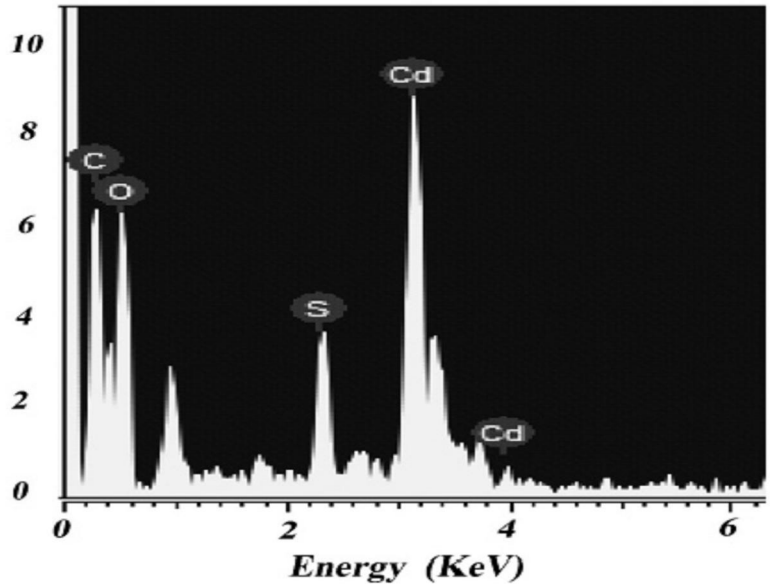

Figure 40: Energy dispersive X-ray (EDAX) spectra of CdS-CRL conjugate

4.1.2. Thermal gravimetric analysis

Thermo gravimetric analysis (TGA) of pristine CdS, functionalized CdS and lipase immobilized on functionalized CdS NP's are shown in Fig 41. In Fig 41(a) pristine CdS nanoparticles shows no significant weight loss upto 900°C. Fig 41(b) reveals the TGA curve of CdS nanoparticles functionalized with APTES and TEOS, with 10 to 15% of weight loss between 200 and 300°C and thereafter a slow decrease of weight loss upto 900°C. This may be due to pyrolysis of silane moieties. On the other hand, Fig 41(c) display the TGA curve of CdS/lipase which is thermally unstable and starts to loose mass upon heating at around 200°C withmuch faster rate as compared to functionalized nanoparticles. A maximum weight loss of 40% was observed at 400°C with constant decrease in weight as the temperature increases. This is mainly due to decomposition of

enzyme as well as loss of bound water molecule to enzyme indicating interaction between enzyme/CdS NP's.

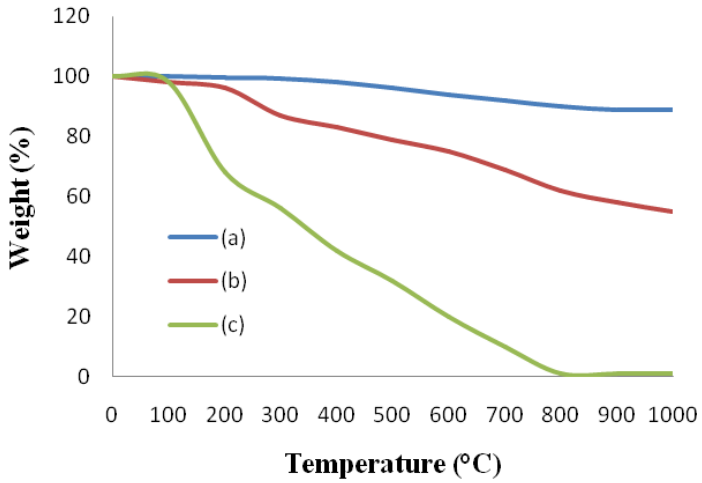

Figure 41: TGA weight loss curves of (a) pristine CdS, (b) functionalized CdS nanoparticles via APTES and TEOS and (c) lipase immobilized functionalized CdS nanoparticles

4.1.3. Fourier Transform Infrared (FTIR) spectroscopy analysis

Binding of lipase on CdS nanoparticles was demonstrated with FTIR analysis. Fig 42 shows the FTIR spectra for free lipase (B), CdS (A) and lipase bound CdS NP's (C). In spectra B (Fig 42), as lipase is a protein, the adsorption at 1639cm^{-1} is possibly due to C=O stretching of the amide moieties in proteins. The stretching of CO at 1639cm^{-1} is shifted to 1632cm^{-1} which is due to interaction of CO moiety of lipase to that of silane functionalized CdS nanoparticles (Fig 42(C)). The NH bending of lipase at ~1561cm^{-1} also shifted to 1559cm^{-1} in lipase bound CdS spectra. The peaks at 779cm^{-1} and 1065 cm^{-1} suggested that Si-O-Si/$SiOCH_3$ moieties presence of silane. The other characteristic band of protein at 1122cm^{-1} and 3425cm^{-1} are also seen in the spectra of pure lipase and lipase bound CdS nanoparticles. The nature of adsorption around 1631 cm^{-1} in lipase bound CdS nanoparticles suggests that there is interaction between C=O moieties of lipase and CdS.

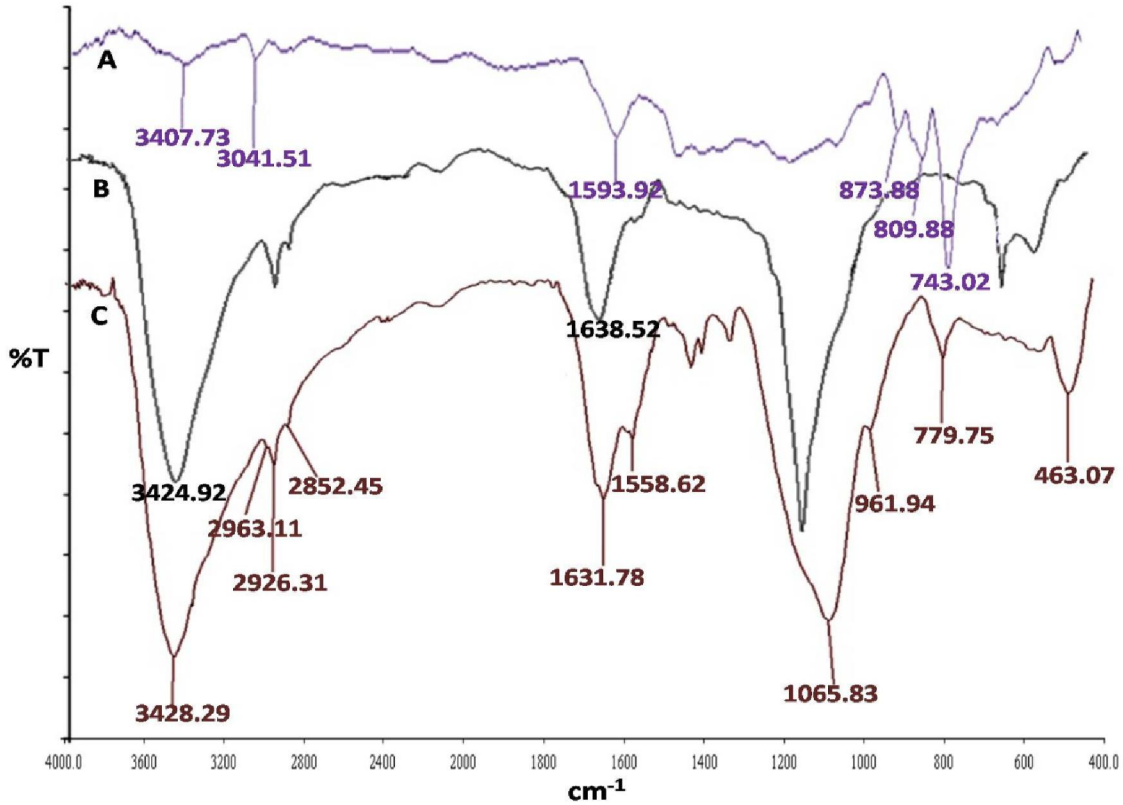

Figure 42: FTIR overlay spectra of lipase immobilized CdS nanoparticles functionalized using APTES and TEOS. (A) pristine CdS nanoparticles, (B) Lipase spectra, (C) lipase bound on silane functionalized CdS nanoparticles

4.2 Hypothesis for enzyme conjugation to that of CdS nanoparticles

In order to investigate the possibility of any structural perturbation of CRL before and after formation of the conjugates, circular dichroism (CD) studies was performed. Fig 43 shows CD spectra of CRL in phosphate buffer (pH) 7.0) and CdS-CRL in water (pH 8.5). It is clearly evident from Figure 42 that CD spectrum of CRL remains essentially similar to that of the CdS-CRL conjugates confirming no perturbation in the secondary structure of the protein after the conjugation of CdS nanoparticles. We also investigated the functionality of the enzyme in its native state and conjugated to CdS nanoparticles by measuring their enzymatic activity on a substrate p-NPP. We found that the activity of the enzyme in the CdS-CRL conjugates was increased by 2 times as compared to that in the pure CRL. This boost of the enzymatic activity in CdS-CRL conjugates could be attributed to the immobilization of the enzyme upon conjugation to CdS nanoparticles.

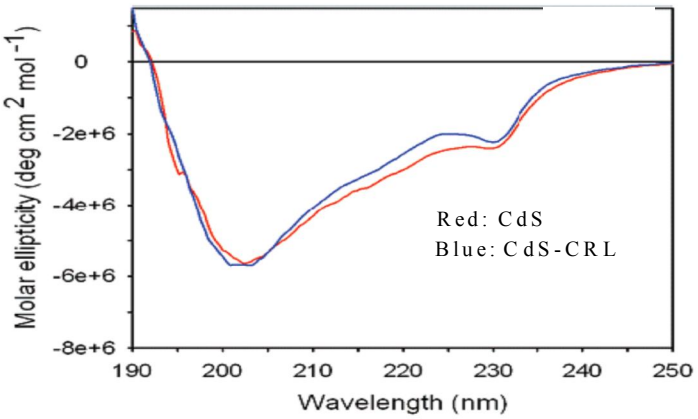

Figure 43: Circular Dichorism (CD) spectra of CdS and CdS-CRL conjugates

4.3 Properties of free and immobilized lipases

4.3.1 Effect of pH and temperature on free and immobilized lipase

The effect of pH on the activity of free and immobilized lipase systems was determined in the pH range from 5.0-9.5. The optimum pH of the free enzyme was 7.0 with 48% of ester production in 6h while the optimum pH for the immobilized lipase was shifted 0.5 unit to the basic region (pH 7.5) producing 79% of ester under same condition (Fig 44).

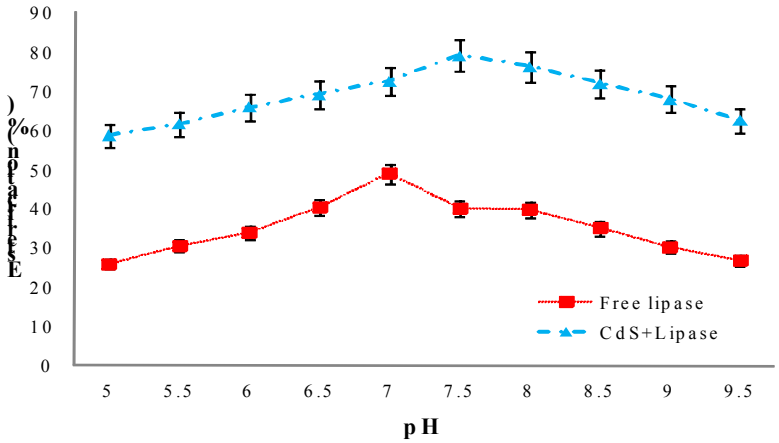

Figure 44: Effect of pH on ester synthesis. Reaction condition: reaction volume 20mL, temperature 40°C, 0.1M pentanol, 0.1M valeric acid,

The activity of lipase (free as well as immobilized) towards esterification reaction was monitored in the temperature range from 20 to 60°C using phosphate buffer (0.05M, pH 7.0 for free lipase and pH 7.5 for immobilized lipase. The results exhibited that optimum

apparent temperature for free enzyme was about 37°C (51% of ester production), while that for immobilized lipase was 40°C (78% of yield in 6h) (Fig. 45). This alteration in temperature might be ascribed to the fact that the configuration of lipase was stabilized as a result of bonding between lipase and the support ensuing higher catalytic activity of the enzyme in immobilized form as compared to that of free counter parts.

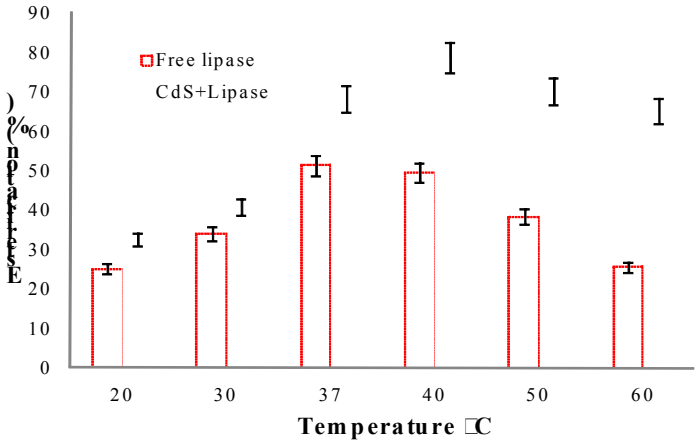

Figure 45: Effect of temperature on ester synthesis. Reaction condition: reaction volume 20mL, temperature 40°C, 0.1M pentanol, 0.1M valeric acid,

4.3.2 Influence of valeric acid/pentanol substrate molar ratios

To examine the dependence of molar ratio of the substrates on the chemical equilibrium of lipase-catalyzed reaction, the concentrations of pentanol and valeric acid were varied one at a time keeping the other constant and carrying out esterification reaction. In one set of experiment concentration of pentanol was maintained at 0.1M and that of valeric acid was varied (0.02 to 0.1M). At concentration 0.08M valeric acid 79% of ester was synthesize (Fig 45), while upon increasing the concentration from 0.08M to 0.1M, the conversion of product started decreasing. The feasible explanation for this may be due to inhibition of lipase activity by soaring valeric acid concentration. When the same experiment was repeated keeping valeric acid constant at 0.08M and varying pentanol concentration (0.02 to 0.14M) highest yield was obtained at 0.12M concentration (Fig 46) with 80% of product formation. Further, the elevated concentration of alcohol displayed an inhibitory effect slowing down the reaction rates. Thus, the molar ratio of valeric acid

to pentanol was found to be 0.08:0.12M corresponding to maximum esterification of 80% in 6h.

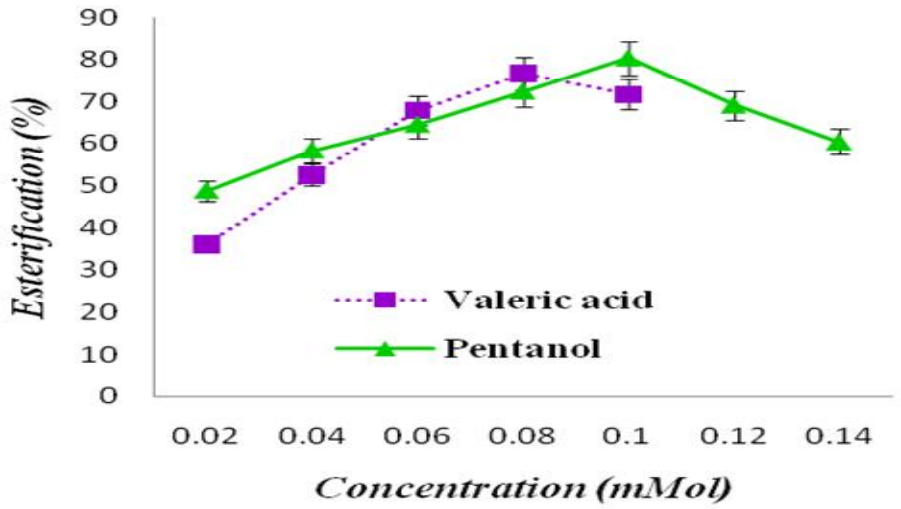

Figure 46: Influence of substrate concentration on the efficiency of ester synthesis where dotted line is for valeric acid and solid line is for pentanol. Reaction conditions: reaction volume 20mL, pH 7.5 and temperature 40°C

4.3.3 Influence of chain length of fatty acid and alcohol on ester synthesis

Influence of fatty acid on lipase catalyzed esterification, the reaction mixture consisting substrate ratio of 0.08:0.12M with cyclohexane (40°C, pH 7.5) was kept on orbital shaker and samples were withdrawn at regular interval. Fig 47(a) demonstrate the rate of esterification by different chain length of fatty acids ranging from acetic acid (C2) to lauric acid (C12). The results showed that there is increase in the conversion rate upto C5 (valeric acid) with the yield of 80% reaching plateau at C6 (hexanoic acid) within 4h. This specifies that the best acyl donor for the synthesis of pentyl esters by *Candida rugosa* lipase is valeric acid. Fig 47(b) demonstrates the influence of alcohol chain length on the esterification of valeric acid. Esterification with butanol showed highest value (80%) while octanol showed the lowest value (25%). This may be due to type of support and method of immobilization employed, since immobilization technique can alter fatty acid specificity.

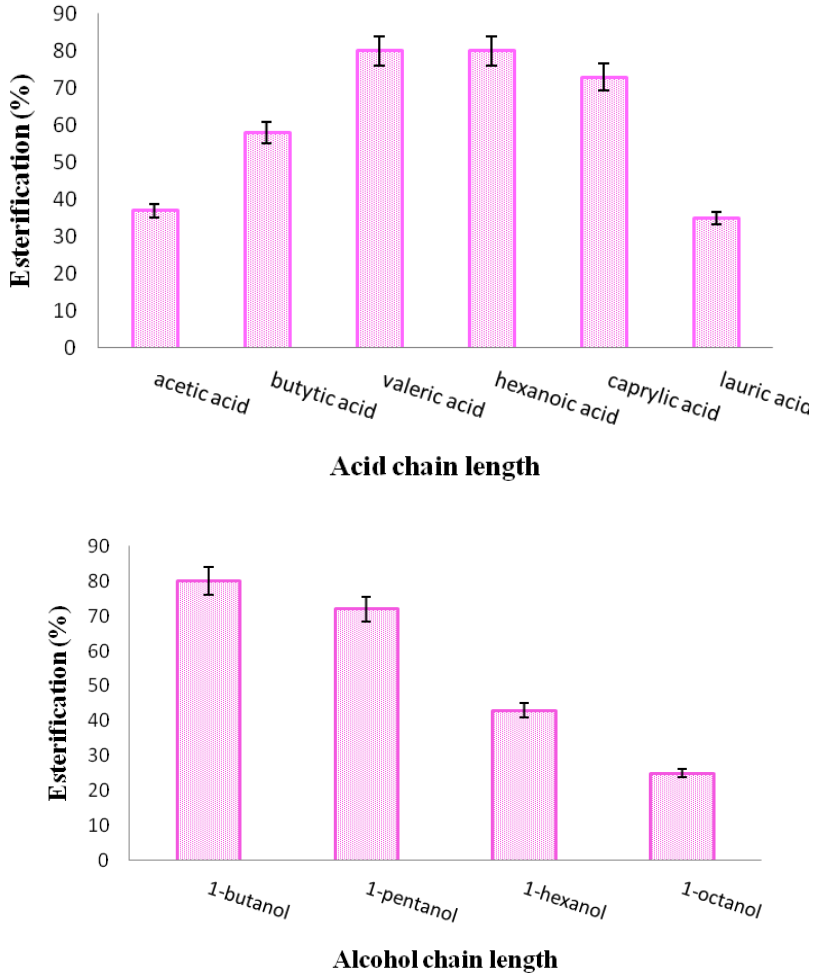

Figure 47: (a) Influence of acid chain length on ester synthesis. (b) Influence of alcohol chain length on ester synthesis. Reaction conditions: reaction volume 20mL, pH 7.5 and temperature 40°C with substrate ration of 0.08:0.1M

4.3.4 Effect of reaction medium on ester synthesis

In the study five organic solvents viz n-hexane, n-heptane, n-octane, cyclo-octane and cyclohexane were used as reaction medium under same optimized condition (40°C, pH 7.5, substrate ratio 0.08:0.12M) for ester synthesis. It can be seen from Fig 48 that immobilized lipase showed exceptionally higher yield (81%) at faster rates in 4h when cyclohexane was used as the medium. This can be attributed to the extreme hydrophobic nature of the solvent stabilizing the hydrated enzyme structure. However, free enzyme showed very poor product formation under similar condition.

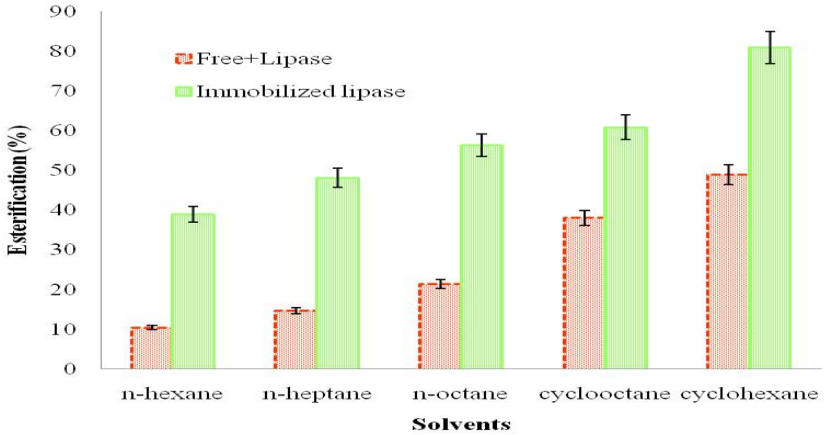

Figure 48: Effects of different solvents (n-hexane, n-heptane, n-octane, cyclo-octane and cyclohexane) as reaction medium on the synthesis of pentyl valerate. Reaction conditions: reaction volume 20mL, pH 7.5 and temperature 40°C

4.4 Kinetic parameters

The K_m value is known as the principle factor for the affinity of enzymes to substrates, and lower value of K_m represents the higher affinity between enzymes and substrates. The apparent K_m value for immobilized lipase was found to be 0.5 mM which is 4-fold lower than free lipase (2.01 mM). However, V_{max} value for the free lipase was 28µmoles/mg/min, while the V_{max} value for immobilized lipase was 6-fold higher with 193µmoles/mg/min. Thus, immobilized lipase-catalyzed pNPP hydrolysis had a 27-fold higher efficiency in comparison to the free lipase. These alterations in kinetic parameters suggest that binding of lipase on CdS nanoparticles resulted in increased affinity for the substrates and enhanced accessibility of the active site. Most likely, the coupling of lipase on nanoparticles leads to a flavored orientation of enzyme on the surface of the carrier.

4.5 Time course for ester production

Pentyl valerate is a short chain ester which has a ‘‘fruity” fragrance and is used as a constituent in various fruity flavors such as apple, banana and pineapple aroma. The synthesis of pentyl valerate by free and immobilized lipase was studied using cyclohexane as reaction medium. The experiment was carried out at 0.08:0.12M acid/alcohol molar ratio under optimized conditions. The utmost esterification yield of 82% was observed within 4h when lipase was immobilized on CdS NP’s. In contrast to

this free lipase exhibited only 50% of ester formation under same condition (Fig 49). One of the reasons for increased esterification activity of immobilizing system could be attributed to the fact that enzyme is dispersed onto a large surface area when adsorbed to a carrier matrix and aggregation of the enzyme is prevented as compared to that of free enzyme in organic synthesis. Another possible reason could be the "lid" structure of lipase. The lid of enzyme is pulled back at the interfaces exposing the active site making *Candida rugosa lipase* highly surface active enzyme. At the oil-water interface, opening of the lid of CRL must have resulted in a self-catalytic bond formation with that of CdS NP's leading to an enhanced activity and stability for immobilized lipase compared with that of free.

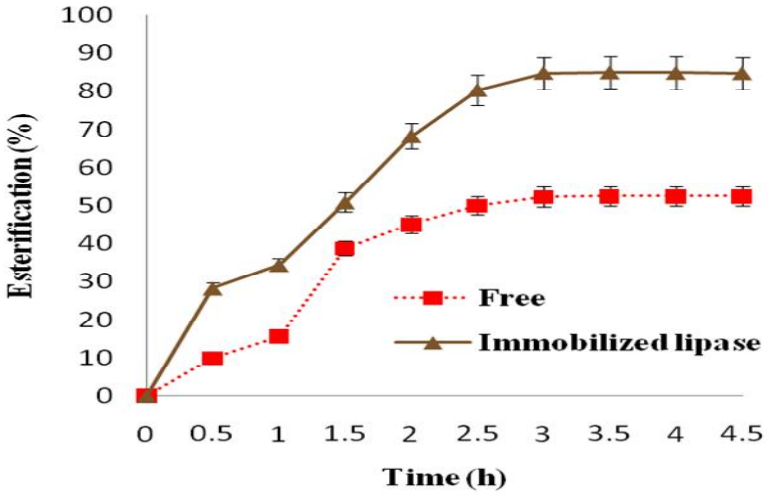

Figure 49: Time course for the synthesis of pentyl valerate using cyclohexane as a medium. Reaction conditions: reaction volume 20mL, pH 7.5 and temperature 40°C with 0.08:0.1M acid to alcohol ratio

Though the main aim for CdS nanoparticles here was to provide support for enzyme, its preliminary study for leeching and toxicity test were also carried out. It was observed that no CdS nanoparticles were found to be released into sytstem and did not show any toxicity.

4.6 Reusability studies of immobilized enzyme

Operational stability of immobilized enzyme was investigated in order to scrutinize potential of lipase for ester synthesis. Immobilized lipase was subjected to check

recyclability by the given standard pentyl valerate synthesis reaction for 4h (Fig 50). After 4h reaction, the enzyme preparation was given solvent washes in order to remove any substrate or product absorbed onto CdS NP's and reused in fresh medium supplemented with substrates. There was marginal decrease in conversion up to 96% after five reuses while, conversion decreased further upto 80% after 15 consecutive cycles. The decrease in conversion was attributed (i) due to frequent exposure to alcoholic substrate in each, cycle which deactivates the catalytic activity of enzyme (ii) and due to leaching of the enzyme from the support upon reuse.

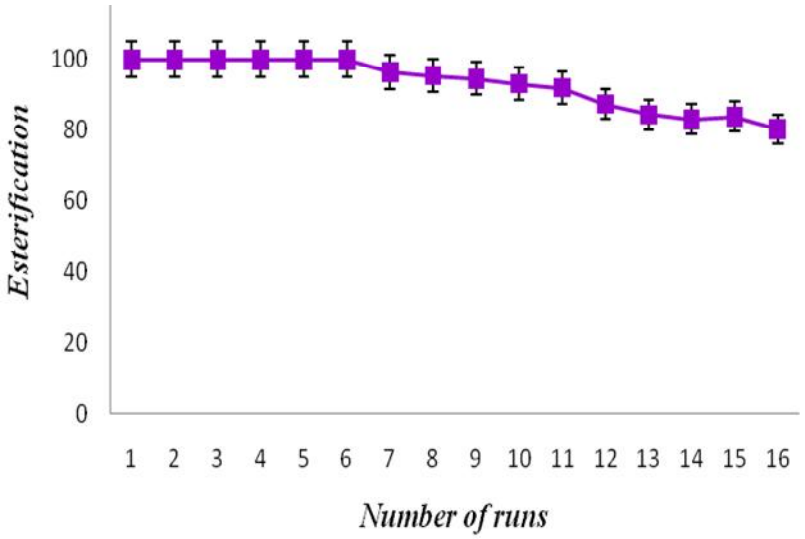

Figure 50: Repeated cycles for pentyl valerate synthesis using lipase immobilized on CdS nanoparticles at pH 7.5 and 40°C

(5) Zinc oxide nanoparticles supported lipase immobilization for biotransformation in organic solvents: A facile synthesis of geranyl acetate, effect of operative variables and kinetic study

5.1 Immobilization of CRL

A protein content and lipase activity assay was performed to determine the immobilization of the protein on the support and to check enzyme catalytic efficiency after immobilization. The present study was designed to apply both adsorption (in the presence of ZnO-PEI and ZnO-PEI-SAA) and covalent attachment via spacer arm of GLU (ZnO-PEI-GLU) for immobilization of CRL as represented in Fig. 51. The protein content for the free as well as immobilized lipase followed the sequence as CRLZnO-

PEI-GLU>ZnO-PEI-SAA>ZnO-PEI (Table 5.1). Lipase fabricated on ZnO-PEI-GLU showed the best results in terms of hydrolytic activity (4.29 U/mL). ZnO-PEI, ZnO-PEI-SAA and ZnO-PEI-GLU showed 49, 61 and 86% of immobilization yield, respectively.

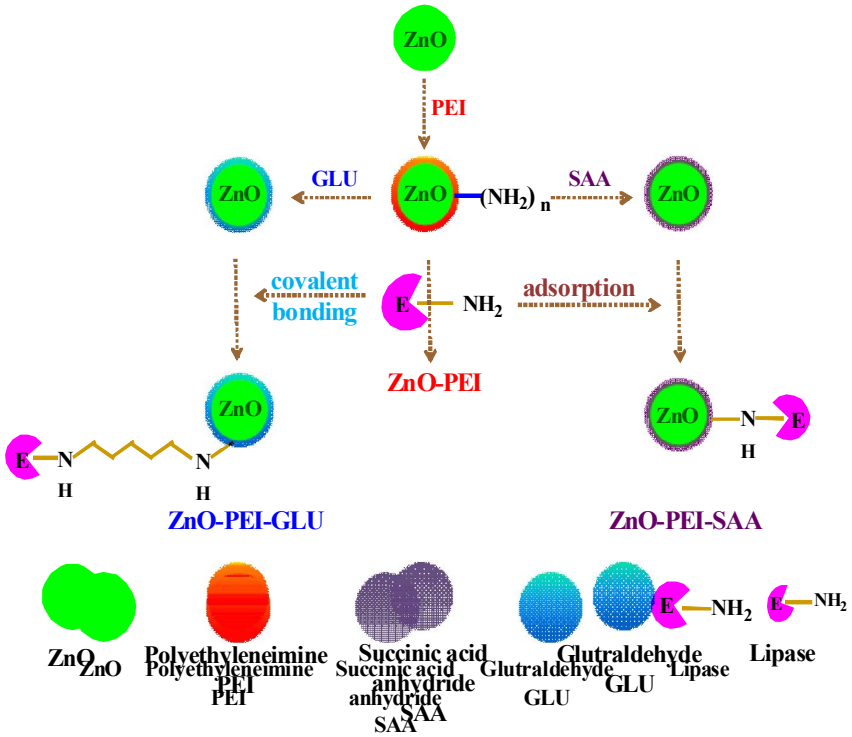

Figure 51: Schematic representation for functionalization of ZnO nanoparticles. ZnO nanoparticles are firstly functionalized using two different linkers i.e glutraldehyde (GLU) and succinic acid anhydride (SAA). Lipase in immobilized by covalent bonding and simple adsorption

Table 5.1: Lipase activity, protein and specific activity

Enzyme	Enzyme Activity (U/mL)	Protein (mg/mL)	Specific activity (U/mg)
CRL	5.68	2.469	2.300
ZnO-PEI	2.96	1.243	2.381
ZnO-PEI-SAA	3.25	0.962	3.371
ZnO-PEI-GLU	4.29	0.325	13.2

5.2 Characterization studies

5.2.1 Microscopic studies

The microstructure investigation of pristine and functionalized ZnO nanoparticles was carried out using transmission electron microscopy (TEM) to reveal the morphology of nanoparticles. Fig. 52(a) illustrates the electron micrograph of pristine ZnO nanoparticles recorded at the accelerating voltage of 200keV. As seen from Fig. 52 it can be assumed that most of the pristine ZnO nanoparticles are quasi-spherical and their diameter is in the range from 15 to 25nm. The micrograph reveals aggregation of some nanoparticles due to large specific surface area and high surface energy. This is generally attributed to a certain degree of compactness existing between the nanoparticles. Also, scanning electron microscopy study was carried out for pristine ZnO nanoparticles. As displayed in Fig. 52(b) ZnO nanoparticles were found to be highly aggregated. It also demonstrates that after the surface of ZnO nanoparticles was modified by PEI, the aggregation of ZnO nanoparticles was greatly reduced. However, using SEM and TEM was no clear difference was found with modified ZnO nanoparticles and lipase immobilization. Thus in order to check whether immobilization has taken place further studies was carried out.

The luminescence properties of functionalized ZnO nanoparticles were recorded by fluorescence microscopy. Pristine ZnO (Fig. 52(c)) have adsorption maximum at about 380nm, however lipase immobilized ZnO (Fig. 52(d)) was excited at 460nm to overcome the strong background fluorescence. The bright green coloration under fluorescence microscopy further confirmed conjugation of ZnO with lipase.

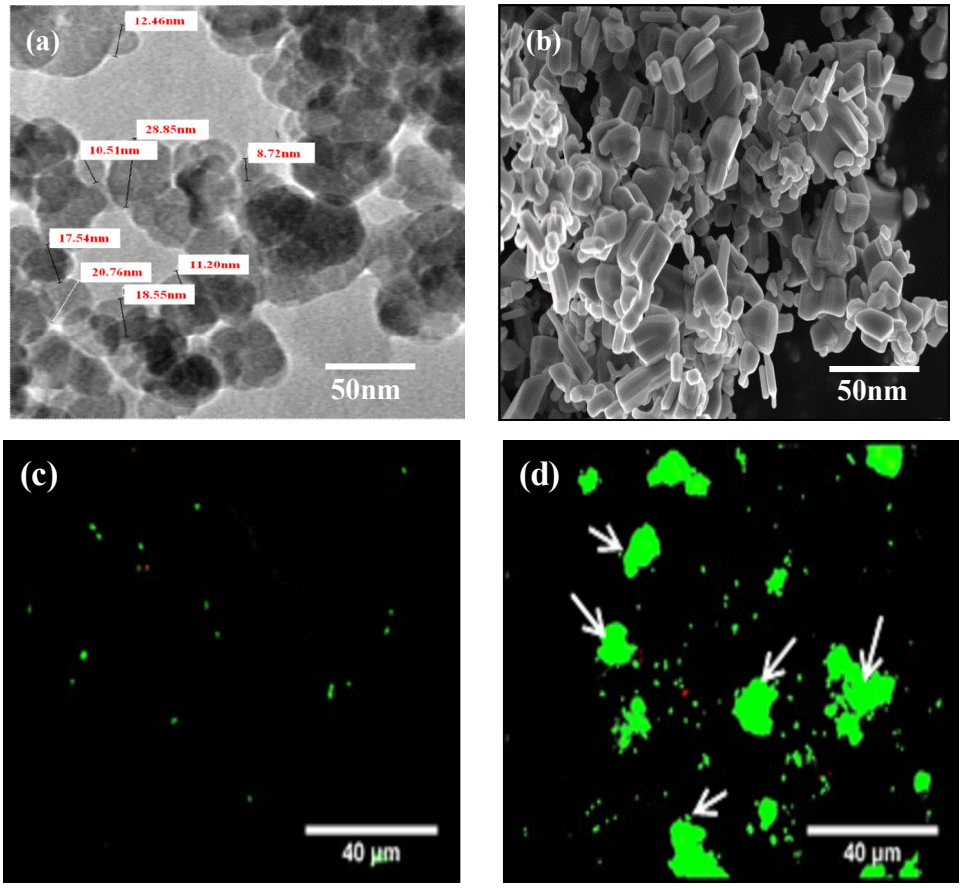

Figure 52: Characterization of ZnO nanoparticles. (a) Transmission electron micrograph for pristine ZnO nanoparticles (b) Scanning electron microscopy for pristine ZnO nanoparticles (c) Fluorescence microscopy analysis for pristine ZnO nanoparticles and (d) Fluorescence microscopy analysis for lipase conjugated ZnO nanoparticles

5.2.2 Fourier transform infrared spectroscopy

To understand better about the functional groups involved in immobilization process, FTIR analysis was performed in the range of 500-4000cm^{-1}. Fig. 53 shows the FT-IR spectra of the (A) ZnO nanoparticles, (B) ZnO-PEI (C) CRL and (D) ZnO-PEI-SAA, respectively. FT-IR band at short wave numbers (range 446-630cm^{-1}) corresponds to the characteristics peak of ZnO nanoparticles and was common for all the spectra (Fig. 53). In addition to this, the broad band of 3429-3439cm^{-1} is due to the -OH stretching and bending vibration indicating the presence of a large number of hydroxyl groups and H_2O molecules on the surface of the particles. The PEI grafting on nanoparticles can be clearly observed, as evident from the strong adsorption band at 1041cm^{-1} and 2928cm^{-1} which

results from the vibration of the Si-O- group and the aliphatic C-H group, respectively (Fig. 53(B)). Shifting the related peak of ZnO to 446 cm^{-1} and the stretching vibration of Si-O- group confirmed anchoring of silanol containing group onto the surface of ZnO nanoparticles. Such results indicate that the active groups have been introduced onto the nanoparticles surface. After immobilization of lipase onto ZnO nanoparticles (Fig. 53(C), the shifting of peak value corresponding to the interaction of -CO group of enzyme with ZnO NPs, while the broadening of peak at 548 cm-1 also revealed uniform adsorption of lipase on the nanomatrix. The peak obtained at 1642 cm-1 was due to amide II of the enzyme, while the peak value observed at 1457 cm-1 confirmed CH vibrations.

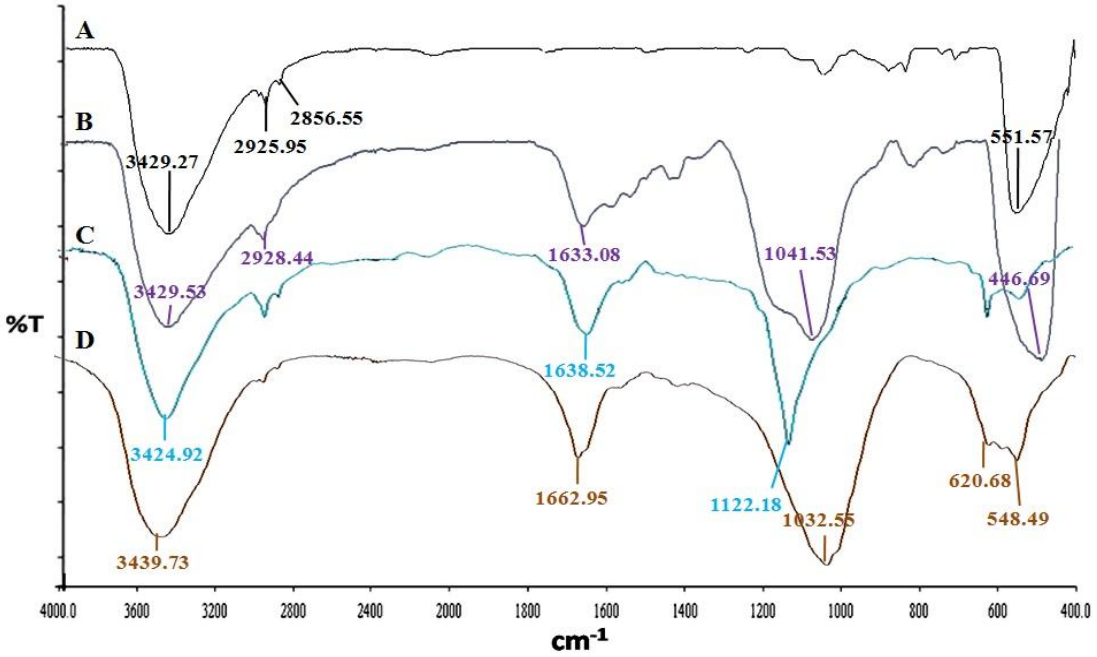

Figure 53: FTIR overlay spectra of (A) pristine ZnO (B) ZnO-PEI (C) Free *Candida rugosa* lipase and (D) ZnO-PEI-SAA

5.2.3 Thermal gravimetric analysis

The successful functionalization was also reflected in TGA curves. The TGA analysis for naked as well as modified ZnO nanoparticles are shown in Fig. 54 and the temperature scale for measurement is from 100 to 1000ºC in nitrogen at heating rate of 20°C min^{-1}. Two step weight loss was found for naked ZnO nanoparticles. The first weight loss of 1%

was acquired at 150ºC associated with desorption of water molecule, while the second weight loss (2.8%) was attain at 550ºC. In comparison to pure ZnO nanoparticles, the related TGA curve for ZnO modified nanocomposites showed weight loss at 105ºC due to vaporization of water formed by the condensation of silanol groups, then at 400ºC associated with oxidative decomposition of organic moiety. In case of lipase immobilized ZnO (for each nanocomposites), nearly 10% of weight loss was observed at around 100°C. This is much obvious due to loss of bound water molecule. This attributes to thermo-decomposition of lipase indicating successful enzyme immobilization on ZnO.

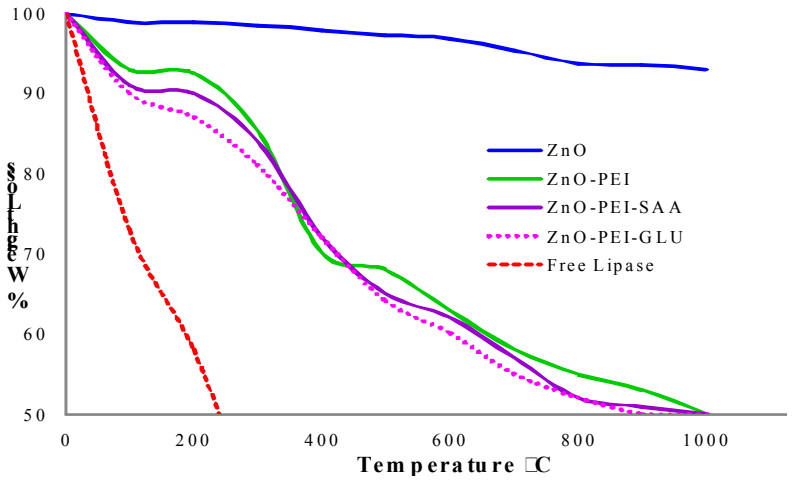

Figure 54: TGA weight loss curves of pristine ZnO, lipase immobilized ZnO nanocomposites. The temperature range was varied from 30-1000°C and with heating rate of 20°C/min, in agron atmosphere

5.3 Effect of operative variables for enhanced synthesis of geranyl acetate

5.3.1 Effect of temperature

In order to check the influence of temperature on enzymatic transesterification the reaction was carried out at different temperatures (30, 37, 40 and 50ºC) using free as well as immobilized lipase nanocomposites. The trends for ester synthesis by prepared nanocomposites of lipase are exhibited in Fig. 55(a) and are more or less similar. Immobilized forms of lipase were found to be quite stable even at higher temperatures, whereas above 40ºC the activity of free CRL started declining. About 90% of ester was synthesized using immobilized lipase (ZnO-PEI-GLU) in 6h at 40ºC while free lipase

was found to be sluggish (52%) for production under same condition. However, ZnO-PEI-SAA and ZnO-PEI produced 82% and 71% of geranyl acetate under same condition and was found to be stable even at 50°C. The stability of immobilized lipase over free CRL can be explained by hydrophobic and electrostatic interaction between ZnO and enzyme which alter the physical and chemical properties of enzyme. Also, the limitation of enzymatic movement after immobilization on the support together with better substrate diffusion at a higher temperature improves the activity of the immobilized enzymes.

The effect of temperature on affinity of free and immobilized enzyme can be seen in Arrhenius plot (Fig. 55(b)). The free and immobilized lipase exhibited a linear relationship in the temperature range of 30-50°C and the corresponding activation energies were calculated to be 19.04 kJ/mol for free lipase and 12.31 kJ/mol for immobilized lipase (ZnO-PEI-GLU). Lower activation energy for immobilized lipase in comparison to that of free lipase suggests less energy requirement and the change in conformation of enzyme during immobilization.

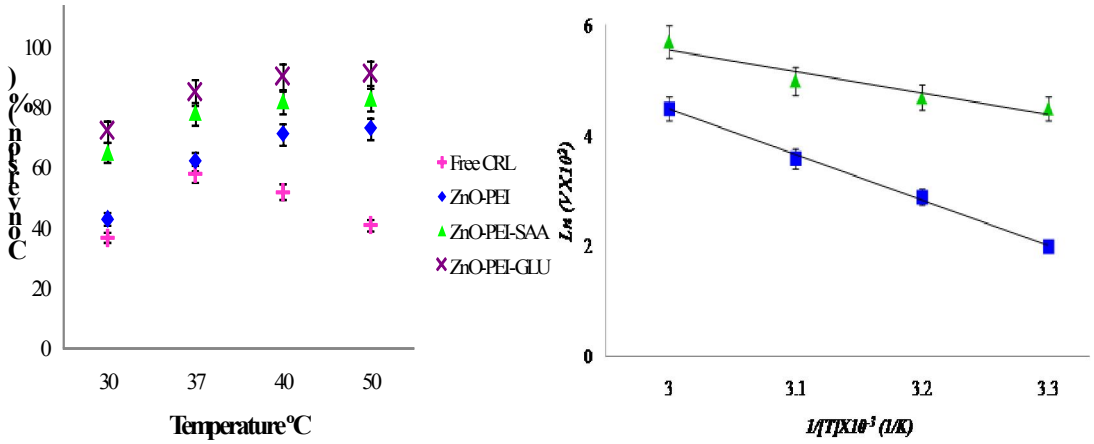

Figure 55: (a) Effect of temperature on free lipase and immobilized lipase nanocomposites. Reaction conditions: 50mg of enzyme (including weight of support), 3mL of n-hexane, 0.1M of each substrate (geraniol and vinyl acetate), temperature 30-50°C, 150rpm. (b) Arrhenius plot for free (■) as well as immobilized lipase (ZnO-PEI-GLU) (▲) over the temperature range of 30-50°C. Reaction conditions: geraniol (0.1M), vinyl acetate (0.4M), reaction volume 3mL, pH 7 and temperature 30-50°C

5.3.2. Effect of organic solvents as reaction medium

In this study, organic solvents with different polarities including tetrahydrofuran, 1,4-dioxane, chloroform, acetone, toluene, benzene and n-hexane were chosen. Fig. 56 displays the yield of geranyl acetate catalyzed by free as well as immobilized forms of lipase in presence of different solvents. The results clearly indicated that n-hexane, a medium polarity organic solvent resulted in higher conversion for all the forms of lipase reaching 92% for ZnO-PEI-GLU in 6h. It is but obvious that immobilized lipase showed higher rate of conversion in comparison to that of free counterpart which was about 53% under similar condition. The enzyme activity is usually high when Log *P* value for solvent is between 2.0 and 4. The conversion obtained from benzene (85%) and toluene (86%) was also good, but their toxicity and odor limits their application in perfume synthesis. Also, the polar solvent like tetrahydrofuran and 1,4-dioxane yield only 48% of ester, whereas chloroform yield only 26% of geranyl acetate. This can be attributed to the stripping off the essential water molecule from the enzyme and enzyme deactivation. As a consequence; the catalytic activity of enzyme was decreased due to the lack of bound water to preserve the enzyme conformation flexibility which in turn is necessary for its catalytic action. However, acetone being an aprotic solvent does on attack protein very strongly. Thus with acetone being reaction medium 68% of geranyl acetate was obtained.

The outcome obtained with present study is in agreement with those reported in the literature, where high hydrophobic solvents with Log*P* values > 4 are considered the most suitable solvents for use in biocatalytic processes. The solvents with Log*P* values between 2 and 4 are moderately effective whereas, polar solvents with Log*P* < 2 are often ineffective.

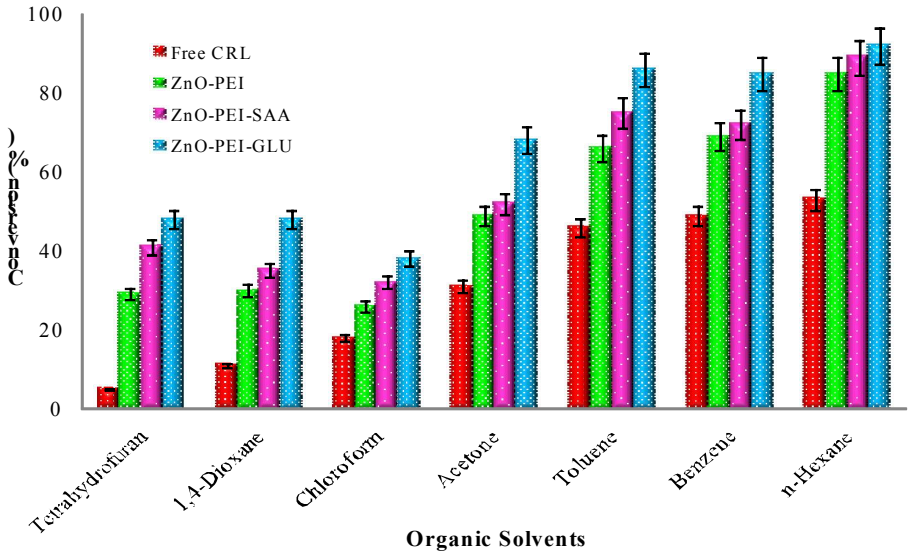

Figure 56: Effects of different solvents as reaction medium on the synthesis of geranyl acetate. Reaction conditions: 0.1M Geraniol, 0.1M vinyl acetate, solvent 3mL, pH 7, temperature 40°C, 150rpm

5.3.3 Substrate concentration

To examine the dependence of the molar ratio of the substrate and acyl donor on the chemical equilibrium of the lipase-catalyzed reaction various experiments were performed. In one set of experiment, the concentration of geraniol was kept constant (0.1M) while the concentration of vinyl acetate was varied from 0.1M to 0.5M (Fig. 57(a)). The molar conversion of the nanocomposites (ZnO-PEI-GLU) with 1:1 ratio of geraniol:vinyl acetate was 87%. Fig. 57(a) revealed that the reaction rate was enhanced when vinyl acetate concentration was increased from 0.1M to 0.4M for all the prepared nanocomposites. But, a slight decrease in molar conversion rate is observed at 0.1:0.5M ratio of geraniol: vinyl acetate in free as well as immobilized lipase. As a consequence this phenomenon in enzymatic reactions revealed that vinyl acetate has no inhibitory effect within the studied range of substrate concentrations.

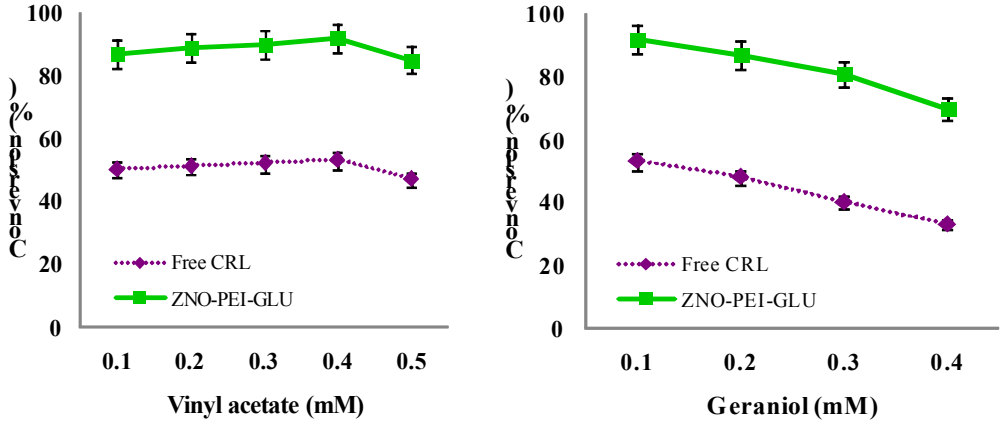

Figure 57: (a) Influence of vinyl acetate concentration on the efficiency of ester synthesis where geraniol concentration was kept constant at 0.1M. Reaction conditions: 0.1M geraniol, 0.1-0.5M vinyl acetate, 3mL n-hexane, pH 7, temperature 40°C, 150rpm. (b) Influence of geraniol concentration on the efficiency of ester production where vinyl acetate concentration was kept constant at 0.4M. Reaction conditions: 0.1-0.5M geraniol, 0.4M vinyl acetate, 3mL n-hexane, pH 7, temperature 40°C, 150rpm

In another set of experiment, concentration of vinyl acetate was kept constant at 0.4M while concentration of geraniol was varied from the 0.1M to 0.5M. As concentration of geraniol increases the yield decreases gradually (Fig. 57(b)). This decrease in reaction rate can be attributed to the inhibitory effect of geraniol on immobilized enzyme. The hydrophobic-hydrophobic interaction between the lipase and geraniol might be the reason to destabilize the active sites of the lipase.

5.3.4 Effect of acyl donor on immobilized lipase

Different acyl donors were used for synthesis of geranyl acetate with immobilized lipase in order to perceive their influence on reaction rate and are exhibited in Fig. 58. The experimental studies showed only 15% yield when acetic acid was used as acyl donor. Acetic acid acts as a potent inhibitor of enzyme activity and hence slower the initial reaction rate and % yield. When ethyl acetate was used as the acyl donor, ethanol was formed as a byproduct which competes with geraniol for nucleophilic attack on carbonyl ester and inhibits the rate of reaction. Herein, highest yield of 90% was achieved in transesterification of the geranyl acetate using vinyl acetate as acyl donor. Thus, vinyl acetate proved to be a good choice of acyl donor for lipase catalyzed transesterification

reactions because vinyl alcohol is formed as bi-product that immediately tautomerizes to acetaldehyde, thereby driving the reaction in a forward direction.

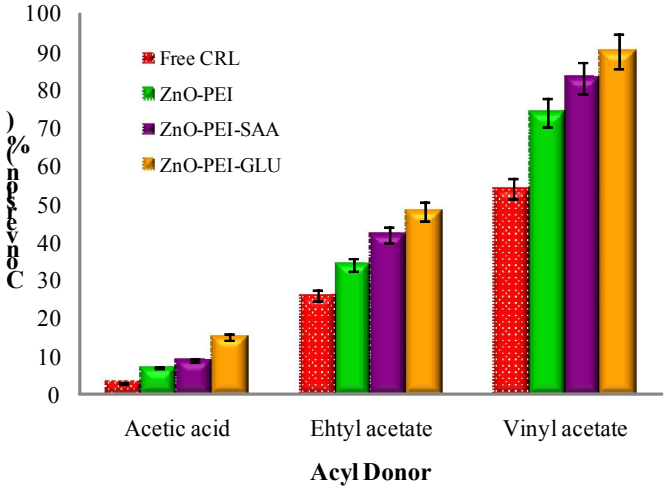

Figure 58: Influence of acyl donor for the synthesis of geranyl acetate. Reaction conditions: 0.1M geraniol, 0.1M acyl donor (Acetic acid, vinyl acetate, ethyl acetate), 3mL n-hexane, pH 7, temperature 40°C, 150rpm

5.4 Enzymatic synthesis of geranyl acetate using ZnO nanocomposites

The trends for geranyl acetate production using three forms of ZnO-enzyme preparations as well as free lipase under optimized conditions are shown in Fig. 59. Also, there was no product formation in negative control (support without enzyme). From Fig. 59 it was noted that in free form of lipase the conversion proceeded at very high rate reaching saturation of 65% after 6h. Immobilized forms of lipase took littler longer time in order to achieve saturation for conversion and utilization of substrates. Among the immobilized forms, CRL cross linked using GLU showed higher conversion (94%) than one coupled with ZnO-PEI and ZnO-PEI-SAA ie. 86% and 90%, respectively in 6h and was stable thereafter. One of the main reason for this can be attributed to the difference in immobilization yield (IY%) (shown in Table 5.1) which is higher for ZnO-PEI-GLU (86%) than ZnO-PEI (61%) and ZnO-PEI-SAA (49%). While, as per calculation hydrolytic activity for free lipase was found to be 5.68U/mL. Another possible reason for this may be due to cross linking of enzyme by glutraldehyde (containing active aldehyde group) on amine based cationic polymer PEI. The results obtained from this study specify

that cross linking of enzyme not only provides good physical stability but also maintain chemical stability of enzyme which can be observed by conversion of ester in organic solvent. Furthermore, it must also be noted that *Candida rugosa* lipase has 'lid' domain (a polypeptide chain near the active site) that helps lipase to change its conformation from 'closed' to an 'open' i.e. active form. Lipase is inactive in aqueous media, but upon binding to a lipid/water interface, its catalytic activity greatly enhances. In other words the activation of lipase depends critically on the structure of the lipid/water interface. In addition, the solubility of the final product of esterification made organic media such as *n*-hexane the best choice for the esterification reaction.

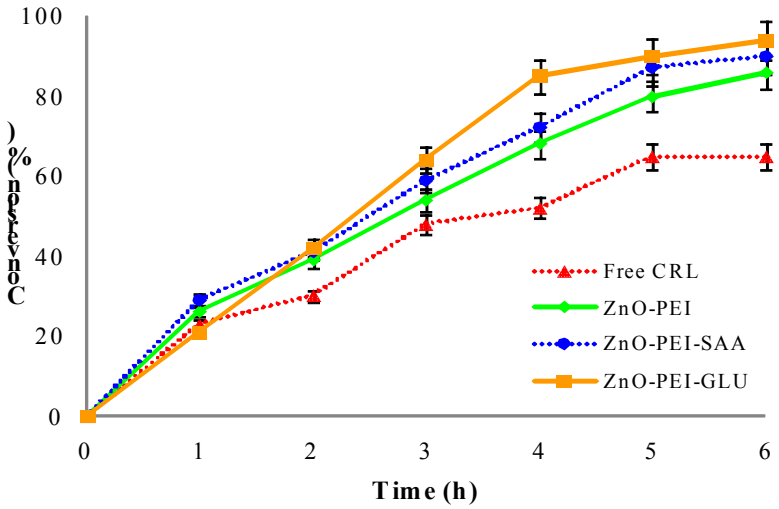

Figure 59: Time course for the synthesis of geranyl acetate by free as well as immobilized lipase using n-hexane as a medium. Reaction conditions: 0.1M geraniol, 0.4M vinyl acetate, 3mL n-hexane, pH 7, temperature 40°C, 150rpm

5.5 Reusability studies

The cost of lipase is one of the limitations in producing terpene esters using the biological enzyme method. If lipase exhibits higher stability during the catalytic reaction and it can be repeatedly used numerous times, then the economic cost can be reduced to a certain extent. However, accumulation of water as byproduct is a major issue for altering the thermodynamic equilibrium of the reaction decreasing activity of lipase. In order to solve this problem, after every 3-4 runs each nanocomposite were treated with 30mg molecular

sieves (4°A) in n-hexane for 24 h. Then these pretreated nanocomposites after dehydration were used for transesterification reaction where significant maintenance in conversion of product was observed demonstrating partial recovery of the lost activity (Fig. 60). The lipase immobilized on ZnO-PEI retained 69% of its initial activity after 20 catalytic rounds, whereas ZnO-PEI-SAA retained 78% of its initial activity. The nanocomposite ZnO-PEI-GLU was the best one, showing only 12% loss of activity retaining 88% of its initial activity after 20 cycles. The results revealed that the strong interactions between lipases and supports significantly increase the enzyme reusability in covalent bonding. However, the gradual decrease in activity of immobilized enzymes arose from the denaturation of protein, the inactivation of the enzyme, and the leakage of protein from the support during sequential application.

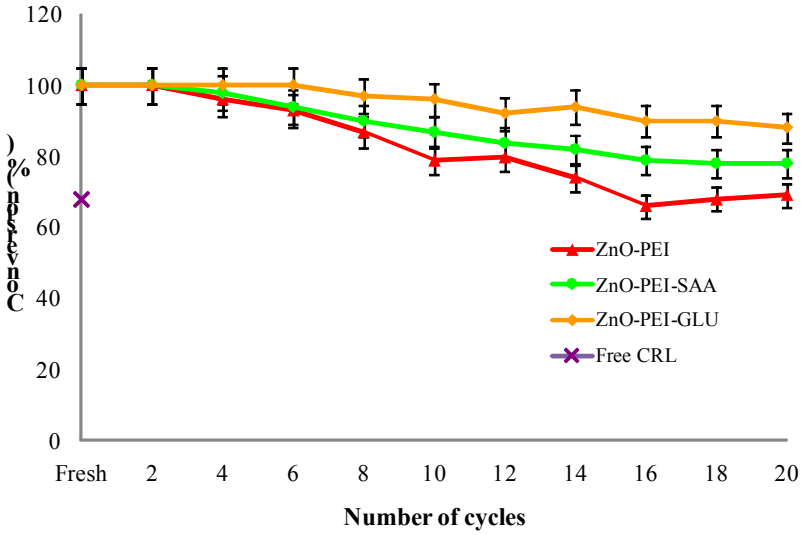

Figure 60: Reusability studies for the synthesis of geranyl acetate using lipase immobilized nanocomposites at pH 7 and 40°C. Reaction conditions: 0.1M geraniol, 0.4M vinyl acetate, 3mL n-hexane, pH 7, temperature 40°C, 150rpm

5.6 Effect of ester and alcohol chain length on synthesis of geraniol acetate

The trend for the effect of the vinyl ester chain length (acetate to butyrate) on synthesis of geranyl ester was studied using nanocomposite of ZnO-PEI-GLU and is exhibited in Fig. 60(a). From the results as describe in Fig. 61(a) it can be depicted that as the ester chain length increases from acetate to butyrate, corresponding yield of product was decreased.

Around 94% of ester was synthesized using acetate whereas only 75% of product was formed using butyrate. There can be two possible reasons for this: (i) higher alkyl chain length leads to decrease in electrophilicity of carbonyl group that slower down nucleophilic attack of geraniol on carbonyl carbon resulting in decreased enzyme-acyl complex formation, (ii) secondly, mass diffusion problem is created with an immobilized enzyme by using higher alkyl groups.

In another set of experiment same nanocomposite (ZnO-PEI-GLU) was used to study the effect of various alcohol chain length (pentanol, hexanol, octanol and geraniol) on synthesis of geranyl acetate. As observed from Fig. 61(b) the synthesis of geraniol acetate using different primary alcohol with shorter chain length was going on increasing from 1-pentanol (78%) to 1-octanol (96%). Accordingly, when geraniol was used as alcohol 93% of ester was synthesized under same condition but was comparatively lower than 1-octanol. The probable reason for this may be steric hindrance effect inhibiting nucleophilic attack that causes slower diffusion of long chain alcohols.

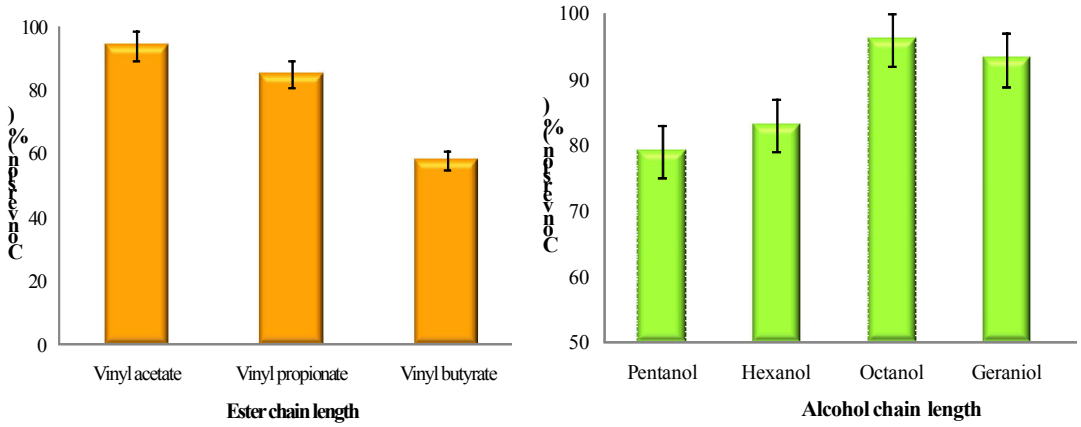

Figure 61: (a) Effect of ester chain length. Reaction condition: Geraniol 0.1M; 0.4M vinyl acetate, 3mL n-hexane, immobilized biocatalyst ZnO-PEI-GLU 50 mg; temperature 40◦C, 150 rpm. (b) Effect of alcohol chain length. Reaction condition: Geraniol 0.1M; 0.4M vinyl acetate, 3mL n-hexane, immobilized biocatalyst ZnO-PEI-GLU 50 mg; temperature 40◦C, 150 rpm

5.7 Kinetic modeling

Kinetic modeling and mechanistic study of a reaction are very important aspects of the reaction designing and to scale up the process. Lipase catalysis involving two substrates

generally follows order bi-bi mechanism. In this study the kinetic model determined for geranyl acetate synthesis was based on Lineweaver-Burk graph constructed by reciprocal of the initial rates at different concentrations of geraniol (as alcohol) for immobilized lipase (ZnO-PEI-GLU) (data not shown). At higher concentration of geraniol, decrease of initial rate with increase in slope was observed which signifies inhibitory effect of alcohol. This fact is also supported by the effect of molar quantity of geraniol (Fig 61(b)). Considering the initial rate, the proposed rate equation for order bi-bi model with inhibition of alcohol is as follows:

$$V = \frac{V_{max}\,[G]\,[VA]}{K_{i(G)}\,K_{m(VA)} + K_{m(G)}\,[VA] + K_{m(VA)}\,[G] + [G]\,[VA]}$$

Where, V= initial rate of reaction, V_{max} = maximum rate of reaction, [G] = initial concentration of geraniol, [VA] = initial concentration of vinyl acetate, $K_{m(G)}$ and $K_{m(VA)}$ = Michaelis-Menten constant of geraniol and vinyl aetate, $K_{i[G]}$ = inhibitory constant of geraniol.

The kinetic parameters were scrutinized by non-linear regression analysis using statistical software XLSTAT version 2015.1.02. According to the kinetic values obtained from order bi-bi mechanism, Michaelis-Menten constant for vinyl acetate i.e. $K_{m(VA)}$ was found to be lower in comparison to that of geraniol $K_{m(G)}$ showing higher affinity of vinyl acetate towards immobilized lipase for formation of acyl-enzyme complex (Table 5.2).

By order bi-bi mechanism (Fig. 62), initially vinyl acetate binds to immobilized lipase (due to higher affinity) and forms acyl-enzyme complex (E-VA). Later on geraniol (alcohol) combines with E-VA complex to form a ternary complex (E-VA-G) and is further isomerized into new complex. This ternary complex was broken down into vinyl alcohol which tautomerized into the acetaldehyde, while binary complex subsequently released desired ester (geranyl acetate) and enzyme.

Table 5.2: Kinetic parameter values for the synthesis of geranyl acetate by lipase immobilized on ZnO-PEI-GLU

Parameters	V_{max} (mmol/L/min)	$K_{m(G)}$ mmol/L	$K_{m(VA)}$ mmol/L	$K_{i(G)}$
Values	2.03 X 10^{-2}	1.3482	0.5743	4.48

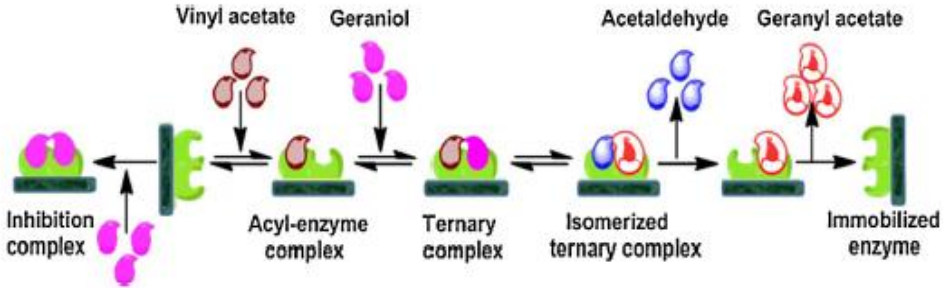

Figure 62: Proposed model for the synthesis of geranyl acetate

(6) Increasing esterification efficiency by double immobilization of lipase-ZnO bioconjugate into AOT-reverse micelles and microemulsion based organogels

6.1 Characterization studies

6.1.1 Physical appearance of MBGs

The prepared MBGs films were uniform and flexible in nature, having slight transparency with white coloration (Figure 63a). While lipase entrapped MBGs exhibited somewhat loss in transparency because of nanocomposite (ZnO-E) (Figure 63b). The control MBGs (without lipase) express thickness values in between 50-65µm; while the MBGs containing lipase presented thickness values in between 65-70µm (using micrometer screw gauge).

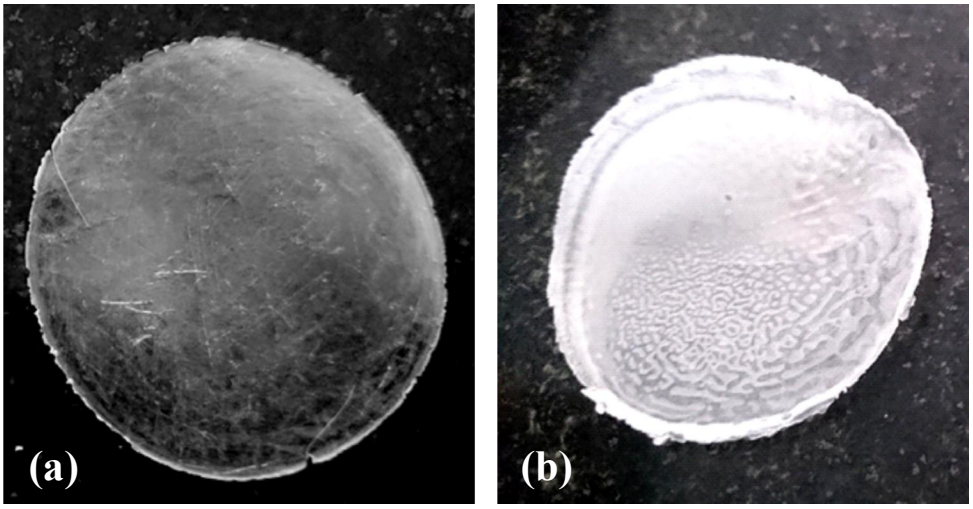

Figure 63: Physical appearance of prepared PVA gels. (a) Control PVA gel without lipase showing transparency and has thickness of 50-65µm. (b) Lipase immobilized PVA gel exhibiting somewhat loss in transparency because of nanocomposite (ZnO-E) and showed thickness values in between 65-70µm.

6.1.2 Fourier Transform Infrared Spectroscopy (FTIR)

The FTIR spectral overlay for all the system studied is shown in Figure 64. FTIR absorption spectrum of lipase (Figure 64(c)) generally shows three major bands caused by peptide group vibrations in the range of 1800-1300 cm-1. Free and immobilized lipase illustrates a characteristic band of amide II with the maximum of 1490 cm-1 due to N-H bending with contribution of C-N stretching vibrations. According to spectra (f), peak at 1451 cm^{-1} indicated C-N stretching of amide bonds hence, showing presence of amide bond formation. This was further supported by peak at 1243 cm^{-1} which can be attributed to the interaction of N-H bending and C-N stretching of amide bond. Furthermore, it is observed that these amide regions are absent in the FT-IR spectrum of ZnO and PVA control (Figure 64(a) and 64(e), respectively addressing strong presence of amide bonds confirming the existence of lipase. Looking at the spectra, it was observed that the immobilization of lipase onto ZnO nanoparticles using reverse micelles as well as organogels proceeded via covalent bonding and not merely physical deposition or adsorption.

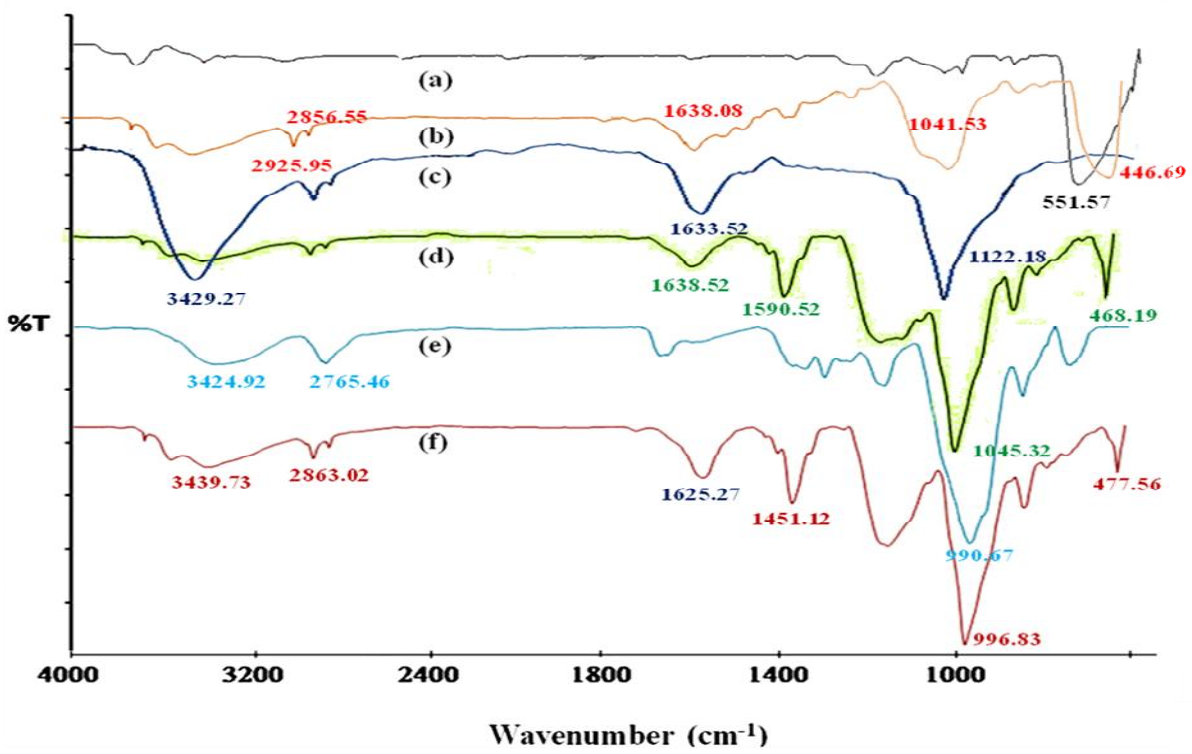

Figure 64: FTIR spectrum for free as well as all the prepared immobilized lipase systems. (a) pristine ZnO, (b) ZnO-E, (c) Free lipase, (d) ZnO-E@RM, (e) PVA control and (f) ZnO-E-RM@PVA.

6.1.3 Thermal Gravimetric Analysis (TGA)

The successful functionalization was also reflected in TGA curves performed using *Mettler Toledo*. Figure 65 shows TGA curves in nitrogen upto 700°C at heating rate of 20°C min^{-1}. It can be observed from the curve that pristine ZnO showed very small weight loss below 200°C, but significant weight loss of 2.8% was attain at 550°C. However, for free lipase gradual decrease in weight loss was observed with increase in the temperature above 100°C. The gradual decrease in weight is much obvious due to loss of bound water molecule. For all the immobilized enzymes curves (i.e. ZnO-E, ZnO-E@RM and ZnO-E-RM@PVA), nearly 10% of weight loss was observed at around 100°C and steeply decreasing thereafter with much faster rate above 400°C. This attributes to thermo-decomposition of lipase indicating successful enzyme immobilization.

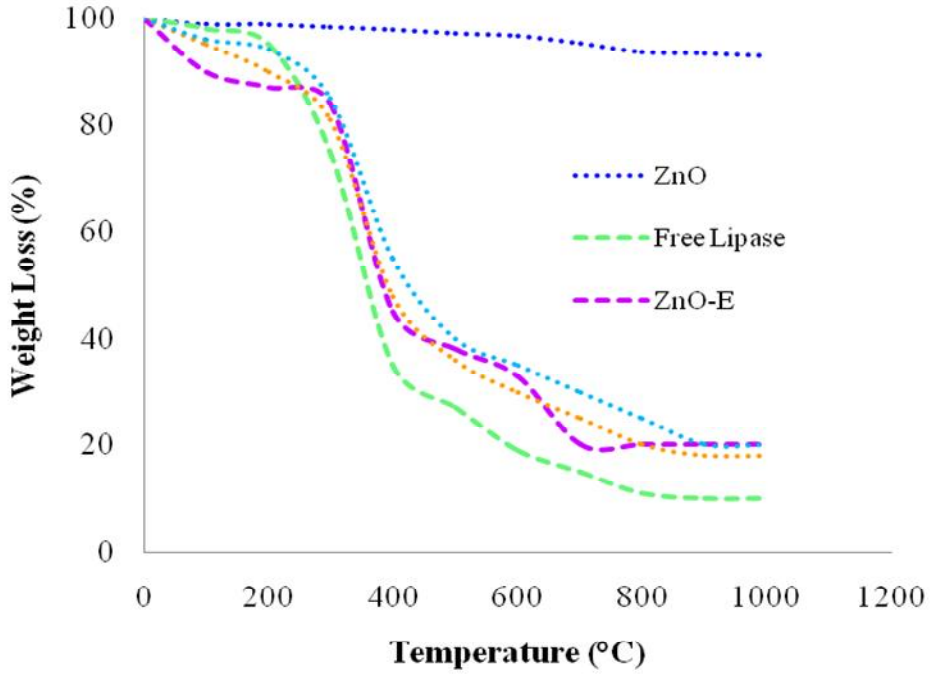

Figure 65: TGA curves showing % weight loss for the respective free as well as immobilized lipase system at temperature ranging from 0 10 1000°C.

6.2 pH, temperature and storage stability

6.2.1 Effect of pH on enzyme stability

The effect of pH on relative activity of the free and immobilized lipase using various immobilization matrix as enzyme supports was determined within the range of 5-10 at 37°C and the results are graphically presented in Figure 66. The obtained results demonstrate that free as well as immobilized lipase preparations exhibit typical bell-shaped curves with maximum relative activity at pH 8. However, immobilized lipase resulted in maintaining excellent adaptability at a wider pH range with higher relative activity. The lipase entrapped into polymer ZnO-E-RM@PVA represented a higher relative activity of 89% at pH 8 than that of ZnO-E@RM and ZnO-E with 80% and 75%, respectively. Free lipase retained 68% of its initial activity under same condition. The quantized increase in the pH stability profile for all the immobilized lipase preparations (viz: ZnO-E-RM@PVA>ZnO-E@RM>ZnO-E) can be argued by two reasons. Firstly, immobilization into reverse micelles supplied much more stable biocatalyst against pH which might be ascribed to the restriction in conformational changes following pH

change. Secondly, the entrapment of such stable enzyme into hydrophilic polymer produces a suitable charge difference by enhancing the electrostatic interaction between enzyme and carrier.

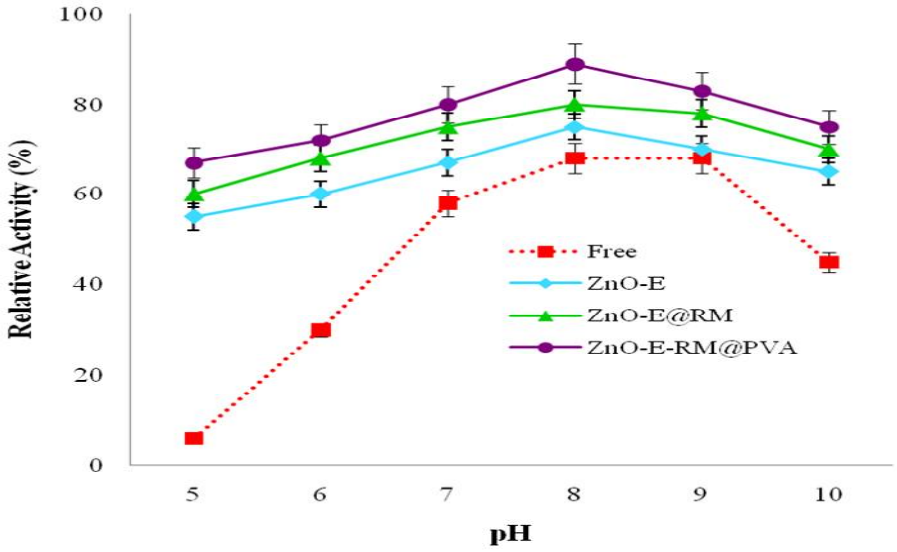

Figure 66: pH stability curves for free and immobilized lipase preparations. The effect of pH on enzyme stability was determined using different buffers of citrate (100mM, pH 5-6), phosphate (100mM, pH 7-8) and Tris-HCl (100mM, pH 9-10) for 1h at 37°C followed by measuring the relative activity of enzyme.

6.2.2 Effect of temperature on enzyme stability

In order to assess the thermal stability profile we have measured relative activity of free as well as all the forms of immobilized enzyme by pre-incubating at different temperatures (20-60°C) for 1h. The results of temperature stability revealed that lipase entrapped in ZnO-E-RM@PVA matrix is much better than that of the corresponding free enzyme (Figure). ZnO-E-RM@PVA exhibited maximum relative activity of 97% within 40-50°C higher in comparison to the free lipase which was only 60% under same condition (Figure 67). However, free enzyme actually decays with time at faster rate as compared to immobilized enzyme. Furthermore, the comparison of the relative activities for ZnO-E@RM (85%) and ZnO-E (80%) at higher temperature indicates the better diffusion of substrate and limitation of enzymatic movement after immobilization on applied support.

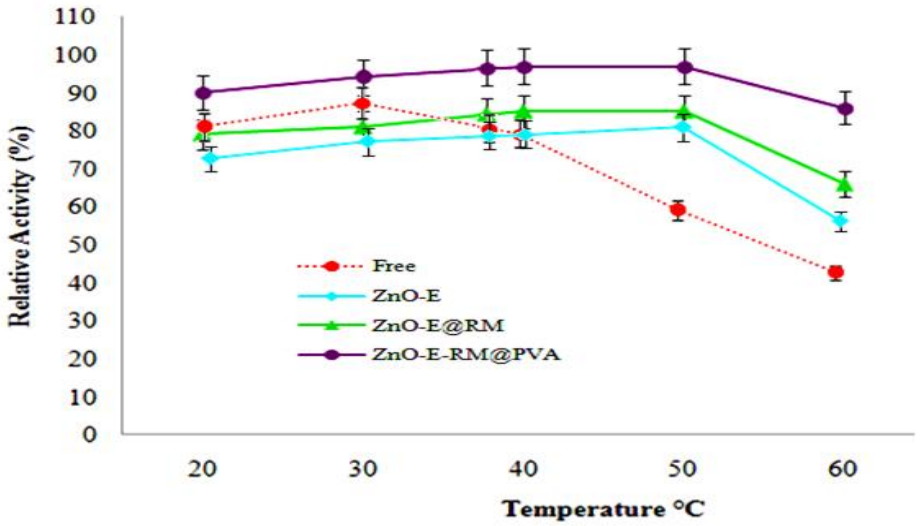

Figure 67: Temperature stability for free and immobilized lipase preparations. The thermal stability of free or immobilized lipases was determined by incubating the enzyme in water bath for 1h at the temperature ranging from 20-50°C followed by measuring the relative activity of enzyme.

6.2.3 Effect of storage on enzyme stability

The storage stability of the free and immobilized lipases was investigated for 20 days in phosphate buffers (pH 8) stored at 4°C. The evaluation of the storage stability for entrapped lipase demonstrated that it increases in the range: ZnO-E-RM@PVA>ZnO-E@RM>ZnO-E>Free lipase. The study revealed that only 26% of the initial activity of free lipase remained after 20 days of incubation at 4°C, whereas ZnO-E, ZnO-E@RM and ZnO-E-RM@PVA retained 81%, 87% and 94% of their initial activities, respectively (Figure 68). The study clearly demonstrates that the prepared double immobilization system (i.e. ZnO-E-RM@PVA) exhibits good stability with no significant decrease in activity during storage periods of 20 days at 4°C. Ample of literatures have stated that enzyme which are entrapped into polymers consist of higher stabilities are most resistant to denaturation effect of organic solvent in biotransformation.

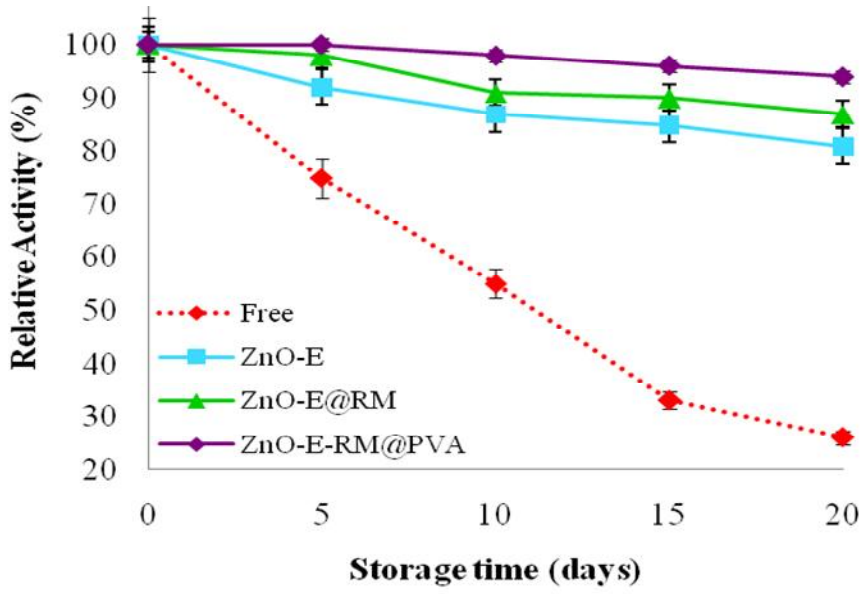

Figure 68: Storage stability curves for free and immobilized lipase preparations. The storage stability was determined by relative activity measurements of free and immobilized lipase for 15 days at 4°C

6.3 Possible reasons for enhanced stability for ZNO-E-RM@PVA immobilization system

There are three main possible reasons for enhanced lipase activity in prepared double immobilization system (ZnO-E-RM@PVA). (i) In the case of ZnO-E, the spacer arm of glutraldehyde assisted the support to covalently attach lipase via surface residues that boost enzyme loading on the surface of ZnO-E. (ii) The confinement of ZnO-E inside the water pool of AOT-reverse micelles led to the formation of larger sized reverse micelle with higher interfacial area. This augmented interfacial area possibly helped in smooth occupancy of lipase and high local concentration of enzyme and substrate resulting in remarkable improvement in lipase activity. Also the enhanced hydrophobic environment due to incorporation of ZnO-E at the interface might lead to the unfolding of the lid and provided accessibility of the substrate to the active region of lipase (iii) Due to entrapment into microemulsion based organogels, limitation of enzymatic movement after immobilization on support together with better substrate diffusion at a higher temperature improves activity of immobilized lipase.

Thus, the developed double immobilization system of lipase was further used for biocatalytic transformation under organic solvents. The MBG consists of a polymer net in which the enzyme-containing microemulsion is entrapped and is actually a semi solid catalyst was preferred for further study rather than working directly with reversed micelles. This decision was based on the advantages presented by heterogeneous catalysis over homogeneous one, such as reuse of the catalyst and easier product isolation.

6.4 Biocatalytic transformation of esters

Synthesis of flavors and fragrance esters using immobilized lipase has received immense attention during the last decades. The study was carried out in order to compare potential of free as well as immobilized lipase (ZnO-E-RM@PVA) for synthesis of esters in organic solvents. The results obtained from optimization revealed that the molar ratio of 2:1 for acid/alcohol at 40°C temperature were the most suitable conditions to get enhanced lipase activity assisted by lipase immobilized on ZnO-E-RM@PVA (Figure 69). Further it was found that increasing alcohol concentration (than that of optimized) leads to decrease in esterification efficiency. This can be attributed to inhibitory effect of higher alcohol concentration on lipase activity which is illustrated in Figure 68. However, as shown in Figure 70, using optimized conditions 90% of ethyl valerate and 86% of pentyl valerate was obtained after 8h of reaction at 40°C while free lipase attain only 50% of ester synthesis under the same condition.

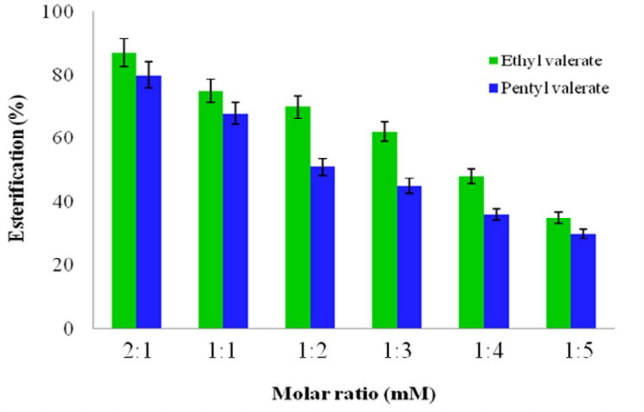

Figure 69: Influence of acid/alcohol concentration on the efficiency of ester synthesis for lipase immobilized into PVA gel. Reaction conditions: n-hexane (2mL), 100mM 1:1 valeric acid/ethanol or valeric acid/1-pentanol separately (acid/alcohol molar ratios of 2:1. 1:1, 1:2, 1:3, 1:4 and 1:5) at 40°C, 150rpm.

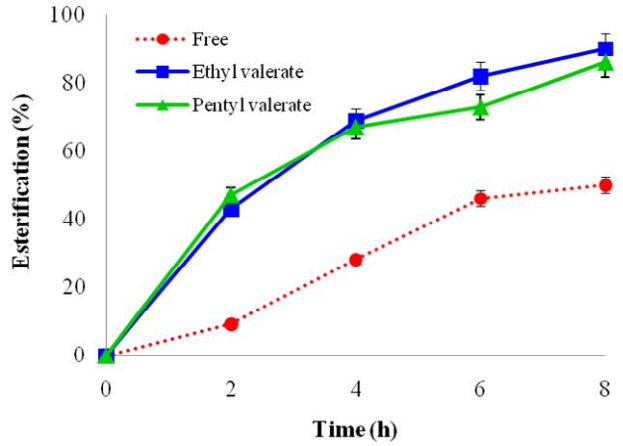

Figure 70: Time course for the synthesis of ethyl and pentyl valerate by free as well as immobilized lipase (ZnO-E-RM@PVA) using n-hexane as a reaction medium. Reaction conditions: 2:1 acid/alcohol molar ratio, 3mL n-hexane, pH 8, temperature 40°C, 150rpm.

The results obtained from reusability experiments of the immobilized lipase (ZnO-E-RM@PVA) in n-hexane showed mild decrease in the activity of lipase after 4 cycles, thereafter a gradual decrease in activity was observed upto 10 cycles. However, the immobilized enzyme retained 87% and 85% of its initial activity for synthesis of ethyl valerate and pentyl valerate, respectively after 10 catalytic rounds (Figure 71). The decrease in catalytic activity may be ascribed to (i) the unfavorable effect of water (released as byproduct during esterification reaction) and (ii) prolonged exposure to the polar organic solvents.

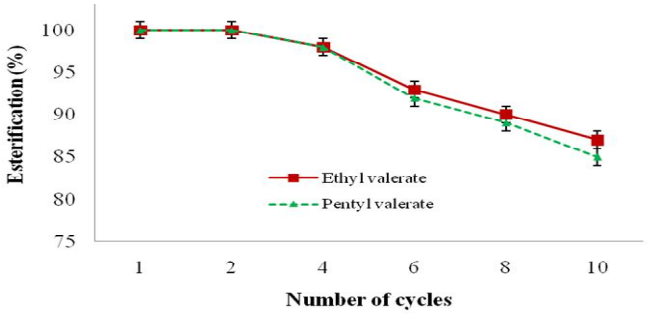

Figure 9: Reusability study for the synthesis of short chain esters using ZnO-E-RM@PVA entrapment lipase at pH 8 and 40°C. Reaction conditions: Reaction conditions: 2:1 acid/alcohol molar ratio, 3mL n-hexane, pH 8, temperature 40°C, 150rpm

✓ ***Summary and Conclusion***

- Present study reflects the detection of microbial diversity across oil stress condition favouring *β-proteobacteria* such as *Chromobacterium, Xanthomonas, Pseudomonas, Burkholderia* and *Acinetobacter sp.* The microbial community analysis at the metagenome level gives an insight into the repertoire of species to deal with oil contamination. We also observed, genes corresponding to enzymes involved in a wide variety of reactions and operating in many unrelated biosynthesis pathways collaborates well with the fact that the site of study has long-term oil contamination. In this regard, obtained knowledge will be useful in understanding the pathways for synthesis and metabolism of fatty acids released for oils and the microbial communities dominating in such stress condition.

- An extracellular lipase from solvent tolerant *Pseudomonas* sp. DMVR46 was purified following simple purification procedure with 29.74% recovery. The molecular mass of the lipase was found to be ~32.0 kDa by SDS-PAGE. It exhibited optimum activity at pH 8.5 and 37°C. Among various p-nitrophenyl esters with different chain lengths, the lipase showed maximum activity on p-nitrophenyl palmitate (C16). The enzyme exhibited significant stability in presence of iso-octane and cyclohexane and was activated by Ca^{+2}, Ba^{+2} and Mg^{+2} but SDS and EDTA has negative influence on its activity. The partially purified lipase showed significant esterification activity for synthesis of pentyl valerate and revealed improved catalytic efficiency upon immobilization in microemulsion based organogels.

- Functionalized EGO's were characterized by Transmission Electron Microscopy (TEM), Scanning Electron Microscopy (SEM), Fourier Transform Infrared spectroscopy (FTIR) analysis, Raman spectroscopy and Thermal Gravimetric Analysis (TGA). Modified EGO were employed as a supporting matrix for *Candida rugosa* lipase immobilization and further applied in the synthesis of flavor ester ethyl caprylate. Various conditions were optimized and maximum ester production was obtained at 40°C with caprylic acid/ethanol ratio of 0.15:0.1M using cyclo-octane as a reaction

medium. A yield of 85% for ethyl caprylate was observed using lipase immobilized on modified EGO which was higher as compared to that of free lipase.

- Immobilization of lipase onto functionalized CdS nanoparticles provides a simple approach to improve activity, stability and reusability of enzyme for enhanced pentyl valerate synthesis. The kinetics of free and immobilized lipase implies that the enzyme undergoes conformational changes during immobilization which results in lower activation energy requirement. Additionally, the altered specificity of the immobilized lipase exhibited higher esterification activity (84%) in comparison to the free enzyme (50%).

- The results obtained from the present study showed that, among the three prepared nanocomposites, ZnO-PEI-GLU was the best biocatalyst, showing higher ester synthesis (94% after 6h incubation at 40ºC) compared with the other nanostructures containing lipase as well as free lipase. The biocatalytic application evaluates the enhancement of immobilized lipase with 2.23 fold over that of free lipase. Various kinetic parameters were refined by nonlinear regression analysis indicating inhibition effect of geraniol. In addition to this energy of activation was determined showing lower energy requirement for immobilized lipase. Furthermore alkyl ester and alcohol chain length effect was studied to understand the influence of the chain length on immobilized enzyme activity. The reusability of covalently immobilized lipase showed that there is not significant leakage of enzyme during repeated use and 88% activity remains after 20 cycles. This approach proved to be a facile, mild and environmental friendly method for synthesizing flavor ester geranyl acetate.

- In particular, a versatile method for double immobilization of Candida rugosa lipase was developed successfully on microemulsion based organogels and was well characterized using FTIR and TGA. Thermal and pH stabilities of lipase immobilized on ZnO-E-RM-@PVA were improved in comparison with those of free and other modified analogues. In addition, esterification experiments revealed that ZnO-E-

RM@PVA was the best immobilization system for the synthesis of ethyl and pentyl valerate compared with that of free lipase. Reusability study revealed meager loss of initial lipase activity even after 10 cycles. In nutshell, the facile synthesis procedure is easy to implement and enables the selective separation of enzymes from reaction mixtures.

- **Publication:**

1. Patel V, Nambiar S, Madamwar D. An extracellular solvent stable lipase from *Pseudomonas sp.* DMVR46: Partial purification, characterization and application in non-aqueous environment. *Process Biochemistry* 2014; 40: 1673-1681.

2. Patel V, Gajera H, Gupta A, Manocha L, Madamwar D. Synthesis of ethyl caprylate in organic media using *Candida rugosa* lipase immobilized on exfoliated graphene oxide: Process parameters and reusability studies. *Biochemical Engineering Journal* 2015; 95: 62-70.

3. Patel V, Madamwar D. Solvent tolerant Pseudomonas sp. DMVR46 strain adsorb on multiwalled caron nanotubes: application for enzymeatic biotransformation in organic solvents. *Applied Biochemistry and Biotechnology* 2015; 117, 1313-1326.

4. Patel V, Sharma A, Lal R and Madamwar D. Response and resilience of soil microbial communities inhabiting in edible oil stress/contamination from industrial estates. *In Press BMC Microbiology* 2016; 16:50.

5. Patel V, Shah C, Deshpandey M, Madamwar D. Zinc oxide nanoparticles supported lipase immobilization for biotransformation in organic solvents: A facile synthesis of geranyl acetate, effect of operative variables and kinetic study. *Applied Biochemistry and Biotechnology* 2016; 178: 1630-1651.

6. Patel V, Deshpande M, Madamwar D. Increasing esterification efficiency by double immobilization of lipase-ZnO bioconjugate into sodium bis(2-ethylhexyl) sulfosuccinate (AOT)-reverse micelles and microemulsion based organogels. *Biocatalysis and Agricultural Biotechnology* 2017; 10: 182-188.

7. Patel V, Deshpandey M, Pandey A, Larroche C, Madamwar D. Nanobiocatalysis for synthesis of pentyl valerate in organic solvents: Characterization, optimization and reusability. Manuscript accepted in *Current Biotechnology*.

8. Patel V, Madamwar D. Advances in nanobiocatalysis: strategies for lipase immobilization and stabilization. A chapter communicated for book :Advances in Nanostructured Composites".

(iii) Has the progress been according to original plan of work and towards achieving the objective. if not, state reasons: **Yes**

(iv) Please indicate the difficulties, if any, experienced in implementing the project: Grant is not available. Remaining grant has to be released at earliest.

(v) If project has not been completed, please indicate the approximate time by which it is likely to be completed. A summary of the work done for the period (Annual basis) may please be sent to the Commission on a separate sheet: **N/A**

(vi) If the project has been completed, please enclose a summary of the findings of the study. One bound copy of the final report of work done may also be sent to University Grants Commission: **N/A**

(vii) Any other information which would help in evaluation of work done on the project. At the completion of the project, the first report should indicate the output, such as (a) Manpower trained (b) Ph. D. awarded (c) Publication of results (d) other impact, if any

(a) Manpower – **Miss Vrutika Patel**.

(b) Ph. D. awarded – **Miss Vrutika Patel** has been awarded Ph.D.

(c) Publication of results – Seven papers has been published and one chapter is communicated.

Paper publication:

1. Patel V, Nambiar S, Madamwar D. An extracellular solvent stable lipase from *Pseudomonas sp.* DMVR46: Partial purification, characterization and application in non-aqueous environment. *Process Biochemistry* 2014; 40: 1673-1681.

2. Patel V, Gajera H, Gupta A, Manocha L, Madamwar D. Synthesis of ethyl caprylate in organic media using *Candida rugosa* lipase immobilized on exfoliated graphene oxide: Process parameters and reusability studies. *Biochemical Engineering Journal* 2015; 95: 62-70.

3. Patel V, Madamwar D. Solvent tolerant Pseudomonas sp. DMVR46 strain adsorb on multiwalled caron nanotubes: application for enzymeatic biotransformation in organic solvents. *Applied Biochemistry and Biotechnology* 2015; 117, 1313-1326.

4. Patel V, Sharma A, Lal R and Madamwar D. Response and resilience of soil microbial communities inhabiting in edible oil stress/contamination from industrial estates. *In Press BMC Microbiology* 2016; 16:50.

5. Patel V, Shah C, Deshpandey M, Madamwar D. Zinc oxide nanoparticles supported lipase immobilization for biotransformation in organic solvents: A facile synthesis of geranyl acetate, effect of operative variables and kinetic study. *Applied Biochemistry and Biotechnology* 2016; 178: 1630-1651.

6. Patel V, Deshpande M, Madamwar D. Increasing esterification efficiency by double immobilization of lipase-ZnO bioconjugate into sodium bis(2-ethylhexyl) sulfosuccinate (AOT)-reverse micelles and microemulsion based organogels. *Biocatalysis and Agricultural Biotechnology* 2017; 10: 182-188.

7. Patel V, Deshpandey M, Pandey A, Larroche C, Madamwar D. Nanobiocatalysis for synthesis of pentyl valerate in organic solvents: Characterization, optimization and reusability. Manuscript accepted in *Current Biotechnology*.

8. Patel V, Madamwar D. Advances in nanobiocatalysis: strategies for lipase immobilization and stabilization. A chapter communicated for book :Advances in Nanostructured Composites".

(d) Other impact, if any – Miss Vrutika Patel has also presented her work in many conferences including International Conferences.

1. International conference on "Advances in biotechnology and bioinformatics" ICABB-2013 and X convention of the Biotech Research Society India (BRSI), November 25-27, 2013, organized by Dr. D.Y. Patil Vidhyapeeth, Pune, India. Presented poster on "Immobilization of *Candida rugosa* lipase on silane modified CdS nanoparticles for multicycle enzymatic production of pentyl valerate under water restricted environment".

2. International conference on Integrating Basic and Translational Research in Modern Biology organized by Department of Microbiology and Biotechnology Center, Maharaja Sayajirao University, Baroda on 27-28th December 2013.

3. Workshop on "Art of Science Communication", February 22, 2014, organized by BRD School of Biosciences, Vallabh Vidhyanagar, Gujarat, India.

4. National symposium on "Microbial biotechnology: Advances and future trends-2014", February 26, 2014, organized by Department of Microbiology and Department of Biotechnology, Genetics and Bioinformatics, N.V. Patel College of Pure and Applied Sciences, Vallabh Vidhyanagar, Anand, India. Presented poster on "Nanobioconjugate of *Candida rugosa* lipase with functionalized graphene oxide: characterization and application in non-aqueous biocatalysis" and secured **THIRD** prize.

5. Science meet – 2014 organized by Gujarat Science Academy (GSA), Charotar University of Science and Technology (CHARUSAT), and CC Patel Community Science Center, Sardar Patel University, Vallabh Vidhyanagar on 9th November, 2014.
6. International conference on "Biotechnology and Bioengineering" (ICBB) organized by Microbiologists Society, Dr, Babasaheb Ambedkar Marathwada University, Aurangabad and Birla Institute of Technology & Science, Pilani, Dubai Campus (U.A.E) during 29th – 30th October 2014. Presented poster on "Immobilization of *Candida rugosa* lipase on silane modified cadmium sulphide nanoparticles for multicycle production of pentyl valerate in organic solvents" and secured **FIRST** prize.

7. 55th Association of Microbiologists of India (AMI) National conference on "Empowering Mankind with Microbial Technologies" organized by Tamil Nadu Agriculture University, Coimbatore on 12th – 14th November 2014. Presented poster on "An extracellular solvent tolerant stable alkaline lipase from *Pseudomonas sp*. DMVR46: Partial purification, characterization and application in non-aqueous environment".

8. 3rd Global Sustainable Biotech Congress, International conference organized by North Maharashtra University, Jalgaon in collaboration with Global Biotech Forum, Nagpur and CETYS University, Mexico on 1st – 5th December 2014. Presented poster on "Synthesis of ethyl caprylate in organic media using *Candida rugosa* lipase immobilized on exfoliated graphene oxide: Process parameters and reusability studies".

9. UGC Sponsored National Conference on "Latest Development in Basic and Applied Sciences" organized by M.B. Patel Science College, Anand on 10th January, 2015. Presented poster on "Nanobioconjugate of *Candida rugosa* lipase and exfoliated graphene oxide: characterization and applications in non-aqueous biocatalysis" and secured **FIRST** prize.

10. Hands on training on the topic entitled "Analysis of metagenomic data using bioinformatics tools" in the Department of Zoology, University of Delhi from 15-28th January, 2015.

11. Hands on training on "Preparation of various polymer based microspheres and their degradation" in Biofouling and Biofilm Processes Section, Water and Steam Chemistry Division, BARC Facilities, Kalpakkam from 5-15th October, 2015.

12. International conference on "New Horizons in Biotechnology" 12th BRSI convention held at NIIST Trivandrum, Kerala on 23-25th November, 2015. Presented poster on "Lipase mediated nanobiocatalysis using zinc oxide nanoparticles: Characterization and application in organic synthesis".

13. International conference on "Recent Trends in Applied Sciences: Building Institutional and Industrial Avenues (ICRTAS – 2015)" held at A.N Patel Post Graduate Institute, Anand on 10-12th December, 2015. Oral presentation on "Lipase mediated nanobiocatalysis: Exploiting ester synthesis in organic solvents" awarded **SECOND** prize.

14. National symposium on "Exploring Advances in Biological Sciences (EABS-2016)" held at MP Patel auditorium organized by BRD School of Biosciences, Vallabh Vidyanagar, Bakrol on 5th March, 2016. Presented poster on "Biodegradable polymeric nanoparticles based drug delivery system for medical application" and secured **BEST POSTER** award.

PRINCIPAL INVESTIGATOR

REGISTRAR

Annexure-IX

UNIVERSITY GRANTS COMMISSION
BAHADUR SHAH ZAFAR MARG
NEW DELHI-110002

PROFORMA FOR SUBMISSION OF INFORMATION AT THE TIME OF SENDING THE FINAL REPORT OF THE WORK DONE ON THE PROJECT

1. **Title of the Project:** Molecular assessment of bacterial community structures of long term oil contaminated soil and screening of lipase producers for lipase production and their application in ester synthesis in organic solvents.

2. Name and address of the Principal Investigator: Prof. Datta Madamwar

3. Name and address of the Institution: BRD School of Biosciences,
Sardar Patel University 388120,
Anand, Gujarat

4. UGC approval letter no. and date: F.42-167/2013(SR) Dated 22-03-2014

5. Date of implementation: April 01, 2013

6. **Tenure of the Project:** Three years and extended for one more year Total 4 Years

7. Total grant allocated: Rs. 13,55,800/-

8. Total grant received: Rs. 12,18,520/-

9. Final Expenditure: Rs. 13,54,053/-

10. Title of the project: Molecular assessment of bacterial community structures of long term oil contaminated soil and screening of lipase producers for lipase production and their application in ester synthesis in organic solvents.

11. Objectives of the project:
Objectives:

1. To isolate and screen indigenous lipase producing microbial strains from oil-contaminated soil sites. Physico-chemical analysis of the oil contaminated soil mainly soil texture, moisture, pH, nutrients, total organic carbon, heavy metals etc.

2. Development of method for the extraction of metagenome from oil contaminated soil which is suitable for further molecular analysis work such as PCR amplification, restriction digestion etc.
3. To assess bacterial community structure of oil contaminated soil using cultivation dependant and cultivation independent analyses.
4. To study the community structure of lipase producers following 16S rRNA gene analysis of oil contaminated sites.
5. Optimization of important parameters effecting lipase production for obtaining high yields, purification and physicochemical characterization of lipases.
6. Exploitation of lipases following various immobilization techniques including microemulsion based organogels to improve esterification in organic solvents.

12. Whether objectives were achieved: Yes

13. Achievements from the project: Principal Investigaton has provided a concept for the enzyme catalysis in apolar organic solvents without the loss of enzyme activity. Bacterial community has been determined following metagenomic approach showing the role of various genes in controlling environment.

14. Summary of findings:

- Present study reflects the detection of microbial diversity across oil stress condition favouring *β-proteobacteria* such as *Chromobacterium, Xanthomonas, Pseudomonas, Burkholderia*and*Acinetobacter sp.* The microbial community analysis at the metagenome level gives an insight into the repertoire of species to deal with oil contamination. We also observed, genes corresponding to enzymes involved in a wide variety of reactions and operating in many unrelated biosynthesis pathways collaborates well with the fact that the site of study has long-term oil contamination. In this regard, obtained knowledge will be useful in understanding the pathways for synthesis and metabolism of fatty acids released for oils and the microbial communities dominating in such stress condition.

- An extracellular lipase from solvent tolerant *Pseudomonas* sp. DMVR46 was purified following simple purification procedure with 29.74% recovery. The molecular mass of the lipase was found to be ~32.0 kDa by SDS-PAGE. It exhibited optimum activity at pH 8.5 and 37°C. Among various p-nitrophenyl esters with different chain lengths, the lipase showed maximum activity on p-nitrophenylpalmitate (C16). The enzyme exhibited significant stability in presence of iso-octane and cyclohexane and was activated by Ca^{+2}, Ba^{+2} and Mg^{+2} but SDS and EDTA has negative influence on its activity. The partially purified lipase showed significant esterification activity for synthesis of pentylvalerate and revealed improved catalytic efficiency upon immobilization in microemulsion based organogels.

- Functionalized EGO's were characterized by Transmission Electron Microscopy (TEM), Scanning Electron Microscopy (SEM), Fourier Transform Infrared spectroscopy (FTIR) analysis, Raman spectroscopy and Thermal Gravimetric Analysis (TGA). Modified EGO were employed as a supporting matrix for *Candida rugosa*lipase immobilization and further applied in the synthesis of flavor ester ethyl caprylate.Various conditions were optimized and maximum ester production was obtained at 40°C with caprylic acid/ethanol ratio of 0.15:0.1M using cyclo-octane as a reaction medium. A yield of 85% for ethyl caprylate was observed using lipase immobilized on modified EGO which was higher as compared to that of free lipase.

- Immobilization of lipase onto functionalized CdS nanoparticles provides a simple approach to improve activity, stability and reusability of enzyme for enhanced pentylvalerate synthesis. The kinetics of free and immobilized lipase implies that the enzyme undergoes conformational changes during immobilization which results in lower activation energy requirement.Additionally, the altered specificity of the immobilized lipase exhibited higher esterification activity (84%) in comparison to the free enzyme (50%).

- The results obtained from the present study showed that, among the three prepared nanocomposites, ZnO-PEI-GLU was the best biocatalyst, showing higher ester synthesis (94% after 6h incubation at 40ºC) compared with the other nanostructures containing lipase as well as free lipase. The biocatalytic application evaluates the enhancement of immobilized lipase with 2.23 fold over that of free lipase. Various kinetic parameters were refined by nonlinear regression analysis indicating inhibition effect of geraniol. In addition to this energy of activation was determined showing lower energy requirement for immobilized lipase. Furthermore alkyl ester and alcohol chain length effect was studied to understand the influence of the chain length on immobilized enzyme activity. The reusability of covalently immobilized lipase showed that there is not significant leakage of enzyme during repeated use and 88% activity remains after 20 cycles. This approach proved to be a facile, mild and environmental friendly method for synthesizing flavor ester geranyl acetate.

- In particular, a versatile method for double immobilization of Candida rugosa lipase was developed successfully on microemulsion based organogels and was well characterized using FTIR and TGA. Thermal and pH stabilities of lipase immobilized on ZnO-E-RM-@PVA were improved in comparison with those of free and other modified analogues. In addition, esterification experiments revealed that ZnO-E-RM@PVA was the best immobilization system for the synthesis of ethyl and pentylvalerate compared with that of free lipase. Reusability study revealed meager loss of initial lipase activity even after 10 cycles. In nutshell, the facile synthesis procedure is easy to implement and enables the selective separation of enzymes from reaction mixtures.

15. Contribution to the Society: Our study has provided information how microbial community get perturbed due to long term oil contamination. Studying microbial community provide indication of contamination which is highly useful for the society.

16. Whether any ph.d enrolled/produced out of the project: Yes, Miss Vrutika Patel got her Ph.D from project work

17. No. Of publication out of the project:

Seven Research Papers in International Journals of high repute and one Book Chapter

Paper publications:

i. Patel V, Nambiar S, Madamwar D. An extracellular solvent stable lipase from *Pseudomonas sp.* DMVR46: Partial purification, characterization and application in non-aqueous environment. *Process Biochemistry* 2014; 40: 1673-1681.

ii. Patel V, Gajera H, Gupta A, Manocha L, Madamwar D. Synthesis of ethyl caprylate in organic media using *Candida rugosa*lipase immobilized on exfoliated graphene oxide: Process parameters and reusability studies. *Biochemical Engineering Journal* 2015; 95: 62-70.

iii. Patel V, Madamwar D. Solvent tolerant Pseudomonas sp. DMVR46 strain adsorb on multiwalledcaron nanotubes: application for enzymeatic biotransformation in organic solvents.*Applied Biochemistry and Biotechnology* 2015; 117, 1313-1326.

iv. Patel V, Sharma A, Lal R and Madamwar D. Response and resilience of soil microbial communities inhabiting in edible oil stress/contamination from industrial estates. *In PressBMC Microbiology*2016; 16:50.

v. Patel V, Shah C, Deshpandey M, Madamwar D. Zinc oxide nanoparticles supported lipase immobilization for biotransformation in organic solvents: A facile synthesis of geranyl acetate, effect of operative variables and kinetic study.*Applied Biochemistry and Biotechnology* 2016; 178: 1630-1651.

vi. Patel V, Deshpande M, Madamwar D. Increasing esterification efficiency by double immobilization of lipase-ZnObioconjugate into sodium bis(2-ethylhexyl) sulfosuccinate (AOT)-reverse micelles and microemulsion based organogels.*Biocatalysis and Agricultural Biotechnology* 2017; 10: 182-188.

vii. Patel V, Deshpandey M, Pandey A, Larroche C, Madamwar D. Nanobiocatalysis for synthesis of pentylvalerate in organic solvents: Characterization, optimization and reusability. Manuscript accepted in *Current Biotechnology*.

viii. Patel V, Madamwar D. Advances in nanobiocatalysis: strategies for lipase immobilization and stabilization. A chapter communicated for book :Advances in Nanostructured Composites".

(PRINCIPAL INVESTIGATOR) **(REGISTRAR)**

Biochemical Engineering Journal 95 (2015) 62–70

Contents lists available at ScienceDirect

Biochemical Engineering Journal

journal homepage: www.elsevier.com/locate/bej

Regular article

Synthesis of ethyl caprylate in organic media using *Candida rugosa* lipase immobilized on exfoliated graphene oxide: Process parameters and reusability studies

Vrutika Patel[a], Hasmukh Gajera[b], Anamika Gupta[a], Lalit Manocha[b], Datta Madamwar[a,*]

[a] BRD School of Biosciences, Satellite Campus, Vadtal Road, P.O. Box # 39, Sardar Patel University, Vallabh Vidhyanagar, Anand 388 120, Gujarat, India
[b] Department of Materials Science, Sardar Patel University, Vallabh Vidhyanagar, Anand 388 120, Gujarat, India

ARTICLE INFO

Article history:
Received 8 October 2014
Received in revised form
27 November 2014
Accepted 13 December 2014
Available online 17 December 2014

Keywords:
Exfoliated graphene oxide
Candida rugosa lipase
Adsorption
Biocatalysis
Immobilization
Kinetic parameters

ABSTRACT

Present work elucidates a general method for biocompatible modification and functionalization of exfoliated graphene oxide (EGO) via direct reaction of organic silane on the surface of nanosheets. Functionalized EGO's were characterized by transmission electron microscopy (TEM), scanning electron microscopy (SEM), Fourier transform infrared spectroscopy (FTIR) analysis, Raman spectroscopy and thermal gravimetric analysis (TGA). Modified EGO were employed as a supporting matrix for *Candida rugosa* lipase immobilization and further applied in the synthesis of flavor ester ethyl caprylate. Various conditions were optimized and maximum ester production was obtained at 40 °C with caprylic acid/ethanol ratio of 0.15:0.1 M using cyclo-octane as a reaction medium. A yield of 85% for ethyl caprylate was observed using lipase immobilized on modified EGO which was higher as compared to that of free lipase. Additionally, the immobilized lipase showed reusability upto 30 cycles retaining 50% of initial activity. Thus, the application of enzyme immobilized on functionalized EGO verifies to be promising system for ester synthesis in non-aqueous environment.

1. Introduction

Biocatalysis has many attractive features in the context of green chemistry, including mild reaction conditions while featuring excellent chemo-, regio-, and stereo-selectivity in multifunctional molecules [1]. Lipases (triacylglycerol acyl hydrolases, E.C. 3.1.1.3) are found to be quite stable in non-aqueous solvents. Due to their exquisite properties lipases are frequently used in organic synthesis for industrial applications [2,3]. Using organic solvents as reaction medium in enzyme catalysis offer many advantages such as (i) increased substrate solubility (ii) increased enzyme stability (iii) possibility of carrying out reactions which are difficult in water (iv) easy recovery of biocatalyst, as it is insoluble in organic solvents. However, free enzyme is associated with the limited operational stability due to deactivation and denaturation as well as difficulties in reusability. In order to obtain an ideal biocatalyst for industrial application, immobilization of the biocatalyst on certain support tends to be a proficient solution for the problems associated with the use of free or soluble enzymes [4,5].

Immobilization of enzymes is one of the most essential facets of modern biotechnology. These processes frequently overcome the problems associated with environmental sensitivity of native enzymes (i.e., heat, pH, ionic strength, metal ions contamination, and mechanical treatment) and enables long-term stability/recyclability of the biocatalyst [6]. Various methodologies for enzyme immobilization include adsorption, ionic bonding, covalent modification, entrapment and encapsulation [7]. The best support for the immobilization of free enzymes should (i) exhibit large surface areas for significant amounts of enzyme immobilization, (ii) facilitate rapid mass transfer of substrates and products, and (iii) provides excellent chemical and mechanical stability [8,9].

Currently, the focus of enzyme immobilization technology is shifting towards the use of nanoparticles [10]. Enzyme immobilization on nanostructured material provides higher enzyme stability and enhanced catalytic activity [11,12]. Among various nanomaterials used, graphene oxide (GO) derivatives have attracted considerable interest for their unique mechanical, thermal and electrical properties, as well as for their biocompatibility. Tight packing of carbon atoms into 2D honeycomb lattice is the key factor for several intrinsic features of GO like large surface area,

* Corresponding author. Tel.: +91 2692 229380; fax: +91 2692 236475.
E-mail addresses: vrutikaptl.19@yahoo.com (V. Patel), datta_madamwar@yahoo.com (D. Madamwar).

http://dx.doi.org/10.1016/j.bej.2014.12.007
1369-703X/

high electrical conductivity, and mechanical strength [13]. Furthermore, GO has large number of hydrophilic functionalities like epoxide, hydroxyl, carboxylic acid that impart hydrophilicity to its surface [14,15]. Silanization is considered to be an another effective method for enhancing adhesion between nanoparticles and enzyme. It is also expected to drastically reduce non-specific binding of molecules by hydrophobic interactions [16]. Recently, some research groups used graphene oxide (GO) based carriers for loading biomacromolecules such as enzymes. Singh et al. [17] immobilized *Cicer* α-galactosidase on functionalized graphene nanosheets. They affirmed that after ten successive runs, the immobilized enzyme still retained approximately 60% activity,with soybean RFOs (*Raffinose oligosaccharides*). Zhou et al. [18] reported use of nanographene oxide (GO) for the immobilization of enzymes, claiming to be an ideal support for protein or enzyme, which can be attributed to its properties such as the incredibly large specific surface area, the abundant oxygen containing surface functionalities, and the high water solubility. Glucose oxidase (GOD) was connected to the Ionic-liquid functionalized graphene (IL-graphene) material based on forceful ionic interaction instead of the usual method of weak physical adsorption. Ionic liquid here acted not only as a structure to bridge graphene and glucose oxidase, but also as a promoter to electron transfer [19]. Thus, we intend to explore the graphene as matrix for biocatalysis in organic solvents.

In present study, we aimed to develop sustainable nanocomposite of exfoliated graphene oxide (EGO) as a host to increase the stability of enzyme by immobilization. These nanobioconjugate of lipase and EGO were further applied for the synthesis of flavor ester ethyl caprylate. To the best of our knowledge this is first report for the synthesis of ethyl caprylate using EGO as immobilizing matrix. The effects of some major influential factors, such as reaction temperature, enzyme concentration, the substrates molar ratio conditions and solvent on the esterification reaction were also scrutinized. Furthermore, the operational stability of immobilized lipase was also examined in order to explore its potential in organic solvents.

2. Materials and methods

2.1. Materials

Exfoliated graphene oxide was procured from Department of Material Sciences, Vallabh Vidhyanagar. *Candida rugosa* lipase with activity of 875 U/g, (3-aminopropyl) triethoxysilane (APTES) and 4-nitrophenyl palmitate (p-NPP) were obtained from Sigma–Aldrich, Germany. Ethyl caprylate (≥98%) and caprylic acid (≥97%) was purchased from Fluka-Chemica (Germany). All organic solvents used were of GC/HPLC grade obtained from Spectrochem (Mumbai, India).

2.2. Experimental

2.2.1. Preparation of lipase functionalized exfoliated graphene oxide (EGO)

The general scheme for immobilization of lipase on functionalized EGO is provided in Fig. 1. Functionalization of lipase on EGO was chiefly carried out in two steps. First step is silanization of EGO: chemical coating of EGO with APTES was performed using procedure described by Yu et al. [16] with some modifications. Briefly, 5 mg of EGO was suspended in 10% APTES (diluted in ethanol) and sonicated for 4 h followed by overnight stirring. The modified EGO was recovered by centrifugation at 13 000 × *g* for 20 min at 4 °C. The pellet was washed thoroughly with ethanol and deionized water in order to remove excess APTES and vacuum dried. Second step includes attachment of lipase on functionalized EGO: silane functionalized EGO was dispersed into 9 mL of 50 mM phosphate buffer (pH 8.5) containing 1 mL of 40 mg/mL *C. rugosa* lipase. The mixture was stirred at 37 °C overnight followed by centrifugation (13 000 × *g* for 20 min) and vacuum dried. The EGO was

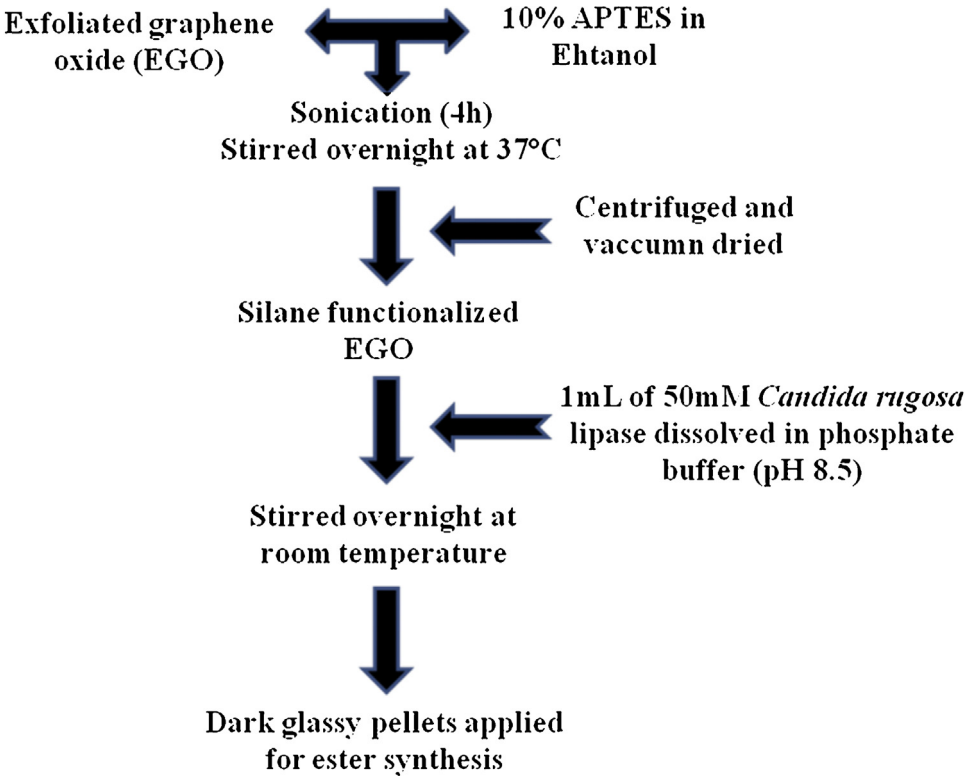

Fig. 1. General scheme for immobilization of lipase on exfoliated graphene oxide.

then washed thrice with phosphate buffer (50 mM) to eliminate unbound lipase. The amount of immobilized lipase adsorbed on nanoparticles was determined by measuring the initial concentration and its final concentration in supernatant after immobilization using lipase assay.

2.2.2. Characterization studies

The morphologies of EGO before and after functionalization of each step were studied by TEM (Philips-Technai 20, Holland) and SEM (Hitachi S-3000N). For TEM analysis, samples were dispersed into isopropanol and a drop was placed on a copper grid. The samples were observed after drying under vacuum. While, for SEM analysis the samples were directly placed on carbon tapes.

The chemical modifications arise on surface of EGO after each step of functionalization was studied by Fourier transform infrared (FT-IR) spectroscopic analysis using Spectrochem GX-IR, PerkinElmer, USA.

Thermal analysis of EGO was carried out in order to study decomposition of oxygen functional groups by TGA-SDTA 851 and DSC 822 (Mettler Toledo) with heating rate of 20 °C/min under N_2 atmosphere. The sample size range from 5 to 7 mg and the mass was recorded as a function of temperature.

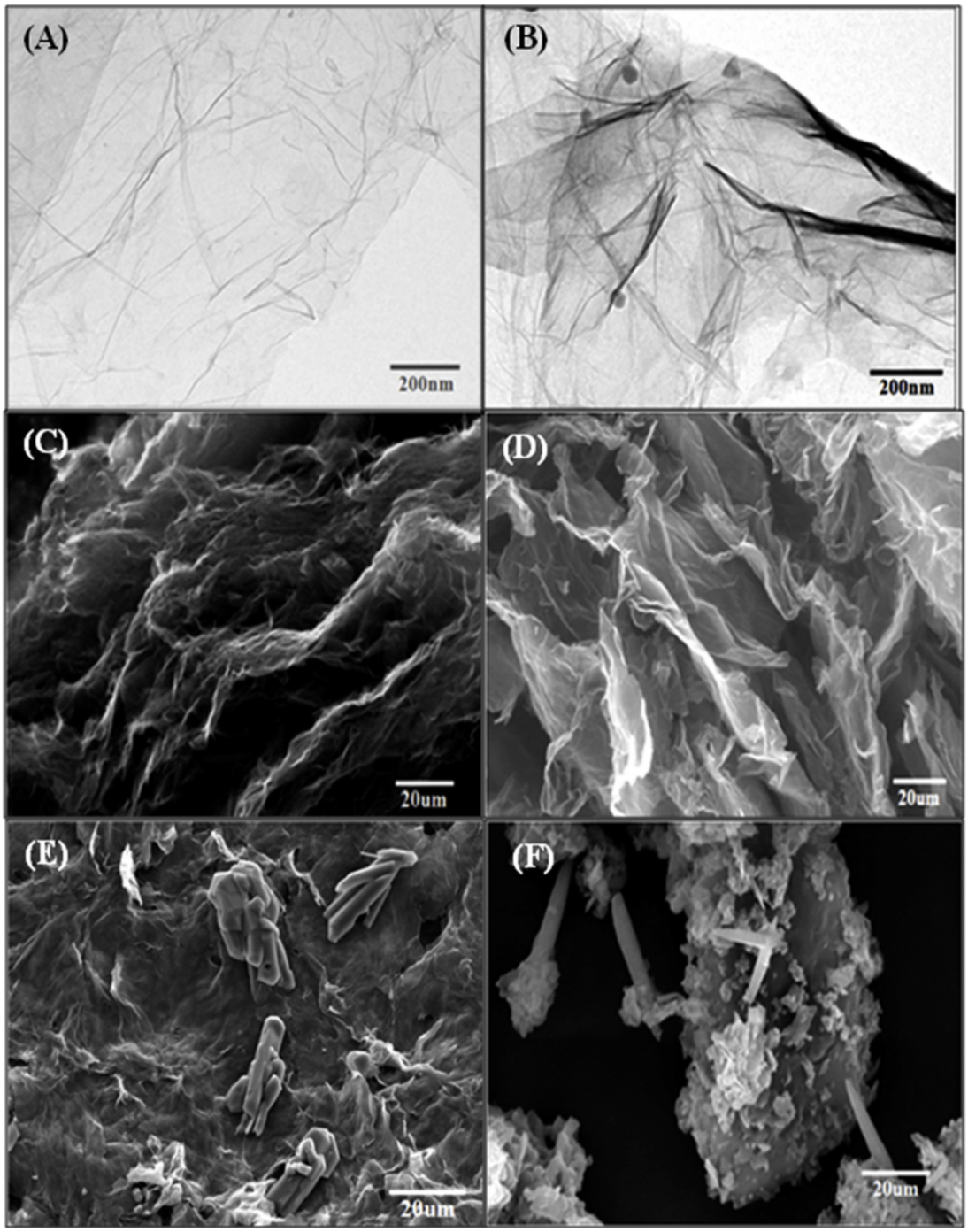

Fig. 2. Images of SEM (C–F) and TEM (A, B). Figure A and C display pristine exfoliated graphene oxide, B and D exhibits APTES treated exfoliated graphene oxide and E demonstrates lipase immobilized on exfoliated graphene oxide while F is control for lipase.

The Raman scattering was performed at room temperature with a Renishaw Raman microscope using laser excitation at 514 nm with 50× objective where the laser beam was focused in an area of ~1 μ (micron).

2.2.3. Application of lipase immobilized EGO in ester synthesis

The immobilized lipase was applied for esterification reaction of ethyl caprylate. Ethanol (0.1 M) and caprylic acid (0.1 M) were used as a substrate and mixed with 20 mL of cyclo-octane in 100 mL stopper flask. The reaction started after addition of enzyme to the substrate where native lipase and EGO-lipase were used separately for catalysis. The experiment was carried out at 37 °C and continuously stirred at 150 rpm to ensure all the enzyme particles were homogeneously dispersed by modulating the operative variables. The operative variables used for the experiment were:

i) Effect of enzyme concentration: ranging from 5 mg to 50 mg/mL.
ii) Effect of temperature: different temperatures measured were 20, 30, 37, 40, 50 and 60 °C.
iii) Effect of substrate concentration: substrate concentration ranges from 0.05 M to 0.25 M. The concentrations of ethanol and caprylic acid were varied one at a time keeping the other constant.
iv) Effect of organic solvents: different solvents used were *n*-hexane, cyclohexane, *n*-octane, and cyclo-octane.

Samples (100 μL) were periodically withdrawn to study the time course of reaction and analyzed by gas chromatograph (GC, PerkinElmer, USA)) in order to establish the product formation profile. No reaction was detected in the absence of the enzyme. All the experiments were repeated thrice at each operating condition and the relative deviation was within ±1%.

2.2.4. Reusability studies

For reusability studies, after completion of each cycle for esterification, the immobilized lipase was recovered by centrifugation at 10 000 × *g* for 25 min. The recovered enzyme was then washed with anhydrous *n*-hexane twice in order to remove any remaining substrate or product accumulated on EGO and subsequently used for next cycle.

2.3. Analytical techniques

2.3.1. Enzyme activity assay

The activity of free and bound lipase was measured colorimetrically at 410 nm using *p*-nitrophenyl palmitate (pNPP) as substrate at 37 °C following the method described by Wrinkler and Stuckmann [20]. One unit of lipase activity was defined as the amount of enzyme releasing 1 μmol *p*-nitrophenol/minute at pH 8.5 and 40 °C.

2.3.2. Gas chromatography analysis

The time course of reaction was determined by a gas chromatograph (PerkinElmer, Model Clarus 500, Germany) equipped with a flame-ionization detector (FID). The column was 30 m Rtx-®-20 (crossbond 80% dimethyl-20% diphenyl polysiloxane) capillary column. The temperature of injector and detector were maintained at 250 °C. The carrier gas served as nitrogen with the split flow rate of 90 mL/min. The column temperature was programmed to increase from 40 to 120 °C at the rate of 3 °C/min, from 120 to 200 °C at the rate of 10 °C/min and from 200 to 220 °C at the rate of 2 °C/min. Ester identification and quantification were done by comparing the retention time and peak area of the sample with the standard. Pure ethyl caprylate (≥98%) was used as external standard.

Table 1
Results for immobilization yield (%) of the lipase immobilized on exfoliated graphene oxide.

Lipase	Enzyme activity (U/mL)	Specific activity (U/mg)	Immobilization yield (%)[a]
Free lipase	6.824	3.06	–
Immobilized lipase	1.250	1.15	88.07

[a] Immobilization conditions: time 14–16 h, temperature 37 °C, Phosphate buffer solution (pH 8.5).

3. Results and discussion

3.1. Characterization of functionalized exfoliated graphene oxide (EGO)

3.1.1. Electron microscopy of surface modified exfoliated graphene oxide (EGO)

SEM (scanning electron microscopy) and TEM (transmission electron microscopy) studies were carried out on pristine EGO as well as functionalized EGO in order to investigate morphological changes during treatment. The samples for TEM were dispersed into isopropanol and a drop was placed onto Cu grids, while samples for SEM were directly placed on carbon tapes.

Fig. 2A and C exhibit TEM and SEM micrographs of pristine EGO. The distortion seen on the surface is caused by the oxygen groups and extremely small thickness of EGO (less than 3 nm) leading to wrinkled topology, with folded features. Oh and his collegues reported similar folding features of graphene oxide paper prepared from amine functionalized poly(glycidyl methacrylate)/graphene oxide core shell microspheres [21]. Yang et al. synthesized chemically converted graphene oxide via functionalization with APTES and observed distortion on the surface of GO [22]. Fig. 2B and D display TEM and SEM images of APTES functionalized EGO. It can be clearly seen from the figure that EGO gets highly agglomerated due to presence of silane moieties. Contrast of SEM micrographs in Fig. 2B and D shows crumpled sheet like structure which confirms the covalent functionalization of graphene oxide via APTES. The surface area of modified EGO was found to be in the range of 1100–1200 m^2/g.

Immobilization of lipase on functionalized EGO is seen in Fig. 2E. The figure demonstrates crystal like agglomerated structure of enzyme (when compared to enzyme as control in Fig. 2F) overlapped between the sheets of functionalized EGO. Fig. 2E also suggests binding of lipase on the surface of functionalized EGO. The results reflected in Table 1, also correlates with the results obtained from imaging analysis. The specific activity of immobilized lipase was found to be 1.156 U/mg of EGO.

3.1.2. Fourier transform infrared spectroscopy (FTIR) studies of chemically modified exfoliated graphene oxide (EGO)

Fourier transform infrared spectroscopy (FTIR) was performed in order to study the alterations in surface functional groups following each chemical/biological functionalization. Although the infrared (IR) spectrum is characteristic of the entire molecule, it is true that certain groups of atom give rise to bands at or near the same frequency regardless of the structure of the rest of the molecule.

The FTIR spectra of pristine EGO, APTES-functionalized EGO and lipase immobilized EGO is shown in Fig. 3. All the functionalized samples i.e., EGO, EGO + APTES and EGO + APTES + LIPASE showed three weak peaks at 2963.11 cm^{-1}, 2924.76 cm^{-1} and 2852.45 cm^{-1} which can be attributed to C—H stretching vibrations of methylene groups [23]. The second peak is at 1632.68 cm^{-1} which is associated with asymmetric vibrations of C=C. The characteristic band at 573.88 cm^{-1} confirms the presence of epoxy groups

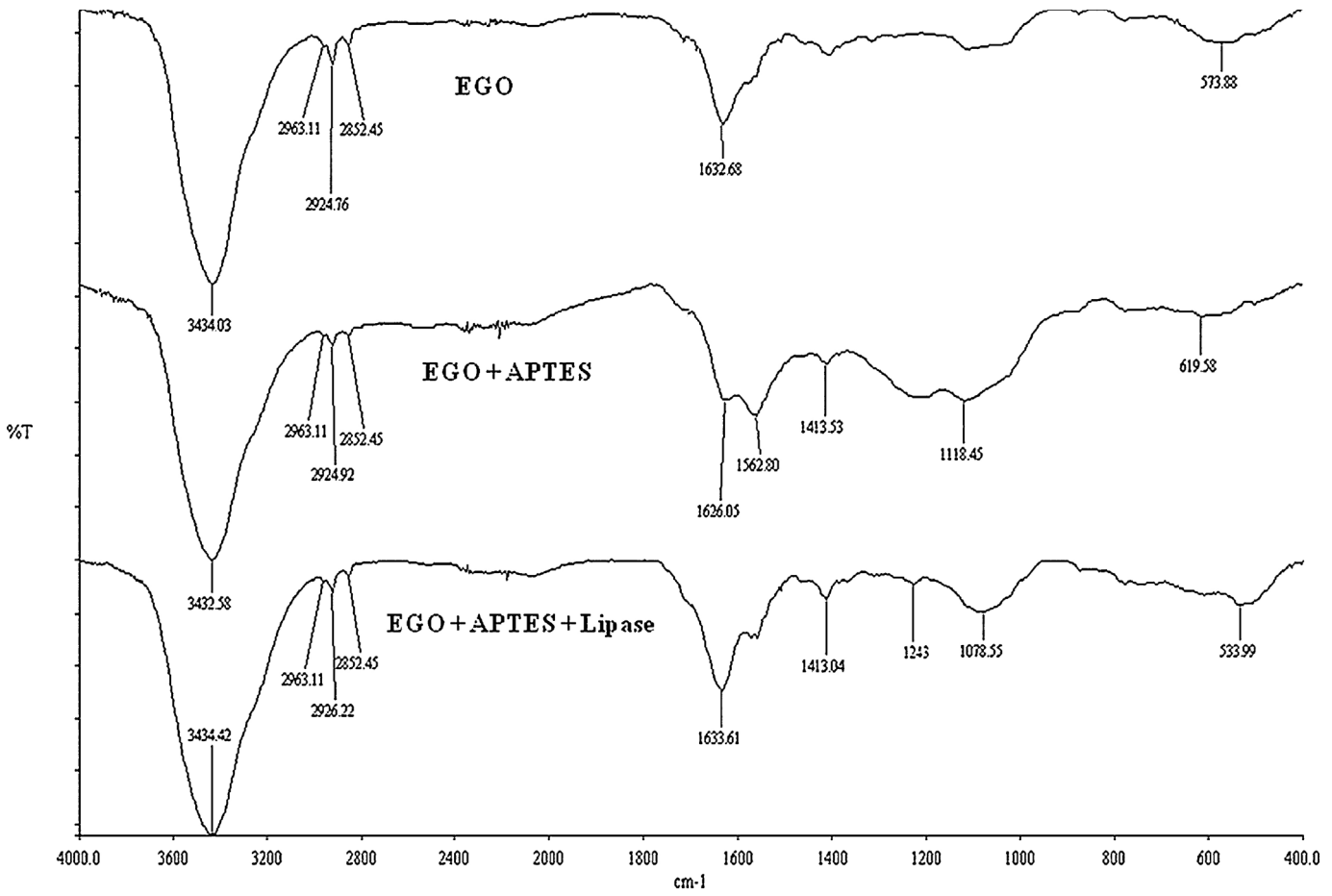

Fig. 3. FTIR overlay spectra of (a) pristine EGO (b) silane functionalized EGO and (c) lipase immobilized EGO.

complying with deformation vibrations. Furthermore, the broad absorption band at 3434.03 cm^{-1} is due to O—H stretching vibration and presence of carboxylic groups in all the three samples [23–25].

In spectra for APTES functionalized EGO, the additional strong and broad absorption peak is observed at 1118.45 cm^{-1} [23] assigning to the formation of Si—O and SiO—C_2H_5 groups due to presence of APTES. The appearance of peak 1118.45 cm^{-1} provides more evidence for successful chemical functionalization. The peaks at 1562.80 cm^{-1} and 1413.53 cm^{-1} are attributed to aromatic C=C bond stretching and C—H bending vibration frequencies, respectively [23]. The NH_2 bending mode is distributed amongst two adsorption peaks at 1626.05 cm^{-1} and 1562.80 cm^{-1}. While in lipase immobilized spectra it can be observed that split peak at 1562.80 cm^{-1} and 1626.05 cm^{-1} was replaced by a single peak shifted to 1633.61 cm^{-1}. The peak at 1413.04 cm^{-1} indicates C—N stretching of amide bond. This is further supported by peak at 1243 cm^{-1} which is due to the interaction of N—H bending and C—N stretching of amide bond. The spectrum of immobilized lipase in Fig. 3 shows successful binding of lipase to functionalized EGO with the disappearance/reduction in intensity of the activating groups, peaks and peak broadening [26].

3.1.3. Raman spectroscopic studies

In present work, Raman spectroscopy was used in order to collect changes in vibration information occurred during functionalization and enzyme immobilization. Fig. 4 shows Raman spectra of exfoliated graphene oxide at each phase of chemical modifications/reactions. A laser excitation of 514 nm was used, and the powdered samples were directly deposited on wafers in the absent of solvent. A Raman spectrum, in Fig. 4 refers to (a) pristine exfoliated graphene oxide (EGO), (b) silane functionalized EGO (EGO + APTES), (c) lipase immobilized EGO (EGO + APTES + LIPASE).

In spectrum of EGO the G band peaks at 1597.2 cm^{-1} (Fig. 4a) corresponds to the first order scattering of tangential C—C [27]. The second, D peak appears at approximately 1358.95 cm^{-1} (Fig. 4a) originating from the disorder in the planar sp^2-hybridized carbon network, which is characteristic of the lattice distortion in the graphene sheets [28]. The strength of this peak is related to the amount of disordered graphite and the degree of conjugation disruption in the graphene sheets. After silanization, both G band and D band were observed to shift at lower frequency (Fig. 4b). Yu et al. [16] reported similar observations who inferred that the shift to lower frequency was caused by APTES, which might be inserted within the nanosheets resulting in the expansion of tube structure and tension stress state of the C—C bond for the peak shift to lower frequency. After APTES treatment G band appears at 1598.33 cm^{-1} while the D band appeared at 1360.60 cm^{-1} (Fig. 4b). Ratios of intensities of the D band/G band have been used as an indicator of the amount of disorder within the sheets. There was no significant change on the intensities of bands after chemical treatment of EGO. The I_D/I_G ratio for EGO was found to be 0.73 indicating mid-order graphitic nature, while the value remained same (0.75) in the case of APTES treatment. For lipase immobilized spectra, in addition to D band and G band a strong peak was observed at 948 cm^{-1} (Fig. 4c). Raman feature for such spectra often indicates presence of inorganic sulfate compound.

3.1.4. Thermo gravimetric analysis

The successful functionalization was also reflected in TGA curves. TGA analysis was performed on as such exfoliated graphene

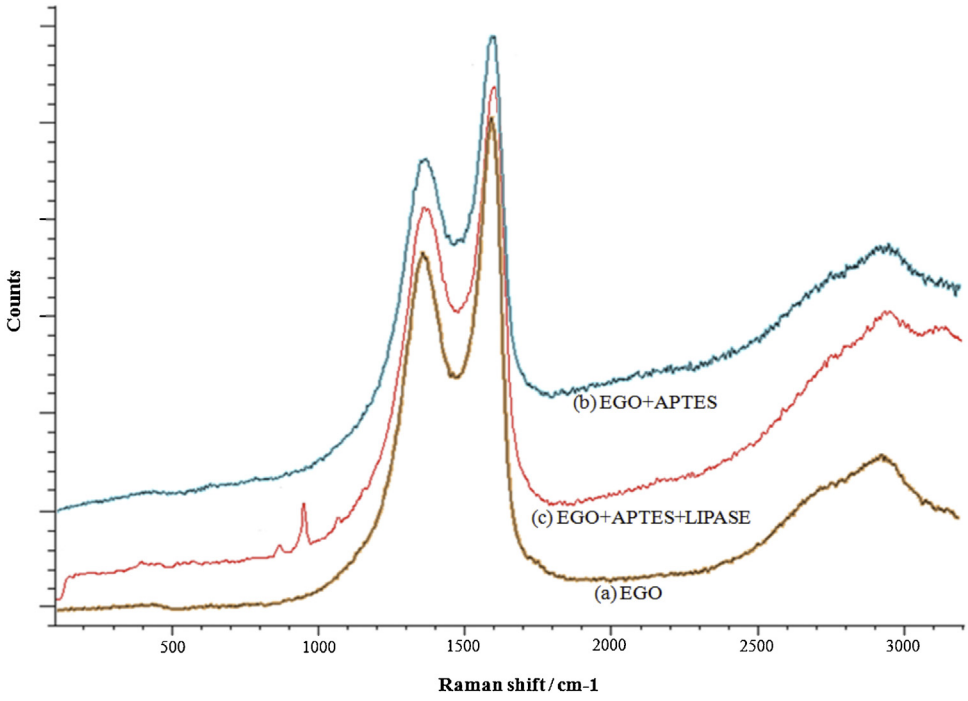

Fig. 4. Raman spectra of (a) pristine EGO (b) silane functionalized EGO and (c) lipase immobilized EGO.

oxide and lipase immobilized EGO using Mettler Toledo. Fig. 5 shows TGA curves in nitrogen upto 700 °C at heating rate of 20 °C min^{-1}. It can be observed from the curve that EGO shows very small weight loss below 100 °C, but significant weight loss occurs after 400 °C due to decomposition of oxygen groups on EGO [29].

In case of lipase immobilized EGO, nearly 10% of weight loss was observed at around 100 °C and steeply decreasing thereafter with much faster rate. This is much obvious due to loss of bound water molecule. This attributes to thermo-decomposition of lipase indicating successful enzyme immobilization on exfoliated graphene oxide.

3.2. Enzymatic esterification experiments

3.2.1. Effect of enzyme concentration

The influence of biocatalyst loading on production of ethyl caprylate was examined by varying enzyme concentration. As shown in Fig. 6, the conversion of the product increased rapidly from 12% to 75% when the amount of biocatalyst increases from 5 mg/mL to 40 mg/mL. However, the conversion of ethyl caprylate decreased slightly when the enzyme concentration was increased up to 50 mg/mL. The excessive amount of the enzyme results in insufficient protein unfolding which causes decrease in the enzymatic activity [6].

3.2.2. Effect of temperature

Study of effect of temperature not only assists in obtaining the optimum working temperature of an enzyme, but also facilitates to understand the tolerance of enzyme to high temperatures [30]. In the present study, the effect of temperature on free and immobilized lipase was carried out at 20, 30, 37, 40, 50 and 60 °C which exhibited more or less similar trend for ester production as shown in Fig. 7. The activity of lipase (both immobilized and free) significantly increased with increase in temperature from 20 to 40 °C, reaching the maximum of 80% for immobilized lipase and 58% for free lipase at 40 °C on second day. Further increase in temperature beyond 40 °C marginally reduces product formation. This is due to the partial inactivation of the enzyme in organic solvent at high temperature for a long time because enzyme undergoes partial unfolding by heat-induced destruction of non-covalent interac-

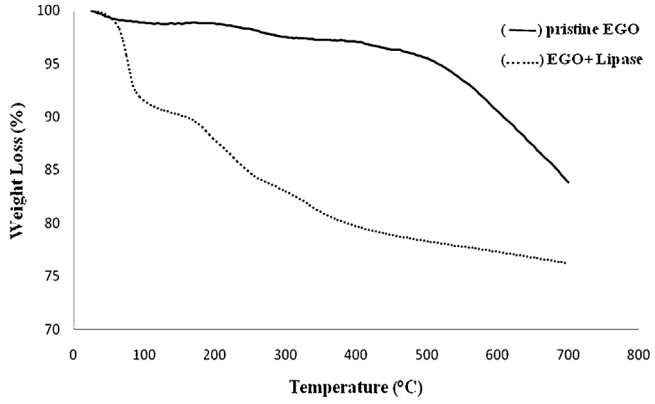

Fig. 5. The TGA weight loss curves of (a) pristine EGO and (b) lipase immobilized functionalized EGO.

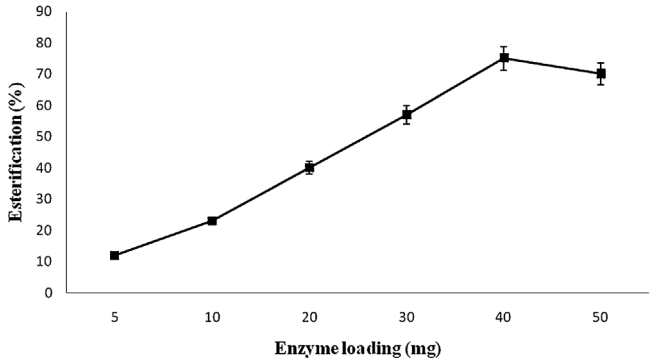

Fig. 6. Effect of enzyme concentration on ester synthesis using 2 mg of EGO as immobilizing matrix. Reaction condition: 20 mL of 0.1 M substrate (ethanol and caprylic acid), 0.1 M cyclo-octane, 37 °C, 150 rpm.

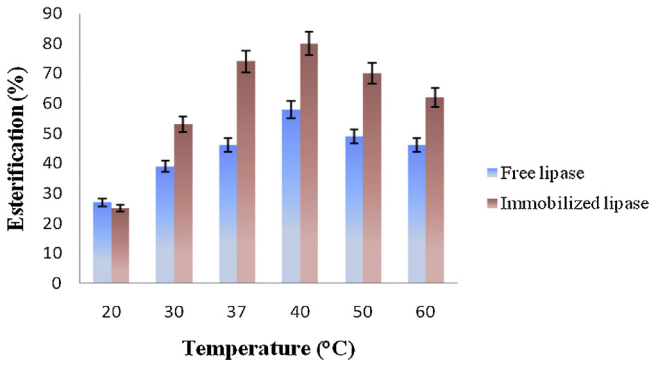

Fig. 7. Effect of temperature on free lipase and immobilized lipase at pH 8.5. Reaction conditions: reaction condition: 40 mg/mL of enzyme, 20 mL of each 0.1 M ethanol and caprylic acid, 0.1 M cyclo-octane, 150 rpm.

tions [31]. For lower temperatures (20 °C), immobilized lipase showed low conversions of only 25% and free lipase used as control showed 27% of ester production (Fig. 7). This suggests that at lower temperatures, the reaction rate is limited by mass transport phenomena. Similar trends of results have also been observed by Rahgavendra et al., Kantaria et al., and Dave and Madamwar [26,32,33], respetively. The results also suggest that increment in temperature to 60 °C did not exhibited drastic decrease in activity which provides a great deal of option in choosing high temperatures for conversions required for solid/semi solid substrates.

3.2.3. Effect of substrate molar ratio

Thermodynamically, an elevated substrate concentration may thrust the reaction towards the product formation and influence on the rate of reaction. In a kinetic study, the presence of possible inhibition on the enzymatic activity, caused by the substrates or products involved in the reaction has to be investigated [34,35]. In order to determine the optimum ratio of the substrates, the concentrations of ethanol and caprylic acid were varied one at a time keeping the other constant and carrying out esterification reaction. In one set of experiment the ethanol concentration was kept constant at 0.1 M varying caprylic acid concentration. As shown in Fig. 8 the maximum amount of ester (83%) was produced with 0.15 M of caprylic acid at 40 °C, pH 8.5 in 48 h. Also, when concentration of caprylic acid was further increased beyond 0.15 M, the ester production was adversely affected. When the same experiment was repeated keeping caprylic acid concentration constant at 0.15 M (obtained from the previous study) and varying ethanol concentration from 0.05 to 0.25 M highest yield was obtained at 0.1 M

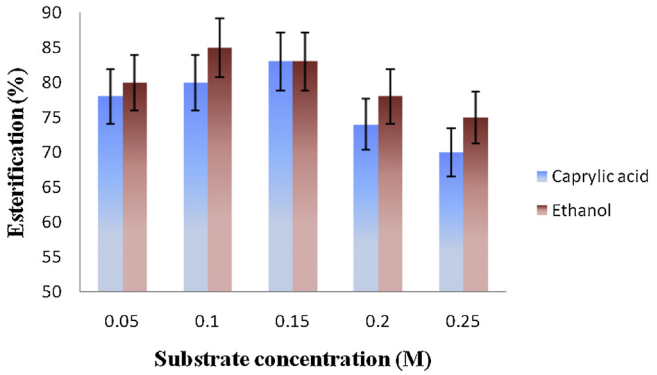

Fig. 8. Influence of substrate concentration on the efficiency of ester synthesis where caprylic acid and ethanol concentration was varied from 0.05–0.25 M. Reaction condition: 40 mg/mL of enzyme, 20 mL of each 0.1 M ethanol and caprylic acid, 0.1 M cyclo-octane, 40 °C, 150 rpm.

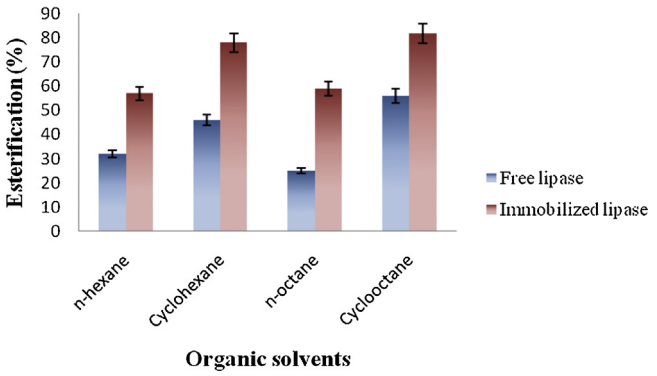

Fig. 9. Effects of different organic solvents (*n*-hexane, cyclohexane *n*-octane and cyclo-octane as reaction medium on the synthesis of ethyl caprylate. Reaction condition: 40 mg/mL of enzyme, 20 mL of each 0.1 M ethanol and caprylic acid, 40 °C, 150 rpm and substrate concentration ethanol/caprylic acid: 0.1 M/0.15 M.

concentration with 85% of product formation in 48 h. The reactions proceeded very quickly at low alcohol content (up to 0.1 M) and the yield reached maximum in 48 h while higher concentrations of alcohol exhibited an inhibitory effect on reaction slowing it down drastically. It is well known that during lipase-catalyzed esterification reaction, the first step consists of the preferential binding of the acid molecule to the enzyme [36]. The acyl transfer is affected by the concentration of free alcohol available. Maximum esterification rates were observed at a molar ratio ethanol/acid of 0.1/0.15 M this is probably the situation where maximum acyl transfer occurs. At higher molar ratios, the large increase in alcohol concentration may promote the binding of alcohol molecules to the lipase, during the first reaction step, competing with the acid. These leads to decrease in the reaction rate, since the reaction will be restricted by the amount of acid in the vicinity of the enzyme [37]. Thus, the molar ratio of caprylic acid to ethanol was found to be 0.15:0.1 M corresponding to maximum esterification of 85% with complete utilization of both substrates.

3.2.4. Effect of organic solvents

Organic solvents produce various physicochemical effects on enzyme molecules, and the effects differ depending on the kinds of organic solvents and enzymes used. Synthetic reactions in microaqueous organic media are also influenced by hydrophobicity and polarity of the medium. It is well known that the solvent polarity can affect enzymatic activity. It is generally accepted that the most suitable solvents are the ones with a log P (where P is the partitioning coefficient of solvent between 1-octanol and water) higher than 2, ideally above 4 [38]. Solvents below these values are known to have a deleterious impact on dehydrated enzymes by stripping the tightly bound water layer from the biocatalyst, resulting in enzyme structure perturbation [39]. Solvents (straight chain and cyclic) such as *n*-hexane, cyclohexane, *n*-octane and cyclo-octane were used as reaction medium for synthesis of ethyl caprylate. Fig. 9 shows the effect of different organic solvents on esterification reaction. In this study free and immobilized lipase exhibited highest esterification of 56% and 82%, respectively, in the presence of cyclo-octane, followed by cyclohexane showing 46% and 78%, whereas *n*-hexane and *n*-octane showed less esterification efficiency. Hence, cyclo-octane as reaction medium was chosen for further experimentation. Also it can be clearly seen from Fig. 9 that cyclic alkanes were found to be better solvents as reaction medium when compared to that of straight chain alkanes. Raghavendra et al. reported similar trend for using cyclic alkanes as solvents for production of pentyl valerate using *C. rugosa* lipase immobilized on functionalized carbon nanotubes [26] where highest esterification as observed in cyclooctane.

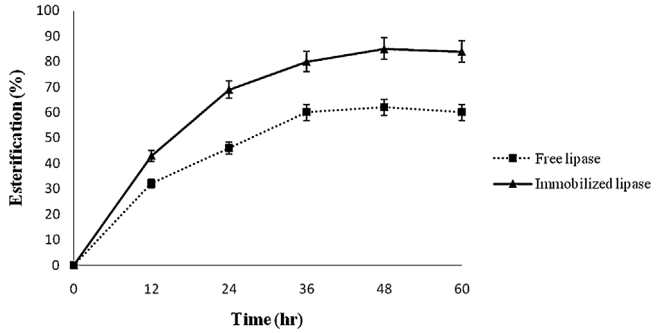

Fig. 10. Time course for the synthesis of ethyl caprylate using free as well as immobilized lipase using cyclo-octane as reaction medium. Reaction condition: 40 mg/mL of enzyme, 20 mL of each 0.1 M ethanol and caprylic acid, 40 °C, 150 rpm and substrate concentration ethanol/caprylic acid: 0.1 M/0.15 M.

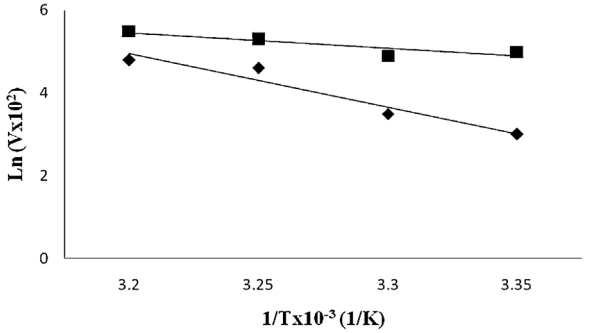

Fig. 11. Arrhenius plot for free and immobilized lipase. Activation energies for free lipase (♦) and immobilized lipase (■) were calculated to be 7.2 and 1.48 KJ/mol, respectively.

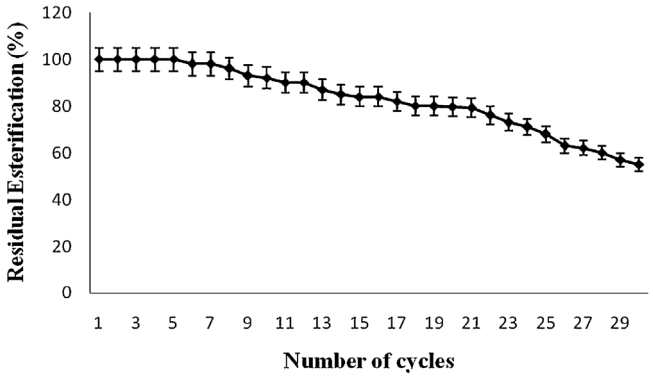

Fig. 12. Operational stability for the synthesis of ethyl caprylate using lipase immobilized on EGO at pH 8.5 and 40 °C.

3.3. Time course for ester synthesis

Alkyl esters are essential part of aroma compounds that plays an important role in food, cosmetic and pharmaceutical industries. Advantages of using the enzymatic synthesis in non-aqueous media significantly expand the possibilities for industrial applications [40]. Ethyl caprylate is a medium chain ester which has a "fruity-flowery" fragrance and is used as a constituent in various fruity flavors such as peach, apple, banana and pineapple aroma. [41]. The synthesis of ethyl caprylate by free and immobilized lipase was studied using cyclooctane as reaction medium. The experiment was carried out at 0.15:0.1 M acid/alcohol molar ratio under optimized conditions. The utmost esterification yield of 85% was observed within 48 h when lipase was immobilized on EGO. In contrast to this free lipase exhibited only 62% of ester formation under same condition (Fig. 10). The increased esterification of the immobilizing system could be attributed to the "lid" structure of the lipase. It is well known that *C. rugosa* lipase (CRL) has a lid consisting of 26 amino acids. This lid is pulled back at the interfaces exposing the active site making CRL a highly surface active enzyme. In this work therefore, at the oil-water interface, opening of the lid of CRL must have resulted in a self-catalytic bond formation with the carboxylic groups of EGOs leading to an enhanced immobilization of enzyme compared with that of free [42]. Another possible reason for enhanced ester synthesis in immobilized system is dispersion of enzyme on large surface area of EGOs in a proper orientation where aggregation of the enzyme is prevented leading to high activities as compared to that of free enzyme in organic synthesis [32].

The kinetic parameters of immobilized lipase were compared to that of free lipase derived from a series of experimental determinations. As observed from Table 2, immobilized lipase showed low K_m value (0.83 mM) and higher V_{max} (0.204 mM/min) value as compared to that of free lipase. These alterations suggest that lipase after immobilization resulted in increased affinity for substrates and enhanced accessibility of active sites. Compared to native lipase, a higher K_{cat}/K_m (0.386 mM^{-1} min^{-1}) value was observed for immobilized lipase which supports observations from Fig. 10, confirming that immobilized lipase shows increased catalytic specificity in non-aqueous system. The effect of temperature on affinity of free and immobilized enzyme can be seen in Arrhenius plot (Fig. 11).

Table 2
Kinetic constants of esterification reaction catalyzed by the free and immobilized lipase.

Sample	V_{max} (mM/min)	K_m (mM)	K_{cat} (min^{-1})	K_{cat}/K_m (mM^{-1} min^{-1})
Free	0.025	1.512	0.238	0.157
Immobilized	0.204	0.83	0.321	0.386

3.4. Reusability studies

To further examine the potential of immobilized lipase for ethyl caprylate production, its operational stability was investigated. The enzyme preparation was given solvent washes after every cycle (48 h for each cycle) in order to remove any substrate or product absorbed onto EGO and reused in fresh medium supplemented with substrates. It was observed that immobilized lipase catalyze reaction appreciably upto 10 cycle retaining 92% (Fig. 12) of its activity, after which lipase activity started declining slowly. This may be due to washing of immobilized biocatalyst which leads to enzyme leaching that limits mass transport and decrease in the exposure of the active sites to substrates [43]. In present work, reusability of immobilized lipase was studied upto 30 consecutive cycles which demonstrate stability of enzyme with meager loss of activity. Moreover, the immobilization of lipase has been reported to improve the catalytic activity of enzyme by providing protection against inhibitory effect of organic solvents as well as aid in reusability of lipase facilitating easy recovery by simple filtration [44]. Also, immobilized lipase exhibited good storage stability without significant decrease in activity after being stored for 68 days under refrigeration. These results further prove that this is promising technique for immobilization and production of ethyl caprylate for industrial purpose.

4. Conclusion

A simple pathway for immobilization of *C. rugosa* lipase on exfoliated graphene oxide has been explored in this work. The

nanobioconjugate was found to be highly efficient in terms of esterification yields, storage stabilities and reusability studies. The characterization methods were affirmative for the physical and chemical modifications occurring after each functionalization step. The immobilized preparations supported conversions in a wide temperature range of 20–60 °C. Immobilized lipase showed good ester production in contrast to free lipase. Moreover, immobilization preparations seem to be sturdy even after 30 cycles.

Acknowledgements

The authors would like to acknowledge University Grants Commission (UGC) grant no. F. 42-167/2013 (SR), New Delhi for financial support. Authors would also like to acknowledge (a) SICART, Vallabh Vidhyanagar for FTIR and TEM facility and (b) Department of Materials Science, Vallabh Vidhyanagar for extending their SEM, TGA and Raman facilities.

References

[1] S.B. Seema, H.N. Steven, Immobilization of lipase using hydrophilic polymers in the form of hydrogel beads, Biomaterials 23 (2002) 3627–3636.
[2] V. Dandavate, H. Keharia, D. Madamwar, Ethyl isovalerate synthesis using *Candida rugosa* lipase immobilized on silica nanoparticles prepared in nonionic reverse micelles, Process Biochem. 44 (2009) 349–352.
[3] M.H. Katsoura, A.C. Polydera, P. Katapodis, F.N. Kolisis, H. Stamatis, Effect of different reaction parameters on the lipase-catalyzed selective acylation of polyhydroxylated natural compounds in ionic liquids, Process Biochem. 42 (2007) 1326–1334.
[4] Y. Lv, Z. Lin, T. Tan, F. Svec, Preparation of reusable bioreactors using reversible immobilization of enzyme on monolithic porous polymer support with attached gold nanoparticles, Biotechnol. Bioeng. 111 (2014) 50–58.
[5] S.S. Deepthi, E. Prasad, B.V.S. Reddy, B. Sreedhar, A.B. Rao, A green approach towards the synthesis of enantio pure diols using horse radish peroxidase enzyme immobilized on magnetic nanoparticles, Green Sustainable Chem. 4 (2014) 15–19.
[6] S. Zhang, W. Shang, X. Yang, X. Zhang, Y. Huang, S. Zhang, J. Chen, Immobilization of lipase with hydrogel beads and the lipase catalyzed kinetic resolution of α-phenyl ethanol, J. Appl. Polym. Sci. (2014) 40178, http://dx.doi.org/10.1002/APP.
[7] J. Kim, J.W. Grate, P. Wang, Nanostructures for enzyme immobilization, Chem. Eng. Sci. 61 (2006) 1017–1026.
[8] R.V. Parthasarathy, C.R. Martin, Synthesis of polymeric microcapsule arrays and their use for enzyme immobilization, Nature 369 (1994) 298–301.
[9] W. Tischer, F. Wedekind, Immobilized enzymes: methods and applications, Top. Curr. Chem. 200 (1999) 95–126.
[10] S. Phadtare, A. Kumar, V.P. Vinod, C. Dash, D.V. Palaskar, M. Rao, P.G. Shukla, S. Sivaram, M. Sastry, Direct assembly of gold nanoparticles shells on polyurethane microspheres cores and their applications as enzyme immobilization templates, Chem. Mater. 15 (2002) 1944–1949.
[11] M. Verma, C. Barrow, M. Puri, Nanobiotechnology as a novel paradigm for enzyme immobilization and stabilization with potential applications in biodiesel production, Appl. Microbiol. Biotechnol. 97 (2013) 23–39.
[12] M.N. Gupta, M. Kaloti, M. Kapoor, K. Solanki, Nanomaterials as matrices for enzyme immobilization, Artif. Cells Blood Substitues Biotechnol. 39 (2011) 98–109.
[13] D. Du, L. Wang, Y. Shao, J. Wang, M.H. Engelhard, Y. Lin, Functionalized graphene oxide as a nanocarrier in a multienzyme labeling amplification strategy for ultrasensitive electrochemical immunoassay of phosphorylated p53 (S392), Anal. Chem. 83 (2011) 746.
[14] S. Park, R.S. Ruoff, Chemical methods for production of graphenes, Nat. Nanotechnol. 4 (2009) 217–224.
[15] J. Zhang, F. Zhang, H. Yang, X. Huang, H. Liu, S. Guo, Graphene oxide as matrix for enzyme immobilization, Langmuir 26 (2010) 6083–6085.
[16] L. Yu, Q. Zhou, Y. Gan, Q.L. Bao, Functionalized multi-walled carbon nanotubes as affinity ligands, Nanotechnology 18 (2007) 115614.
[17] N. Singh, G. Srivastava, M. Talat, H. Raghubanshi, O. Nath Srivastava, A.M. Kayastha, *Cicer* α-galactosidase immobilization onto functionalized graphene nanosheets using response surface method and its applications, Food Chem. 142 (2014) 430–438.
[18] L. Zhou, Y. Jiang, J. Gao, K. Zhao, Q. Zhou, Oreiented immobilization of glucose oxidase on graphene oxide, Biochem. Eng. J. 69 (2012) 28–31.
[19] Y. Jiang, Q. Zhang, F. Li, L. Niu, Glucose oxidase and graphene nanobiocompositebridged by ionic liquid unit of glucose biosensing application, Sens. Actuators B 161 (2012) 728–733.
[20] U.K. Winkler, M. Stuckmann, Glycogen, hyaluronate and some other polysaccharides greatly enhance the formation of exolipase by *Serratia marcescens*, J. Bacteriol. 138 (1979) 663–670.
[21] J. Oh, J.H. Lee, J.C. Koo, H.R. Choi, Y. Lee, T. Kim, N.D. Luong, J.D. Nam, Graphene oxide porous paper from amine-functionalized poly(glycidyl methacrylate)/graphene oxide core–shell microspheres, J. Mater. Chem. 20 (2010) 9200–9204.
[22] H. Yang, F. Li, C. Shan, D. Han, Q. Zhang, L. Niu, A. Ivaska, Covalent functionalization of chemically converted graphene sheets via silane and its reinforcement, J. Mater. Chem. 19 (2009) 4632–4638.
[23] P.C. Ma, J.K. Kim, B.Z. Tang, Functionalization of carbon nanotubes using a silane coupling agent, Carbon 44 (2006) 3232–3238.
[24] Q. Li, F. Fan, Y. Wang, W. Feng, P. Ji, Carboxyl-functionalized graphene oxide for catalysis in organic solvents, Ind. Eng. Chem. Res. 52 (2013) 6343–6348.
[25] X. Li, G. Zhang, X. Bai, X. Sun, X. Wang, E. Wang, H. Dai, Highly conducting graphene sheets and Langmiur–Blodgett films, Nat. Nanotechnol. 3 (2008) 538–542.
[26] T. Raghavendra, A. Basak, L. Manocha, A. Shah, D. Madamwar, Robust nanobioconjugates of *Candida antarctica* lipase B-multiwalled carbon nanotubes: characterization and application for multiple usages in non-aqueous biocatalysis, Bioresour. Technol. 140 (2013) 103–110.
[27] V.A. Sinani, M.K. Gheith, A.A. Yaroslavov, A.A. Rakhnyanskaya, K. Sun, A.A. Mamedov, J.P. Wicksted, N.A. Kotov, Aqueous dispersions of single-wall and multiwall carbon nanotubes with designed amphiphillic polycations, J. Am. Chem. Soc. 127 (2005) 3463.
[28] Y. Gao, I. Kyratzis, Covalent immobilization of proteins on carbon nanotubes using the cross linker 1-ethyl-3-(3-dimethylamino-propyl) carbodiimide–a critical assessment, Bioconjugate Chem. 19 (2008) 1945.
[29] S. Stankovich, D.A. Dikin, R.D. Piner, K.A. Kohlhaas, A. Kleinhammes, Y. Jia, Y. Wu, S.T. Nguyen, R.S. Ruoff, Synthesis of graphene based nanosheets via chemical reduction of exfoliated graphene oxide, Carbon 45 (2007) 1558–1565.
[30] S.Y. Han, Z.Y. Pan, D.F. Huang, M. Ueda, X.N. Wang, Y. Lin, Highly efficient synthesis of ethyl hexanoate catalyzed by CALB-displaying *Saccharomyces cerevisiae* whole-cells in non-aqueous phase, J. Mol. Catal. B: Enzym. 59 (2009) 168–172.
[31] N.S. Dosanjh, J. Kaur, Immobilization, stability and esterification studies of a lipase from *Bacillus* sp, Biotechnol. Appl. Biochem. 36 (2002) 7–12.
[32] S. Kantaria, G.D. Rees, M.J. Lawrence, Formulation of electrically conducting microemulsion based organogels, Int. J. Pharm. 250 (2003) 65–83.
[33] R. Dave, D. Madamwar, Esterification in organic solvents by silica gel immobilized *Candida rugosa* lipase, in: C. Larroche, A. Pandey, C.-G. Dussap (Eds.), Current Topic on Bioprocesses in Food Industry, Asiatech Press, New Delhi, 2005, pp. 71–80.
[34] Y. Xu, D. Wang, X.Q. Mu, G.A. Zhao, K.C. Zhang, Biosynthesis of ethyl esters of short chain fatty acids using whole-cell lipase from *Rhizopus chineses* CCTCC M201021 in non-aqueous phase, J. Mol. Catal. B: Enzym. 18 (2002) 29–37.
[35] M. Karra-Chaabouni, H. Ghamgui, S. Bezzine, A. Rekik, Y. Gargouri, Production of flavor esters by immobilized *Staphylococcus simulans* lipase in a solvent-free system, Process Biochem. 41 (2006) 1692–1698.
[36] W. Chulalaksananukul, J.S. Condoret, D. Combes, Geranyl acetate synthesis by lipase-catalyzed transesterification in supercritical carbon dioxide, Enzyme Microb. Technol. 15 (1992) 691–698.
[37] G. Ozyilmaz, E. Gezer, Production of aroma esters by immobilized *Candida rugosa* and porcine pancreatic lipase into calcium alginate gel, J. Mol. Catal. B: Enzym. 64 (2010) 140–145.
[38] B. Yang, S.J. Kuo, P. Hariyadi, K.L. Parkin, Solvent suitability for lipase mediated acyl-transfer and esterification reactions in microaqueous milieu is related to substrate and product polarities, Enzyme Microb. Technol. 16 (1994) 577–583.
[39] A.M. Klibanov, Improving enzymes by using them in organic solvents, Nature 409 (2001) 241–246.
[40] E.J. Vandamme, W. Soetaert, Bioflavors and fragrances via fermentation and biocatalysis, J. Chem. Technol. Biotechnol. 77 (2002) 1323–1332.
[41] V. Tesevic, N. Nikicevic, A. Jovanovic, D. Djokovic, L.V. Vujisic, V. Vuckovic, M. Bonic, Volatile compounds from old plum brandies, Food Technol. Biotechnol. 4 (2005) 367–372.
[42] T. Raghavendra, U. Vahora, A. Shah, D. Madamwar, Enhanced conjugation of *Candida rugosa* lipase onto multiwalled carbon nanotubes using reverse micelles as attachment medium and application in nonaqueous biocatalysis, Biotechnol. Progr. 30 (2014) 828–836.
[43] R. Ben Salah, H. Ghamghui, N. Miled, H. Mejdoub, Y. Gargouri, Production of butyl acetate ester by lipase from novel strain of *Rhizopus oryzae*, J. Biosci. Bioeng. 103 (2007) 368–372.
[44] V. Dandavate, D. Madamwar, Novel approach for the synthesis of ethyl isovalerate using surfactant coated *Candida rugosa* lipase immobilized in microemulsion based organogels, Enzyme Microb. Technol. 41 (2007) 265–270.

Patel et al. BMC Microbiology (2016) 16:50
DOI 10.1186/s12866-016-0669-8

BMC Microbiology

RESEARCH ARTICLE Open Access

Response and resilience of soil microbial communities inhabiting in edible oil stress/contamination from industrial estates

Vrutika Patel[1], Anukriti Sharma[2], Rup Lal[2], Naif Abdullah Al-Dhabi[3] and Datta Madamwar[1*]

Abstract

Background: Gauging the microbial community structures and functions become imperative to understand the ecological processes. To understand the impact of long-term oil contamination on microbial community structure soil samples were taken from oil fields located in different industrial regions across Kadi, near Ahmedabad, India. Soil collected was hence used for metagenomic DNA extraction to study the capabilities of intrinsic microbial community in tolerating the oil perturbation.

Results: Taxonomic profiling was carried out by two different complementary approaches i.e. 16S rDNA and lowest common ancestor. The community profiling revealed the enrichment of phylum "*Proteobacteria*" and genus "*Chromobacterium*," respectively for polluted soil sample. Our results indicated that soil microbial diversity (Shannon diversity index) decreased significantly with contamination. Further, assignment of obtained metagenome reads to Clusters of Orthologous Groups (COG) of protein and Kyoto Encyclopedia of Genes and Genomes (KEGG) hits revealed metabolic potential of indigenous microbial community. Enzymes were mapped on fatty acid biosynthesis pathway to elucidate their roles in possible catalytic reactions.

Conclusion: To the best of our knowledge this is first study for influence of edible oil on soil microbial communities via shotgun sequencing. The results indicated that long-term oil contamination significantly affects soil microbial community structure by acting as an environmental filter to decrease the regional differences distinguishing soil microbial communities.

Keywords: Oil perturbation, β-proteobacteria, 16S rRNA gene, Bacterial community structure, Fatty acid biosynthesis, Enzymes

Background

Oil spills have been pivotal in delineating microbial diversity at the affected site in contrast to the pristine soil. Thus, it becomes important to understand how indigenous microbial communities respond to the stress in order to understand their role in degradation process. Implementation of efficacious bioremediation strategies relies on innate microbial community dynamics, structure, and function [1]. Depending on biotic and abiotic factors, microorganisms adapt to the environment and accordingly environmental conditions select for microorganisms featuring specific capabilities. Other environmental variables also influence microbial distribution, such as regional climate [2, 3] soil type and characteristics [4] and vegetation [5].

Interestingly, microbial community interacts with each other to adapt under extreme environmental changes via modulating genome architecture [6, 7]. The vast majority of these organisms have been characterized through culture-independent molecular surveys using conserved marker genes like the small subunit ribosomal RNA or more recently the shotgun sequencing [8, 9]. The ongoing development of next generation sequencing (NGS) methods can now be combined with advanced bioinformatics method to replace more traditional approach of metagenomic library screening [10–12]. Consequently, more and more complete microbial genomes as well as

* Correspondence: datta_madamwar@yahoo.com
[1]Post Graduate Department of Biosciences, Centre of Advanced Study in Bioresource Technology, Sardar Patel University, Satellite Campus, Vadtal Road, Bakrol 388 315, Gujarat, India
Full list of author information is available at the end of the article

environmental metagenomes are being sequenced to gain insights into functional aspects besides species composition [13].

Till date microbial community studies in oil-polluted sites have been carried out either for crude oil contamination (marine and coastal sites) [14–16] or petroleum oil contamination [17, 18] or desert soils [19, 20] but limited efforts have been made in the direction of studying role of bacterial community at sites tainted with edible oil. Consequently, the intrinsic microbial community has to be active degrader organic pollutants (fats and lipids). The process of biodegradation mainly depends on microorganisms which enzymatically attack the pollutants and convert them into innocuous products [21]. Major group of extracellular hydrolytic enzymes disrupt chemical bonds in the toxic molecules and results in the reduction of their toxicity. This mechanism is effective for biodegradation of oil spill as well as organophosphate and carbamate insecticides. Bacteria such as *Bacillus sp.*, *Pseudomonas sp.*, *Chromobacterium vinosum* and the fungi *Aspergillus niger* and *Humicola lanuginose, Rhizopus delemar* and *Candida rugosa* secrete hydrolytic enzyme i.e. lipase that hydrolyse triacylglycerides to fatty acids and glycerol [22] and catalyze the degradation of lipids. Recent reports have shown that lipase activity is closely related with organic pollutants present in the soil and for the drastic reduction of total hydrocarbon from contaminated soil. Hence, research undertaken in this area is likely to progress the knowledge in the bioremediation of oils spill [23].

The study aims at the metagenomic-analysis of the microbial community inhabiting long-term edible oil contaminated site for both taxonomic profile and catabolic gene potential. Taxonomic profiling will provide insights into the composition of the microbial community capable of tolerating and/or degrading fatty acid compounds. Functional characterization of metagenome sequence reads on the basis of Clusters of Orthologous Groups of proteins (COG) accessions and Kyoto Encyclopedia of Genes and Genomes (KEGG) database entries will lead to elucidation of the catabolic potential of the indigenous microbial community. This approach will facilitate identification of genes essential for key catalytic steps in biodegradation pathways with respect to edible oil. Concisely, the obtained data will improve our understanding for the dynamics of bacterial community inhabiting oil stress and will also assess the genomic potential of the indigenous microbial community of the contaminated soil habitat.

Methods

Survey of the sampling site and physicochemical analysis of soil samples

To study the shift in microbial community structure across the oil polluted sites we collected bulk soil samples from the depots of oil contamination located near industrial area of Kadi, Ahmedabad. Three different sampling sites (i.e. P1, P2, P3) of soil were selected that represents accumulated edible cotton seed oil contamination since 20 years, resulted from oil spillage in ginning mills (GPS location for polluted site 23 degrees 17′ 46.2624″N_72 degrees 20′37.2840″E). Another sampling site was located within the industrial estate area 500 meter without any contamination i.e. control soil sample (C1, C2, C3) and was considered as a reference to demonstrate changes in microbial community under oil stress (GPS location for control site 23 degrees 17′ 17.1780″N_72 degrees 21′36.6048″E). At each site sampling was performed in replicates and collected soil was archived at 4 °C until further use. Physicochemical analysis of soil samples such as soil moisture, soil texture, organic carbon content, soil carbon/nitrogen ratio (C:N) were determined. This soil sample is collected from the soil where the cluster of edible oil industries are available, does not involve any ethical issues. No prior permission was required as this land does not belong to any specific agency. However, field studies do not create any destruction to endangered or protected species.

Community DNA extraction and sequencing

Metagenomic DNA from each soil samples i.e. polluted and control (P1, P2, P3, C1, C2 and C3) was extracted using protocol described by Zhou et al. [24]. In all 50 μL MilliQ water was used to dissolve DNA at the final step.

Soil sample (5 g) was pre-washed with double distilled water before DNA extraction according to the method of Zhou et al. [24]. Briefly, after adding 5 g glass beads (d = 3 mm) and 15 mL DNA extraction buffer (100 mM Tris, 100 mM EDTA, 1.5 M NaCl, 10 % Sucrose, 1 % CTAB, 100 mM sodium phosphate buffer pH = 8.0) to the pretreated soil, the sample was vortexed for 5 min followed by incubation for 30 min at 37 °C on environmental shaker. Subsequently, 2 ml SDS (20 %) was added and mixed with hand-shaking for 5 min. The sample was incubated at 60 °C for 30 min and inverted every 10 min. Further, 0.5 g of powdered activated charcoal (PAC) was added and incubated for 30 min more [25]. After centrifugation at 12000 rpm for 15 min at room temperature, DNA was extracted with an equal volume of phenol and chloroform-isoamyl alcohol (24:1, v/v), precipitated with isopropanol and washed with 70 % ethanol.

Total DNA concentration and quality was analyzed by NanoDrop spectrophotometer and electrophoresed on 0.8 % agarose gel, respectively. Equal concentration of environmental metagenomic DNA (obtained by Qubit reading) from each subsequent sites were mixed to form a composite genetic pool (i.e. P1 + P2 + P3 = P and C1 + C2 + C3 = C) representing total DNA composition for each site. Isolated DNA was sheared and sized to produce DNA library according to the manufacturer's protocol

from Ion Xpress™ Plus gDNA Fragment Library Preparation Kit. DNA Sequencing was performed on Ion Torrent PGM platform using sequencing chip 318 to generate short reads with an average insert size of 300 bp. All the outsourcing for DNA sequencing was done at Xcelris Lab Pvt Ltd, Ahmedabad, India.

Assembly and taxonomic analysis for sequencing data

Sequences generated for polluted as well as control sample was assembled individually by MetaVelvet assembler (1.20.02) [26, 27] set at $k = 31$, –exp cov = auto, –cov_cutoff = auto and insertion length with standard deviation = 300 bp ± 20. Both raw reads and contigs were used for further analysis. The taxonomic positions of sequenced reads was analysed and studied using two complementary approaches: (1) LCA: classification based on lowest common ancestor using MEGAN [28] and (2) Ribosomal Database Project (RDP) classifier: classification based on 16S rRNA gene sequences. MEGAN platform uses the lowest common ancestor (LCA) algorithm to classify reads to certain taxa based on their blast hits [29, 30]. The LCA parameters were set as Min Score = 35.0, Top Percent = 50, and Min Support = 2. In addition, the 16S rRNA sequences were extracted from the results of BLASTN analysis against the nt/nr database [26] and submitted to the RDP classifier [29, 31] with E value < $1X10^{-1}$ and 80 % confidence level. The RDP classifier predicted the taxonomic origin of 16S rRNA up to the rank of genus. Moreover, in order to rectify diversity picture other reference databases such WebCARMA (based on Environmental gene tags i.e. EGTs) and non-redundant database M5NR were also used with standard parameters.

Rarefaction analysis, Diversity indices and multivariate component analysis

Rarefaction curve was generated for all reads, except unassigned reads. Species richness was plotted according to the data obtained from RDP dataset [31], whereas, additional species likely to be discovered was addressed by plotting the discovery rate of dataset, which is obtained by repeatedly selecting random subsample of the dataset at 10, 20, upto- 90 % of the original size and then plotting the number of leaves predicted by LCA algorithm using MEGAN [28]. The diversity index i.e. Shannon's evenness index for general diversity (at genus level) and Simpson's dominance index on the basis of genus were calculated as described previously [25, 32, 33]. Multivariate principle component analysis (PCA), contour plot and correspondence analysis plot was plotted using data of phylum in PAST3 software [34].

Mapping of metagenomic reads

Polluted metagenomic single reads were mapped on available microbial genomes by aligning to the sequenced genome(s). An E-value cut off of $1Xe^{-3}$ and $\log_2$ as abundance scale was set. The coverage of reference genome sequence by reads was visualized using the Circos [35, 36].

Functional characterization and classification of genes

Functional characterization of reads was done on the basis of assembled data obtained from polluted sample. Gene calling was performed on the contigs using FragGeneScan [37] in order to predict operon reading frame (ORF). The ORFs were functionally annotated and assigned to the Clusters of Orthologous Groups of proteins (COG) [38] with an E value cut-off 10^{-5}. The metabolism analysis was performed on KEGG Orthology (KO)-identifiers by using KAAS tool (KEGG Automatic Annotation Server) based on bi-directional best hit approach (60). Gene annotation was based on Enzyme Commission (EC)-numbers based on the Kyoto Encyclopedia of Genes and Genomes (KEGG) Orthology database [39].

Screening of bacterial strains having oil degradation ability

Soil obtained from polluted sample was serially diluted and spread on Nutrient agar, Luria agar, Plate count agar and Tributyrin agar plates supplemented with tributyrin oil as a carbon source. Bacterial strains were selected on the bases of their ability to hydrolyze tributyrin oil by producing a clear zone around bacterial colonies [22, 40–42]. A total of 40 strains were isolated based on their distinct morphological characteristics of the colonies and hydrolysis of trybutyrin oil. All the isolated culture on plates was observed for 48 h and sub cultured once in every month. Further, all the bacterial strains were maintained at 4 °C in pure form for further use.

Data availability

The sequence data for both soil samples i.e. polluted and control obtained from Ion Torrent PGM platform has been deposited at MGRAST server (version 3). MGRAST IDs for the datasets are 4508969.3 and 4516462.3 for polluted soil and control soil, respectively. MGRAST IDs for the contig obtained from both the samples are 4515485.3 and 4512472.3, respectively. The sequences obtained from the culturable diversity study have been submitted to GenBank, NCBI and their accession numbers are from KR140170 to KR140186 (polluted soil) and KR140187 to KR140201 (control soil).

Results

Multiple studies have demonstrated the applications of high throughput sequencing in the study of microbial distributions and functional genes in different microbial communities. However, there are limited reports on bacterial community structural studies for edible oil contamination sites. Therefore, we took this opportunity to

explore effect of oil on bacterial community shift in long term edible oil-contaminated sites from industrial area of Kadi, Ahmedabad. Innate microbial community inhabiting contaminated environment was analyzed in terms of its composition and diversity by high-throughput shotgun sequencing approach via ion-torrent PGM platform provided by Xcelris Lab Pvt Ltd, Ahmedabad, India.

Physicochemical analysis of soils

The physicochemical analysis of soil samples from both (control and polluted) sites are tabulated in Table 1 showing significant difference (*P-value* <0.05) in all the corresponding parameters. Soil with oil stress exhibited higher nitrogen (1.5 times) and potassium (1–3 times) content as compared to that of control soil sample. This difference could be attributed to the characteristic feature of soil ecosystems with inherent bioremediation potential [43]. Total organic carbon was found to be 1.05 % and 0.71 % for polluted and pristine soil, respectively.

Metagenomic DNA extraction and analysis

Soil collected from the industrial area was used for metagenomic DNA extraction using the protocol of Zhou et al. [24]. The obtained DNA was of high molecular weight (Additional file 1: Figure S1) and was pure enough for further sequencing studies. Details about purity ratio and quality of metagenomic DNA (after pooling up DNA for each respective site i.e. P and C) with respect to humic acids is described in Table 1.

Sequencing of two DNA libraries (viz. polluted soil and control soil) was performed and data from the experiments are summarized in Table 2. The sequencing run resulted in 17, 06,040 reads (an average read length of 339 bp) for polluted sample and 39,98,015 reads (an average read length of 356 bp) for control sample. In total 31,284,971 numbers of bases were assembled into 201,285 contigs for polluted soil and 58,039,898 number of bases were assembled into 262,608 contigs for control soil sample using MetaVelvet assembler [26, 27].

Table 1 Characteristics features of sample for both polluted and control soil

Sr. No	Parameters tested	Polluted soil	Control soil
1	Texture of soil	Fine loamy soil	Fine loamy soil
2	Temperature (°C)	37	37
2	pH	8.10	8.26
3	Organic carbon (%)	1.05	0.71
4	Total Nitrogen ($Kgha^{-1}$)	2070	1371
5	Available P_2O_5 ($Kgha^{-1}$)	37.75	26.78
6	Available K_2O ($Kgha^{-1}$)	170.45	122.21
7	EC (dSm^{-1})	0.33	0.19
8	DNA concentration (ng/μL)	404	358

Table 2 Summary of sequencing result

	Polluted	Control
Number of reads	17,06,040	39,98,015
Average read length	339	356
Total number of contigs	201,285	262,608
Max contig length	1347	1258
Number of bases in contigs	31,284,971	58,039,898
N50	157	221

The sequences were assembled separately using MetaVelvet assembler

Bacterial diversity analysis

The taxonomic positions of sequenced reads was analysed and studied using two complementary approaches: (1) LCA: classification based on lowest common ancestor using MEGAN [28] and (2) RDP classifier: classification based on 16S rRNA gene sequences [31]. The predominance of bacterial reads was equally observed in all two approaches used to characterize indigenous bacterial community structure with RDP suggesting 97 % dominance of bacteria and 98 % reads were accounted to bacteria in LCA for perturbed environment.

Since 16S rRNA is widely used for taxonomic and phylogenetic studies due to its highly conserved sequences, its hypervariable region can also be used for accurate taxonomic evaluation [44]. The reads assigned to the superkingdom Bacteria are ~97.6 % for polluted and ~95.8 % in pristine indicating dominance of domain bacteria. The niche generated due to perturbed environment was dominated by phylum *Proteobacteria* (60.9 %), followed by *Bacteroidetes* (5.6 %) responsible for lipid metabolism. Only 30 % of *Proteobacteria* and 7.4 % of *Bacteroidetes* was dominant in control sample. The 3rd most abundant taxon in both samples (i.e. polluted and control) is *Verrucomicrobia* (2.4 % and 4.3 %) which was followed by *Firmicutes* (0.6 % and 4.2 %) and *Actinobacteria* (1.3 % and 3.4 %), respectively (Additional file 1: Figure S2).

At the class level community shift can be clearly seen between polluted and control soil samples. *Gammaproteobacteria* (14.9 %) showed dominancy in control soil while *Betaproteobacteria* (56.3 %) is in abundance for polluted soil sample (Fig. 1). The second most abundant class found in polluted soil is *Sphingobacteria* (2.5 %) followed by *Gammaproteobacteria* (2.2 %), *Cytophagia* (2 %) and *Verrucomicrobiae* (1.4 %). *Betaproteobacteria* (6 %) was found to be second dominant class in control soil sample followed by *Alphaproteobacteria* (5 %), *Actinobacteria* (3.5 %), *Deltaproteobacteria* (3.3 %), *Flavobacteria* (2.9 %) and *Verrucomicrobiae* (2.7 %). At rank genus *Chromobacterium* (45.5 %) (family *Neisseriaceae*) showed dominancy for polluted sample followed by

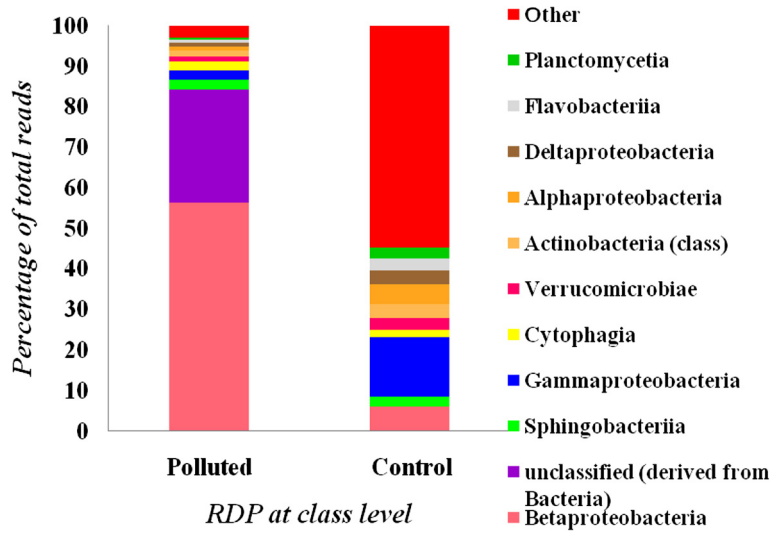

Fig. 1 Distribution of taxa among bacteria at rank class classified according to 16S rDNA using RDP classifier for both polluted as well as control sample

Neisseria (4.9 %) (family *Neisseriales), Cupriavidus* (4.5 %) (family *Burkholderiaceae*) and *Pedosphaera* (1.06 %) belonging to the family *Verrucomicrobia.* Genus *Klebsiella* (5 %) (family *Enterobacteriaceae*) was found to be abundant in control sample followed by 2.2 % *Flavobacterium* (family *Flavobacteriaceae*), 1.7 % *Brevibacillus* (family *Paenibacillaceae*) and 1.6 % *Xantomonas* (family *Xanthomanadaceae*). (Data for genus level is not shown)

Meanwhile, we also analyzed microbial community compositions based on lowest common ancestor (LCA). The statistics for both the sample (i.e. polluted and control) are shown in Additional file 1: Figure S3 at rank phylum. However, data for only polluted sample is explained in text. Comparable to the taxonomic structure generated from the output on reads, our analysis revealed that polluted soil sample showed *Proteobacteria* (47 %), followed by *Bacteroidetes* (20 %), *Verrucomicrobia* (15.5 %), *Plantomycetes* (4 %) and *Acidobacteria* (3 %) as most dominant classified phylum (Additional file 1: Figure S3). For polluted site the dominant classes (Fig. 2) in bacteria are *Alphaproteobacteria* (19 %), *Betaproteobacteria* (13 %), *Gammaproteobacteria* (7 %), *Spartobacteria* (7 %) and *Cytophagia* (7 %). At rank genus *Chthoniobacter* (10 %) (family unclassified from

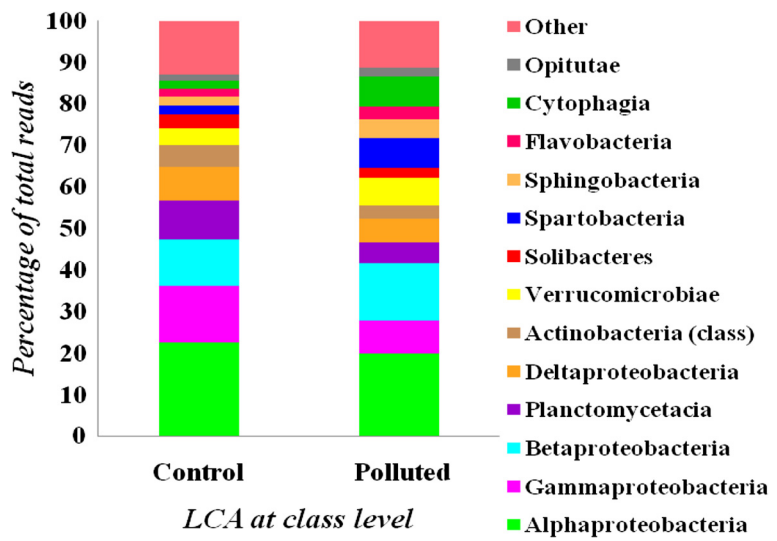

Fig. 2 Distribution of taxa among bacteria at rank class classified according to lowest common ancestor (LCA) for both polluted as well as control sample

Spartobacteria), *Chromobacterium* (7 %) (family *Neisseriaceae*) showed dominancy for polluted sample followed by *Candidatus Solibacter* (3.5 %) (family *Solibacteraceae*), *Verrucomicrobium* (2.9 %) (family *Verrucomicrobiaceae*) and *Chitinophaga* (2.8 %) belonging to the family *Sphingobacteriales.*

In addition to this, the diversity picture for both samples was also compared with EGTs using WebCARMA algorithm and non-redundant database M5NR. The comparison is not described in text but displayed through figures in Additional file 1: Figure S4. Among all the databases used for analysis we found that there is influence of oil contamination on soil and can be clearly seen by the dominance of betaproteobacteria at class level and *Chromobacterium* (widely known for its oil degrading capability) at genus level.

Comparison of microbial composition between soil samples

Statistical analysis of biodiversity provides interesting insights as reflected in rarefaction curves. Rarefaction analysis was carried out in order to assess species richness of the system. Using RDP, we analyzed the microbial richness, based on sequence reads, between libraries of polluted and control soil samples (Fig. 3a). Whereas, plotting the number of leaves predicted by LCA algorithm revealed that the number of taxonomic leaves or clades of control soil are all higher than those of polluted ones. Also, control and polluted soil contains 629 and 396 leaves for all assigned taxa, respectively (Fig. 3b). Furthermore, the rarefaction curves of both libraries appear close to saturation at 100 % of the total reads. Our results suggest that the current sampling depth is not yet close to the natural status for bacteria.

Shannon index was used to indicate diversity and complexity, and the Simpson index was used to measure abundance. As exhibited in Fig. 3c, the lowest Shannon diversity in polluted sample indicates presence of phylotypes while in control sample the diversity indices showed a higher level of species richness. Simpson index showed the dominance in polluted sample as compared to that of control. Consistently, the data collected from phylotype distributions of 16S rRNA gene sequences of total bacterial community of both the samples were treated by PCA plot, contour plot and correspondence analysis (CA) plot in order to check differences between the sites in terms of bacterial community structures. The entire three analysis viz. PCA plot, Contour plot and CA plot (Fig. 3d (a, b, c)) was able to separate control site from that of polluted ones. The data set of both the samples showed that sites were well separated from each other and as well as no cluster formation showed difference in bacterial community structure.

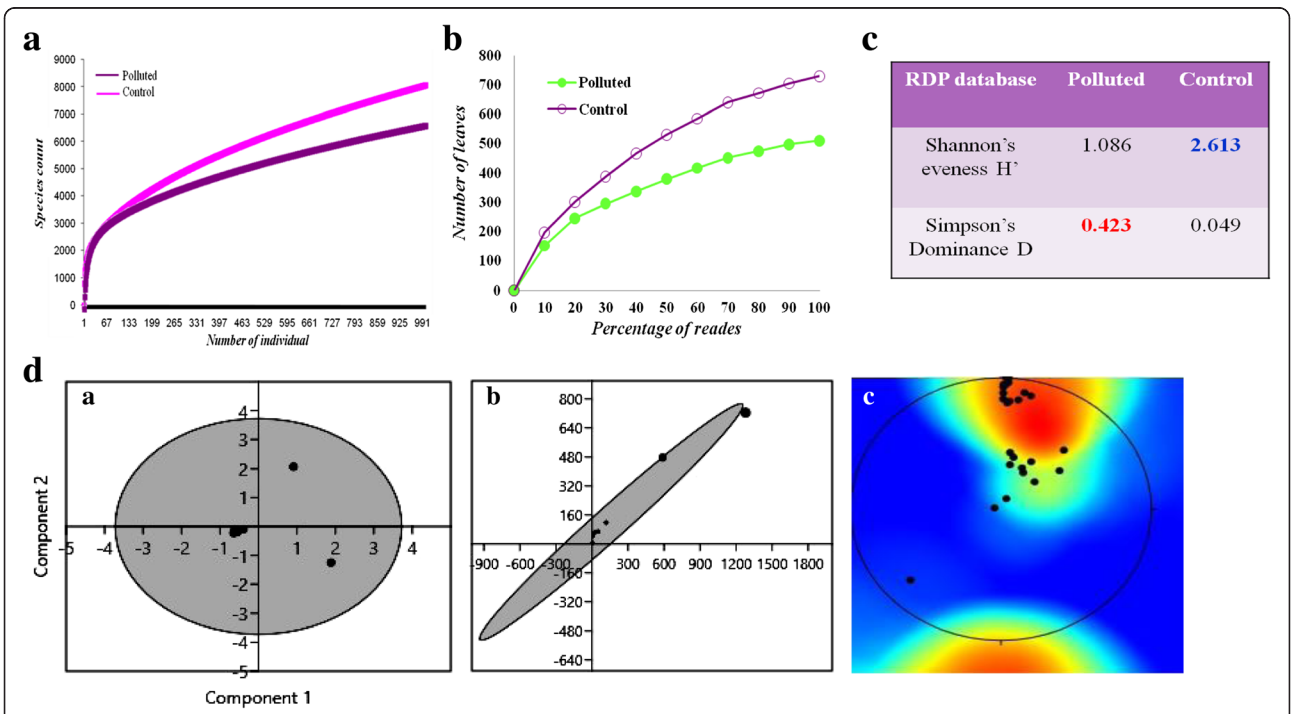

Fig. 3 Statistical comparative analysis for the reads assigned between control as well as polluted soil sample (**a**) rarefaction curves on species counts using RDP dataset (**b**) rarefaction curve using percentage of reads, (**c**) diversity indices and (**d**) multivariate analysis *a*) PCA plot, *b*) CA plot, *c*) contour plot

Annotation and mapping of metagenome single reads to the microbial genomes

Metagenomic reads of polluted sample were mapped for assessing genome coverage. Maximum hits for metagenome were attributed to the genome of *Candidatus solibacter ellin* (Fig. 4a). Maximum identity percentile of metagenomic reads with whole genome of *Candidatus solibacter ellin* was found to be 5.76 %. List of top 50 microorganisms mapped with highest number of reads are shown in Fig. 4b. The highest number of reads was allocated to *Chthoniobacter flavus* Ellin428 genome followed by *Chitinophaga penensis* DSM2588, *Candidatus solibacter* usitatus Ellin6076, *Verrucomicrobium spinosum* DSM4136, *Spirosoma lingual, Optitutus terrae PB90-1, Dyadobacter fermentans DSM18053, Marivirga tractuosa DSM4126.* The list also includes *Algoriphagus, Sorangium, Pirellula, Mesorhizobium, Halangium, Cytophaga* and others. This suggested that these organisms were enriched at polluted site and can play significant role in fatty acid metabolism and synthesis.

Gene function annotation and classification

Metabolic profile for bacterial community structure of polluted soil sample was annotated using COG and KEGG databases. Assembled contigs were analyzed by assigning predicted functions to genes based on COG [45]. In total 22 classes based on functional categories were identified by COG database (Fig. 5). In the category "metabolism" large amount of reads are distributed among "amino acid transport and metabolism (E)", "energy production and conversion (C)", "carbohydrate transport and metabolism (G)", and "lipid transport and metabolism (I)". The class "lipid transport and metabolism (I)" was further characterized for various kinds of enzymes responsible for fatty acid metabolism under stress conditions. Classes such as "inorganic ion transport and metabolism (P)" and "coenzyme metabolism (H)," "secondary metabolites biosynthesis, transport, and catabolism (Q)," and "signal transduction mechanisms (T)" are associated with transport of ions/compounds and other metabolic processes (Fig. 5). COG categories/accessions important in lipid metabolism are described in Table 3. In the KEEG analysis, metabolism term including carbohydrate metabolism, lipid metabolism, metabolism of cofactors and vitamins, amino acid metabolism and metabolism of other amino acids are among the top five most popular categories (Fig. 6a). KEGG terms in lipid metabolism are displayed in Fig. 6b. The enzymes involved in lipid metabolism were detected in reads assigned to fatty acid biosynthesis, glycerophospholipid metabolism, sphingolipid metabolism, glycerolipid metabolism as the four most dominant groups which are involved in the processing of lipids and fatty acids. The 20 most abundant enzymes mapped according to KEGG

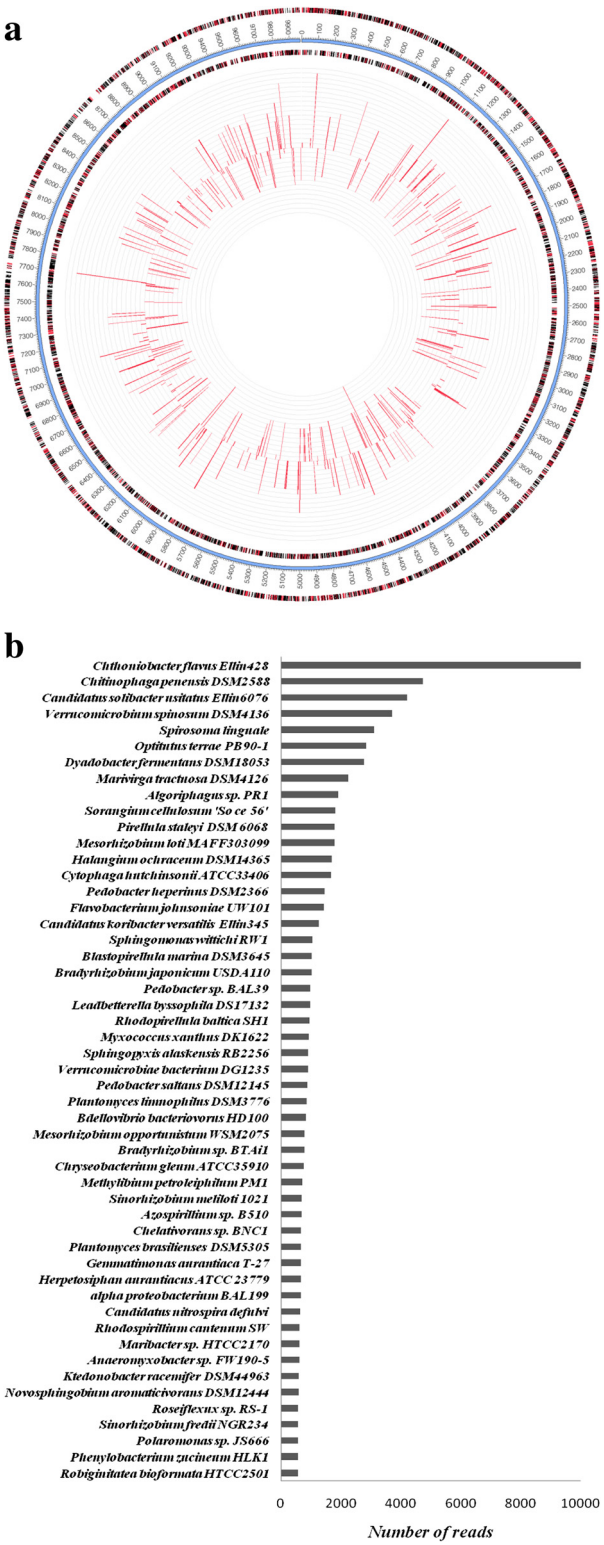

Fig. 4 **a** Mapping of metagenomic reads from polluted soil sample on the genome of *Candidatus solibacter ellin* 6076 and **b** Metagenomic reads assigned to microbial genomes sequences. The x-axis denoted the number of reads assigned to the 50 most prevalent microbial strain genomes

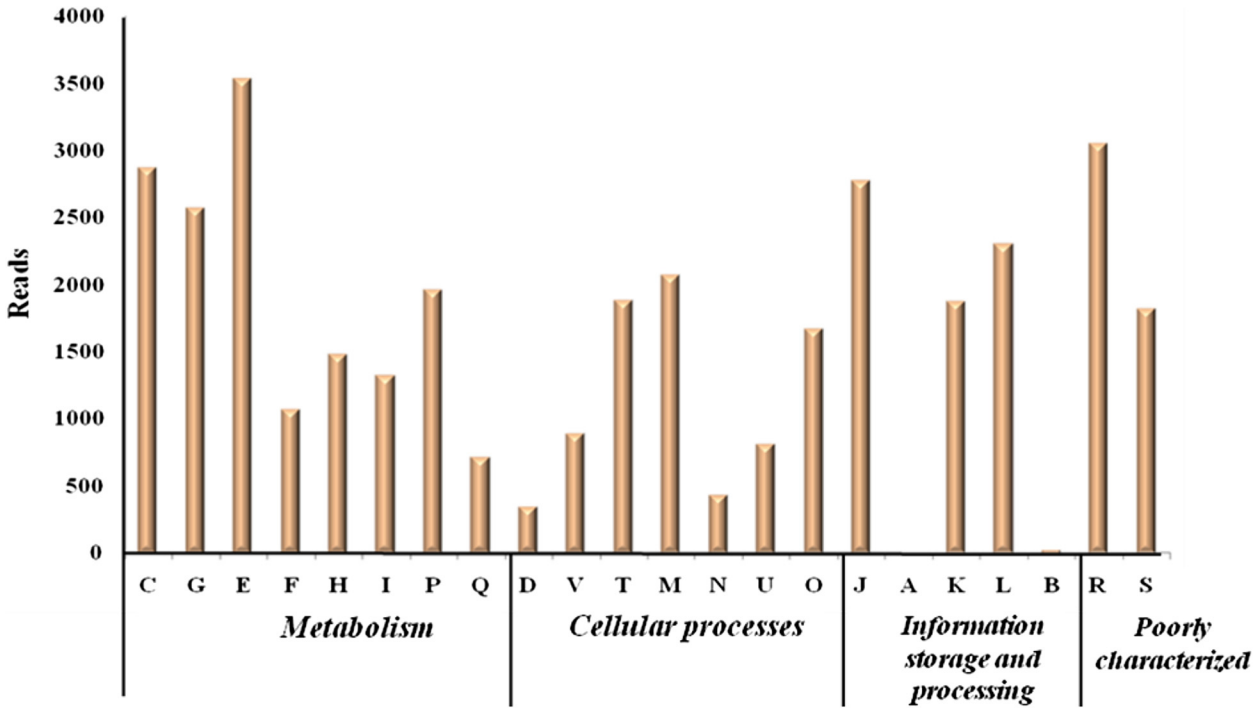

Fig. 5 Characterization of metagenomic sequencing reads of contaminated soil sample according to the Cluster of Orthologous Groups of protein (COGs). The categories for COG are abbreviated as follows: C- energy production and conversation; G- carbohydrate transport and metabolism; E- amino acid transport and metabolism; F- nucleotide transport and metabolism; H- coenzyme transport and metabolism; I- lipid transport and metabolism; P- inorganic ion transport and metabolism; Q- secondary metabolites and biosynthesis; D- cell cycle control, cell division, chromosome partitioning; T- signal transduction mechanism; M- cell wall/membrane/envelope biogenesis; N- cell motility; U- intracellular trafficking, secretion and vesicular transport; O- post translational modification, protein turnover, chaperones; J- translation, ribosomal structure and biogenesis; A- RNA processing and modification; K- transcription; L- replication, recombination and repair; B- chromatin structure and dynamics; R- general function prediction only, S- function unknown

database from metagenomic data is tabulated in Table 4. This observation is consistent with the findings that many species in polluted sample are involved in fatty acid biosynthesis and fatty acid metabolism.

The main focus of the study was on fatty acid biosynthesis. The expression of genes involved in lipid metabolism pathways such as fatty acid biosynthesis (PATH: ko00061), fatty acid degradation (PATH: ko00071) mapped from KEEG database are displayed in Additional file 1: Table S1.

Bacterial community structure using culture dependent approach

Since the contaminated site of the study is oil perturbed soil attempts were made to isolate organisms on tributyrin agar plates containing tributyrin oil as carbon source. Total bacterial counts of $1.8X10^2$ CFU/mL were obtained from oil contaminated soil whereas <30 bacterial counts were obtained from control sample when screened on tributyrin agar plates. The possible reason for this could be production of extracellular enzymes by particular microorganisms to combat these stressed condition in such contaminated environment. Different species of *Bacillus such as (B. subtilis, B. methylotrphicus, B. pumilis, B. endophyticus)*, *Pseudomonas (P. stutzeri, P. sp)* as well as *Exiqobacterium (E. profundum)* known for their lipolytic activities were identified.

Discussion

Deciphering bacterial community structure using shotgun sequencing approach

Novel technologies continue to expand our understanding of microbial diversity and community structure. Metagenomic analysis [10, 45] has previously identified 'unexpectedly' high bacterial phylogenetic and functional diversity. The long-term sustainability of soil contamination requires detailed knowledge of its biodiversity coupled to profound understanding for its functioning. Previous studies with 16S rRNA-based analyses using clone libraries [46–48], microarrays (for example, PhyloChip and GeoChip) [49–52], pyrosequencing [7, 53] and other approaches [54] showed that soil microbial communities are highly diverse and complex.

Here, we took opportunity to explore microbial diversity and its functioning in edible oil contaminated soil using 16S rRNA shotgun sequencing approach. This study

Table 3 COG categories as discovered from the metagenomic reads for lipid metabolism

COG No.	Name of the protein
COG3425	3-hydroxy-3-methylglutaryl CoA synthase
COG0304	3-oxoacyl-(acyl-carrier-protein) synthase
COG0332	3-oxoacyl-[acyl-carrier-protein] synthase III
COG4247	3-phytase (myo-inositol-hexaphosphate 3-phosphohydrolase)
COG1211	4-diphosphocytidyl-2-methyl-D-erithritol synthase
COG0439	Biotin carboxylase
COG2272	Carboxylesterase type B
COG4589	CDP-diglyceride synthetase
COG1024	Enoyl-CoA hydratase/carnithine racemase
COG0821	Enzyme involved in the deoxyxylulose pathway of isoprenoid biosynthesis
COG0657	Esterase/lipase
COG1398	Fatty-acid desaturase
COG1022	Long-chain acyl-CoA synthetases (AMP-forming)
COG3127	Lysophospholipase
COG1443	Isopentenyldiphosphate isomerase
COG2185	Methylmalonyl-CoA mutase, C-terminal domain/subunit (cobalamin-binding)
COG1260	Myo-inositol-1-phosphate synthase
COG2867	Oligoketide cyclase/lipid transport protein
COG0558	Phosphatidylglycerophosphate synthase
COG1562	Phytoene/squalene synthetase
COG3243	Poly(3-hydroxyalkanoate) synthetase
COG4553	Poly-beta-hydroxyalkanoate depolymerase
COG1657	Squalene cyclase
COG0020	Undecaprenyl pyrophosphate synthase

provides a comprehensive survey of the microbial richness and composition of long-term oil contaminated soil microbial communities. Upon taxonomic analysis using different approaches (RDP classifier and LCA algorithm), *Proteobacteria* was the well-represented phylum along with β-, α-, γ-, and δ-*Proteobacteria*. This group of bacteria has considerable morphological, physiological and metabolic diversity, which are of great importance to global carbon, nitrogen and sulfur cycling [50]. *Bacteroidetes* are the second most prevalent group of bacteria detected in polluted sample, with three major classes (*Sphingobacteria, Cytophagia and Flavobacteriia*). *Gammaproteobacteria* is dominant group of bacteria followed by β-, α-*Proteobacteria* in pristine soil sample. The results showed significantly altered microbial community diversity, composition and structure, especially for particular microbial populations at class level.

The members of the *Proteobacteria* phylum are a group of Gram-negative bacteria that have an important role in decomposition of organic matter and carbon cycling [53]; *Neisseriaceae* and *Burkholderiaceae* were found to be major families. *Proteobacteria* has been previously detected at high abundance in soil samples, including polluted ones [55–58], and shift in their community were also observed upon contamination with oil or during bioremediation. While, *Proteobacteria* accounted for 60 % of total sequences in our polluted soil sample, they accounted for 86 % in long-term diesel-contaminated soil from Poland [58], 45 % in contaminated permafrost soils along a crude oil pipeline in china [59], 42 % in gradient of petroleum contaminated desert soil [17] and 50-60 % in contaminated mangrove sediments from Brazil [57]. Members of *Betaproteobacteria* and *Gammaproteobacteria* are known to be highly versatile for their degradation ability [7, 60, 61]. The strains of genera *Chromobacterium, Xanthomonas, Pseudomonas, Burkholderia* and *Acenitobacter* which prevailed the classes *Betaproteobacteria* and *Gammaproteobacteria* were found to possess oil-degrading capabilities [17, 18, 22]. Various microbial populations that are capable of degrading different oil and petroleum products including species of *Pseudomonas, Flavobacterium, Arthrobacter, Alcaligenes, Nocardia, Micrococcus, Corynebacterium* and *Mycobacterium* have been isolated from soil [62], while *Pseudomonas, Arthrobacter, Sphingomonas, Rhodococcus, Ochrobactrum, Psychrobacter, Pseudoalteromonas, Acinetobacter* and *Bacillus* are isolated from marine environment [63–66]. Among the detected genera known for degradation are *Actinobacteria*, *Microbacterium* and *Micrococcus* [40, 67].

Rarefaction analysis for particular ecosystem is a prerequisite to deduce the complete taxonomic profile of the community. The rarefaction curves are nearly reaching saturation for classifications based on RDP. Moreover, results from PCA plot, CA plot and contour plot also suggested there is variation in community structure for both samples and appropriate depth of sampling is also covered. Mapping of metagenome reads onto bacterial genomes suggested that organisms related to the identified species were enriched at the site contaminated with oil and presumably play an active role in biodegradation.

Understanding the factors that influence microbial community structure is an important goal in microbial ecology [51]. Our analysis results indicate that oil has a significant impact on soil microbial functional communities in contaminated soil. On one hand oil contamination could be toxic to many microbial populations reducing microbial diversity and on the other hand, the vast range on carbon substrates and subsequent metabolites present in oil-contaminated soil could facilitate the development of rather complex microbial communities. In this study, microbial functional genes encoded for lipid metabolism was analyzed using KEEG database [39]. The

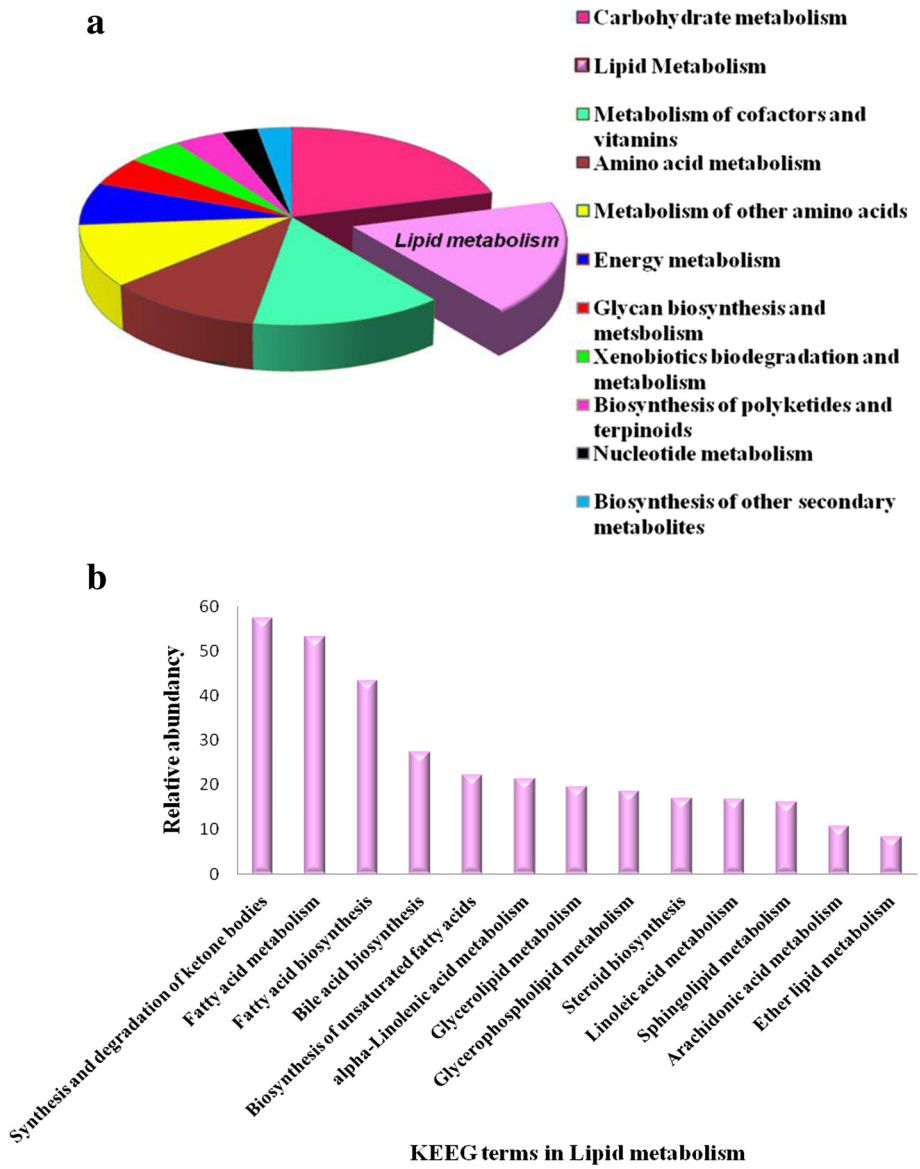

Fig. 6 a Characterization of metagenomic sequencing reads of contaminated soil sample according to KEEG database. **b** Popular terms on lipid metabolism based on KEEG analysis. The Y-axis refers to the percentage of reads within the reads mapping to metabolism terms

pathways of fatty acid biosynthesis and the enzymes involved in them are well conserved. The abundance of several functional genes involved in fatty acid synthesis and metabolism such as *acc*, *fab* and *fad* genes were detected. These genes are directly involved in the synthesis and metabolism of free fatty acids [68]. The increase in these functional genes might be due to the natural selection of organisms capable of utilizing fatty acids/lipids. The degradation of PAHs by microorganisms through a complex enzymatic process was well documented by Patel et al. [63] with increase in frequencies of *nahA* genes in polluted water. Bestawy et al. [22] reported a positive correlation between oil contamination and abundance of *fab* genes from gram-negative bacteria removing oil and grease in industrial effluent.

Metabolic pathway analysis for fatty acid biosynthesis

Fatty acid biosynthesis in almost all the organisms culminates in formation of saturated fatty acids. All organisms produce fatty acids via a repeated cycle of reactions involving the condensation, reduction, dehydration and reduction of carbon-carbon bonds. First step in fatty acid biosynthesis (Fig. 7) is the ATP dependent formation of malonyl-CoA from acetyl-CoA and bicarbonate by acetyl-CoA carboxylase (*acc*, EC 6.4.1.2) enzyme. All

Table 4 Abundance of enzymes mapped from metagenomic reads identified in KEEG database

Sr. No	Enzyme mapped	Abundance/Hits
1	ABC transporter related	237
2	binding-protein-dependent transport systems inner membrane component	192
3	TonB-dependent receptor	186
4	TonB-dependent receptor plug	141
5	short-chain dehydrogenase/reductase SDR	119
6	acriflavin resistance protein	118
7	ABC transporter related protein	116
8	NAD-dependent epimerase/dehydratase	114
9	oxidoreductase domain protein	104
10	sulfatase	94
11	protein of unknown function DUF214	90
12	transcriptional regulator	80
13	histidine kinase	76
14	ABC transporter ATP-binding protein	69
15	extracellular solute-binding protein	69
16	inner-membrane translocator	69
17	aldo/keto reductase	68
18	AMP-dependent synthetase and ligase	64
19	beta-lactamase	64
20	glycoside hydrolase family protein	64

bacterial organisms contain a type II synthase (FAS II) for which each reaction is catalyzed by a discrete protein and reaction intermediates are carried in the cytosol as thioesters of the small acyl carrier protein (ACP) [45]. Malonyl CoA:ACP transferase encoded by *fabD* gene (EC 2.3.1.39) undergoes transacylation of malonyl from CoA to ACP. The chain elongation step in fatty acid biosynthesis consists of the condensation of acyl groups, which are derived from acyl- CoA or acyl-ACP, with malonyl-ACP by two types of 3-ketoacyl-ACP synthases. The first class of 3-ketoacyl-ACP synthase III (*fabH*, EC 2.3.1.180) is responsible for the initiation of fatty acid elongation and utilizes acyl-CoA primers. The second class of enzymes (*fabF* EC 2.3.1.179 and *fabB,* EC 2.3.1.41) is responsible for the subsequent rounds of fatty acid [68–70]. Thus, produced acyl-ACP is catalyzed by three enzymes [NADPH-dependent 3-ketoacyl-ACP reductase (*fabG*, EC 1.1.1.100), 3-hydroxyacyl-ACP dehydratase (*fabZ,* EC 4.2.1.59) and NAD(P)H-dependent enoyl-ACP reductase (*fabI,* EC 1.3.1.9, 1.3.1.10)] for reduction, dehydration and reduction of carbon-carbon bonds,respectively. Further, additional cycles are initiated by *fabF* and *fabB*. The $fadR_{Ec}$ protein is a global regulator of fatty acid degradation, is a transcriptional activator that binds to the *fabA* promoter region [71].

Finally, input to fatty acid synthesis is acetyl CoA and the output is free fatty acid synthesis. The *fab* and *fad* proteins are highly conserved in many gram-positive bacteria including *Bacillus*, *Clostridium*, *Streptomyces* and other related genera [70–72]. Moreover, its orthologues are unexpectedly present in more diverse genera, such as *Metanosarcina* (*Archaea*), and *Bordetella*, *Burkholderia* and *Chromobacteria* (*β*-proteobacteria) [70]. Also, genome analysis indicated that only the α-, β and γ-proteobacteria have the proteins of this pathway [73, 74].

Bacterial isolates by culture dependent approach

Using culturable approach higher number of total bacterial count was observed in presence of tributyrin from

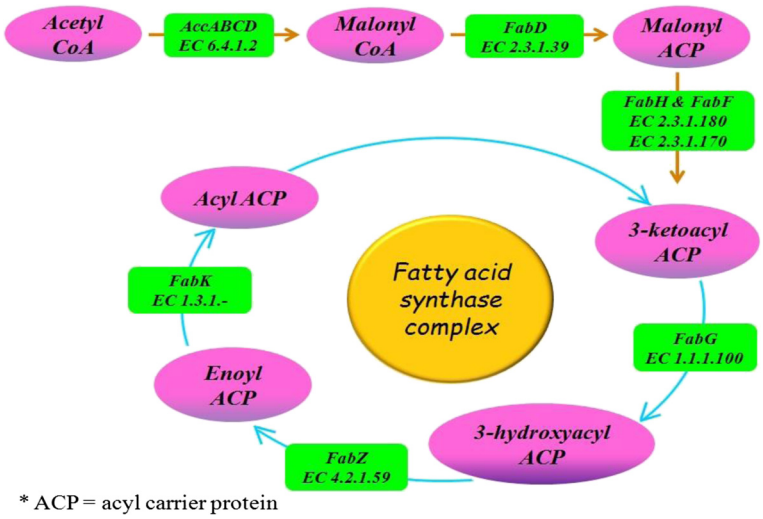

Fig. 7 Fatty acid synthesis and metabolism pathway predicted in polluted soil sample based on KEEG analysis. Pink colors indicate formation of compounds within the reactions and green labels indicates presence of genes detected in metagenomic reads

polluted environment in comparison to that of pristine. Result clearly indicates the adaption of organism toward oil stress. Biodegradation by intrinsic microbial populations is the key and reliable system through which thousands of organic contaminants are eradicated from the environment [75]. Different species of *Bacillus* (*B. subtilis, B. pumilis, B. endophyticus)* and *Pseudomonas (P. stutzeri, Pseudomonas sps.)* were found in abundance from oil stressed soil which depicts their significant role in degradation of oil. These microbial strains have ability for producing extracellular lipase enzymes that hydrolyze triglycerides (the main component of oils and fats) to fatty acids and glycerol [21, 22]. The enzymatic versatility of these bacteria is well known and has been suggested as their importance in ecosystem. As noted by Ahmad et al., *Bacillus* strains play an important role in biodegradation of oil contaminated soil in combination with that of *Pseudomonas sp* [41]. Apart from this species such as B. *thuringiensis, Micrococcus sp, Corynebacterium sp.,* and *Acinetobacter sp.* also has significant role in degradation of pollutants [75, 76].

Conclusion

In conclusion, present study reflects the detection of microbial diversity across oil stress condition favouring *β-proteobacteria* such as *Chromobacterium, Xanthomonas, Pseudomonas, Burkholderia* and *Acinetobacter sp.* The microbial community analysis at the metagenome level gives an insight into the repertoire of species to deal with oil contamination. We also observed, genes corresponding to enzymes involved in a wide variety of reactions and operating in many unrelated biosynthesis pathways collaborates well with the fact that the site of study has long-term oil contamination. Moreover, the isolation of different genera of *β-proteobacteria* is in correspondence with results obtained by culture dependent approach reporting abundance of *β-proteobacteria* in polluted samples. These isolates are well documented for biodegradation processes. In this regard, obtained knowledge will be useful in understanding the pathways for synthesis and metabolism of fatty acids released for oils and the microbial communities dominating in such stress condition.

Availability of supporting data

The sequence data for both soil samples i.e. polluted and control obtained from Ion Torrent PGM platform has been deposited at MGRAST server (version 3). MGRAST IDs for the datasets are 4508969.3 and 4516462.3 for polluted soil and control soil, respectively. MGRAST IDs for the contig obtained from both the samples are 4515485.3 and 4512472.3, respectively. The DOI link for the server is http://metagenomics.anl.gov/metagenomics.cgi?page=Home. The sequences obtained from the culturable diversity study have been submitted to GenBank, NCBI and their accession numbers are from KR140170 to KR140186 (polluted soil) and KR140187 to KR140201 (control soil). The DOI link for GenBank is http://www.ncbi.nlm.nih.gov/genbank.

Additional file

Additional file 1: Figure S1. Metagenomic DNA extracted from polluted as well as control soil sample and electrophoresed on 0.8 % agarosa gel. Lane M is of marker, Lane 1, is for polluted sample (representing pooled metagenomic DNA for P1 + P2 + P3 = P) and Lane 2 is for control soil sample (representing pooled metagenomic DNA for C1 + C2 + C3 = C). **Figure S2.** Distribution of taxa among bacteria at rank phylum classified according to 16S rDNA using RDP classifier for both polluted as well as control sample. **Figure S3.** Distribution of taxa among bacteria at rank phylum classified according to lowest common ancestor (LCA) for both polluted as well as control sample. **Figure S4.** Comparative distribution of taxa among bacteria at rank class classified according to WebCARMA and M5NR datasets for both polluted as well as control sample. **Table S1.** Enzymes mapped for lipid metabolism pathways in KEEG database. (DOC 300 kb)

Competing interests

All the authors declare that they have no competing interest. DNA sequencing was carried out as outsourcing by Xcelris Lab Pvt. Ltd.

Authors' contributions

Conceived and designed the experiments: DM. Performed the experiments: VP Analyzed the data: VP AS RL. Contributed reagents/materials/analysis tools: RL, NAA-D. Wrote the paper: VP DM. Sample Collection: VP DM. All authors read and approved the final version of the manuscript.

Acknowledgments

We are grateful to University Grants Commission (UGC) grant no. F.42-167/2013(SR) and Department of Biotechnology (DBT) sponsored Centre of Excellence and Innovation in Biotechnology (CEIB) programme supported grant no. BT/01/CEIB/09/V/05 for financial assistance. Vice Deanship of Research Chair, King Saud University, Kingdom of Saudi Arabia is duly acknowledged.

Author details

[1]Post Graduate Department of Biosciences, Centre of Advanced Study in Bioresource Technology, Sardar Patel University, Satellite Campus, Vadtal Road, Bakrol 388 315, Gujarat, India. [2]Department of Zoology, University of Delhi, Delhi, India. [3]Department of Botany and Microbiology, Addiriya Chair for Environmental Studies, College of Science, King Saud University, P.O. Box # 2455, Riyadh 11451, Saudi Arabia.

Received: 10 September 2015 Accepted: 9 March 2016
Published online: 22 March 2016

References

1. Desai C, Pathak H, Madamwar D. Advances in molecular and "-omics" technologies to gauge microbial communities and bioremediation at xenobiotic/anthropogen contaminated sites. Bioresour Technol. 2010;101:1558–69.
2. Bhattacharya D, Sarma P, Krishnan S, Mishra S, Lal B. Evaluation of genetic diversity among *Pseudomonas citronellolis* strains isolated from oily sludge-contaminated sites. Appl Environ Microbiol. 2003;69:1435–41.
3. Maila M, Randima P, Dronen K, Cloete T. Soil microbial communities: Influence of geographic location and hydrocarbon pollutants. Soil Biol Biochem. 2006;38:303–10.
4. Hamamura N, Olson S, Ward D, Inskeep W. Microbial population dynamics associated with crude-oil biodegradation in diverse soils. Appl Environ Microbiol. 2006;72:6316–24.
5. Joner E, Johansen A, Loibner A, Cruz M, Szolar O, Portal J, et al. Rhizosphere effects on microbial community structure and dissipation and toxicity of

polycyclic aromatic hydrocarbons (PAHs) in spiked soil. Environ Sci Technol. 2001;35:2773–7.
6. Nikolaki S, Tsiamis G. Microbial Diversity in the Era of Omic Technologies. 2013; doi:10.1155/2013/958719.
7. Shah V, Zakrzewski M, Wibberg D, Eikmeyer D, Schluter A, Madamwar D. Taxonomic profiling and metagenome analysis of a microbial community from a habitat contaminated with industrial discharges. Microb Ecol. 2013; 66:533–50.
8. Rajendhran J, Gunasekaran P. Microbial phylogeny and diversity: small subunit ribosomal RNA sequence analysis and beyond. Microbiological Res. 2011;166(2):99–110.
9. Gilbert JA, Dupont CL. Microbial metagenomics: beyond the genome. Annual Review of Marine Science. 2011;3:347–71.
10. Venter JC, Remington K, Heidelberg JF, et al. Environmental genome shotgun sequencing of the Sargasso Sea. Science. 2004;304(5667):66–74.
11. Tringe SG, Hugenholtz P. A renaissance for the pioneering 16S rRNA gene. Curr Opi Microbiol. 2008;5:442–6.
12. Rusch DB, Halpern AL, Sutton G, et al. The Sorcerer II GlobalOcean Sampling expedition: northwest Atlantic through eastern tropical Pacific. Plos Biology. 2007;5(3):e77.
13. Handelsman J. Metagenomics: application of genomics to uncultured microorganisms. Microbiol Mol Biol Rev. 2004;68:669–85.
14. Al-Saleh E, Drobiova H, Obuekwe C. Predominant culturable crude oil-degrading bacteria in the coast of Kuwait. Int Biodeterior Biodegrad. 2009; 63:400–6.
15. Miralles G, Nerini D, Mante C, Acquaviva M, Doumenq P, et al. Effects of spilled oil on bacterial communities of Mediterranean coastal anoxic sediments chronically subjected to oil hydrocarbon contamination. Microb Ecol. 2007;54:646–61.
16. Orcutt BN, Joye SB, Kleindienst S, Knittel K, Ramette A, et al. Impact of natural oil and higher hydrocarbons on microbial diversity, distribution, and activity on Gulf of Mexico cold-seep sediments. Deep Sea Res Part2 Top Stud Ocean org. 2010;57:2008–21.
17. Raeid MM, Al-Kindi S, Al-Kharusi S. Diversity of bacterial communities along a petroleum contamination gradient in desert soils. Microb Ecol. 2015;69: 95–105.
18. Raeid MM, Al-Kharusi S, Al-Hinai M. Effect of biostimulation, temperature and salinity on respiration activities and bacterial community composition in an oil polluted desert soil. Int Biodeterior Biodegrad. 2015;98:43–52.
19. Radwan S. Microbiology of oil-polluted contaminated desert soils and coastal areas in the Arabian Gulf Region. In: Dion P, Nautiyal CS, editors. Microbiology of extreme soils. Soil biology 13. Berlin: Springer; 2008. p. 275–98.
20. Radwan S. Phytoremediation for oily desert soils. In: Singh A, Kuhad RC, Ward OP, editors. Advances in applied bioremediation. Berlin: Springer; 2009. p. 279–98.
21. Karigar CS, Rao SS. Role of microbial enzymes in the bioremediation of pollutants: A review. Enzym Res. 2011. doi:10.4061/2011/805187.
22. Bestawy E, Mohamed H, Nawal E. The potentially of free gram-negative bacteria for removing oil and grease from contamination industrial effluents. World J Microbiol Biotechnol. 2005;21:815–22.
23. Riffaldi R, Minzi R, Cardelli R, Palumbo S, Saviozzi A. Soil biological activities in monitoring the bioremediation of diesel oil contaminated soil. Water, Air and Soil pol. 2006;170:3–15.
24. Zhou J, Bruns MA, Tiedje JM. DNA recovery from soils of diverse composition. Appl Environ Microbiol. 1996;62:316–22.
25. Desai C, Parikh R, Vaishnav T, Shouche Y, Madamwar D. Tracking the influence of long-term chromium pollution on soil bacterial community structures by comparative analyses of 16S rRNA gene phylotypes. Res Microbiol. 2009;160:1–9.
26. Ludwig W, Strunk O, Westram R, Richter L, Meier H, Yadhukumar BA, Lai T, Steppi S, Jobb G, Forster W, et al. ARB: a software environment for sequence data. Nucleic Acids Res. 2004;32:1363–71.
27. Zerbino DR, Birney E. Velvet: Algorithms for de novo short read assembly using de Bruijn graphs. Genome Res. 2008;18:821–9.
28. Huson DH, Auch AF, Qi J, Schuster SC. Megan analysis of metagenomic data. Genome Res. 2007;17:377–86.
29. Wang Q, Garrity GM, Tiedje JM, Cole JR. Naïve Bayesian classifier for rapid assignment of rRNA sequences into the new bacterial taxonomy. Appl Environ Microbiol. 2007;73:5261–7.
30. Clemente JC, Jansson J, Valiente G. Accurate taxonomic assignment of short pyrosequencing reads. Pac Symp Biocomput. 2010;24:3–9.
31. Cole JR, Wang Q, Cardenas E, Fish J, Chai B, Farris RJ. The Ribosomal Database Project: improved alignments and new tools for rRNA analysis. Nucleic Acids Res. 2009;37:D141–5.
32. Wani AA, Surakasi VP, Siddharth J, Raghavan RG, Patole MS, Ranade D, Shouche YS. Molecular analyses of microbial diversity associated with the Lonar soda lake in India: An impact crater in a basalt area. Res Microbiol. 2006;157:928e937.
33. Kapley A, Baere TD, Purohit HJ. Eubacterial diversity of activated biomass from a common effluent treatment plant. Res Microbiol. 2007;158:494e500.
34. Hammer O, Harper DAT, Ryan PD. PAST: Paleontological statistics software package for education and data analysis. Palaeontol Electron. 2001;4(1):9.
35. Albertsen M, Hugenholtz P, Skarshewski A, Nielsen KL, Tyson GW, Nielsen PH. Genome sequences of rare, uncultured bacteria obtained by differential coverage binning of multiple metagenomes. Nat Biotechnol. 2013;31(6): 533–8.
36. Krzywinski M, Schein J, Birol I, Connors J, Gascoyne R, Horsman D, Steven J, Marco A. Circos: An information aesthetic for comparative genomics. Genome Res. 2009;19:1639–45.
37. Rho M, Tang H, Ye Y. FragGeneScan: predicting genes in short and error-prone reads. Nucleic Acids Res. 2010;38:20–191.
38. Tatusov RL, Galperin MY, Natale DA, Koonin EV. The COG database: a tool for genome-scale analysis of protein functions and evolution. Nucleic Acids Res. 2001;28:33–6.
39. Ogata H, Goto S, Sato K, Fujibuchi W, Bono H, Kanehisa M. KEGG: Kyoto Encyclopedia of Genes and Genomes. Nucleic Acids Res. 1999;27:29–34.
40. Ilori MO, Amund D, Robinson CK. Ultrastructure of two oil degrading bacteria isolated from the tropical soil environment. Folia Microbiol. 2000;45: 259–62.
41. Ahmad M, Sajjad W, Rehman ZU, Hayat M, Khan I. Identification and characterization of intrinsic petrophillic bacteria from oil contaminated soil and water. Int J Curr Microbiol App Sci. 2015;4(2):338–46.
42. Kumar D, Kumar L, Nagar S, Raina C, Prasad R, Gupta VK. Screening isolation and production of lipase/esterase producing *Bacillus sp*. Strain DVL2 and its potential evaluation in esterification and resolution reaction. Arc Appl Sci Res. 2012;4(4):1763–70.
43. Sangwan N, Lata P, Dwivedi V, Singh A, Niharika N, et al. Comparative metagenomic analysis of soil microbial communities across three hexachlorocyclohexane contamination levels. Plos ONE. 2012;7(9):e46219. doi:10.1371/journal.pone.0046219.
44. Li A, Chu Y, Wang X, Ren L, Yu J, Liu X, Yan J, Zhang L, Wu S, Li S. A pyrosequencing based metagenomic study of methane-producing microbial community in solid-state biogas reactor. Biotechnol for Biofuels. 2013;6:3.
45. DeLong EF, Preston CM, Mincer T, Rich V, Hallam SJ, Frigaard NU, et al. Community genomics among stratified microbial assemblages in the oceans interior. Science. 2006;311:496–503.
46. Janssen PH. Identifying the dominant soil bacterial taxa in libraries of 16S rRNA and 16S rRNA genes. Appl Environ Microbiol. 2006;72:1719–28.
47. Lesaulnier C, Papamichail D, McCorkle S, Ollivier B, Skiena S, Taghavi S, et al. Elevated atmospheric CO_2 affects soil microbial diversity associated with trembling aspen. Environ Microbiol. 2008;10:926–41.
48. Patel V, Munot H, Shouche Y, Madamwar D. Response of bacterial community structure to seasonal fluctuation and anthropogenic pollution on coastal water of Alang-Sosiya ship breaking yard, Bhavnagar. India Bioresour Technol. 2014;161:362–70.
49. DeAngelis KM, Brodie EL, DeSantis TZ, Andersen GL, Lindow SE, Firestone MK. Selective progressive response of soil microbial community to wild oat roots. ISME J. 2009;3:168–78.
50. Zhili H, Piceno Y, Ye D, Meiying X, et al. The phylogenetic composition and structure of soil microbial communities shifts in response to elevated carbon dioxide. ISME J. 2012;6:259–72.
51. Liang Y, Joy D, Nostrand V, Deng Y, Zhili H, Liyou W, Xu Z, Guanghe L, Zhou J. Functional gene diversity of soil microbial communities from five oil-contaminated fields in China. ISME J. 2011;5:403–13.
52. Yang Y, Gao Y, Wang S, Xu D, Yu H. The microbial gene diversity along an elevation gradient of the Tibetan grassland. ISME J. 2014;8:430–40.
53. Campbell BJ, Polson SW, Hanson TE, Mack MC, Schuur EAG. The effect of nutrient deposition on bacterial communities in Arctic tundra soil. Environ Microbiol. 2010;12:1842–54.

54. Shade A, Capraso JG, Handelsman J, Knight R, Fierer N. A meta-analysis of changes in bacterial and archaeal communities with time. ISME J. 2013;7:1493–506.
55. Kersters K, De Vos P, Gillis M, Swings J, Vandamme P, Stackebrandt E. Introduction to the *Proteobacteria*. In: Dwarkin M, Falkow S, Rosenberg E, Schleifer K-H, Stackebrandt E, editors. The Prokaryotes, 5. 3rd ed. New York: Springer; 2006. p. 3–37.
56. Adetutu EM, Smith RJ, Weber J, Aleer S, Mitchell JG, Ball AS, Juhasz AL. A polyphasic approach for assessing the suitability of bioremediation for the treatment of hydrocarbon impacted soil. Sci Total Environ. 2013;450–451:51–8.
57. dos Santos HF, Cury JC, do Carmo FL, dos Santos AL, Tiedje J, van Elsas JD, Rosado AS, Peixoto RS. Mangrove bacterial diversity and the impact of oil contamination revealed by pyrosequencing: bacterial proxies for oil pollution. PloS ONE. 2011;6.
58. Sutton NB, Maphosa F, Morillo JA, Abu Al-Soud W, Langenhoff AAM, Grotenhuis T, Rijnaarts HHM, Smidt H. Impact of long-term diesel contamination on soil microbial community structure. Appl Environ Microbiol. 2013;79:619–30.
59. Yang S, Wen X, Jin H, Wu Q. Pyrosequencing investigation into the bacterial community in permafrost soils along the China-Russia crude oil pipeline (CRCOP). PLoS One. 2012;7:e52730.
60. Alonso-Gutierrez J, Costa MM, Figueras A, Albaiges J, Vinas M, Solanas AM, Novoa B. *Alcanivorax* strain detected among the cultured bacterial community from sediments affected by the 'Prestige' oil spill. Mar Ecol Prog Ser. 2008;362:25–36.
61. Kostka JE, Prakash O, Overholt WA, Green SJ, Freyer G, Canion A, Delgardio J, Norton N, Hazen TC, Huettel M. Hydrocarbon degrading bacteria and the bacterial community response in Gulf of Mexico beach sands impacted by the deepwater horizon oil spill. Appl Environ Microbiol. 2011;77:7962–74.
62. Malik Z, Ahmed S. Degradation of petroleum hydrocarbons by oil field isolated bacterial consortium. African J Biotechnol. 2014;11(3):650–8.
63. Patel V, Patel J, Madamwar D. Biodegradation of phenanthrene in bioaugmented microcosm by consortium ASP developed from coastal sediment of Alang-Sosiya ship breaking yard. Mar Pollut Bull. 2013;74:199–207.
64. Hou D, Shen X, Luo Q, He Y, Wang Q, Liu Q. Enhancement of the diesel oil degradation ability of a marine bacterial strain by immobilization on a novel compound carrier material. Mar Pollut Bull. 2012;67:146–51.
65. Song X, Xu Y, Li G, Zhang Y, Huang T, Hu Z. Isolation, characterization of *Rhodococcus sp.* P14 capable of degrading high-molecular-weight polycyclic aromatic hydrocarbons and aliphatic hydrocarbons. Mar Pollut Bull. 2011;62:2122–8.
66. Arulazhagan P, Vasudevan N. Role of a moderately halophilic bacterial consortium in the biodegradation of poly aromatic hydrocarbons. Mar Pollut Bull. 2009;58:256–62.
67. Prince R, Gramain A, Mc Genity T. Prokaryotic hydrocarbon degraders. In: Timmis K, editor. Handbook of hydrocarbon and lipid microbiology. Berlin: Springer; 2010. p. 1672–92.
68. Campbell JW, Cronan JE. Bacterial fatty acid biosynthesis: Targets for Antibacterial Drug Discovery. Annu Rev Microbiol. 2001;55:305–32.
69. Waltermann M, Steinbüchel A. Neutral lipid bodies in prokaryotes: recent insights into structure, formation, and relationship to eukaryotic lipid depots. J Bacteriol. 2005;187:3607–19.
70. Sampath H. Polyunsaturated fatty acid regulation of genes of lipid metabolism. Annu Rev Nutr. 2005;25:317–40.
71. Fujita Y, Matsuoka H, Hirooka K. Regulation of fatty acid metabolism in bacteria. Mol Microbiol. 2007;66(4):829–39.
72. Matsuoka H, Hirooka K, Fujita Y. Organization and function of the YsiA regulon of *Bacillus subtilis* involved in fatty acid degradation. J Biol Chem. 2007;282:5180–94.
73. Cronan JE, Subrahmanyam S. FadR, transcriptional co-ordination of metabolic expediency. Mol Microbiol. 1998;29:937–43.
74. Cronan Jr JE, Waldrop GL. Multi-subunit acetyl-CoA carboxylases. Prog Lipid Res. 2002;41:407–35.
75. Cappello S, Caruso G, Zampino D, Monticelli LS, Maimone G, et al. Microbial community dynamics during assay of harbor oil spill bioremediation: a microscale stimulation study. J Appl Microbiol. 2007;122:184–94.
76. Archaya S, Gopinath LR, Sangaatha S, Bhuvaneshwari R. Molecular characterization of kerosene degrading bacteria isolated from kerosene polluted soil. Int J Adv Res. 2014;2(4):1117–24.

Process Biochemistry 49 (2014) 1673–1681

Contents lists available at ScienceDirect

Process Biochemistry

journal homepage: www.elsevier.com/locate/procbio

An extracellular solvent stable alkaline lipase from *Pseudomonas* sp. DMVR46: Partial purification, characterization and application in non-aqueous environment

Vrutika Patel, Shruti Nambiar, Datta Madamwar*

BRD School of Biosciences, Sardar Patel University, Vadtal Road, Satellite Campus, Post Box # 39, Vallabh Vidhyanagar 388 120, Gujarat, India

ARTICLE INFO

Article history:
Received 22 April 2014
Received in revised form 31 May 2014
Accepted 12 June 2014
Available online 19 June 2014

Keywords:
Organic solvent stable lipase
Pseudomonas sp.
Purification
Microemulsion based organogels (MBGs)
Ester synthesis

ABSTRACT

The biosynthesis of esters is currently of much commercial interest because of the increasing popularity and demand for natural products among consumers. Biotransformation and enzymatic methods of ester synthesis are more effective when performed in non-aqueous media. In present study, an organic solvent stable *Pseudomonas* sp. DMVR46 lipase was partially purified by acetone precipitation and ion exchange chromatography with 28.95-fold purification. The molecular mass of the lipase was found to be ~32 kDa. The partially purified lipase was optimally active at 37 °C and pH 8.5. The enzyme showed greater stability toward organic solvents such as isooctane, cyclohexane and n-hexane retaining more than 70% of its initial activity. The metal ions such as Ca^{2+}, Ba^{2+} and Mg^{2+} had stimulatory effects on lipase activity, whereas Co^{2+} and Zn^{2+} strongly inhibited the activity. Also lipase exhibited variable specificity/hydrolytic activity toward different 4-nitrophenyl esters. DMVR46 lipase was further immobilized into AOT-based organogels used for the synthesis of flavor ester pentyl valerate in presence of organic solvents. The organogels showed repeated use of enzyme with meager loss of activity even upto 10 cycles. The solvent-stable lipase DMVR46 thus proved to be an efficient catalyst showing an attractive potency for application in biocatalysis under non-aqueous environment.

1. Introduction

Lipases known as triacylglycerol acylhydrolases (E.C. 3.1.1.3) are ubiquitous enzymes of considerable physiological significance and industrial prospective. Lipases catalyze the hydrolysis of triacylglycerols to glycerols and free fatty acids. Compared to esterases, lipases are activated only when adsorbed to an oil–water interface [1] and do not hydrolyze dissolved substrates in bulk fluid. Besides, lipases accept a wide range of substrates and are quite stable in non-aqueous solvents, thus they are frequently used for the synthesis of enantiopure compounds for industrial applications [2,3].

Though solvents are extremely lethal to microorganisms, there are numerous advantages of conducting enzymatic conversions in organic solvents such as (i) shifting of thermodynamics equilibrium in favor of synthesis, (ii) regiospecificity and stereoselectivity, (iii) enabling use of hydrophobic substrate, (iv) controlling substrate specificity and (v) thermal stability of enzymes and relative use of product recovery [4]. Solvent stable lipases are obligatory in biotechnological applications, specifically in the production of chiral compounds, high value pharmaceutical substances, modifications of fats and oils, synthesis of flavor esters and food additives, production of biodegradable polymers, biodiesel and in synthesis of fine chemicals [5]. Organic solvents offer advantages on enzyme activity such as synthesis of esters from their constituent acids and alcohol, enzyme stability and possess "pH memory" i.e. catalytic activity of enzyme reflects pH of last solution to which it was exposed [6,7]. So far, the number of solvent tolerant bacterial lipases is inadequate [8], thus it becomes crucial to explore novel lipases with high activity in organic solvents to expand their application in practical catalysis.

Substantial efforts are made to exploit new species of microorganisms that secretes solvent-stable lipase. Baharum et al. [9] reported solvent tolerant lipase produced by *Pseudomonas* sp. strain S5 that was stable in organic solvents such as n-hexane, cyclohexane, toluene and 1-octanol. Rahman et al. [10] described organic solvent tolerant lipase which was not only stable in n-hexane but its activity was stimulated in presence of n-hexane. Cao et al. [8]

* Corresponding author. Tel.: +91 2692 229380; fax: +91 2692 236475; mobile: +91 98256 86025.
E-mail addresses: vrutikaptl.19@yahoo.com (V. Patel), datta_madamwar@yahoo.com (D. Madamwar).

http://dx.doi.org/10.1016/j.procbio.2014.06.007
1359-5113/

studied characterization of an organic solvent stable lipase purified from *Pseudomonas stutzeri* LC2-8 and showed its application for efficient resolution of (R, S)-1-phenylethanol. Dandvate et al. [11] purified a solvent tolerant lipase from *Burkholderia multivorans* V2 and showed its application for the synthesis of ethyl butyrate under non-aqueous environment. Conversely, the stability and reusability of the enzyme are of major concern in non-aqueous enzymatic synthesis. The conceivable answer to this problem is recovery and reuse by immobilizing in/on a solid support which makes it cost effective [12,13].

Lipase immobilization is known to allow easier product recovery, flexibility of reactor design and, in some cases, enhanced storage and operational, thermal and conformational stability [14]. Variety of methods has been used for immobilization of biocatalyst such as adsorption, covalent attachment and entrapment in polymer gels, microencapsulation [15] and sol–gel entrapment [16]. One of the well explored methods for immobilization in non-aqueous biocatalysis is encapsulation of enzyme in microemulsion based organogels (MBGs). The arrangement of MBGs consists of solid network of gelatin/water rods stabilized by monolayer of surfactant, in co-existence with a population of conventional water-in-oil microemulsion droplets. Thus, enzyme immobilized in MBGs has considerable advantages in organic media as direct exposure of enzyme to organic solvent is nullified [17,18].

In this paper, we report production, partial purification and characterization of solvent tolerant lipase produced from solvent stable *Pseudomonas* sp. DMVR46 isolated from oil contaminated soil. There are scanty reports for the production of pentyl valerate ester immobilized in MBGs from purified lipase. Thus, we intend to use this lipase for esterification of pentanol and valeric acid to produce pentyl valerate, a compound with fruity aroma used in industries. The main purpose for the study was exploitation of DMVR46 lipase in non-aqueous environment and its reusability.

2. Materials and methods

2.1. Chemicals

DEAE-cellulose and gelatin were procured from Sigma–Aldrich (Germany). Tributyrin oil and bovine serum albumin (BSA) were obtained from HiMedia (India). All p-nitrophenyl esters were purchased from Sigma–Aldrich (Germany). Sodium bis-2-(ethylhexyl) sulfosuccinate (AOT), valeric acid, pentanol and pentyl valerate were obtained from Fluka (Switzerland). All other solvents (methanol, butanol, iso-propanol, ethanol, acetone, cyclohexane, iso-octane, chloroform) used during the experiment were of HPLC/GC grade.

2.2. Screening of organic solvent tolerant lipolytic microorganism

Soil samples were collected from various oil spilling sites near industrial area of Kadi, Ahmedabad, Gujarat, India. Solvent tolerance was determined by plate overlay method as described by Ogino et al. [19]. Five microliters of overnight grown cultures was transferred to tributyrin agar plates (1% (m/v) tributyrin oil, 0.3% (m/v) yeast extract and 0.5% (m/v) peptone extract, 1.5% (m/v) agar–agar). The plates were kept for 20 min until the drops get dry followed by flooding with 18 mL of different solvents like iso-octane, cyclohexane, toluene, isopropanol, methanol, DMSO. Colonies were examined for solvent tolerance after incubation at 37 °C for 24 h. The ability of the cultures to grow and produce lipase in presence of solvents was observed.

2.3. Identification of solvent stable lipase producing culture using 16S rRNA approach

Bacterial strain designated as DMVR46 was selected on the basis of its solvent tolerance and was identified using 16S rRNA gene sequencing. Genomic DNA was extracted using protocol standardized by Asubel et al. [20] The genomic DNA of DMVR46 was used as template of PCR reaction (30 μL) using universal primers 8F (5′-AGAGTTTGATCCTGGCTCAG-3′) and 1492R (5′-GGTTACCTTGTTACGACTT-3′). The amplification of 16S rRNA gene was done in BioRad PCR cycler (Biorad iCycler version 4.006, Biorad, U.S.A.). Each PCR cycle (total 35 cycles) consisted of 1 min denaturation step at 94 °C, followed by 1 min annealing step at 55 °C and 1 min elongation step at 72 °C, with an initial denaturation step at 94 °C for 5 min and a final extension step at 72 °C for 15 min. PCR products were resolved on 1.2% low melting agarose gel in 1× TAE buffer and was visualized with ethidium bromide staining in Gel Documentation (Alpha-Inotech, U.S.A.). The amplified PCR product was subjected to sequencing by automated DNA Analyzer 3730 using ABI PRISM® BigDye™ cycle sequencing kit (Applied Biosystems, USA). The nearly complete sequence (>95%) was submitted to Genbank at NCBI. BLAST (n) program at NCBI server was used to identify and download nearest neighbor sequence from BLAST database [20].

2.4. Optimization of process parameters for maximum lipase production

Optimization of process parameters for lipase production from isolate DMVR46 was aimed to evaluate the effect of a single parameter at a time, and later manifesting it as standardized condition before optimizing the next parameter. The isolate DMVR46 was cultured in 100 mL medium containing 0.5% (m/v) peptone, 0.3% (m/v) yeast extract and 1% (v/v) tributyrin oil with pH 7.0 and incubated at different temperature (30 °C, 37 °C, 40 °C, 45 °C and 50 °C) to determine the effect of temperature. Similarly, to test the effect of initial pH the culture was investigated at varying pH ranging from 6.0 to 11.0 incubated at 37 °C. The standardized temperature 37 °C and pH 8.0 were used in each step for optimizing the effect of additional inducers, nitrogen sources and carbon sources. The effect of different inducers for lipase production was studied by addition of cotton seed oil, soybean oil, sunflower oil, tributyrin oil, maize oil, olive oil and groundnut oil (each at initial concentration of 1% (v/v). Nitrogen sources such as peptone, yeast extract, tryptone, casein, urea, ammonium sulphate and ammonium nitrate were used to observe the influence of nitrogen sources (1%, m/v) on lipase production. To test the influence of additional carbon sources, media were supplemented with dextrose, lactose and sucrose at 1% (m/v). The best carbon, nitrogen and inducer sources obtained were further tested for varied concentration of 0.2%, 0.5%, 1%. 1.5% and 2%. All experiments were performed in triplicates and the results shown are the average of three independent experiments. Data are represented as mean with standard deviation.

2.5. Growth profile for lipase production

A Erlenmeyer flask of 500 mL capacity containing 200 mL of production medium (0.3% (m/v) yeast extract, 0.5% (m/v) peptone as a basal medium and 1.5% (m/v) tryptone, 0.5% (m/v) dextrose and 1% (m/v) cotton seed oil) was inoculated with an overnight grown culture of DMVR46 to obtain an initial culture density (A_{600}) 0.05 and incubated at 37 °C in an orbital shaker (150 rpm). The samples were withdrawn at regular intervals of 24 h and analyzed for cell growth and enzyme activity. The enzyme activity was estimated

from supernatant (crude lipase) obtained upon centrifugation and cell growth was observed by suspending pellet in distilled water.

2.6. Partial purification of lipase

Solvent tolerant lipase from DMVR46 was purified in two sequential steps. *Step 1*: The culture supernatant was obtained by centrifugation at 10,000 × *g* (Kubota, Model 6500 Japan) for 20 min followed by precipitation using acetone as solvent. Chilled acetone was added slowly to the culture supernatant of strain DMVR46 upto 60% (v/v) concentration with continuous stirring and kept at −20 °C for O/N to allow protein precipitation. The precipitates were harvested by centrifugation at 10,000 × *g* for 20 min at 4 °C and resuspended in 50 mM sodium phosphate buffer (pH 8.0). *Step 2*: The enzyme containing solution was applied to a DEAE-cellulose column previously equilibrated with 50 mM sodium phosphate buffer (pH 8.0). The flow rate was adjusted to 15 mL/h (approx.) having the fraction volume of 1 mL and each fraction was further assayed for enzyme activity and protein content. The lipase preparations (crude and purified fractions) were electrophoresed on SDS-PAGE as described by Laemmli [21]. The protein bands on the gel were visualized upon silver staining.

2.7. Characterization of purified lipase

2.7.1. Effect of pH and temperature on lipase activity and thermal-stability of lipase

Optimum pH of the solvent tolerant lipase was determined by measuring the enzyme activity over a pH value ranging from 6.0 to 10.0 at 37 °C for 30 min. Different buffers used for determination of lipase activity were: pH 6.0–8.5 sodium phosphate buffer, pH 9.0–10.0 glycine–NaOH buffer.

The effect of temperature on the lipase was studied by carrying out the enzymatic reactions at different temperature in the range of 30–50 °C at pH 8.5 (50 mM sodium phosphate buffer). The reactions were carried out for 0–30 min and proceed for enzyme activity. The thermal-stability of the lipase was assayed at various temperatures ranging from 30 to 50 °C for different time interval from 0 to 4 h. At each time interval, 1 mL sample was pipette out and then assayed for residual activity, which was expressed as percentage of initial activity.

2.7.2. Effects of metal ions, inhibitors and surfactants on the lipase activity

The effects of different metal ions (Ca^{2+}, Mg^{2+}, Fe^{2+}, Co^{2+}, Zn^{2+} and Ba^{2+}) and inhibitors (EDTA and β-mercaptoethanol) were investigated by pre incubating the purified lipase with 10 mM solutions of these ions or inhibitors at pH 8.5 for 30 min at 37 °C. Similarly, the effects of surfactants (SDS, CTAB, Triton X-100, Tween 20 and Tween 80) at the concentration of 0.5% were investigated.

2.7.3. Stability of lipase DMVR46 in different organic solvents

The effects of different organic solvents on the activity and the stability of the purified lipase were investigated following method defined by Ogino et al. [19]. The stability of lipase in organic solvents was investigated by appropriately mixing 3 mL of purified enzyme and 1 mL of solvent in crew cap vials to obtain a final solvent concentration of 25% (v/v). The solution was incubated in shaker (150 rpm) at 37 °C for 0–4 h and lipase activity was assayed in the aqueous phase.

2.7.4. Substrate specificity to various p-nitrophenyl esters

The substrates, p-nitrophenyl fatty acid esters, of varying chain length (C2, C4, C8, C12, C16 and C18) were used at the final concentration of 0.3 mg/mL and the lipase activity was measured according to the pNPP method [22].

2.8. Synthesis of pentyl valerate under water restricted environment using free and immobilized DMVR46 lipase

Pentyl valerate was synthesized by the condensation of pentanol and valeric acid using free as well as immobilized lipase as described by Dandavate et al. [23]. For immobilization, the partially purified lipase was first entrapped in a surfactant solution comprising of 0.1 M sodium bis (2-ethylhexyl) sulfosuccinate (AOT) with Wo = 60 in isooctane by vigorously mixing the two solutions to create a clear reverse micellar system of AOT/50 mM phosphate buffer (pH 8.5) – lipase/isooctane (1 mL). The amount of purified lipase used for immobilization was 108 μL having specific activity of 64.57 U/mg. This system was then polymerized by the addition of 14% gelatin (1.5 mL) maintained at 55 °C followed by vigorous mixing to obtain homogenous AOT based organogel (MBGs). The gel was poured into plastic Petri plates, dried overnight, and cut into small pieces (1 cm × 1 cm with 110 ± 10 μm thickness). The reaction mixture consisted of 20 mL cyclohexane and equimolar concentrations (100 mM) of pentanol and valeric acid. The esterification reaction was initiated by addition of free lipase and the pieces of MBGs to the reaction mixture in glass-stoppered flasks kept on orbital shaker at 37 °C and 150 rpm. At every 24 h interval 100 μL of the reaction mixture was withdrawn and analyzed by gas chromatograph.

2.9. Reusability studies

For reusability studies, upon completion of each cycle for ester production the immobilized enzymes was recovered by washing with neat cyclohexane twice for removal of unwanted substrate or product formed, air dried and reused for next cycle of esterification. This procedure was repeated for several cycles.

2.10. Analytical procedures

2.10.1. Lipase assay

The pH stat method: Lipase activity was measured under controlled temperature using a pH 718 STAT Titrino Titrator (Metrohm, Switzerland). The buffer used for the activity determination comprised of 10% (m/v) Gum Arabic, 0.2% (m/v) bile salt, and 20% (m/v) $CaCl_2$, 5% (v/v) cotton oil as substrate and 0.1 M NaOH as the titrant. The insoluble triglycerides were dispersed by vigorous stirring. One unit of enzyme activity was defined as the amount of enzyme that liberates 1 μmol of fatty acid/min at 37 °C [24].

In order to check hydrolytic activity of lipase exclusively for different p-nitrophenyl esters lipase activity was measured with spectrophotometric method using p-nitrophenyl esters as substrate [22]. The substrate with a final concentration of 0.3 mg/mL was dissolved in 1 mL of isopropanol and mixed with 9 mL of 50 mM sodium phosphate buffer (pH 8.5) containing gum Arabic (0.1%) and Triton X-100 (0.6%). The reaction mixture was composed of 240 μL of substrate solution and 10 μL of appropriately diluted enzyme solution, and incubated at 37 °C for 10 min. The p-nitrophenol (p-NP) produced in the reaction mixture was quantified spectrophotometrically at 410 nm. One unit of enzyme activity was defined as the amount of enzyme that liberated 1 μmol p-nitrophenol/min under standard assay conditions.

2.10.2. Protein assay

Soluble protein was estimated by Lowry's method [25] using bovine serum albumin as standard.

2.10.3. Quantification of ester production by gas chromatography

Quantification of accumulated ester was done by using gas chromatograph using FID as detector described by Raghavendra et al. [26]. After initiation of esterification, 100 μL sample was periodically collected and analyzed by gas chromatograph (Perkin Elmer, Model Clarus 500, USA) equipped with the flame ionization detector and a 30 mRtx-R-20 (cross bond 80% dimethyl-20% diphenyl polysiloxane) capillary column. Nitrogen served as a carrier gas at a split flow rate of 90 mL/min. The injector and detector temperatures were 250 and 280 °C respectively and oven temperature was programmed to increase from 100 to 160 °C at the rate of 20 °C/min, from 160 to 280 °C at the rate of 2 °C/min and from 165 to 175 °C at the rate of 1 °C/min. Ester identification and quantification was done by comparing the retention time and peak area of the sample with a standard. Pure pentyl valerate (>98%) was used as external standard.

3. Results and discussion

3.1. Isolation and identification of solvent tolerant lipase producing bacteria

Lipases are inducible enzymes that are produced in the presence of lipids such as oils, triaclyglycerols, fatty acids and glycerols in addition to carbon sources [27]. Organic solvents are often lethal to microorganisms and thus can denature or inactivate enzymes. Therefore, we assumed that organic solvent tolerant bacteria are ought in producing enzyme that can tolerate the toxic effect of organic solvent to a certain degree and will be very useful in industry. In the present study, we have screened solvent tolerant lipase explored by its ability to grow on tributyrin agar plates flooded with different solvents. Out of all isolates showing clearance zone on tributyrin agar plate, the isolate DMVR46 showed the highest lipase activity (9 U/mL), and hence was used for further studies. Organic solvent tolerant lipase produced by strain DMVR46 was identified as *Pseudomonas* sp. on the basis of 16 S rRNA gene sequencing followed by BLAST analysis which showed sequence homology (100%) with the complete 16S rRNA gene sequence of *Pseudomonas* sp. The sequence of strain DMVR46 was deposited in NCBI with an Accession number KF636492. Phylogenetic affiliation of isolate DMVR46 with related *Pseudomonas* sp. is shown in Fig. 1.

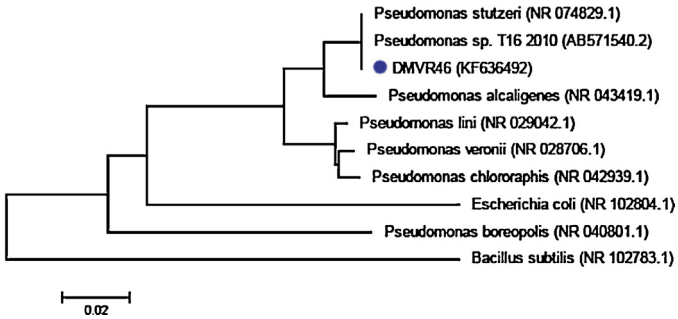

Fig. 1. Phylogenetic tree based on 16S rRNA gene sequence of *Pseudomonas* sp. DMVR46. (GenBank accession No. KF636492) and sequence of closest phylogenetic neighbors obtained by NCBI BLAST (n) analysis, numbers in the parenthesis indicate accession numbers of corresponding sequence. The tree was constructed using MEGA 5.0 software. *Bacillus subtilis* strain NR 102783 has been taken as an out-group.

3.2. Growth profile for lipase production

Various physico-chemical parameters were scrutinized for maximum lipase production. The optimum temperature and pH for initial lipase activity was found to be 37 °C and pH 8.0 (Fig. 2(a) and (b)). Cao et al. [8] showed maximum lipase production at pH 8.0 and at 30 °C from *P. stutzeri* LC2-8. Among various inducers tested for lipase production, cotton seed oil (1% (v/v)) with an activity of 48 U/mL (Fig. 2(c)) was the best inducer followed by soya bean and maize oil. The best lipase production (75.54 U/mL lipase activity) was obtained with 1.5% tryptone (Fig. 2(d)) as organic nitrogen supplement. However, all the inorganic nitrogen sources resulted in the reduction of bacterial growth as well as lipase production. Also, as shown in Fig. 2(e) cotton oil used at the concentration of 1% (v/v) and tryptone with concentration of 1.5% (m/v) stimulated lipase activity. Using optimized conditions the maximum lipase activity of 79.54 U/mL was observed on 2nd day with cell mass of 16.571 (including dilution factor) absorbance at 600 nm (assay done using pH STAT method [24]). On 3rd day decline in lipase activity as well as growth was observed (Fig. 3). The decrease of lipase production and growth of the bacterial cells at the later stage could be possibly due to pH inactivation, proteolysis, or both [28].

3.3. Purification of solvent tolerant lipase DMVR46

The extracellular lipase secreted by DMVR46 was purified by acetone precipitation and DEAE-cellulose anion-exchange chromatography. About 28.95 fold purification with 29.74% recovery was achieved (Table 1). The purified lipase showed a single band on SDS-PAGE (Fig. 4). The purified lipase was homogenous and its molecular mass was estimated to be ~32.0 kDa.

Cao et al. [8] reported purification of lipase from *P. stutzeri* by acetone precipitation with 32.8% recovery. Ogino et al. [19] reported purify cation of *Pseudomonas aeruginosa* LST-03 lipase by ion-exchange and hydrophobic interaction chromatography achieving 34.7-fold purification and 12.6% yield. Rahman et al. [10] succeeded in getting higher recovery but they employed affinity chromatography in combination with ion-exchange chromatography. *P. aeruginosa* PseA lipase was purified by ultrafiltration and gel exclusion chromatography with 8.6 fold purification and 51.6% recovery [29]. Meanwhile, *Pseudomonas mendocina* PK-12CS lipase was purified to 240 fold with 14.8% recovery using acetone precipitation and anion exchange chromatography [30].

3.4. Characterization of purified lipase

3.4.1. Effect of pH and temperature on activity and stability of the lipase

The optimum pH for purified lipase was found to be 8.5 (Fig. 5) and it retained 100% of its maximum activity, while remarkable drop was obtained below pH 8.0 and above pH 9.0 indicating alkaline nature of enzyme. Gilbert et al. [31] reported *P. aeruginosa* EF2 lipase with a maximum activity in the range of pH 8.5–9.0.

The optimum temperature for lipase activity was observed to be 37 °C as indicated in Fig. 6(a). Whereas, Cao et al. [8] showed lipase from *P. stutzeri* LC2-8 having optimum activity at 30 °C and organic solvent stable *P. aeruginosa* LST-03 lipase screened by Ogino

Table 1
Purification of lipase produced by *Pseudomonas* sp. DMVR46.

Purification steps	Total activity (Units)	Total protein (mg)	Specific activity (U/mg)	Fold purification	Yield (%)
Crude enzyme	3951	1764.5	2.23	1	100
Acetone precipitation	2780.4	112.5	24.71	11.08	70.37
DEAE-cellulose	1175.3	18.2	64.57	28.95	29.74

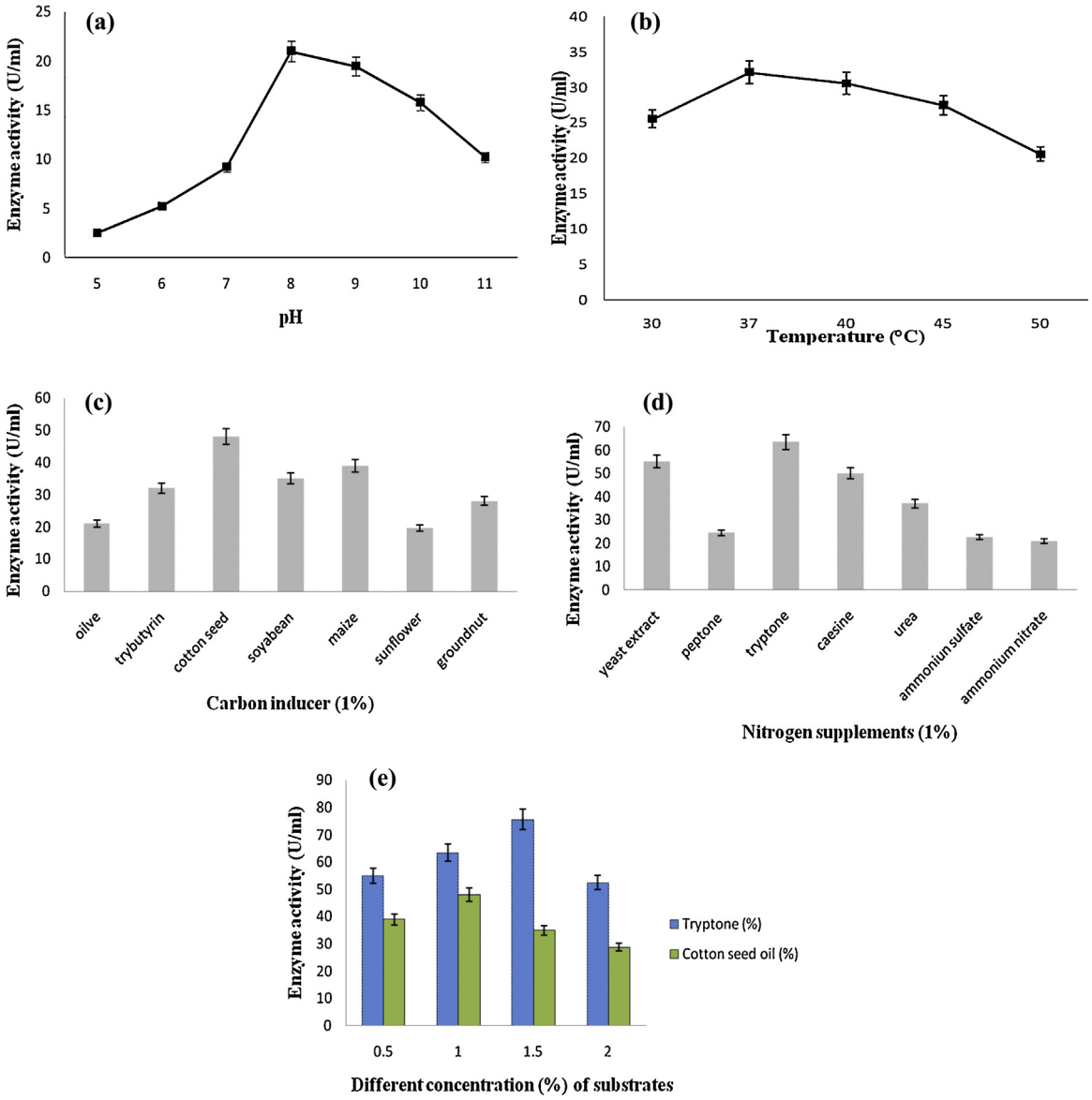

Fig. 2. Effect of (a) pH, (b) temperature, (c) carbon inducer, (d) nitrogen supplements, (e) different substrate i.e. tryptone (%) and cotton seed oil (%) concentration on lipase production by DMVR46.

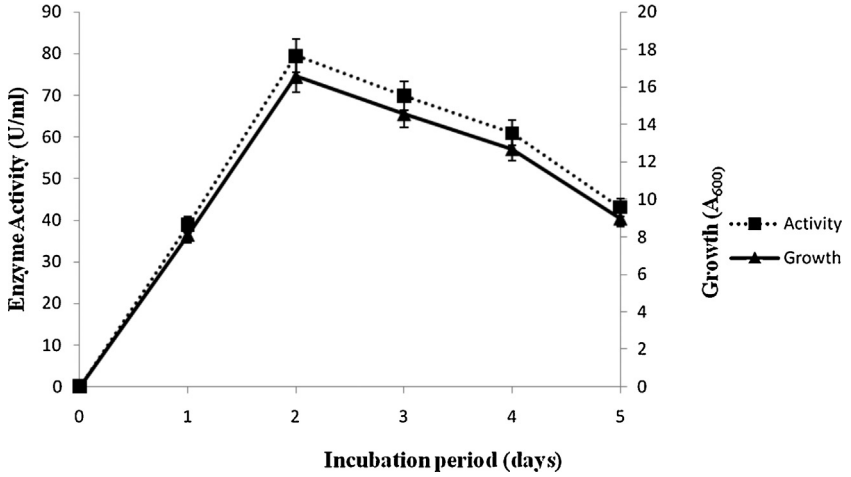

Fig. 3. Growth profile of lipase produced by *Pseudomonas* sp. DMVR46. The production was carried out at 37 °C under shaking condition (150 rpm) in presence of cotton seed oil with pH 8.

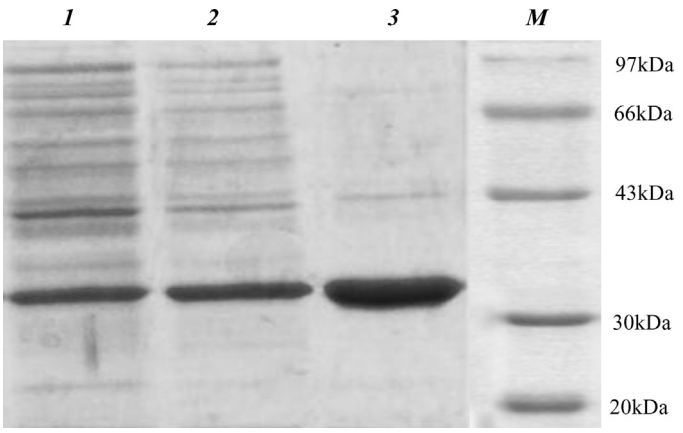

Fig. 4. SDS-PAGE of lipase DMVR46 at different stages of purification. Lane M: protein marker; Lane 1: supernatant; Lane 2: lipase concentrated by acetone precipitation; Lane 3: lipase purified by DEAE-cellulose.

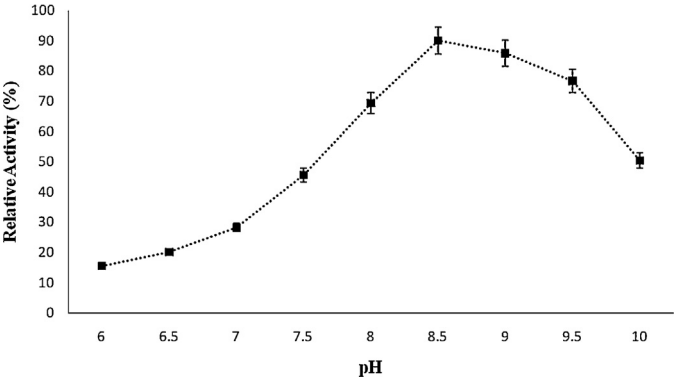

Fig. 5. Effect of pH on activity of lipase obtained from purified *Pseudomonas* sp. DMVR46. The enzyme was added to various buffer systems (pH 6.0–10.0) of 50 mM at 37 °C for 30 min. The buffer systems used were pH 6.0–8.5 sodium phosphate buffer and pH 9.0–10.0 glycine–NaOH buffer.

et al. [19] showed maximum activity at 37 °C. The trend for thermal stability of purified lipase on different temperature is shown in Fig. 6(b). Lipase DMVR46 retained approximately 68% of its initial activity at 37 °C when incubated for 4 h. With increase in temperature, at 40 °C enzyme retained only 28% of initial activity, while at 50 °C enzyme was drastically inactivated as shown in Fig. 6(b). Similar trends of reports were seen in organic solvent-stable LST-03 lipase having maximal activity at 37 °C as reported by Ogino et al. [19]. Thermal stability profile of PseA purified by Gaur et al. [29] was found to be stable at 40 °C upto 4 h. Sharma et al. [32] reported that *Pseudomonas* sp. AG-8 lipase has optimal activity at 45 °C. In contrast, organic solvent stable LST-03 lipase showed a lower stability (below 40 °C for 10 min) then DMVR46 lipase.

3.4.2. Substrate specificity

Substrate specificity of lipases may be attributed to alterations in the geometry and dimensions of their active sites [33]. The substrate specificity of purified lipase was determined by testing the lipolytic activities against p-nitrophenyl fatty acid esters according to the spectrophotometric method [22]. The trend for hydrolytic activity of enzyme toward substrate is evident from Fig. 7. The result indicates higher hydrolytic activity for long chain substrate (p-nitrophenyl palmitate) p-NPP; this can be explained in the terms of lipase structure. Lipases exist in two forms, closed (inactive) and open (active) forms. *Pseudomonas* sp. lipase has been characterized of lacking interfacial activation and 'lid' in contrast to most of other lipases [34]. The CMC (critical micelle concentration) values for

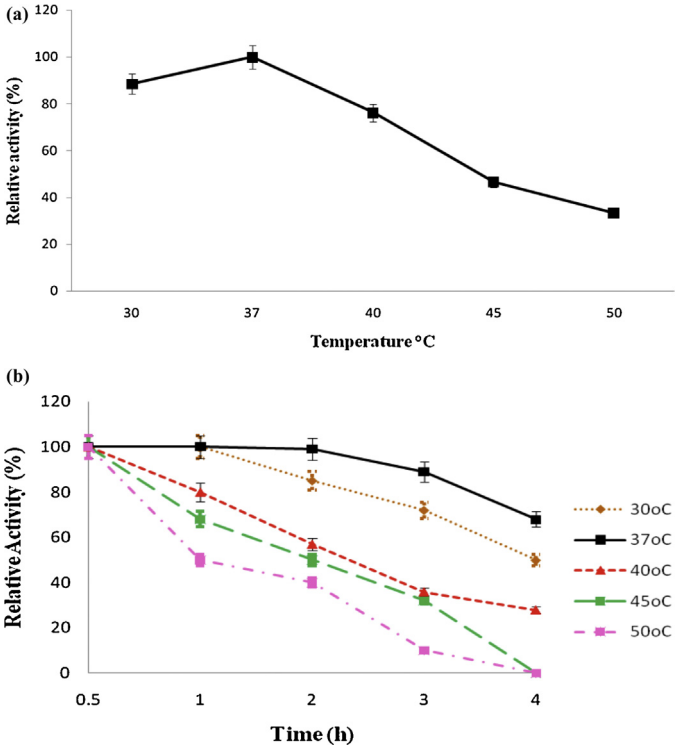

Fig. 6. (a) Temperature profile of purified DMVR46 lipase. The effect of temperature on lipase activity was studied by carrying out the enzyme reaction at different temperature in the range of 30–50 °C at pH 8.5 using sodium phosphate buffer (50 mM). The reaction was carried out for 4 h. (b) Thermal stability of purified lipase was measured by incubating the lipase in 50 mM sodium phosphate buffer (pH 8.5) at 30 °C, 37 °C, 40 °C, 45 °C and 50 °C for 4 h. Residual lipase activity (%) was calculated relative to the initial activity.

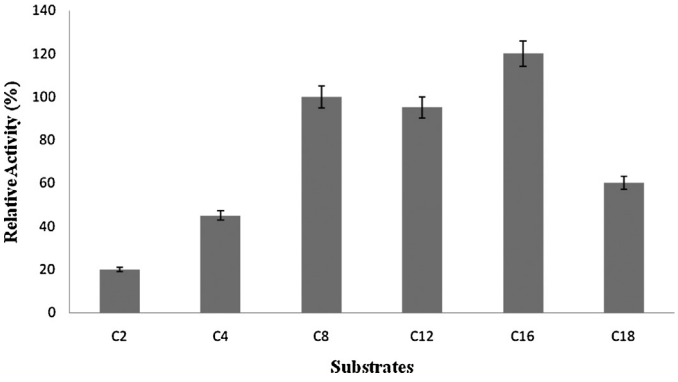

Fig. 7. Substrate specificity of purified DMVR46 lipase against various fatty acid esters. The activity of lipase toward different p-nitrophenyl esters were determined and calculated relative to the maximum activity measured toward p-nitrophenyl caprylate (taken as 100%). The composition of the reaction mixture was 0.1 mg/mL of lipase and 0.3 mg/mL of synthetic pNP esters (where C2 = p-nitrophenyl acetate, C4 = p-nitrophenyl butyrate, C8 = p-nitrophenyl caprylate, C12 = p-nitrophenyl laurate, C16 = p-nitrophenyl palmitate, C18 = p-nitrophenyl sterate).

different substrates were found to be (p-nitrophenyl butyrate) p-NPB 200 μM, (p-nitrophenyl caprylate) p-NPC 5 μM, (p-nitrophenyl laurate) p-NPL 100 μM, p-NPP 50 μM and (p-nitrophenyl stearate) p-NPS 20 μM. Thus, from the results it could be concluded that i) no interfacial activation was noted with short and moderate chain substrates, while activation was observed at point using substrate of long chain (p-NPP) and ii) the lack of interfacial activation of lipases could be caused not only by the structural features of the enzyme but also by very low CMC values of the substrate [34–36]. Generally, lipases from *Pseudomonas* sp. prefer

Table 2
Effect of various metal ions, inhibitors and surfactants on DMVR46[a] lipase activity at pH 8.5 and 37 °C.

Metal ions	Relative lipase activity (%)
Control[b]	100
Ca^{2+}	135.1
Mg^{2+}	119.4
Fe^{2+}	98.3
Co^{2+}	7.7
Zn^{2+}	3.6
Ba^{2+}	110.3
EDTA	40.44
2-Mercaptoethanol	98.89
PMSF	95.7
Iodoacetate	36.12
SDS*	80.65
Triton X-100*	137.5
Tween 20*	92.49
Tween 80*	96.39
CTAB*	12.5

[a] Lipase DMVR46 was incubated with various metals, inhibitors (10 mM) and detergents (0.5%) with the superscript * in 50 mM sodium phosphate buffer (pH 8.5) at 37 °C for 30 min.
[b] Lipase activity is shown as value relative to the initial activity without addition of effectors (control).

small or medium chain fatty acids triglycerides or their methyl esters [19,37,38]. However, lipase from *P. aeruginosa* AAU2 [39], *Pseudomonas alcaligenes* EF2 [31], *Pseudomonas* sp. S5 [10] and *Pseudomonas cepacia* [33] shows specificity for longer chain fatty acids substrates.

3.4.3. Effects of metal ions, inhibitors and surfactants on lipase activity

Among the tested metal ions Ca^{2+}, Mg^{2+} and Ba^{2+} significantly stimulate activity while Zn^{2+} and Co^{2+} strongly inhibit lipase activity (Table 2). Many lipases have been found to display enhanced activity in the presence of Ca^{2+} [10,11,29,31]. The presence of Ca^{2+}, Ba^{2+} and Mg^{2+} increase lipase activity this may be due to binding of metal complex to the active site of the enzyme which leads to the conformational changes in protein [10]. Alternatively, Ca^{2+} might complex with fatty acids produced during catalysis eliminating the possibility of product inhibition [40]. The chelating agent EDTA significantly reduce the lipase activity suggesting that purified lipase may be a metalloenzyme, whereas in presence of disulphide reducing agent β-mercaptoethanol slight reduction in activity was observed. PMSF, a serine inhibitor has a marginal effect on DMVR46 lipase at 10 mM concentration exhibiting 95% of relative lipase activity. This may be attributed to the fact that the catalytic serine residue is inaccessible owing to the presence of lid covering the active site which is a characteristic feature for most of the lipases [8,29,39].

Surfactants facilitate access of substrate to the enzyme by reducing the interfacial tension between oil and water increasing the lipid–water interfacial area where catalytic reactions takes place [41]. Non-ionic detergent Triton X-100 stimulated lipase activity (Table 2). Whereas, Tween 80 has modest influence on lipase activity by reducing it, while anionic surfactant sodium dodecyl sulphate (SDS) showed 20% decrease in activity. Cationic surfactant (CTAB) completely inactivated the enzyme, as CTAB has been thought to destroy the conformation of lipase [42].

3.4.4. Stability of lipase in organic solvents

High activity and stability of lipases in organic solvents is considered as novel attributes. Effects of different organic solvents (25%) on the stability of *Pseudomonas* sp. DMVR46 lipase are shown in Table 3. The enzyme was found to be quite stable and active in most of the organic solvents. The highest stability was achieved in isooctane, cyclohexane and n-hexane with the relative lipase activity of 120%, 80% and 78% respectively after 4 h. The activation of lipase could be explained by the interaction of organic solvents with hydrophobic amino residues present in the lid that covers the catalytic site of the enzyme, thereby maintaining the lipase in its open conformation [43]. When organic solvents such as toluene, butanol and chloroform was added to purified lipase solution and incubated for 1 h, the enzyme got drastically inactivated. The possible reason for this may be the incubation of enzyme in polar solvents (Log *P* values <3.0), remove water molecules necessary for its catalytic function which leads to decrease in activity of enzyme. The results suggested DMVR46 lipase exhibited fairly good stability, retaining more than 70% of its activity in presence of organic solvents with Log *P* value of 3.00 or higher. The reasonably high stability of DMVR46 lipase in organic solvents makes it potentially useful for practical application in many synthetic reactions in non-conventional media.

Table 3
Organic solvent stability of *Pseudomonas* sp. DMVR46 lipase at pH 8.5 and 37 °C.

Organic solvents (25%)	Log *P*	Relative lipase activity (%)
Control	–	100
Methanol	−0.76	8.90
Ethanol	−0.24	30.5
Butanol	0.89	0
Iso-propanol	0.28	40.8
Toluene	2.64	0
Acetone	−0.23	45.23
Iso-octane	4.7	120.41
Cyclohexane	3.2	80.52
n-Hexane	3.5	78.98
Chloroform	2.0	0

Note: Data are means of triplicate determinations. The purified enzyme and organic solvents were mixed in a 3:1 ratio, and the mixture was incubated at 37 °C with shaking at 150 rpm for 4 h and assayed for lipase activity. Activities of DMVR46 in presence of various organic solvents are shown as a value relative to those in the absence of organic solvent (control).

3.5. Kinetic study

The maximum specific activities (V_{max}) and Michaelis constants (K_m) for free and immobilized lipase were estimated from double reciprocal plots of thee initial rates of pNPP hydrolysis. The K_m of immobilized lipase (0.45 mM) was ~3-folds lower than that of free lipase (1.437 mM), while the V_{max} of immobilized lipase (257 μmol/mg/min) was ~9-folds higher than that of free lipase (25.18 μmol/mg/min). The lower K_m value indicated the higher affinity of enzyme for substrate and higher V_{max} value indicates higher activity of enzyme. The immobilized enzyme was found to be 35 times more efficient catalyst for pNPP hydrolysis in comparison to that of free lipase. Immobilization of lipase in organogels induces some structural changes, which probably is responsible for enhancing its esterification activity. The changes in parameters suggest that immobilization of lipase resulted in an increased affinity for the substrate by improving accessibility of the active site [23].

The effect of temperature on affinity of free and immobilized enzyme can be seen in Arrhenius plot (Fig. 8) The free and immobilized lipase exhibited a linear relationship in the temperature range of 30–40 °C and the corresponding activation energies were calculated to be 9.2 kJ/mol for free lipase and 2.48 kJ/mol for immobilized lipase. The activation energy of the immobilized lipase is lower in comparison to that of free lipase which suggests the change in conformation of enzyme during immobilization.

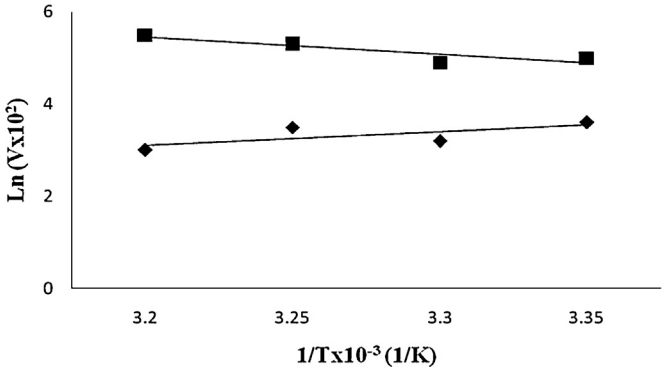

Fig. 8. Arrhenius plot for initial hydrolysis rate of pNPP catalyzed by free and immobilized lipase. Activation energy for free (♦) and immobilized lipase (■) was calculated to be 9.2 and 2.48 kJ/mol, respectively.

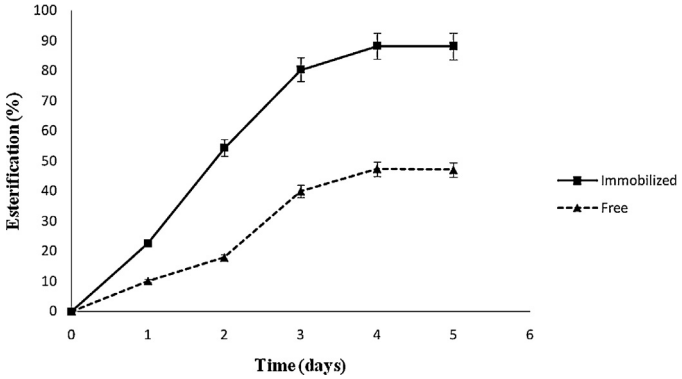

Fig. 9. Time course of pentyl valerate production catalyzed by free and immobilized DMVR46 lipase using pentanol (0.1 M) and valeric acid (0.1 M). The reaction was carried out in presence of cyclohexane as solvent at 37 °C with shaking (150 rpm).

3.6. Application of purified lipase for ester synthesis under water restricted environment using free and immobilized DMVR46 lipase

The biosynthesis of esters is currently of much commercial interest as the fatty acid esters synthesized using enzymes offer better odor and flavor characteristics when compared to those produced chemically [44]. Lipase from DMVR46 was used for the synthesis of industrially important ester "pentyl valerate". Fig. 9 shows the trend of synthesizing ester using free and immobilized lipase. The partially purified lipase from DMVR46 exhibited significant esterification efficiency with 88% ester production after 4 days of reaction when immobilized into AOT-organogels. While the free lipase showed only 47% of ester synthesis after 4 days of reaction. The immobilized enzyme has been more active than crude extract. This phenomenon can be attributed to the fact that the catalytic activity of lipase extract is lower than immobilized form due to the better dispersion of enzyme molecules on the support surface which improves its activity in organic medium [45]. Moreover, the immobilization of lipase in MBGs has been reported to improve the catalytic efficiency of enzyme by providing protection against inhibitory effect of organic solvents as well as aid in reusability of lipase facilitating easy recovery by simple filtration [23]. Hence, DMVR46 lipase may prove to be promising in esterification and standardization of reaction parameters may increase its efficiency as a biocatalyst.

3.7. Reusability of DMVR46 lipase

To prove the potential of an immobilized enzyme for application in industry, the most important criterion is to demonstrate its high reusability. The MBGs were subjected to reusability examination for determining the efficiency of immobilization. The enzyme preparation was given solvent washes after every cycle where the reaction time for each cycle was 4 days and reused in fresh media supplemented with substrates. The reusability studies showed that immobilized enzyme was stable up to 6 cycles of esterification, during which no significant decrease in esterification efficiency was noticed. However, activity started declining slowly after 6th cycle (Fig. 10). This may be due to accumulation of water formed as a by-product of reaction. Lipase DMVR46 exhibited 70% of its residual activity even after 10th run indicating meager loss of activity.

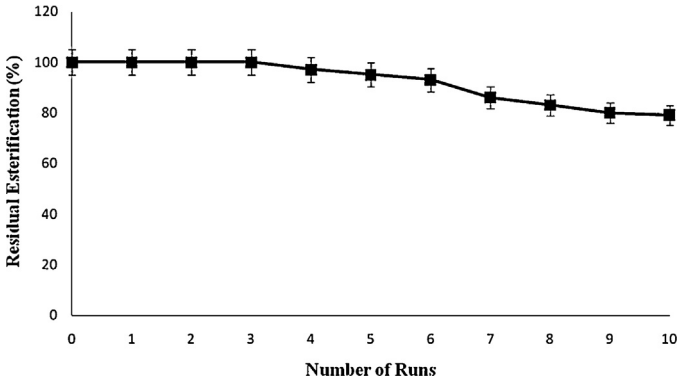

Fig. 10. Reusability of DMVR46 lipase immobilized into AOT-based organogels. The reaction was carried out at 37 °C and 150 rpm.

4. Conclusion

In this study, an extracellular lipase from solvent tolerant *Pseudomonas* sp. DMVR46 was purified following simple purification procedure with 29.74% recovery. The molecular mass of the lipase was found to be ~32.0 kDa by SDS-PAGE. It exhibited optimum activity at pH 8.5 and 37 °C. Among various p-nitrophenyl esters with different chain lengths, the lipase showed maximum activity on p-nitrophenyl palmitate (C16). The enzyme exhibited significant stability in presence of iso-octane and cyclohexane and was activated by Ca^{2+}, Ba^{2+} and Mg^{2+} but SDS and EDTA has negative influence on its activity. The partially purified lipase showed significant esterification activity for synthesis of pentyl valerate and revealed improved catalytic efficiency upon immobilization in microemulsion based organogels. These results make solvent-tolerant lipase DMVR46 more potentially valuable for biotechnological applications in non-aqueous catalysis.

Acknowledgements

The authors are thankful to University Grants Commission (UGC) (grant no. F. 42-167/2013 (SR)) New Delhi, India for financial assistance. The authors would also extend their acknowledgment to Dr. Yogesh Souche of NCCS, Pune, India for 16S rDNA sequencing.

References

[1] Martinelle M, Holmquist M, Hult K. On the interfacial activation of *Candida antarctica* lipase A and B as compared with *Humicola lanuginosa* lipase. Biochim Biophys Acta 1995;1258:272–6.
[2] Katsoura MH, Polydera AC, Katapodis P, Kolisis FN, Samatis H. Effect of different reaction parameters on the lipase-catalyzed selective acylation of polyhydroxylated natural compounds in ionic liquids. Process Biochem 2007;42:1326–34.
[3] Cai XQ, Wang N, Lin XF. The preparation of polymerizable, optically active non-steroidal anti-inflammatory drugs derivatives by irreversible enzymatic methods. J Mol Catal B: Enzym 2006;40:51–7.
[4] Koops BC, Verheij HM, Soltboom AJ, Egmond MR. Effect of chemical modification on the activity of lipases in organic solvents. Enzyme Microb Technol 1999;25:622–31.

[5] Sulong MR, Rahman RNZRA, Salleh AB, Basri M. A novel organic solvent tolerant lipase from *Bacillus sphaericus* 205y: extracellular expression of a novel OST-lipase gene. Protein Expr Purif 2006;49:190–5.
[6] Klibanov AM. Improving enzymes by using them in organic solvents. Nature 2001;409:241–6.
[7] Hazarika S, Goswami P, Dutta NN, Hazarika AK. Ethyl oleate synthesis by Porcine pancreatic lipase in organic solvents. Chem Eng J 2002;85:61–8.
[8] Cao Y, Zhuang Y, Yao C, Wu B, He B. Purification and characterization of an organic solvent-stable lipase from *Pseudomonas stutzeri* LC2-8 and its application for efficient resolution of (R, S)-1-phenylethanol. Biochem Eng J 2012;64:55–60.
[9] Baharum SN, Salleh AB, Razak CNA, Basri M, Rahman MBA, Rahman RNZRA. Organic solvent tolerant lipase by *Pseudomonas* sp. strain S5: stability of enzyme in organic solvent and physical factors affecting its production. Anal Microbiol 2003;53:75–8.
[10] Rahman RNZRA, Baharum SN, Salleh AB, Basri M. S5lipase: an organic solvent tolerant enzyme. J Microbiol Biotechnol 2006;44:583–90.
[11] Dandvate V, Jinjala J, Keharia H, Madamwar D. Production, partial purification and characterization of organic solvent tolerant lipase from *Burkholderia multivorans* V2 and its application for ester synthesis. Bioresour Technol 2009;100:3374–81.
[12] Perraud R, Laboret F. Optimization of methyl propionate production catalyzed by *Mucor miehei* lipase. Appl Microbiol Biotechnol 1995;44:321–6.
[13] Balcao VM, Paiva AL, Malcata FX. Bioreactors with immobilized lipases: state of art. Enzyme Microb Technol 1996;18:392–416.
[14] Cabral PP, da Fonsece MMR, Dias SF. Esterification activity and operational stability of *Candida rugosa* lipase immobilized in polyurethane foams in the production of ethyl butyrate. Biochem Eng J 2010;48:246–52.
[15] Chen B, Hu J, Miller EM, Xie W, Cai M, Gross RA. *Candida antarctica* lipase B chemically immobilized on epoxy activated micro and nanobeads: catalysts for polyester synthesis. Biomacromolecules 2008;9:463–547.
[16] Soni K, Madamwar D. Ester synthesis by lipase immobilized on silica and microemulsion based organogels (MBGs). Process Biochem 2001;36:607–12.
[17] Atkinson PJ, Grimson MJ, Heenan RK, Howe AM, Robinson BH. Structure of microemulsion based organogels. J Chem Soc Chem Commun 1989;23:1807.
[18] Atkinson PJ, Robinson BH, Howe AM, Heenan RK. Structure and stability of microemulsion based organogels. J Chem Soc Faraday Trans 1991;87:3389–97.
[19] Ogino H, Nakagawa S, Shinya K, Muto T, Fujimura N, Yasuda M, Ishikawa H. Purification and characterization of organic solvent-stable lipase from organic solvent tolerant *Pseudomonas aeruginosa* LST-03. J Biosci Bioeng 2000;89:451–7.
[20] Ausubel FM, Brent R, Kingston RE, Moore DD, Seidman JA, Smith JG, Struhl DJ. Current protocols in molecular biology. New York: John Wiley and Sons; 1997 [unit (24)].
[21] Laemmli UK. Cleavage of structural protein during assembly of the head of bacteriophage T4. Nature 1970;227:680–5.
[22] Winkler UK, Stuckmann M. Glycogen, hyaluronate, and some other polysaccharides greatly enhance the formation of exolipase by *Serratia marcescens*. J Bacteriol 1979;138:663–70.
[23] Dandavate V, Madamwar D. Novel approach for the synthesis of ethyl isovalerate using surfactant coated *Candida rugosa* lipase immobilized in microemulsion based organogels. Enzyme Microb Technol 2007;41:265–70.
[24] Ahmed EH, Raghavendra T, Madamwar D. A thermostable alkaline lipase from a local isolate *Bacillus subtilis* EH 37: characterization, partial purification, and application in organic synthesis. Appl Biochem Biotechnol 2010;160:2102–13.
[25] Lowry OH, Rosebrough NJ, Farr AL, Randall RJ. Protein measurement with the Folin phenol reagent. J Biol Chem 1951;31:426–8.
[26] Raghavendra T, Sayania D, Madamwar D. Synthesis of the 'green apple ester' ethyl valerate in organic solvents by *Candida rugosa* lipase immobilized in MBGs in organic solvents: effects of immobilization and reaction parameters. J Mol Catal B: Enzym 2010;63:31–8.
[27] Treichel H, Oliveira D, Mazutti MA, Luccio MD, Oliveira JV. A review on microbial lipases production. Food Bioprocess Technol 2010;3:182–96.
[28] Bayoumi AR, El Louboudey SS, Sidkey MN, Abd-el-rahman AM. Production, purification and characterization of thermoalkalophilic lipase for application in bio-detergent industry. J Appl Sci Res 2007;3:1752–65.
[29] Gaur R, Gupta A, Khare SK. Purification and characterization of lipase from solvent tolerant *Pseudomonas aeruginosa* PseA. Process Biochem 2008;43:1040–6.
[30] Jinwal UK, Roy U, Chowdhury AR, Bhaduri AP, Roy PK. Purification and characterization of an alkaline lipase from a newly isolated *Pseudomonas mendocina* PK-12CS and chemoselective hydrolysis of fatty acid ester. Bioorg Med Chem 2003;11:1041–6.
[31] Gilbert EJ, Cornish A, Jones CW. Purification and properties of extracellular lipase from *Pseudomonas aeruginosa* EF-2. J Gen Microbiol 1991;137:2223–9.
[32] Sharma AK, Tiwari RP, Hoondal GS. Properties of a thermostable and solvent stable extracellular lipase from *Pseudomonas* sp. AG-8. J Basic Microbiol 2001;41:363–6.
[33] Pleiss J, Fisher M, Schimid RD. Anatomy of lipase binding sites: the scissile fatty acid binding site. Chem Phys Lipids 1998;93:67–80.
[34] Surinenaite B, Bendikiene V, Juodka B. The hydrolytic activity of *Pseudomonas mendocina* 3121-1 lipase. A kinetic study. Biologica 2009;55:71–9.
[35] Nini L, Sarda L, Comeau LC, Boitard E, Dubes JP, Chahinian H. Lipase-catalysed hydrolysis of short-chain substrates in solution and in emulsion: a kinetic study. Biochem Biophys Acta 2001;1534:34–44.
[36] Chahinian H, Nini L, Boitard E, Dubes JP, Sarda L, Comeau LC. Kinetic properties of *Penicillium cyclopium* lipases studied with vinyl esters. Lipids 2000;35:919–25.
[37] Kojima Y, Shimizu S. Purification and characterization of the lipase from *Pseudomonas fluorescens* HU380. J Biosci Bioeng 2003;96:219–26.
[38] Kordel M, Hofmann B, Schomberg D, Schmid RD. Extracellular lipase from *Pseudomonas* sp. strain ATCC21808; purification, characterization, crystallization and preliminary X-ray diffraction data. J Bacteriol 1991;173:4836–41.
[39] Bose A, Keharia H. Production, characterization and application of organic solvent tolerant lipase by *Pseudomonas aeruginosa* AAU2. Biocatal Agric Biotechnol 2014, http://dx.doi.org/10.1016/j.bcab.2013.03.009.
[40] Zhang AJ, Gao RJ, Diao NB, Xie GQ, Gao G, Cao SG. Cloning expression and characterization of an organic solvent tolerant lipase from *Pseudomonas fluorescens* JCM5963. J Mol Catal B: Enzym 2009;56:78–84.
[41] Gupta R, Gupta N, Rathi P. Bacterial lipase: an overview of production, purification and biochemical properties. Appl Microbiol Biotechnol 2004;64:763–81.
[42] Peng R, Lin J, Wei D. Purification and characterization of an organic solvent tolerant lipase from *Pseudomonas aeruginosa* CS-2. Appl Biochem Biotechnol 2010;162:733–43.
[43] Singh M, Banerjee UC. Enantioselective transesterification of (RS)-1-chloro-3-(3,4-difluorophenoxy)-2-propanol using *Pseudomonas aeruginosa* lipase. Tetrahedron: Asymmetry 2007;18:2079–85.
[44] Rizzi M, Stylos P, Reik A, Reuss M. A kinetic study of immobilized lipase catalyzing the synthesis of isoamyl acetate by transesterification in hexane. Enzyme Microb Technol 1992;14:709–14.
[45] Mendes AA, Oliveira PC, Velez AM, Giordano RC, Giordano RLC, de Castro HF. Evaluation of immobilized lipase on poly-hydroxybutyrate beads to catalyse biodiesel synthesis. Int J Biol Macromol 2012;50:503–11.

Appl Biochem Biotechnol (2015) 177:1313–1326
DOI 10.1007/s12010-015-1816-7

Lipase from Solvent-Tolerant *Pseudomonas* sp. DMVR46 Strain Adsorb on Multiwalled Carbon Nanotubes: Application for Enzymatic Biotransformation in Organic Solvents

Patel Vrutika[1] · **Madamwar Datta**[1]

Received: 8 May 2015 / Accepted: 17 August 2015 /
Published online: 2 September 2015

Abstract Immobilization of biocatalysts onto particulate carriers has been widely explored for recycling of biocatalyst. However, surface properties often affect the amount of biocatalysts immobilized, their bioactivity and stability, hampering their wide applications. The aim of this work was to elucidate the importance of nanoimmobilization system in organic synthesis. The surface of multiwalled carbon nanotubes (MWCNTs) was functionalized with a mixture of concentrated acids to create an interface for enzyme immobilization. Successful functionalization and enzyme immobilization was structurally evidenced by transmision electron microscopy analysis and Fourier-transform infrared spectroscopy analysis. Furthermore, immobilized enzyme was exploited for the synthesis of flavoured ester ethyl butyrate in the presence of *n*-heptane. Optimized conditions for enhanced ester synthesis was found to be 8.5 pH, 40 °C, 150 rpm, 0.15:0.2 M substrate molar ratio (ethanol/butyric acid) and *n*-heptane as reaction medium. Utmost 81 % of ester synthesis was obtained using immobilized lipase quite higher in comparison to that of free lipase. The activation energy indicated a lower energy requirement for immobilization of lipase on the surface of functionalized MWCNTs. In summary, immobilization of lipase on functionalized MWCNTs by simple adsorption method displayed excellent properties for enzyme stability and reusability, indicating its potential for application in organic synthesis.

Keywords Multiwalled carbon nanotubes · Ethyl butyrate · *Pseudomonas* sp · Kinetic study · Biotransformation

✉ Madamwar Datta
datta_madamwar@yahoo.com

Patel Vrutika
vrutikaptl_19@yahoo.com

[1] Environmental Genomics and Proteomics Laboratory, BRD School of Biosciences, Sardar Patel University, Sardar Patel Maidan, Vadtal Road, Satellite Campus, Post Box # 39, Vallabh Vidhyanagar 388 120 Gujarat, India

Introduction

Non-aqueous enzymology emerged as a major part of biotechnological research and development area that offers valuable product such as fine chemicals using reactions that are not feasible in aqueous media [1]. Using organic solvents as reaction medium in enzyme catalysis offers many advantages such as (1) increased substrate solubility, (2) increased enzyme stability, (3) possibility of carrying out reactions which are difficult in water and (4) easy recovery of biocatalyst, as it is insoluble in organic solvents [2]. Among several enzymes studied, lipase (triacyl slycerol acyl hydrolases, EC 3.1.1.3) has been one of the dominant hydrolase enzymes explored for the synthesis of several important chemicals in organic solvents and neoteric solvents such as ionic liquids, supercritical fluids and eutectic solvents [3, 4]. Lipases are attractive in organic chemistry because of their enantioselectivity, regioselectivity and stereoselectivity, and these granted them the broad spectrum of industrial applications covering domains such as fine chemical synthesis, pharmaceutical chemistry, food and dairy industries and also in the production process for biodiesel [3, 5, 6]. Apart from all the benefits, the main drawback in carrying out the reaction under a water-restricted environment is the tendency of organic solvents to strip away water molecules from the enzyme surface especially from the active site, leaving the enzyme inactive [7]. Thus, in order to overcome these limitations and for enhancing the enzyme activity and stability, several strategies such as immobilization of catalyst onto porous support by adsorption or deposition, entrapment in gel matrix or covalently attaching the enzyme to immobilization carrier, etc., have been demonstrated [8, 9]. However, the immobilization of enzymes, including lipases, on solid supports is among the most effective methods to improve their stability, separation and reusability [10–12].

Nanostructured materials are highlighted as one of the most important research and development frontiers in modern science. Nanostructured materials emerged as a supporting material for lipase immobilization due to their high specific surface area to favor the binding, lower transfer resistance to solve the diffusion problem, easy separation, versatile surface chemistry and lower operational cost [6, 13]. Carbon nanotubes (CNTs) represent an important class of nanosupports that have been widely investigated for immobilization of enzymes and proteins based on their unique electrical and mechanical properties. CNTs comprise of two different types, i.e. single-walled carbon nanotubes (SWCNTs) and multi-walled carbon nanotubes (MWCNTs). MWCNTs are 1D nanoparticles of high surface area, excellent physicochemical stability and less cytotoxic than their single-wall counterparts [14, 15]. Functionalization of these MWCTNs makes it possible for further binding of additional components, significantly increasing their physico-chemical properties. These modifications are frequently explored in the conjugation of bioactive molecules [16].

To date, there are numerous reports for the immobilization of commercially available lipases on nanostructured materials [6, 7, 13, 16]. Several authors have reported the purification, characterization and optimization of lipase production from *Pseudomonas* sp. isolated by means of different sources [17–19], but there are scanty reports on its applications in nanobiocatalysis. Combining two aspects—(1) industrial demand for organic synthesis and (2) tunability of MWCNTs hydrophilicity, we present the development of the potential biocatalytic system on MWCNTs as porous support for immobilization of purified lipase. In the present study, lipase from *Pseudomonas* sp. DMVR46 was immobilized on MWCNTs, where nanotubes were previously carboxylated with some oxygen-bearing functional groups such as hydroxyl, carbonyl, ester and nitro groups. The immobilized lipase was further characterized using TEM and FTIR spectroscopic techniques, also applied for the synthesis of short-chain flavor compound ethyl butyrate and reusability studies.

Materials and Methods

Materials

Purified *Pseudomonas* sp. DMVR46 lipase with activity of 64.57 U/mg protein, *p*-nitropenyl palmitate, *p*-nitrophenol, butyric acid and ethyl butyrate (≥99.5 %) were procured from Sigma-Aldrich, Germany. Gum arabic, Triton X-100 and bovine serum albumin were purchased from Hi-Media, India. Other solvents such as isopropanol, *n*-hexane, 1-ethanol were of HPLC/GC grade as obtained from Sprectrochem, India, whereas the sulfuric acid and nitric acid used were from Merck, India.

Carboxylation of Multiwalled Carbon Nanotubes (MWCNTs)

Acid functionalization of pristine MWCNTs was followed using the method described by Raghvendra et al. [7] with some modifications. Briefly, 10 mg of pristine MWCNTs was suspended in a mixture of concentrated sulfuric acid/nitric acid (3:1 *v*/*v*) and sonicated for 6 h. The suspension was centrifuged at 15,000 ×*g* for 30 min at 4 °C. The residue was suspended in milliQ by sonication and centrifuged again under the same condition. This centrifugation process was repeated several times in order to remove the acid. Finally, semi-solid residue was collected and vacuum-dried at 37 °C for 1 h to obtain acid-functionalized MWCNTs, abbreviated as f-MWCNTs.

Immobilization of DMVR46 Lipase on f-MWCNTs

Enzyme solution was prepared by suspending lipase (50 mg/mL) in 50 mM phosphate buffer (pH 8.5), vigorously vortexing and centrifugation at 1000 x*g* for 5 min where the supernatant was collected. Ten mg of f-MWCNTs in 9 mL of phosphate buffer (50 mM, pH 8.5) was sonicated for 10 mins. Then, 1 mL of previously prepared enzyme solution was added in the mixture of f-MWCNTs, stirred overnight at 37 °C for immobilization of lipase. Finally, the nanobioconjugate was separated by centrifugation at 13,000 ×*g* for 20 min at 4 °C from supernatant and washed twice with buffer solution in order to remove loosely bound enzyme. After centrifugation, the supernatant was collected (for activity measurements), and the resulting solid was vacuum-dried for 1 h at 37 °C.

Determination of Lipase Activity

The activity of free and immobilized lipase was assayed using Wrinkler and Stuckmann method [20] with some modifications. *p*-Nitrophenyl palmitate was used as a substrate with a final concentration of 0.3 mg/mL dissolved in 1 mL of isopropanol and mixed with 9 mL of 50 mM sodium phosphate buffer (pH 8.5) containing gum arabic (0.1 %) and Triton X-100 (0.6 %). The reaction mixture comprised of 240 μL substrate solution and 10 μL of appropriately diluted enzyme solution, and incubated at 40 °C for 10 min. The amount of immobilized enzyme was measured by calculating the difference between the activity of enzyme before immobilization and after immobilization (from supernatant). The *p*-nitrophenol (p-NP) produced in the reaction mixture was quantified spectrophotometrically at 410 nm. One unit of enzyme activity was defined as the amount of enzyme liberating 1 μmol *p*-nitrophenol/min under standard assay conditions. The amount of protein in the supernatant was determined by Lowry's method [21] using bovine serum albulin (BSA) as standard.

Characterization

The size and morphologies of MWCNTs before and after lipase immobilization was assayed by transmission electron microscopy (TEM) (Philips-Technai 20, Holland). The KBr pellet technique was used for determining Fourier transform infrared spectroscopy (FTIR) spectra for free and immobilized lipase using Spectrochem GX-IR, Perkin Elmer, USA.

Studies on the Applications of Immobilized Lipase for Biocatalysis

Lipase immobilized on f-MWCNTs was repeatedly washed with *n*-hexane in order to remove water. The reaction system consisted of 20 mL *n*-heptane supplemented with equimolar (0.1 M) concentrations of 1-ethanol and butyric acid in a 100-mL stopper flask. The reaction was initiated by addition of immobilized lipase (50 mg, including the weight of f-MWCNTs) and f-MWCNT without lipase (as a negative control) kept on an orbital shaker at 37 °C and 150 rpm. Esterification reaction using the free enzyme equivalent to the amount immobilized on MWCNTs was also performed. Process parameters such as effect of organic solvents, solvent stability, temperature, agitation and substrate molar ratio were scrutinized in order to get enhanced ester production. Samples (100 μL) were withdrawn at regular intervals, and ester accumulation was monitored by gas chromatography (Perkin Elmer, Clarus-500, USA) equipped with a flame ionization detector in order to establish the product formation profile. The column was 30m Rtx-®-20 (Crossbond 80 % dimethyl−20 % diphenyl polysiloxane) capillary column. The temperature of the injector and detector were maintained at 250 °C. The carrier gas was nitrogen with a split flow rate of 30 mL/min. The column temperature was programmed to increase from 70 to 190 °C at the rate of 15 °C/min. Ester identification and quantification were done by comparing the retention time and peak area of the sample with the standard. Pure ethyl butyrate (≥99 %) was used as an external standard. No reaction was detected in the absence of the enzyme. All the experiments were repeated thrice at each operating condition, and the relative standard deviation was within ±1 %.

Operational Stability of Immobilized Lipase

After completion of one reaction cycle (48 h), immobilized lipase was recovered by centrifugation (10,000 ×*g* for 15 min) separation and washed two to three times with fresh hexane for complete removal of residual substrates and products, followed by air-drying. The next reaction cycle was initiated by addition of new substrates where the residual activity determined after each cycle was analyzed using gas chromatography under standard conditions. The conversion achieved in the initial batch was set to be 100 %.

Results and Discussions

Immobilization of the enzyme has been granted as an imperative cornerstone to cover the way for enzyme technology from lab curiosity to an industrially viable process. In principle, the carriers for enzyme immobilization should be chemically stable and inert to microbiological contamination. In the present work, –COOH functional groups were introduced onto the surface of MWCNTs through carboxylation (Scheme 1). The resulting surface functionalized MWCNTs were employed for lipase immobilization with *Pseudomonas* sp. lipase

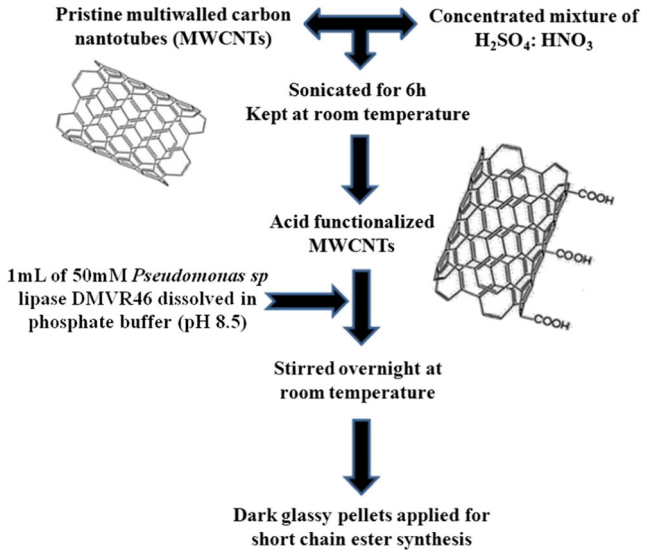

Scheme 1 General scheme for acid functionalization of multi-walled carbon nanotubes (f-MWCNTs) and immobilization for solvent tolerant lipase

DMVR46 having a molecular weight of close to 32 kDa, employed as a model enzyme and assessed for immobilization efficiency, specific activity, ester synthesis and stability studies. Immobilization yield (%) calculated from the protein content in free lipase against protein in supernatant after immobilization was about 81 % with equivalent binding efficiency of enzyme. Moreover, recovered enzyme activity and specific activity for immobilized lipase was also calculated and found to be 2.145 U/mL (recovered enzyme activity) and 9.53 U/mg MWCNTs (specific activity), respectively. Surface functionalization was confirmed and characterized by FTIR and TEM analysis where, the corresponding details are described in the following sections.

Characterization of Functionalized MWCNTs: Morphological and Chemical Properties

FTIR Characterization

To confirm the occurrence and alterations of functional groups on the surface of MWCNTs due to carboxylation, FTIR analysis was employed, and the related spectrum was demonstrated in Fig. 1. As can be seen from Fig. 1, the IR spectrum of raw MWCNT (Fig. 1a) showed weak absorption at ~3430 cm^{-1} (possibly due to adsorbed water); additionally, no other peak was observed in the spectra, indicating the absence of functional groups. The spectrum of f-MWCNT (Fig. 1b) showed weak absorption at around 2926 cm^{-1} which can be attributed to the stretching vibrations of alkyl groups [22]. Moreover, peak at 3435 cm^{-1} traced to OH stretching and a significant absorption at 1634 cm^{-1} assigned to C = O stretching suggest the carboxylation of MWCNTs. In spectra C (Fig. 1), as lipase is a protein, the adsorption at 1638 cm^{-1} is possibly due to C = O stretching of the amide moieties present in protein. Additionally, the peak at 1122 cm^{-1} in lipase may be assigned to C–N stretching. Interestingly,

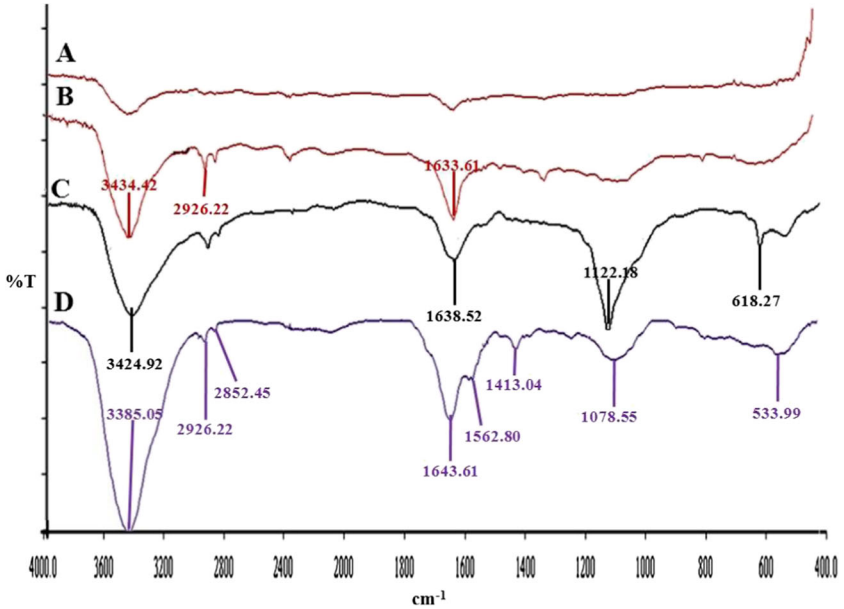

Fig. 1 FTIR overlay for **a** functionalized MWCNTs (f-MWCNT) and **b** lipase immobilized on functionalized MWCNTs

the spectrum of carboxylated MWCNTs with immobilized lipase (Fig. 1d) showed all the prominent peaks of lipase and carboxyl group. The absorption at 3385 cm^{-1} became stronger, possibly due to the contribution from both OH and NH groups. The stretching of CO at 1638 cm^{-1} is shifted to 1643 cm^{-1} which indicates that the interaction with 'N' of the amide group increased the CO stretching frequency. The peaks of 1563 and 1413 cm^{-1} in spectrum D may be due to traces of asymmetric and symmetric stretching of C = O moieties. Also, it is important to notice that some functional groups such as NH and OH groups may overlap [23]. Furthermore, the broad absorption band at 3434 cm^{-1} is due to O–H stretching, vibration and presence of carboxylic groups [24], while the same adsorption band is shifted to 3385 cm^{-1} in immobilized lipase. The simultaneous shifting and peak broadening at 1643 cm^{-1} in the spectrum of immobilized lipase clearly shows the utilization of the intermediate groups for the stable bond formation.

Imaging Analysis of Immobilized Lipase on Functionalized MWCNTs by TEM

In this work, the size and morphology of functionalized MWCNTs with and without immobilized lipase were viewed by TEM at the same resolution (Fig. 2a, b). Carboxylation of nanotubes resulted in highly jagged surface with a diameter of 28 nm. Prolonged exposure to concentrated acid resulted in oxidation of carbon atoms, rendering the surface accessible for chemical and biological reactions [7]. A slight increment in the diameter of f-MWCNT was observed after immobilization of lipase. A higher roughness with the immobilization of lipase and the presence of visible bud-like projections might be the adsorbed enzymes. Similar observations were also noted by Rastian et al. [23] while working with surface functionalization of MWCNTs for *Candida rugosa* lipase immobilization.

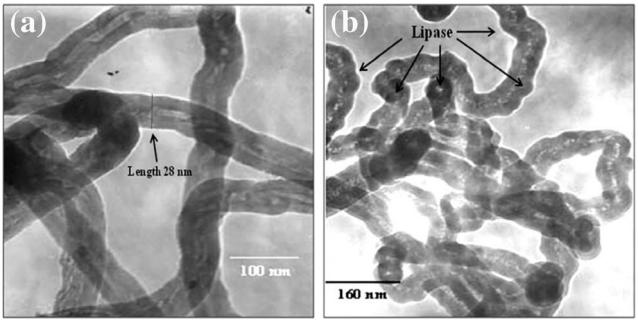

Fig. 2 TEM analysis of **a** functionalized MWCNTs and **b** lipase immobilized with bud like projections on surface of f-MWCNT

Optimization of Experimental Parameters for Enhanced Ester Synthesis

Effect of Organic Solvents

Organic solvent plays a key role for any enzymatic transformation which significantly influences the catalytic power of an enzyme. The most important criteria for solvent selection in biocatalysis are a high substrate and product recovery, biocompatibility, chemical and thermal stability, non-biodegradability, non-hazardous nature and low cost [25]. The most commonly used parameter to classify solvents in terms of biocompatibility is the log *P* value, which is defined as the partition coefficient of a given compound in a two-phase *n*-octanol and water system [25, 26]. In the current study, a series of organic solvents covering a wide range of log *P* values was chosen, and results are revealed in Fig. 3a. The results suggested that non-polar solvents have good compatibility with enzyme molecule in comparison to that of polar solvents. Higher rate of esterification was noticed with *n*-heptane and *n*-hexane where immobilized lipase showed 74 and 68 % ester synthesis, while free lipase displayed only 52 and 48 % ester formation, respectively. The higher rate of esterification could be attributed to the effect of solvent on the enzyme performance influenced by the bulkiness and hydrophobicity of solvent [26, 27]. Polar solvents like acetonitrile and DMSO were too sluggish to give only 36 % of conversion with immobilized lipase. The hydrophilic solvent may deactivate the enzyme in the way of disrupting the functional structure of enzyme or stripping off the essential water from the enzyme [26, 28]. This alters the native conformation of lipase by disturbing hydrogen bonding and hydrophobic interactions. As a consequence, the catalytic activity of enzyme was decreased due to the lack of bound water to preserve the enzyme conformation flexibility. This structural mobility is necessary for its catalytic action [25, 28]. Abreu et al. showed the synthesis of ethyl butyrate using organic solvent tolerant lipase from *Staphylococcus warneri* EX17 immobilized on porous styrene-divinylbenzene beads and reported only 14 % of ethyl butyrate synthesis using polar solvents, showing that polar solvents not suitable for catalytic activity of enzyme [29]. Also, Hun et al. reported that high-polarity solvents such as acetonitrile (log P=−0.33) caused a complete deactivation of the lipase from *Bacillus sphaericus* 205y, whereas *n*-hexane (log P=3.5) enhanced the lipase activity [30].

Effect of Organic Solvent on the Stability of Immobilized Lipase

Organic solvents may change the parent conformation of the lipase by disturbing the hydrogen bonding and hydrophobic interactions, which leads to affect the activity and stability of the

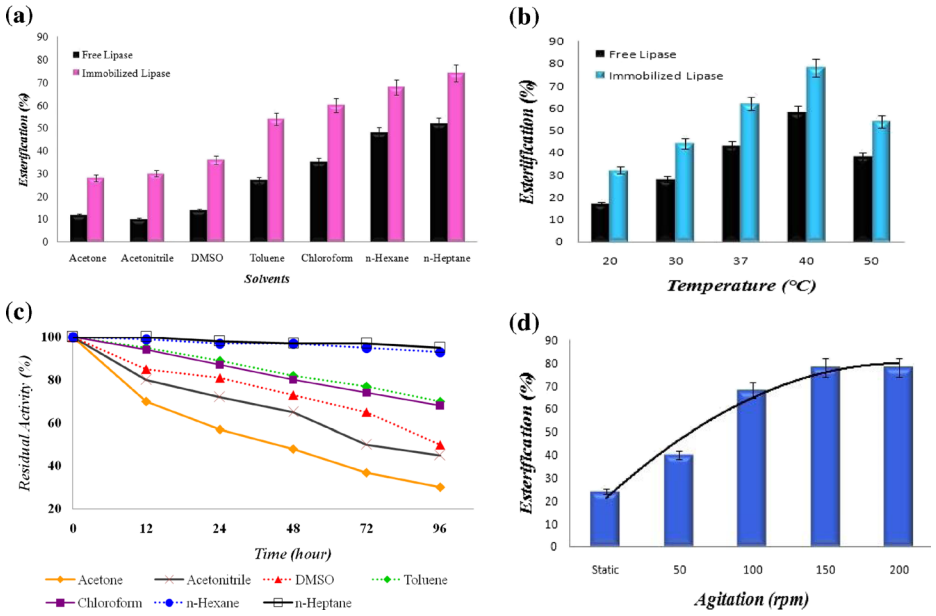

Fig. 3 **a** Effect of different organic solvents on synthesis of ethyl butyrate. Reaction conditions: ethanol (0.1 M), butyric acid (0.1 M), 150 rpm, pH 8.5, temperature (37 °C), time (24 h). **b** Effect of organic solvent on the stability of immobilized lipase. Reaction conditions: ethanol (0.1 M), butyric acid (0.1 M), 150 rpm, pH 8.5, temperature (37 °C), time (96 h). **c** Effect of temperature on ester synthesis. Reaction conditions: ethanol (0.1 M), butyric acid (0.1 M), *n*-heptane (20 mL), 150 rpm, pH 8.5, time (24 h). **d** Influence of agitation on esterification. Reaction conditions: ethanol (0.1 M), butyric acid (0.1 M), *n*-heptane (20 mL), 150 rpm, pH 8.5, temperature (40 °C), time (24 h)

enzymes [26]. In the present study, the stability of immobilized lipase was studied in different organic solvents by measuring the residual activity versus time as exhibited in Fig. 3b. The solvent stability study showed that immobilized lipase has better stability in the non-polar solvents such as *n*-heptane, *n*-hexane and toluene which gave almost 95, 93 and 68 % of residual activity after 96 h at 40 °C, respectively, while in the case of polar solvents such as DMSO, acetonitrile and acetone activity was reduced to almost 50, 45 and 30 %, respectively. The results clearly specify that non-polar solvents have good compatibility with enzymes in comparison to that of polar solvents, as stripping of water layer around the enzyme is not possible in the case of non-polar solvents [25, 28]. These results are in good agreement with many reports where non-polar organic solvents showed better stability for the enzymes [7, 27, 31].

Effect of Temperature

The reaction temperature is a crucial factor which helps to enhance the catalytic interaction with the substrate, reduces the viscosity of reaction medium and improves the solubility of reactant/substrate in reaction media. The effect of reaction temperature on the enzymatic synthesis of ethyl butyrate was investigated over a range from 20 to 50 °C. As shown in Fig. 3c, it was observed that the initial rate of synthesis increases linearly with the increase in temperature from 20 to 40 °C. The activity of lipase reached a maximum of 78 % for immobilized lipase and 58 % for free lipase at 40 °C in 72 h. However, further increment in temperature beyond 40 °C resulted in a relatively rapid loss of enzyme stability, pulling down

the reaction yield. Indeed, above a certain temperature, enzyme inactivation occurs, and stability decreases. This is due to (1) the partial inactivation of the enzyme in organic solvent at high temperature for a long time because protein undergoes partial unfolding by heat-induced destruction of non-covalent interactions [32] and (2) increase in temperature which may alter the confirmation of lipase, resulting in decreased activity and stability. The results clearly showed that immobilized enzyme possesses better stability up to 40 °C. Thus, 40 °C was considered to be the optimum temperature for the corresponding biotransformation and used for further experiments.

Effect of Agitation

In immobilized catalysts, reactants have to pass from the bulk liquid phase to the enzyme particle's surface and then diffuse from the external surface to the enzyme active site. The external mass transfer resistance and intraparticle diffusion rate play significant roles during the reaction. Thus, it is necessary to check the effect of mass transfer in the solid liquid system where both substrates are in liquid phase while the polymer-supported biocatalyst is in solid form [33–35]. Several experiments were performed in the range of 50 to 200 rpm by taking 0.1 M ethanol and butyric acid each at 40 °C using *n*-heptane as solvent. It can be clearly seen from the results displayed in Fig. 3d that increase in speed of agitation exerted ester production up to 78 % from 0 to 150 rpm and later remains almost constant with increase in agitation speed from 150 to 200 rpm. The result conveys that, for this system, shaking at 150 rpm is optimum for transporting the substrates to the enzyme at the same time sufficient enough for moving out the product from the site as well. This clearly indicates that there was no significant effect of external mass transfer diffusion when rotation speed increased from 150 to 200 rpm for the corresponding system in an orbital shaker.

Substrate Molar Ratio

In order to determine the optimum ratio of the substrates, the concentrations of ethanol and butyric acid were varied one at a time, keeping the other constant and carrying out esterification reaction. In one set of experiment, the ethanol concentration was kept constant at 0.1 M varying butyric acid concentration. The maximum amount of ester (80 %) was produced with 0.2 M of butyric acid at 40 °C, pH 8.5 in 48 h (data not shown). Also, when the concentration of acid was further increased beyond 0.2 M, ester production was adversely affected. When the same experiment was repeated keeping butyric acid concentration constant at 0.2 M (obtained from the previous study) and varying ethanol concentration from 0.1 to 0.25 M, highest yield was obtained at 0.15 M concentration with 81 % of product formation in 48 h (data not shown). The reactions proceeded very quickly at low alcohol content (up to 0.15 M) and reached a maximum in 48 h, while higher concentrations of alcohol exhibited an inhibitory effect on reaction, slowing it down drastically. Thus, the molar ratio of butyric acid to ethanol was found to be 0.2:0.15 M, corresponding to maximum esterification of 81 % with complete utilization of both substrates.

Synthesis of Ethyl Butyrate

Short-chain esters are volatile compounds in flavor and fragrance applications in food, beverages, pharmaceuticals and personal care industries [27, 36, 37]. Among them, ethyl butyrate has been widely used in the food industry due to its pleasant fruity flavor similar to

that of pineapple. The purified lipase immobilized on f-MWCNT was subjected for the synthesis of ethyl butyrate in the presence of *n*-heptane under optimized conditions. It can be clearly seen from the results (Fig. 4a) that free enzyme catalyzes reaction at a very slow rate, exhibiting only 47 % of conversion in 48 h, while immobilized lipase showed higher ester synthesis (80 % in 48 h) and remains stable up to 72 h under the same condition. This conveys that a large amount of enzyme has been adsorbed on the surface of f-MWCNT, which can be explained by binding of enzyme molecules on the surface of f-MWCNT, involving hydrophobic interactions engrossed with active sites, leading to conformational change which alters the substrate specificity of the enzyme [38].

Boncel [39] described the potential of alkaline lipase from *P. fluorescence* immobilized on pristine and oxidized MWCNTs for the synthesis of solketal esters. These authors found that depending upon the structures of acyl donor, immobilized lipase showed nine times higher

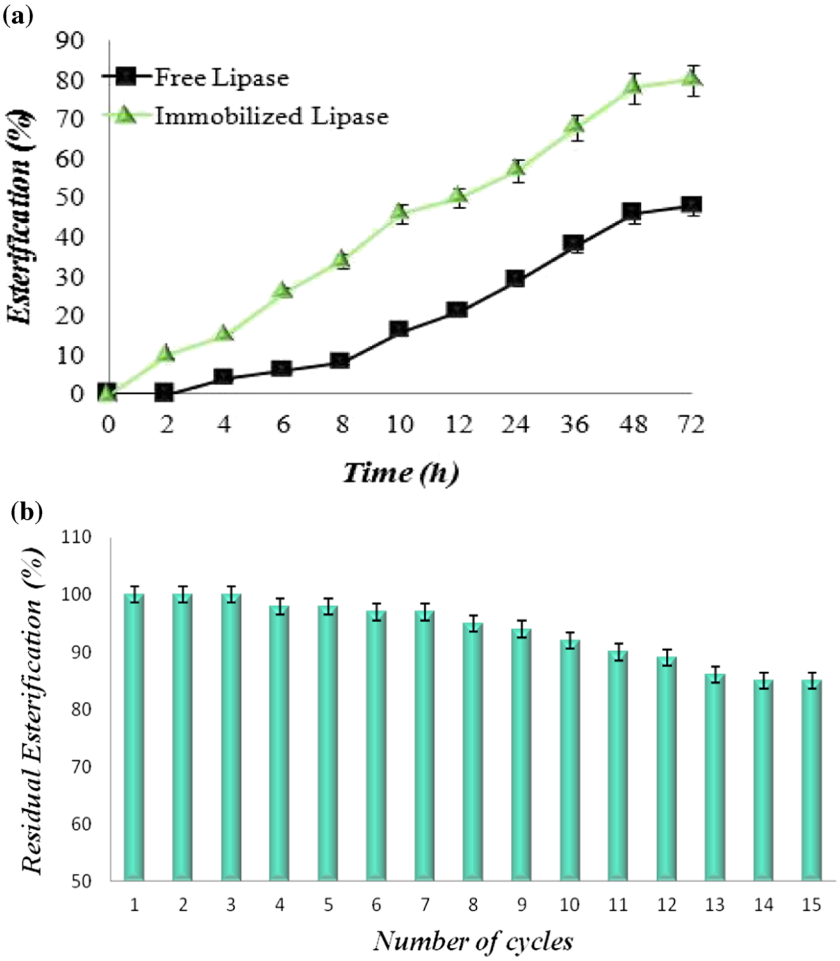

Fig. 4 **a** Synthesis of ethyl butyrate using free lipase (*filled square*) and immobilized lipase (*filled circle*). Reaction conditions: ethanol (0.15 M), butyric acid (0.2 M), *n*-heptane (20 mL), 150 rpm, pH 8.5, temperature (40 °C). **b** Reusability study for the immobilized lipase. Reaction conditions: ethanol (0.15 M), butyric acid (0.2 M), *n*-heptane (20 mL), 150 rpm, pH 8.5, temperature (40 °C), time (48 h)

activity as compared to that of the native enzyme for pristine MWCNTs. Abreu [29] purified and immobilized lipase from *Staphylococcus warneri* EX17 (SWL) via interfacial adsorption using the hydrophobic support octyl-sepharose. Octyl-SWL preparations were used for the synthesis of ethyl butyrate, showing 28 % conversion in 24 h of reaction. Compared to these reports, the results of our work suggest that f-MWCNT preparations have promising application in organic synthesis considering the higher rate of ester conversion. *Candida antarctica* lipase B (CALB) was covalently attached on MWCNTs using two different methods by Raghavendra et al. [40]. The lipase-MWCNTs conjugate was applied for the synthesis of flavor ester pentyl valerate and showed reusability of up to 50 cycles without meager loss of activity.

However, it is difficult to compare results reported in the literature on lipase activities because conversion varies depending upon the lipase preparations, their specificities, the nature of support and the amount of enzyme immobilized.

Operational Stability

One of the important criteria to prove the potential of an immobilized enzyme for industrial application is its reusability [41]. In the present study, immobilized lipase was subjected to reusability examination for determining the efficiency of immobilization. After 48 h of reaction of each cycle, the immobilized lipase was recovered by centrifugation and regenerated by *n*-hexane washing and air drying and then subjected to the next reaction cycle by supplementing with fresh substrates. Interestingly, the results presented in Fig. 4b showed that ester synthesis by immobilized lipase was not significantly affected up to 3 cycles, retaining 100 % of its initial activity. This could be attributed to the better absorption and dispersion of immobilized lipase on the surface of f-MWCNT, increasing the availability of substrates to the enzyme's active site [7, 23]. Also, the immobilization of lipase has been reported to improve the catalytic activity of enzyme by providing protection against the inhibitory effect of organic solvents [42]. Furthermore, the results in Fig. 4b also depicted that the activity of immobilized lipase starts declining slowly after the third cycle. The decrease in the activity of the biocatalyst after three consecutive cycles may be due to (1) accumulation of water formed as a byproduct during the esterification reaction, (2) inactivation of enzyme molecules by the influence of solvent [43] and (3) desorption of lipase from the support surface during repeated use [44], even though the results showed that lipase immobilized on f-MWCNT can be used successfully in industrial applications requiring long-term reaction stability.

Kinetic Parameters

The kinetics for the hydrolytic activity of free and immobilized lipase was studied by varying the substrate concentration. The kinetics constant K_m (affinity of enzyme to substrate) and V_{max} (maximum specific activity) was determined from Lineweaver–Burk equation. K_m value for free lipase was found to be 7.9 mM, which is 2.25 times higher than that of the immobilized lipase (3.5 mM). The lower value of K_m represents a higher affinity between enzyme and substrate. Hence, the affinity of lipase towards the substrate upon immobilization on f-MWCNT was boosted. However, V_{max} value for immobilized lipase (646 mmol/mg/min) was 5.20-folds higher as compared to that of free lipase (124 mmol/mg/min), suggesting a higher enzyme activity. The ratio of V_{max}/K_m defines a measure of catalytic activity of an enzyme–substrate pair. The catalytic efficiencies for free and immobilized enzyme were found to be 15.69 and 184.57, respectively. Thus, immobilized lipase has 11.76-fold higher efficiency in comparison

Table 1 Kinetic parameters for reaction catalyzed by the free and immobilized lipase

Sample	V_{max} (mM/min)	K_m (mM)	V_{max}/K_m (min^{-1})	E_a (kJ/mol)
Free	124	7.9	15.69	9.7
Immobilized	646	3.5	184.57	2.85

to free lipase for substrate hydrolysis. These outcomes imply that adsorption of lipase on f-MWCNT resulted in increased affinity for the substrate and improved accessibility for the active site. The activation energy (E_a) for the effect of temperature on the affinity of free and immobilized lipase was determined by Arrhenius equation and shown in Table 1. The E_a of immobilized enzyme was 2.85 kJ/mol lower than free lipase (9.75 kJ/mol), which indicates that lipase have higher affinity for active site and lower sensitivity towards temperature. Moreover, lower activation energy of immobilized enzyme suggests a conformational change in enzyme, leading to lower energy requirement for the immobilization at f-MWCNT surface.

Conclusion

One of the most important aims of enzyme technology is to enhance the conformational stability of the enzyme. The extent of stabilization depends upon enzyme structure, immobilization methods and types of support. In this study, we demonstrate simple immobilization of purified solvent-tolerant lipase on carboxylated multiwalled carbon nanotubes which was mainly focused on stability and reusability of lipase DMVR46 for enhanced ethyl butyrate synthesis. Immobilization of lipase was confirmed by spectroscopic analysis (FTIR) and imaging analysis (TEM). Higher ester yield was observed in the case of immobilized lipase. The operational stability study indicated that this approach might provide an important tool for the application of immobilized lipase in ester synthesis.

Acknowledgments The authors would like to acknowledge University Grants Commission (UGC) grant no. F. 42-167/2013 (SR), New Delhi, for financial support. The authors would also like to acknowledge SICART, Vallabh Vidhyanagar, for FTIR and TEM facility and Department of Material Sciences, Vallabh Vidhyanagar, for providing MWCNTs.

References

1. Madamwar, D., & Dave, R. (2005). Lipase mediated catalysis in water restricted microenvironment under microemulsion based organogels. *Chemica Oggi, 23*(5), 16.
2. Soni, K., Shah, C., & Madamwar, D. (2000). Role of surfactant on activity of acid phosphatase incorporated in reverse micelles. *Biocatalysis and Biotransformation, 18*(5), 331–341.
3. Jaeger, K. E., & Egger, T. (2002). Lipase for biotechnology. *Current Opinion in Biotechnology, 13*, 390–397.
4. Lozano, P. (2010). Enzymes in neoteric solvents: from one phase to multiphase systems. *Green Chemistry, 12*, 555–569.
5. Ribeiro, D. S., Henrique, S. M. B., Oliveria, L. S., Macedo, G. A., & Fleuri, L. F. (2010). Enzymes in juice processing: a review. *International Journal of Food Science and Technology, 4*, 635–641.
6. Verma, M. L., Barrow, C. J., & Puri, M. (2013). Nanobiotechnology as a novel paradigm for enzyme immobilization and stabilization with potential applications in biodiesel production. *Applied Microbiology and Biotechnology, 97*, 23–39.

7. Raghavendra, T., Vohra, U., Shah, A. R., & Madamwar, D. (2014). Enhanced conjugation of *Canida rugosa* lipase onto multiwalled carbon nanotubes using reverse micelles as attachment medium and application in non-aqueous biocatalysis. *Biotechnology. Progress, 30*, 828–836.
8. Lv, Y., Lin, Z., Tan, T., & Svec, F. (2014). Preparation of reusable bioreactors using reversible immobilization of enzyme of monolithic porous polymer support with attached gold nanoparticles. *Biotechnology and Bioengineering, 111*, 50–58.
9. Klibanov, A. M. (1983). Immobilized enzymes and cells as practical catalysts. *Science, 219*, 722–727.
10. Garcia-Galan, C., Berenguer-Múrcia, A., Fernandez-Lafuente, R., & Rodrigues, R. C. (2001). Potential of different enzyme immobilization strategies to improve enzyme performance. *Advanced Synthesis and Catalysis, 353*, 2885–2904.
11. Rodrigues, R. C., Ortiz, C., Berenguer-Múrcia, A., Torres, R., & Fernandez-Lafuente, R. (2013). Modifying enzyme activity and selectivity by immobilization. *Chemical Society Reviews, 42*, 6290–6307.
12. Mateo, C., Palomo, J. M., Fernandez-Lorente, G., Guisan, J. M., & Fernandez-Lafuente, R. (2007). Improvement of enzyme activity, stability and selectivity via immobilization techniques. *Enzyme and Microbial Technology, 40*, 1451–1463.
13. Gupta, M. N., Kaloti, M., Kapoor, M., & Solanki, K. (2011). Nanomaterials as matrices for enzyme immobilization. *Artificial Cells Blood Substitute Biotechnology, 39*, 98–109.
14. Singh, C., Shaffer, M., Koziol, K., Kinloch, I., & Windle, A. (2003). Towards the production of large scale aligned carbon nanotubes. *Chemical Physics Letters, 372*, 860–865.
15. Jia, G., Wang, H., Yan, L., Wang, X., Pie, R., Yan, T., et al. (2005). Towards the production of large scale aligned carbon nanotubes. *Environmental Science and Technology, 39*, 1378–1383.
16. Shi, J., Cjaussen, J. C., McLamore, E. S., Haquel, A., Jaroch, D., Diggs, A. R., et al. (2011). A comparative study of enzyme immobilization strategies for multiwalled carbon nanotube glucose biosensors. *Nanotechnology, 22*, 355502.
17. Patel, V., Nambiar, S., & Madamwar, D. (2014). An extracellular solvent stable alkaline lipase from *Pseudomonas sp* DMVR46: partial purification, characterization and application in non-aqueous environment. *Process Biochemistry, 49*, 1673–1681.
18. Cao, Y., Zhuang, Y., Yao, C., Wu, B., & He, B. (2012). Purification and characterization of an organic solvent-stable lipase from *Pseudomonas stutzeri* LC2-8 and its application for efficient resolution of (*R*, *S*)-1-phenylethanol. *Biochemical Engineering, 64*, 55–60.
19. Dandvate, V., Jinjala, J., Keharia, H., & Madamwar, D. (2009). Production, partial purification and characterization of organic solvent tolerant lipase from *Burkholderia multivorans* V2 and its application for ester synthesis. *Bioresource Technology, 100*, 3374–3381.
20. Winkler, U. K., & Stuckmann, M. (1979). Glycogen, hyaluronate and some other polysaccharides greatly enhance the formation of exolipase by *Serratia marcescens*. *Journal Bacteriology, 138*, 663–670.
21. Lowry, O. H., Rosebrough, N. J., Farr, A. L., & Randall, R. J. (1951). Protein measurement with the folin phenol reagent. *Journal of Biological Chemistry, 193*, 265–275.
22. Ma, P. C., Kim, J. K., & Tang, B. Z. (2006). Functionalization of carbon nanotubes using a silane coupling agent. *Carbon, 44*, 3232–3238.
23. Rastian, Z., Khodadadi, A., Vahabzdeh, F., Bortilini, C., Docg, M., Mortazavi, Y., Mogharei, A., Naseh, M., & Guo, Z. (2014). Facile surface fuctionalization of multiwalled carbon nanotubes by soft dielectric barrier discharge plasma: general composite interface for lipase immobilization. *Biochemical Engineering Journal, 90*, 720–726.
24. Teng, L. H. (2008). IR study on surface chemical properties of catalytic grown carbon nanotubes and nanofibers. *Journal of Zhejiang University Science A, 9*, 720–726.
25. Isabel, H., Vanessa, D., Silva, G., & Nascimento, M. (2011). Enantioselective resolution of (*R*, *S*)-1-phenylethanol catalyzed by lipases immobilized in starch films. *Journal of the Brazilian Chemical Society, 22*, 1559–1567.
26. Badgujar, K. C., & Bhanage, B. M. (2014). Synthesis of geranyl acetate in non-aqueous media using immobilized *Pseudomonas cepacia* lipase on biodegradable polymer film: kinetic modelling and chain length effect study. *Process Biochemistry, 49*, 1304–1313.
27. Dhake, K. P., Tambade, P. J., Qureshi, Z. S., Singhal, R. S., & Bhanage, B. M. (2011). HPMC-PVA filmimmobilized *Rhizopus oryzae* lipase as a biocatalyst for transesterification reaction. *ACS Catalysis, 1*, 316–322.
28. Lee, S. C., & Mohamad, R. S. (2006). Effect of solvent and initial water content on (*R*, *S*)-1-phenylethanol resolution. *Enzyme and Microbial Technology, 38*, 551–556.
29. de Ligia, A., Roberto, F. L., Rafael, C. R., Giandra, V., & Marco, A. Z. A. (2014). Efficient purification-immobilization of an organic solvent-tolerant lipase from *Staphylococcus warneri* EX17 on porous styrene-divinylbenzene beads. *Journal of Molecular Catalysis B: Enzymatic, 99*, 51–55.
30. Hun, C., Rahman, R., Salleh, A., & Basri, M. A. (2003). Newly isolated organic solvents tolerant *Bacillus sphaericus* 205y producing organic solvent stable lipase. *Biochemical Engineering Journal, 15*, 147–151.

31. Patel, V., Gajera, H., Gupta, A., Manocha, L., & Madamwar, D. (2015). Synthesis of ethyl caprylate in organic media using *Candida rugosa* lipase immobilized on exfoliated graphene oxide: process parameters and reusability studies. *Biochemical Engineering Journal, 95*, 62–70.
32. Doshanj, N. S., & Kaur, J. (2002). Immobilization stability and esterification studies of a lipase from a *Bacillus* sp. *Biotechnology and Applied Biochemistry, 36*, 7–12.
33. Devendran, S., & Yadav, G. (2014). Lipase-catalyzed kinetic resolution of (±)-1-(2-furyl) ethanol in nonaqueous media. *Chirality, 26*, 286–292.
34. Yadav, G. D., & Pawar, S. V. (2012). Synergism between microwave irradiadition and enzyme catalysis in transesterification of ethyl-3-phenylpropanoate with *n*-butanol. *Bioresource Technology, 109*, 1–6.
35. Yadav, G. D., & Borkar, I. V. (2008). Kinetic modelling of immobilized lipase catalysis in synthesis of *n*-butyl levulinate. *Industrial and Engineering Chemistry Research, 47*, 3358–3363.
36. Bayromoglu, G., Karagoz, B., Allintas, B., Arica, M. Y., & Bicak, N. (2011). Poly(styrene-divinylbenzene) beads surface functionalized with di-block polymer grafting and multi-modal ligand attachment: performance of reversibly immobilized lipase in ester synthesis. *Bioprocess and Biosystems Engineering, 34*, 735–746.
37. Lorenzoni, A. S., Graebin, N. G., Martins, A. B., Fernandez-Lafuente, R., Ayub, M. A. Z., & Rodrigues, R. C. (2012). Optimization of pineapple flavor synthesis by esterification catalyzed by immobilized lipase from *Rhizomucor miehie. Flavour and Fragrance Journal, 27*, 196–200.
38. Zhang, D. H., Zhang, Y. F., Zhi, G. Y., & Xie, Y. L. (2011). Effect of hydrophobic/hydrophilic characteristics of magnetic microspheres on the immobilization of BSA. *Colloids and Surfaces B: Biointerfaces, 82*, 302–306.
39. Boncel, S., Zniszczol, A., Szymansha, K., Bailon, J. M., Jarzebski, A., & Walczak, K. Z. (2013). Alkaline lipase from *Pseudomonas fluorescens* non-covalently immobilized on pristine verses oxidized multiwall carbon nanotubes as efficient and recyclable catalytic systems in the synthesis of solketal esters. *Enzyme and Microbial Technology, 53*, 263–270.
40. Raghavendra, T., Basak, A., Manocha, L., Shah, A., & Madamwar, D. (2013). Robust nanobioconjugates of *Candida antarctica* lipase B-multiwalled carbon nanotubes: characterization and application for multiple usages in non-aqueous biocatalysis. *Bioresource Technology, 140*, 103–110.
41. Dandavate, V., & Madamwar, D. (2007). Novel approach for the synthesis of ethyl isovalerate using surfactant coated *Candida rugosa* lipase immobilized in microemulsion based organogels. *Enzyme and Microbial Technology, 41*, 265–270.
42. Lee, D. G., Ponve, K. M., Kim, M., Hwang, S., Ahn, I. S., & Lee, C. H. (2009). Immobilization of lipase on hydrophobic nano-sized magnetic particles. *Journal of Molecular Catalysis B: Enzymatic, 57*, 62–66.
43. Zou, B., Hu, Y., Yu, D., Xia, J., Tang, S., Liv, W., & Huang, H. (2010). Immobilization of porcine pancreatic lipase onto ionic liquid modified mesoporous silica SBA-15. *Biochemical Engineering Journal, 53*, 150–153.
44. Abdullah, A. Z., Sukaimann, N. S., & Kamaruddin, A. H. (2009). Biocatalytic esterification of citronellol with lauric acid by immobilized lipase on aminopropyl-grafter mesoporous SBA-15. *Biochemical Engineering Journal, 44*, 263–270.

Zinc Oxide Nanoparticles Supported Lipase Immobilization for Biotransformation in Organic Solvents: A Facile Synthesis of Geranyl Acetate, Effect of Operative Variables and Kinetic Study

Vrutika Patel, Chandani Shah, Milind Deshpande & Datta Madamwar

Applied Biochemistry and Biotechnology
Part A: Enzyme Engineering and Biotechnology

ISSN 0273-2289
Volume 178
Number 8

Appl Biochem Biotechnol (2016)
178:1630-1651
DOI 10.1007/s12010-015-1972-9

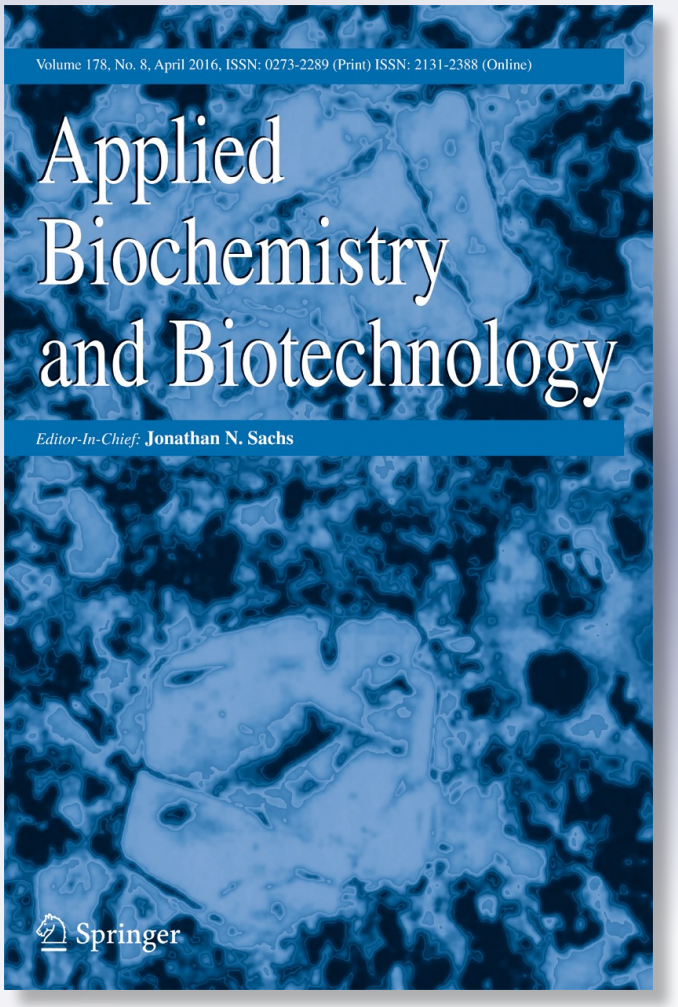

Springer

Appl Biochem Biotechnol (2016) 178:1630–1651
DOI 10.1007/s12010-015-1972-9

Zinc Oxide Nanoparticles Supported Lipase Immobilization for Biotransformation in Organic Solvents: A Facile Synthesis of Geranyl Acetate, Effect of Operative Variables and Kinetic Study

Vrutika Patel[1] · Chandani Shah[1] · Milind Deshpande[2] · Datta Madamwar[1]

Received: 13 October 2015 / Accepted: 28 December 2015 /
Published online: 9 January 2016

Abstract The present study describes grafting of zinc oxide (ZnO) nanoparticles with polyethyleneimine (PEI) followed by modification with glutraldehyde used as the bridge for binding the enzyme to support. The prepared nanocomposites were then characterized using Fourier transform infrared spectroscopy, thermogravimetric analysis, and transmission electron microscopy, utilized for synthesis of geranyl acetate in n-hexane. Among all the three prepared nanocomposites (ZnO + PEI, ZnO + PEI + SAA, ZnO + PEI + GLU), *Candida rugosa* lipase immobilized on ZnO-PEI-GLU was found to be best for higher ester synthesis. The operating conditions that maximized geranyl acetate resulted in the highest yield of 94 % in 6 h, molar ratio of 0.1:0.4 M (geraniol/vinyl acetate) in the presence of n-hexane as reaction medium. Various kinetic parameters such as V_{max}, $K_{i(G)}$, $K_{m(G)}$, and $K_{m(VA)}$ were determined using nonlinear regression analysis for order bi–bi mechanism. The kinetic study showed that reaction followed order bi–bi mechanism with inhibition by geraniol. Activation energy (E_a) was found to be lower for immobilized lipase (12.31 kJ mol^{-1}) than crude lipase (19.04 kJ mol^{-1}) indicating better catalytic efficiency of immobilized lipase. Immobilized biocatalyst demonstrated 2.23-fold increased catalytic activity than crude lipase and recycled 20 times. The studies revealed in this work showed a promising perspective of using low-cost nanobiocatalysts to overcome the well-known drawbacks of the chemical-catalyzed route.

✉ Datta Madamwar
datta_madamwar@yahoo.com

Vrutika Patel
vrutikaptl_19@yahoo.com

[1] Environmental Genomics and Proteomics Lab, BRD School of Biosciences, Sardar Patel Maidan, Satellite campus, Sardar Patel University, Sardar Patel Maidan, P.O. Box # 39, Vallabh Vidyanagar, Anand 388 120 Gujarat, India

[2] Department of Physics, Sardar Patel University, Vallabh Vidyanagar, Anand 388 120 Gujarat, India

Keywords Geranyl acetate · Polyethyleneimine · Immobilization · Biosynthesis · Lipase

Introduction

Lipases (triacylglycerol acyl hydrolases, E.C. 3.1.1.3) are one of the most common applied enzymes from hydrolases class used in wide range of organic reactions [1, 2]. The biocatalytic route involving lipase (triacylglycerol hydrolases, E.C. 3.1.1.3) has gained special importance because of the wide substrate array and the ability to carry out variety of organic reactions [3, 4]. *Candida rugosa* lipase (CRL), a stable mesophilic lipase, has been commonly used due to its high activity and broad specificity in reaction medium [5]. Like other well-known lipases, CRL present two physical conformations: an open (more active form) and a closed, relatively inactive form [6]. In presence of drop of oil, "lid" domain (partially cover the active site of enzyme) helps lipase to change its conform from "close" to "open" (more active) form. This mechanism is known as "interfacial activation" of lipase [7–9].

Enzyme immobilization confers a multitude of advantages such as structural stability, specificity and selectivity, reduction of inhibition, and increased flexibility with enzyme/substrate contact [10–13]. Over the past few years, several methods have been developed for lipase immobilization, including enzyme entrapment in solid porous polymers, enzyme encapsulation in semipermeable organic and/or inorganic membranes, physical adsorption, and covalent bonding using a cross-linker among which, the multipoint covalent attachment of enzymes with host materials and physical adsorption of biocatalyst on the surface of suitable supports has received considerable attention during last decades [14–17]. Presently, immobilization on nanostructure materials such as nanoparticles [8, 18, 19], carbon nanotubes [14, 20], nanofibers [21, 22], and nanosheets [23] is gaining more attention over traditional supports because of their extremely high surface area to volume ratios and easy to use features. Nanostructures are very attractive for enzymatic immobilization processes, since (i) they possess the ultimate characteristics to equilibrate principal factors that determine biocatalyst efficiency, (ii) ease of surface functionalization, (iii) specific surface area, (iv) mass transfer resistance, (v) effective enzyme loading, and (vi) high stability in a wide range of temperature and pH, compared to free enzymes [3, 19, 21, 23, 24]. However, nanoparticles may also have some drawbacks which includes enzymes exposed to external interfaces, may suffer proteolysis, etc. Among several nanoparticles, ZnO nanoparticles have been extensively investigated for several technological applications such as catalysis, gas sensing, cancer treatment, chemical absorbent, antibacterial, and UV blocking function and in cosmetic and pharmaceutical industries [25, 26]. Apart from this, Zn compounds have been currently listed as generally regarded as safe (GRAS) by the US Food and Drug Administration (21CFRI82.8991). However, naked ZnO nanoparticles are not sufficient for stabilizing enzymes due to the lack of appropriate functional groups. There are many reports on the protective effect of polyethyleneimine (PEI), a water-soluble cationic polymer with large number of primary amino groups, on the activity of enzymes such as lipases especially in organic media [9, 18]. PEI grafting onto inert, inorganic supports and then cross-linking with bi-functional agents such as glutraldehyde (GLU), hexamethylene diisocyanate (HMDI) is an extensively used approach for immobilization of various enzymes, such as lipase [9, 18], β-galactosidase [26, 27], and tyrosinase [28].

The present study aimed for utilization of ZnO nanoparticles as immobilizing matrix for CRL and their exploitation in organic solvents. The effect of immobilization on the catalytic

activity and stability of lipase is studied thoroughly. These immobilized biocatalysts are used for geranyl acetate (GA) synthesis. GA is a colorless liquid with pleasant floral or fruity rose aroma, which is insoluble in water but soluble in alcohol and oil. It is an important flavor and fragrance ester compound used in food, pharmaceutical, and cosmetic industries [21, 29]. Furthermore, to improve ester synthesis, operating parameters like temperature, molar ratio of substrates, and organic solvents are scrutinized.

Materials and Methods

Chemicals and the Enzyme

Readily synthesized zinc oxide nanoparticles (size varying from 8 to 25 nm) were procured from the Department of Physics, Vallabh Vidyanagar. *Candida rugosa* lipase with activity of 875 U g^{-1} (3-aminopropyl) triethoxysilane (APTES), polyethyleneimine (PEI), succinic anhydride (SAA), glutraldehyde (GLU), and 4-nitrophenyl palmitate (p-NPP) were obtained from Sigma-Aldrich, Germany. Geraniol (≥98 %), vinyl acetate (≥98 %), and geranyl acetate (≥97 %) was purchased from Fluka-Chemica (Germany). Acetic acid and ethyl acetate were procured from Hi-Media, India. All organic solvents used were of GC/HPLC grade obtained from Spectrochem (Mumbai, India).

PEI Coating of ZnO Nanoparticles and Its Modification with SAA

The grafting of PEI onto the surface of naked ZnO nanoparticles was carried out in two steps. In first step, PEI (1.5 mL) was suspended in a solution containing 10 % APTES (1 mL in 9 mL ethanol). To this mixture, 10 mg of ZnO nanoparticles were added and stirred vigorously to react for 24 h. The composite obtained was isolated by centrifugation (10,000×*g* for 15 min) and repeatedly washed with ethanol and milliQ in order to remove excess PEI. Secondly, to introduce amide and acid groups onto the surface of nanoparticles, 10 mg of PEI-coated ZnO nanoparticles was suspended in 10-mL solution of SAA (10 mg mL^{-1}), followed by stirring of the mixture at room temperature for 4 h. The prepared succinated nanocomposites (ZnO-PEI-SAA) were separated by centrifugation and washed thrice with deionized water to remove excess SAA and by product.

Characterization of Prepared Nanocomposites

The chemical modification on the surface of nanoparticles before and after functionalization was studied by Fourier transform infrared (FT-IR) spectroscopic analysis using Spectrochem GX-IR (Perkin Elmer, USA) in order to confirm binding of lipase on nanoparticles. The surface morphologies for each ZnO samples before and after functionalization were studied by TEM (Philips-Technai 20, Holland) and SEM. Samples were prepared by placing a droplet of sample (dispersed into isopropanol) on a copper grid covered by Formvar foil (200 mesh). The samples were then dried and analyzed. The fluorescence microscopy images of ZnO and ZnO + lipase were recorded on a fluorescence microscope (Olympus U-CMAD3) using an excitation filter of 460–495 nm and a band absorbance filter covering wavelengths below 505 nm. The samples were excited with a 50-W mercury arc lamp. Fluorescent microscopy images of several randomly selected sites were captured with a digital camera connected to the

microscope. The measurement of mass change during modification was analyzed using TGA/DTA-7200 thermal analyzer (Seiko SII-EXSTAR). The system was employed with PtRh furnace capable of operating from 25 to 1500°C, the temperature being measured using type R thermocouple. The measurements are conducted under controlled atmosphere as the system is vacuum tight. TGA-DSC analysis was performed using 10 mg of samples in alumina crucible without lid, in argon atmosphere. The temperature range was varied from 30 to 1000 °C and with heating rate of 20 °C min^{-1}.

Immobilization of Lipase on Modified ZnO Nanoparticles

Immobilization of lipase on ZnO was done by two different methods: (i) adsorption of lipase on PEI- and succinated PEI-grafted ZnO nanoparticles: ZnO-PEI and ZnO-PEI-SAA (10 mg each) were suspended in 10mL phosphate buffer (50 mM, pH 7) containing 1 mL *Candida rugosa* lipase (50 mg mL^{-1}). The mixture was incubated at 4 °C for 16 h, followed by centrifugation and then vacuum-dried at 37 °C for 1 h. (ii) Covalent immobilization using glutraldehyde (GLU) as cross linker: the covalent immobilization procedure was developed using GLU as cross-linking agents between the lipase and the amino groups located on the surface of the ZnO-PEI. In a typical procedure, 10 mg of ZnO-PEI was incubated in 10 mL phosphate buffer solution (50 mM, pH 7.0) containing 1 % (*w*/*v*) GLU and allowed to react for 10 min. Then, 1 mL of lipase solution (50 mg mL^{-1}) was incorporated into the mixture and stirred for overnight. The resultant nanobioconjugant obtained from both the procedures (physical adsorption and covalent attachment) were dried under vacuum (37 °C for 1 h) and further preceded for transesterification of geranyl acetate in organic solvents. The amount of enzyme immobilized is calculated based on the residual enzyme remaining in the supernatant.

Enzyme Activity and Protein Assay

The enzymatic activity of free and immobilized lipase was measured using the lipase assisted hydrolysis of *p*-nitrophenyl palmitate (*p*-NPP) as the substrate and the spectrophotometric determination of liberated *p*-nitrophenol (*p*-NP) according to a modified method described by Wrinkler and Stuckman [30]. The reaction mixture was prepared by addition of free (0.1 mL) or immobilized enzyme (10 mg) to 0.9 mL of substrate solution [*p*-NPP (0.4 mmol L^{-1}) in phosphate buffer (100 mM L^{-1}, pH 7.0)] and incubated at 37 °C for 10 min, followed by measuring the absorbance at 410 nm. One enzyme unit was defined as the amount of enzyme that liberates 1 μmol of *p*-NP per minute under assay conditions. The protein concentration for free and immobilized enzyme was estimated by Lowry's method at 595 nm [31] by means of bovine serum albumin as a standard.

Enzymatic Synthesis of Geranyl Acetate Catalyzed by Free CRL As Well As Immobilized Lipase Preparations

Synthesis of geranyl acetate as industrially important ester was studied using free as well as immobilized biocatalyst in presence of organic solvent as reaction medium. In 10 mL screw cap glass vials, equimolar concentration of geraniol (0.1 M) and vinyl acetate (0.1 M) were used as a substrate and mixed with 3 mL of n-hexane. Later on, the reaction was initiated after addition of enzyme to the substrate where native lipase and immobilized lipases were used separately for catalysis. The experiment was carried out at 37 °C and continuously stirred at

150 rpm to ensure all the enzyme particles were homogeneously dispersed. Reaction sample of 100 μL was withdrawn periodically and analyzed using Perkin Elmer Clarus-500 Gas Chromatograph equipped with flame ionization detector and 30m Rtx-®-20 capillary column. The carrier gas was nitrogen at split flow rate of 90 mL min^{-1}. The temperature of the detector and injector was maintained at 250 °C. The oven temperature was programmed to increase from 40 to 180 °C at the rate of 3 °C min^{-1} up to 180–230 °C (20 °C min^{-1}) and maintained at 230 °C for 20 min [14, 29]. Ester identification and quantification were done by comparing the retention time and peak area of the sample with the standard.

Effect of Operative Variables on Enzymatic Production of Geranyl Acetate

In order to obtain enhanced geranyl acetate synthesis, different operative variables were used for the experiment. The operative variables used in the study are as follows:

1. Effect of temperature: 30, 37, 40, and 50 °C.
2. Effect of organic solvents: different solvents used were tetrahydrofuran, 1,4-dioxane, acetone, chloroform, benzene, toluene, and n-hexane.
3. Effect of substrate concentration: substrate concentration ranges from 0.1 to 0.5 M. The concentrations of geraniol and vinyl acetate were varied one at a time keeping the other constant.
4. Effect of acyl donor: acetic acid, ethyl acetate, and vinyl acetate were used as acyl donor.

Samples (100 μL) were periodically withdrawn to study the time course of reaction and analyzed by gas chromatograph (GC, Perkin Elmer, USA)) in order to establish the product formation profile. No reaction was detected in the absence of the enzyme. All the experiments were repeated thrice at each operating condition and the relative deviation was within ±1 %.

Reusability Studies for Immobilized Lipase Preparations

After establishing the conditions for maximum geranyl acetate production, the reusability study for all the immobilized lipase nanocomposites was carried out. After the first run of lipase activity determination, the immobilized lipase was collected using centrifugation and washed three times with n-hexane in order to remove excess substrate and product. The activity during the first run was defined as 100 % and that during the succeeding runs was regarded as relative activity. All the experiments were performed in triplicate, and data were shown as relative deviation within ±1 %. Also, after every three to four cycles of reusability, dehydration treatment was given in order to remove accumulated water formed as by-product. The nanocomposites were treated with molecular sieves (30 mg) for overnight in 2-mL n-hexane solution.

Results and Discussion

Immobilization of CRL

A protein content and lipase activity assay was performed to determine the immobilization of the protein on the support and to check enzyme catalytic efficiency after immobilization. The

present study was designed to apply both physical adsorption (in the presence of ZnO-PEI and ZnO-PEI-SAA) and covalent attachment via spacer arm of GLU (ZnO-PEI-GLU) for immobilization of CRL as represented in Scheme 1. The protein content for the free as well as immobilized lipase followed the sequence as CRL > ZnO-PEI-GLU > ZnO-PEI-SAA > ZnO-PEI (Table 1). Lipase fabricated on ZnO-PEI-GLU showed the best results in terms of hydrolytic activity (4.29 U mL^{-1}). ZnO-PEI, ZnO-PEI-SAA, and ZnO-PEI-GLU showed higher immobilization of lipase in terms of specific activity (Table 1). The results obtained in present study were in agreement with the study of Khoobi et al. [9] determining maximum immobilization yield of 88 % for covalent attachment of TTL on MCM-41@PEI-GLU nanocomposite. Nicoletti et al. [32] reported 70 % of immobilization yield for CaLB lipase immobilized on polyurethane foam modified with PEI and activated by GLU.

One of the reason in using PEI as support is to ensure greater mechanical strength. The electrostatic interaction between the negatively charged lipase and positively charged PEI might be the reason for noticeable immobilization yield for ZnO-PEI due to their high accessible amine groups on the surface of nanoparticles [9, 33]. In the case of ZnO-PEI-GLU, the spacer arm of glutraldehyde might assist the support to covalently attach CRL via surface residues that boost the loading of CRL on the surface of ZnO-PEI-GLU [18].

Characterization Studies

The microstructure investigation of pristine and functionalized ZnO nanoparticles was carried out using transmission electron microscopy (TEM) to reveal the morphology of nanoparticles. Figure 1a illustrates the electron micrograph of pristine ZnO nanoparticles recorded at the accelerating voltage of 200 keV. As seen from Fig. 1, it can be assumed that most of the

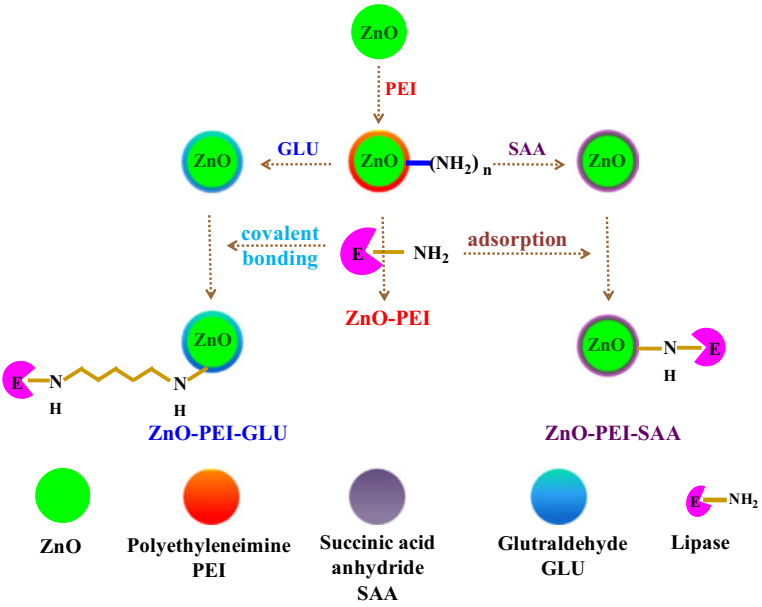

Scheme 1 Preparation of various ZnO-nanocomposites using different cross-linkers and immobilization of lipase. Polyethyleneimine (PEI), succinic acid anhydride (SAA), and glutraldehyde (GLU) are used as cross-linking agents

Table 1 Lipase activity under various immobilization systems

Enzyme	Enzyme activity (U mL^{-1})	Protein (mg mL^{-1})	Specific activity (U mg^{-1})
CRL	5.68	2.469	2.300
ZnO-PEI	2.96	1.243	2.381
ZnO-PEI-SAA	3.25	0.962	3.371
ZnO-PEI-GLU	4.29	0.325	13.2

pristine ZnO nanoparticles are quasi-spherical and their diameter is in the range from 15 to 25 nm. The micrograph reveals aggregation of some nanoparticles due to large specific surface area and high surface energy [34]. This is generally attributed to a certain degree of compactness existing between the nanoparticles. Also, scanning electron microscopy study was carried out for pristine ZnO nanoparticles. As displayed in Fig. 1b, ZnO nanoparticles were found to be highly aggregated. It also demonstrates that after the surface of ZnO nanoparticles was modified by PEI, the aggregation of ZnO nanoparticles was greatly reduced (results not shown). However, using SEM and TEM, there was no clear difference found with modified

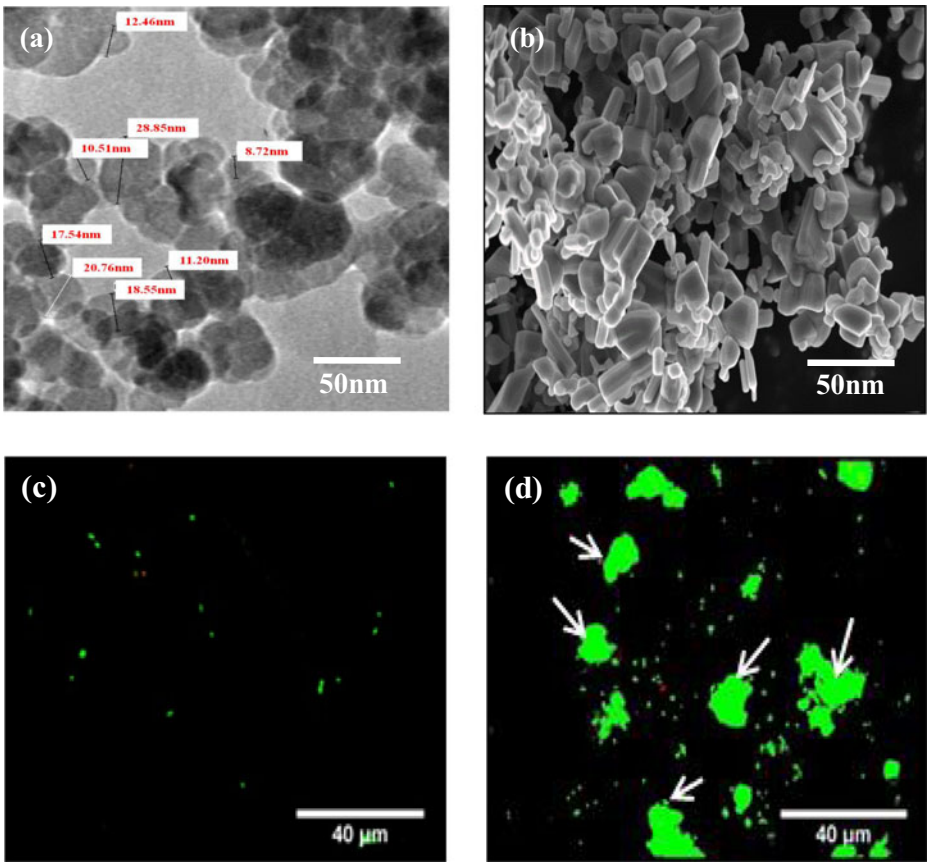

Fig. 1 Characterization of ZnO nanoparticles. **a** Transmission electron micrograph for pristine ZnO nanoparticles. **b** Scanning electron microscopy for pristine ZnO nanoparticles. **c** Fluorescence microscopy analysis for pristine ZnO nanoparticles. **d** Fluorescence microscopy analysis for lipase conjugated ZnO nanoparticles

ZnO nanoparticles and lipase immobilization (results not shown). Thus, in order to check whether immobilization has taken place, further studies were carried out.

The luminescence properties of functionalized ZnO nanoparticles were recorded by fluorescence microscopy. Pristine ZnO (Fig. 1c) have adsorption maximum at about 380 nm; however, lipase immobilized ZnO (Fig. 1d) was excited at 460 nm to overcome the strong background fluorescence. The bright green coloration under fluorescence microscopy further confirmed conjugation of ZnO with lipase.

To understand better about the functional groups involved in immobilization process, FTIR analysis was performed in the range of 500–4000 cm^{-1}. Figure 2 shows the FT-IR spectra of the ZnO nanoparticles (A), ZnO-PEI (A), CRL (C), and ZnO-PEI-SAA (D), respectively. FT-IR band at short wave numbers (range 446–630 cm^{-1}) corresponds to the characteristics peak of ZnO nanoparticles and was common for all the spectra (Fig. 2). In addition to this, the broad band of 3429–3439 cm^{-1} is due to the –OH stretching and bending vibration, indicating the presence of a large number of hydroxyl groups and H_2O molecules on the surface of the particles. The PEI grafting on nanoparticles can be clearly observed, as evident from the strong adsorption band at 1041 and 2928 cm^{-1} which results from the vibration of the Si–O– group and the aliphatic C–H group, respectively (Fig. 2b). Shifting the related peak of ZnO to 446 cm^{-1} and the stretching vibration of Si–O– group confirmed anchoring of silanol containing group onto the surface of ZnO nanoparticles. Such results indicate that the active groups have been introduced onto the nanoparticles surface. After immobilization of lipase onto ZnO nanoparticles (Fig. 2c), the shifting of peak value corresponding to the interaction of –CO group of enzyme with ZnO NPs, while the broadening of peak at 548 cm^{-1} also revealed uniform adsorption of lipase on the nanomatrix. The peak obtained at 1642 cm^{-1} was due to amide II of the enzyme, while the peak value observed at 1457 cm^{-1} confirmed CH vibrations [26, 35].

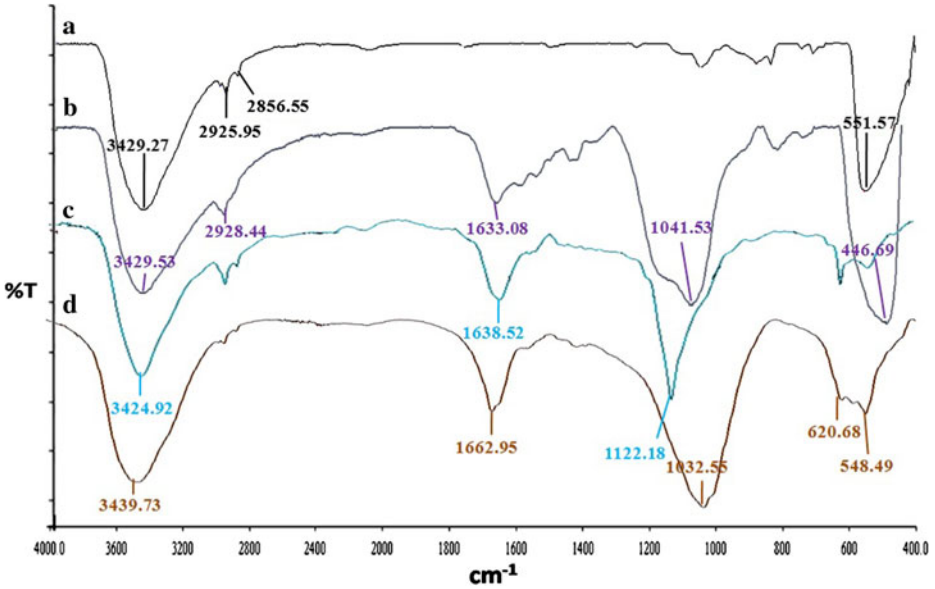

Fig. 2 FTIR overlay spectra of **a** pristine ZnO, **b** ZnO-PEI, **c** lipase, and **d** ZnO-PEI-SAA

The successful functionalization was also reflected in TGA curves. The TGA analysis for naked as well as modified ZnO nanoparticles are shown in Fig. 3, and the temperature scale for measurement is from 100 to 1000 °C in nitrogen at heating rate of 20 °C min^{-1}. Two-step weight loss was found for naked ZnO nanoparticles. The first weight loss of 1 % was acquired at 150 °C associated with desorption of water molecule, while the second weight loss (2.8 %) was attained at 550 °C. In comparison to pure ZnO nanoparticles, the related TGA curve for ZnO modified nanocomposites (data not shown) showed weight loss at 105 °C due to vaporization of water formed by the condensation of silanol groups, then at 400 °C associated with oxidative decomposition of organic moiety. In case of lipase immobilized ZnO (for each nanocomposites), nearly 10 % of weight loss was observed at around 100 °C. This is much obvious due to loss of bound water molecule. This attributes to thermo-decomposition of lipase indicating successful enzyme immobilization on ZnO.

Effect of Reaction Parameter for Enhanced Synthesis of Geranyl Acetate

Effect of Temperature

In order to check the influence of temperature on enzymatic transesterification, the reaction was carried out at different temperatures (30, 37, 40, and 50 °C) using free as well as immobilized lipase nanocomposites. The trends for ester synthesis by prepared nanocomposites of lipase are exhibited in Fig. 4a and are more or less similar. Immobilized forms of lipase were found to be quite stable even at higher temperatures, whereas above 40 °C, the activity of free CRL started declining. About 90 % of ester was synthesized using immobilized lipase (ZnO-PEI-GLU) in 6 h at 40 °C while free lipase was found to be sluggish (52 %) for production under same condition. However, ZnO-PEI-SAA and ZnO-PEI produced 82 and 71 % of geranyl acetate under same condition and was found to be stable even at 50 °C. The stability of immobilized lipase over free CRL can be explained by hydrophobic and electrostatic interaction between ZnO and enzyme which alter the physical and chemical properties of

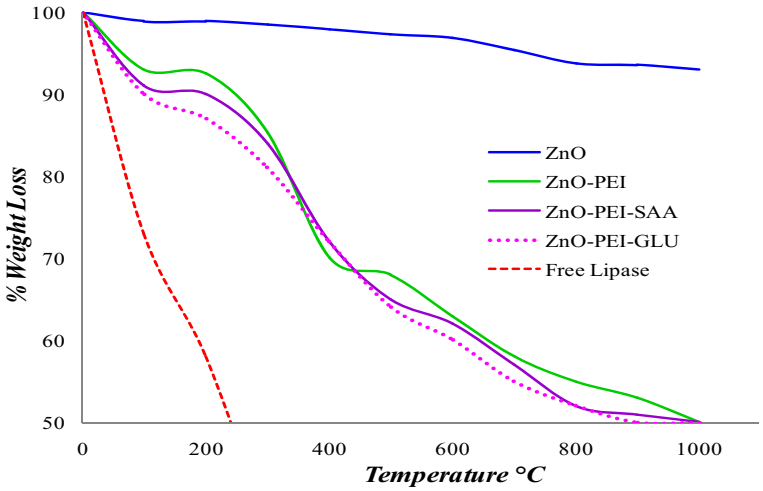

Fig. 3 The TGA weight loss curves of pristine ZnO, lipase immobilized ZnO nanocomposites. The temperature range was varied from 30 to 1000°C and with heating rate of 20 °C min^{-1}, in agron atmosphere

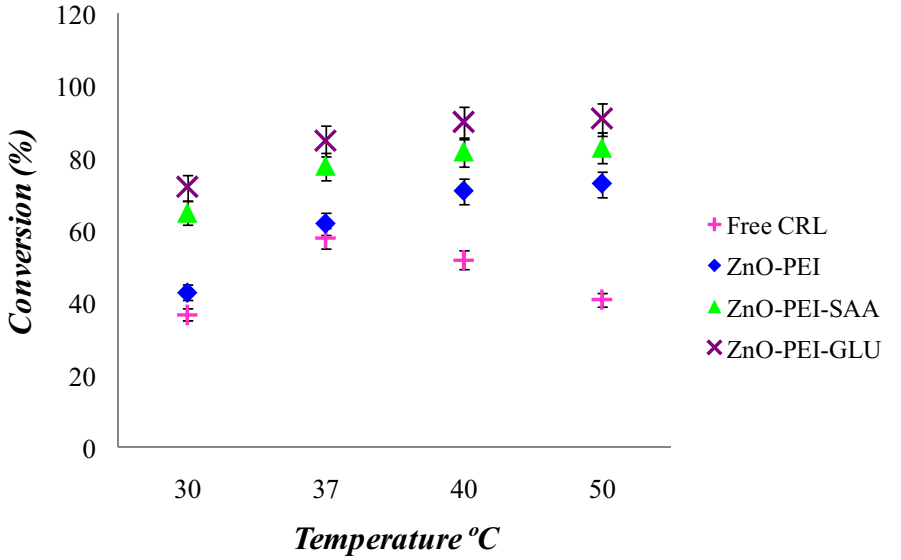

(a)

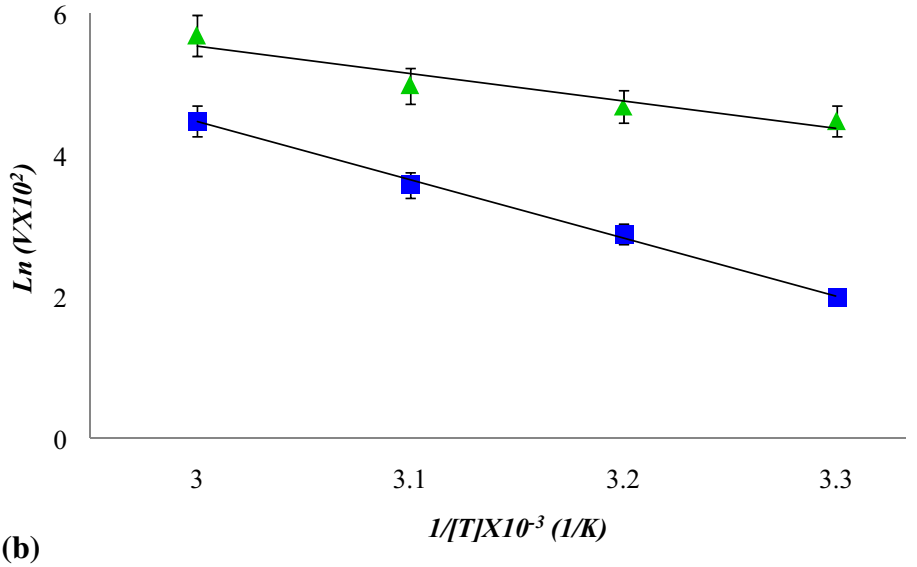

(b)

Fig. 4 **a** Effect of temperature on free lipase and immobilized lipase nanocomposites. Reaction conditions: 50 mg of enzyme (including weight of support), 3 mL of n-hexane, 0.1 M of each substrate (geraniol and vinyl acetate), temperature 30–50 °C, 150 rpm. **b** Arrhenius plot for free (*squares*) as well as immobilized lipase (ZnO-PEI-GLU) (*triangles*) over the temperature range of 30–50 °C. Reaction conditions: geraniol (0.1 M), vinyl acetate (0.4 M), reaction volume 3 mL, pH 7, and temperature 30–50 °C

enzyme [35, 36]. Also, the limitation of enzymatic movement after immobilization on the support together with better substrate diffusion at a higher temperature improves the activity of

the immobilized enzymes [37]. Ozyilmaz et al. reported the optimum temperature of the immobilized lipase of *Candida rugosa* on β-cyclodextrin grafted magnetic nanoparticles shifted to 40 °C due to consequent conformational limitations on enzyme movement [38]. The effect of temperature on affinity of free and immobilized enzyme can be seen in Arrhenius plot (Fig. 4b). The free and immobilized lipase exhibited a linear relationship in the temperature range of 30–50 °C, and the corresponding activation energies were calculated to be 19.04 kJ mol^{-1} for free lipase and 12.31 kJ mol^{-1} for immobilized lipase (ZnO-PEI-GLU). Lower activation energy for immobilized lipase in comparison to that of free lipase suggests less energy requirement and the change in conformation of enzyme during immobilization.

Effect of Organic Solvents as Reaction Medium

The solvent as reaction medium not only affects the catalytic power of enzyme by changing the three-dimensional structure of protein but also significantly alters the conversion rate of product [39]. Log*P* value (*P* is the partition coefficient of a given solvent between n-octanol and water) is widely used parameter to describe solvent hydrophobicity and its possible effects on enzyme activity [38, 40]. In this study, organic solvents with different polarities including tetrahydrofuran, 1,4-dioxane, chloroform, acetone, toluene, benzene, and n-hexane were chosen. Figure 5 displays the yield of geranyl acetate catalyzed by free as well as immobilized forms of lipase in presence of different solvents. The results clearly indicated that n-hexane, a medium polarity organic solvent, resulted in higher conversion for all the forms of lipase reaching 92 % for ZnO-PEI-GLU in 6 h. It is but obvious that immobilized lipase showed higher rate of conversion in comparison to that of free counterpart which was about 53 % under similar condition. The enzyme activity is usually high when Log*P* value for solvent is between 2.0 and 4. The conversion obtained from benzene (85 %) and toluene (86 %) was also good, but their toxicity and odor limits their application in perfume synthesis. Also, the polar solvent like tetrahydrofuran and 1,4-dioxane yield only 48 % of ester, whereas chloroform

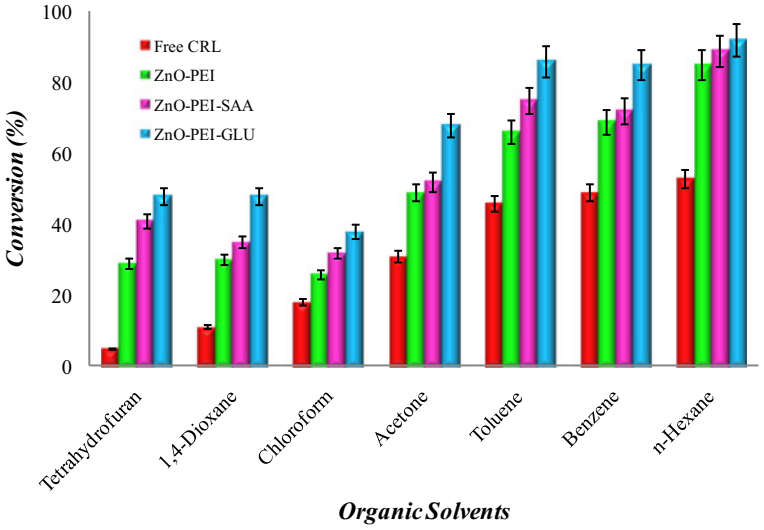

Fig. 5 Effects of different solvents as reaction medium on the synthesis of geranyl acetate. Reaction conditions: 0.1 M geraniol, 0.1 M vinyl acetate, solvent 3 mL, pH 7, temperature 40 °C, 150 rpm

yield only 26 % of geranyl acetate. This can be attributed to the stripping off the essential water molecule from the enzyme and enzyme deactivation [23]. As a consequence, the catalytic activity of enzyme was decreased due to the lack of bound water to preserve the enzyme conformation flexibility which in turn is necessary for its catalytic action [23, 41]. However, acetone, being an aprotic solvent, attacks protein very strongly. Thus, with acetone being reaction medium, 68 % of geranyl acetate was obtained.

The outcome obtained with present study is in agreement with those reported in the literature, where high hydrophobic solvents with Log*P* values >4 are considered the most suitable solvents for use in biocatalytic processes. The solvents with Log*P* values between 2 and 4 are moderately effective, whereas polar solvents with Log*P* <2 are often ineffective [23, 40, 41].

Substrate Concentration

To examine the dependence of the molar ratio of the substrate and acyl donor on the chemical equilibrium of the lipase-catalyzed reaction, various experiments were performed. In one set of experiment, the concentration of geraniol was kept constant (0.1 M) while the concentration of vinyl acetate was varied from 0.1 to 0.5 M (Fig. 6a). The molar conversion of the nanocomposites (ZnO-PEI-GLU) with 1:1 ratio of geraniol/vinyl acetate was 87 %. Figure 6a revealed that the reaction rate was enhanced when vinyl acetate concentration was increased from 0.1 to 0.4 M for all the prepared nanocomposites. As a consequence, this phenomenon in enzymatic reactions revealed that vinyl acetate has no inhibitory effect within the studied range of substrate concentrations.

In another set of experiment, concentration of vinyl acetate was kept constant at 0.4 M while concentration of geraniol was varied from the 0.1 to 0.5 M. As concentration of geraniol increases, the yield decreases gradually (Fig. 6b). This decrease in reaction rate can be attributed to the inhibitory effect of geraniol on immobilized enzyme [42]. The hydrophobic–hydrophobic interaction between the lipase and geraniol might be the reason to destabilize the active sites of the lipase [42, 43]. Similar kind of inhibitory effect for geraniol was observed in case of the geranyl acetate synthesis [29] and geraniol propionate synthesis [44]. Hence, optimum molar ration of 0.1:0.4 M geraniol/vinyl acetate was considered synthesizing up to 92 % of geranyl acetate. Similar molar ratio of 1:5 was found to be optimum for the synthesis of geranyl acetate catalyzed by TTL immobilized on nanofiber membrane [29]. Paroul et al. observed 99 % conversion for the substrates at the molar ratio of 5:1 propionic acid/geranyl acetate [45].

Effect of Acyl Donor on Immobilized Lipase

Different acyl donors were used for synthesis of geranyl acetate with immobilized lipase in order to perceive their influence on reaction rate and are exhibited in Fig. 7. The experimental studies showed only 15 % yield when acetic acid was used as acyl donor. Acetic acid acts as a potent inhibitor of enzyme activity and hence slows the initial reaction rate and % yield. When ethyl acetate was used as the acyl donor, ethanol was formed as a by-product which competes with geraniol for nucleophilic attack on carbonyl ester and inhibits the rate of reaction [46, 47]. Herein, highest yield of 90 % was achieved in transesterification of the geranyl acetate using vinyl acetate as acyl donor. Thus, vinyl acetate proved to be a good choice of acyl donor for lipase catalyzed

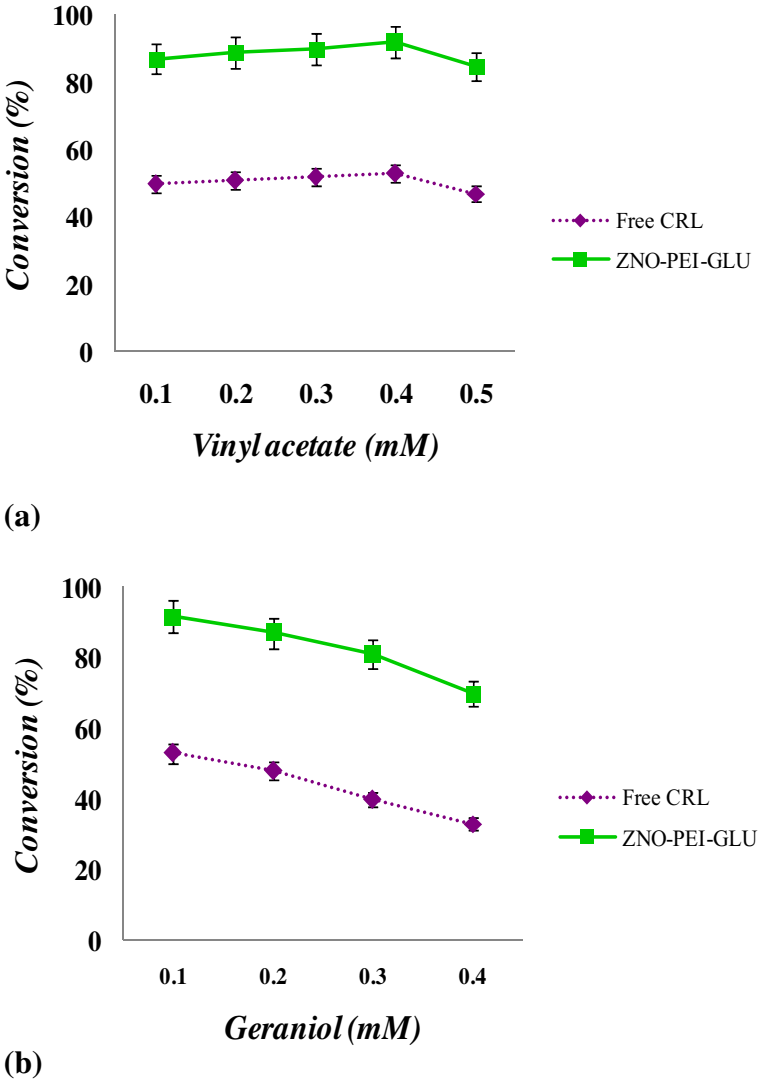

Fig. 6 **a** Influence of vinyl acetate concentration on the efficiency of ester synthesis where geraniol concentration was kept constant at 0.1 M. Reaction conditions: 0.1 M geraniol, 0.1–0.5 M vinyl acetate, 3 mL n-hexane, pH 7, temperature 40 °C, 150 rpm. **b** Influence of geraniol concentration on the efficiency of ester production where vinyl acetate concentration was kept constant at 0.4 M. Reaction conditions: 0.1–0.5 M geraniol, 0.4 M vinyl acetate, 3 mL n-hexane, pH 7, temperature 40 °C, 150 rpm

transesterification reactions because vinyl alcohol is formed as by-product that immediately tautomerizes to acetaldehyde, thereby driving the reaction in a forward direction [40].

Enzymatic Synthesis of Geranyl Acetate

Biotechnological approaches are predominantly used in bioprocess of flavor compounds in modern food industries. Some of the flavor esters have been prepared by esterification

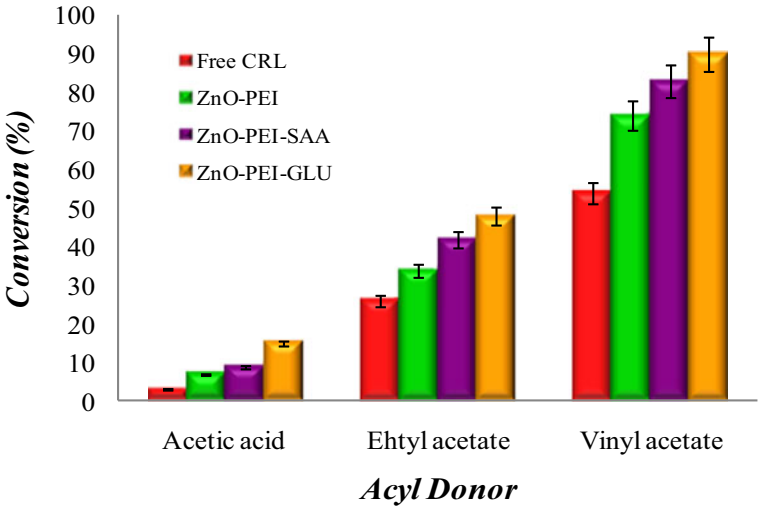

Fig. 7 Influence of acyl donor for the synthesis of geranyl acetate. Reaction conditions: 0.1 M geraniol, 0.1 M acyl donor (acetic acid, vinyl acetate, ethyl acetate), 3 mL n-hexane, pH 7, temperature 40 °C, 150 rpm

reactions via enzymes. In many cases, stable enzyme-support conjugation takes place but the activity of the enzyme is lost due to change in enzyme configuration during the immobilization process [48]. Therefore, characterization studies were followed by application to scrutinize the activity of enzyme after immobilization by its ability to catalyze ester synthesis in organic solvents. The trends for geranyl acetate production using three forms of ZnO-enzyme preparations as well as free lipase under optimized conditions are shown in Fig. 8a. Also, there was no product formation in negative control (support without enzyme). From Fig. 8a, it was noted that in free form of lipase, the conversion proceeded at very high rate reaching saturation of 65 % after 6 h. Immobilized forms of lipase took littler longer time in order to achieve saturation for conversion and utilization of substrates. Among the immobilized forms, CRL cross-linked using GLU showed higher conversion (94 %) than one coupled with ZnO-PEI and ZnO-PEI-SAA, i.e., 86 and 90 %, respectively, in 6 h and was stable thereafter. One of the main reason for this can be attributed to the difference in Specific activity (U/mL) (shown in Table 1) which is higher for ZnO-PEI-GLU (13.2) than ZnO-PEI (3.371) and ZnO-PEI-SAA (2.381). While, as per calculation, hydrolytic activity for free lipase was found to be 5.68 U mL^{-1}. Another possible reason for this may be due to cross-linking of enzyme by glutraldehyde (containing active aldehyde group) on amine-based cationic polymer PEI. Khoobi et al. and co-workers [9] prepared magnetically separable nanospheres consisting of polyethyleneimine (PEI) and succinated PEI grafted on silica coated magnetite (Fe_3O_4) and reported 79 % of ethyl valerate synthesis in h-hexane. Badgujar and Bhagane [29] reported 99 % of geranyl acetate conversion in 3 h using *Pseudomonas cepecia* lipase immobilized on biodegradable polymer film of HPMC/PVA. In another study, the researchers obtained 90 % of geranyl acetate yield by covalent linkage of *Thermomyces lanuginosus* lipase (TLL) on electrospun polyacrylonitrile nanofiber membrane [14]. The results obtained from this study specify that cross-linking of enzyme not only provides good physical stability but also maintain chemical stability of enzyme which can be observed by conversion of ester in organic solvent.

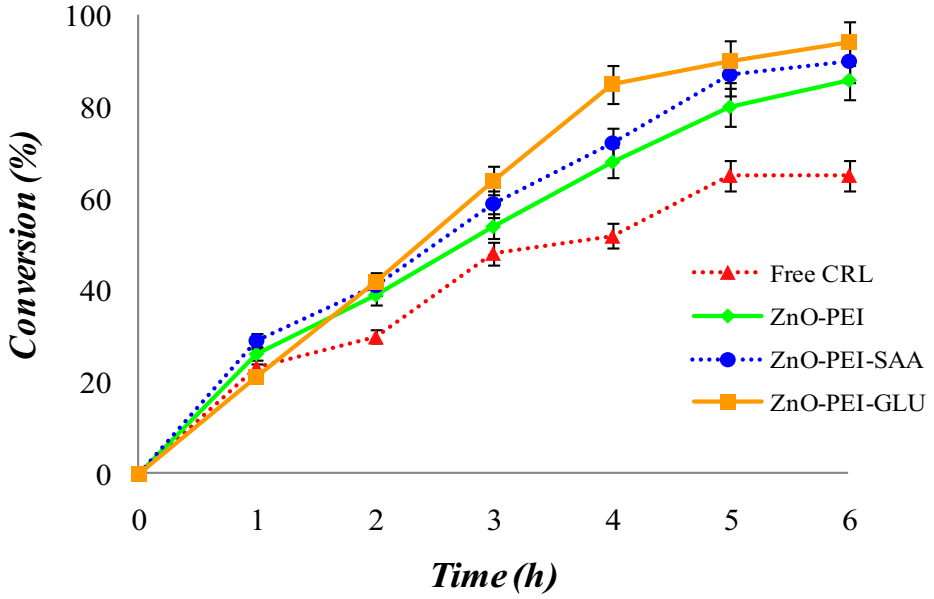

(a)

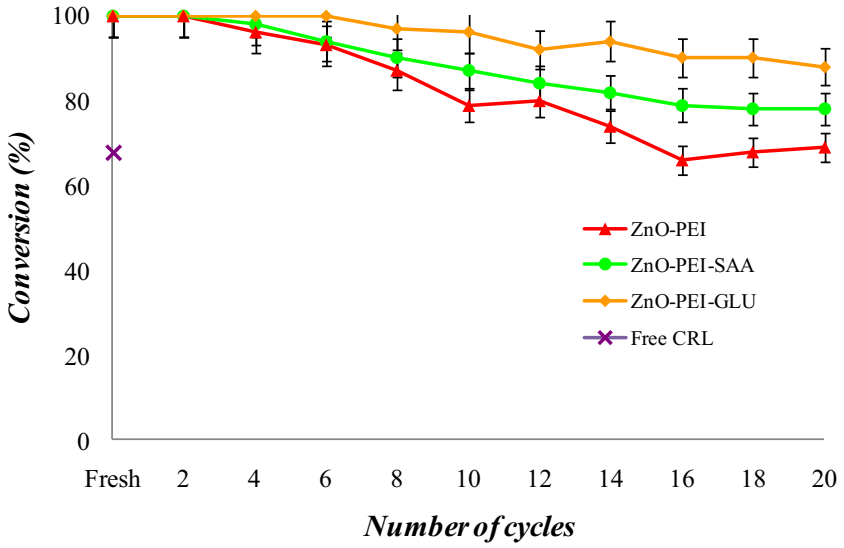

(b)

Fig. 8 **a** Time course for the synthesis of geranyl acetate by free as well as immobilized lipase using n-hexane as a medium. Reaction conditions: 0.1 M geraniol, 0.4 M vinyl acetate, 3 mL n-hexane, pH 7, temperature 40 °C, 150 rpm. **b** Operational stability for the synthesis of geranyl acetate using lipase immobilized nanocomposites at pH 7 and 40 °C. Reaction conditions: 0.1 M geraniol, 0.4 M vinyl acetate, 3 mL n-hexane, pH 7, temperature 40 °C, 150 rpm

Furthermore, higher esterification activity for immobilized lipase can be hypothesized by following reasons: (i) immobilized lipase scattered into immobilization matrix could easily contact with the substrate molecules, which enhances the catalytic rate; (ii) immobilization matrix could benefit the "open state" conformation of lipase and offered easy access of substrates to active sites of enzyme; (iii) the interfacial activation causes a change in enzyme conformation after immobilization, which improves the biocatalytic activity of the lipases; and (iv) free enzyme aggregation is avoided after immobilization, which facilitates easy mass transfer of the substrates to active catalytic sites [2, 21, 23, 29, 49–51].

Reusability Studies

The cost of lipase is one of the limitations in producing terpene esters using the biological enzyme method. If lipase exhibits higher stability during the catalytic reaction and it can be repeatedly used numerous times, then the economic cost can be reduced to a certain extent. However, accumulation of water as by-product is a major issue for altering the thermodynamic equilibrium of the reaction decreasing activity of lipase. In order to solve this problem, after every three to four runs, each nanocomposite were treated with 30 mg molecular sieves (4°A) in n-hexane for 24 h. Then, these pretreated nanocomposites after dehydration were used for transesterification reaction where significant maintenance in conversion of product was observed demonstrating partial recovery of the lost activity (Fig. 8b). The lipase immobilized on ZnO-PEI retained 69 % of its initial activity after 20 catalytic rounds, whereas ZnO-PEI-SAA retained 78 % of its initial activity. The nanocomposite ZnO-PEI-GLU was the best one, showing only 12 % loss of activity retaining 88 % of its initial activity after 20 cycles. The results revealed that the strong interactions between lipases and supports significantly increase the enzyme reusability in covalent bonding. However, the gradual decrease in activity of immobilized enzymes arose from the denaturation of protein, the inactivation of the enzyme, and the leakage of protein from the support during sequential application [19, 23]. Kumar et al. immobilized the partially purified lipase from *Bacillus* sp. DVL2 on the glutraldehyde-activated aluminum oxide reported a 25 % of loss in the activity of immobilized biocatalyst after ten cycles [52]. Khoobi et al. prepared nanocomposite of MCM-41@PEI-GLU that retains 85 % of its initial activity after 12 catalytic rounds, whereas the lipase immobilized on MCM-41 retains only 70 % of its initial activity [9].

Effect of Ester and Alcohol Chain Length on Synthesis of Geraniol Acetate

The trend for the effect of the vinyl ester chain length (acetate to butyrate) on synthesis of geranyl ester was studied using nanocomposite of ZnO-PEI-GLU and is exhibited in Fig. 9a. From the results described in Fig. 9a, it can be depicted that as the ester chain length increases from acetate to butyrate, corresponding yield of product was decreased. Around 94 % of ester was synthesized using acetate whereas only 75 % of product was formed using butyrate. There can be two possible reasons for this: (i) higher alkyl chain length leads to decrease in electrophilicity of carbonyl group that slower down nucleophilic attack of geraniol on carbonyl carbon resulting in decreased enzyme-acyl complex formation; (ii) secondly, mass diffusion problem is created with an immobilized enzyme by using higher alkyl groups [29, 53]. Similar results for decrease in the conversion of geranyl acetate by using higher alkyl chain length were reported by Badgujar and co-workers [29].

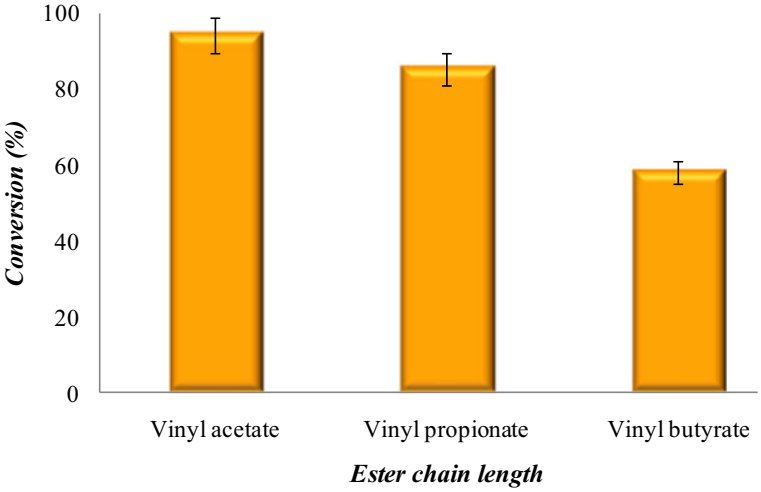

(a)

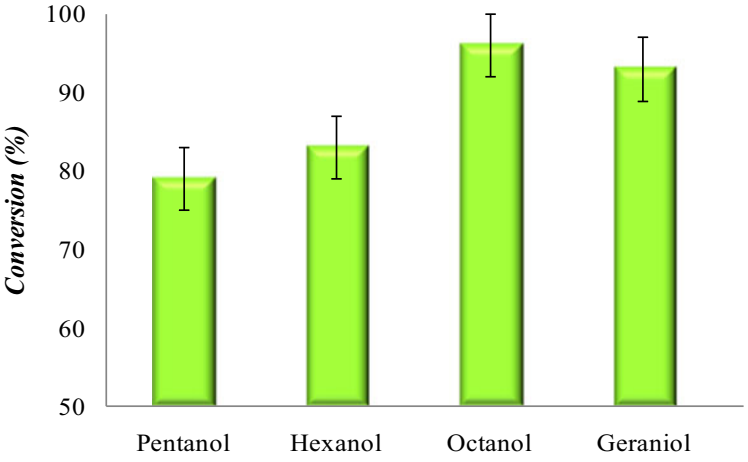

(b)

Fig. 9 **a** Effect of ester chain length. Reaction condition: geraniol 0.1 M, 0.4 M vinyl acetate, 3 mL n-hexane, immobilized biocatalyst ZnO-PEI-GLU 50 mg; temperature 40 °C, 150 rpm. **b** Effect of alcohol chain length. Reaction conditions: geraniol 0.1 M, 0.4 M vinyl acetate, 3 mL n-hexane, immobilized biocatalyst ZnO-PEI-GLU 50 mg, temperature 40 °C, 150 rpm

In another set of experiment, the same nanocomposite (ZnO-PEI-GLU) was used to study the effect of various primary alcohol chain lengths (pentanol, hexanol, octanol, and geraniol) on synthesis of geranyl acetate. As observed from Fig. 9b, the synthesis of geraniol acetate using different primary alcohol with shorter chain length was going on increasing from 1-pentanol (78 %) to 1-octanol (96 %). Accordingly, when geraniol was used as alcohol, 93 % of ester was synthesized under same condition but was comparatively lower than 1-octanol. The

probable reason for this may be steric hindrance effect inhibiting nucleophilic attack that causes slower diffusion of long-chain alcohols [29, 53, 54]. Similar type of steric effect for the short-chain alcohol and the mass diffusion effect for the longer-chain alcohols was studied by Ozturk [53] and Badgujar et al. [29] when reaction was catalyzed by the porcine pancreatic lipase and *Candida rugosa* lipase, respectively, for synthesis of geranyl acetate.

Kinetic Modeling

Immobilization of enzymes on a support may alter the performance of an enzyme in many interesting processes, such as selective hydrolysis or oxidations, kinetic resolutions of racemic mixtures, or kinetically controlled synthesis [55]. The enzyme fully dispersed on the support surface after immobilization prevents aggregation or other inactivation phenomena [56]. Moreover, multipoint covalent immobilization produces more rigid structure which is less sensitive to conformational changes; thus, enzyme activity under drastic conditions becomes higher than that of the free enzyme. The surface of the support is likely to produce some effects that may affect enzyme performance, by partitioning of substrates, products, or components of the reaction medium [56, 57].

Kinetic modeling and mechanistic study of a reaction are very important aspects of the reaction designing and to scale up the process. Lipase catalysis involving two substrates generally follows order bi–bi mechanism. In this study, the kinetic model determined for geranyl acetate synthesis was based on Lineweaver–Burk graph constructed by reciprocal of the initial rates at different concentrations of geraniol (as alcohol) for immobilized lipase (ZnO-PEI-GLU) (data not shown). At higher concentration of geraniol, decrease of initial rate with increase in slope was observed which signifies inhibitory effect of alcohol. This fact is also supported by the effect of molar quantity of geraniol (Fig. 6b).

Considering the initial rate, the proposed rate equation for order bi–bi model with inhibition of alcohol is as follows:

$$V = \frac{V_{\max}[G][VA]}{K_{i(G)}K_{m(VA)} + K_{m(G)}[VA] + K_{m(VA)}[G] + [G][VA]}$$

where V = initial rate of reaction, $V_{\max}$ = maximum rate of reaction, $[G]$ = initial concentration of geraniol, $[VA]$ = initial concentration of vinyl acetate, $K_{m(G)}$ and $K_{m(VA)}$ = Michaelis–Menten constant of geraniol and vinyl aetate, and $K_{i[G]}$ = inhibitory constant of geraniol.

The kinetic parameters were scrutinized by nonlinear regression analysis using statistical software XLSTAT version 2015.1.02. According to the kinetic values obtained from order bi–bi mechanism, Michaelis–Menten constant for vinyl acetate, i.e., $K_{m(VA)}$ was found to be lower in comparison to that of geraniol $K_{m(G)}$ showing higher affinity of vinyl acetate towards immobilized lipase for formation of acyl-enzyme complex (Table 2).

By order bi–bi mechanism, initially, vinyl acetate binds to immobilized lipase (due to higher affinity) and forms acyl-enzyme complex (E-VA). Later on, geraniol (alcohol) combines with E-VA complex to form a ternary complex (E-VA-G) and is further isomerized into

Table 2 Kinetic parameter values for the synthesis of geranyl acetate by lipase immobilized on ZnO-PEI-GLU

Parameters	$V_{\max}$ (mmol L^{-1} min^{-1})	$K_{m(G)}$ (mmol L^{-1})	$K_{m(VA)}$ (mmol L^{-1})	$K_{i(G)}$
Values	2.03×10^{-2}	1.3482	0.5743	4.48

new complex. This ternary complex was broken down into vinyl alcohol which tautomerized into the acetaldehyde, while binary complex subsequently released desired ester (geranyl acetate) and enzyme [29, 43].

Conclusion

Different approaches to improve the conformational stability of enzymes have been studied. Enzyme type, immobilization route, and structure of support play significant roles in the extent of stabilization. The lipase-catalyzed transesterification synthesis of geranyl acetate in a nonaqueous system was systematically studied in this research, including the effects of various parameters. In a nutshell, the results obtained from the present study showed that, among the three prepared nanocomposites, ZnO-PEI-GLU was the best biocatalyst, showing higher ester synthesis (94 % after 6 h incubation at 40 °C) compared with the other nanostructures containing lipase as well as free lipase. The biocatalytic application evaluates the enhancement of immobilized lipase with 2.23-fold over that of free lipase. Various kinetic parameters were refined by nonlinear regression analysis indicating inhibition effect of geraniol. In addition to this, energy of activation was determined showing lower energy requirement for immobilized lipase. Furthermore, alkyl ester and alcohol chain length effect was studied to understand the influence of the chain length on immobilized enzyme activity. The reusability of covalently immobilized lipase showed that there is not significant leakage of enzyme during repeated use and 88 % activity remains after 20 cycles. This approach proved to be a facile, mild, and environmental friendly method for synthesizing flavor ester geranyl acetate.

Acknowledgments The authors would like to acknowledge University Grants Commission (UGC) grant no. F. 42-167/2013 (SR), New Delhi, for financial support. Authors would also like to acknowledge (a) SICART, Vallabh Vidyanagar for FTIR and TEM facility and (b) Department of Physics for extending their TGA facility.

References

1. Motevalizadeha, S. F., Khoobi, M., Sadighi, A., Khalilvand-Sedagheh, M., Pazhouhandeh, M., Ramazani, A., et al. (2015). Lipase immobilization onto polyethylenimine coated magnetic nanoparticles assisted by divalent metal chelated ions. *Journal of Molecular Catalysis B: Enzymatic, 120*, 75–83.
2. Fernandez-Lorente, G., Cabrera, Z., Godoy, C., Fernandez-Lafuente, R., Palomo, J. M., & Guisan, J. M. (2008). Interfacially activated lipases against hydrophobic supports: effect of the support nature on the biocatalytic properties. *Process Biochemistry, 43*, 1061–1067.
3. Hasan-Beikdashti, M., Forootanfar, H., Safiarian, M. S., Ameri, A., Ghahremani, M. H., Khoshayand, M. R., et al. (2012). Optimization of culture conditions for production of lipase by a newly isolated bacterium *Stenotrophomonas maltophilia*. *Journal of the Taiwan Institute of Chemical Engineers, 43*, 670–677.
4. Adlercreutz, P. (2013). Immobilization and application of lipases in organic media. *Chemical Society Reviews, 42*, 6406–6436.
5. Kapoor, M., & Gupta, M. N. (2012). Lipase promiscuity and its biochemical applications. *Process Biochemistry, 47*, 555–569.
6. Manoel, E. A., dos Santos, J. C. S., Freire, D. M. G., Rueda, N., & Fernandez-Lafuente, R. (2015). Immobilization of lipases on hydrophobic supports involves the open form of the enzyme. *Enzyme and Microbial Technology, 71*, 53–57.
7. Zhou, G., Wu, C., Jiang, X., Ma, J., Zhang, H., & Song, H. (2012). Active biocatalysts based on *Candida rugosa* lipase immobilized in vesicular silica. *Process Biochemistry, 47*, 953–959.
8. Fernandez-Lafuente, R. (2010). Lipase from *Thermomyces lanuginosus*: Uses and prospects as an industrial biocatalyst. *Journal of Molecular Catalysis B: Enzymatic, 62*, 197–212.

9. Khoobi, M., Motevalizadeh, S. F., Asadgol, Z., Forootanfarc, H., Shafiee, A., & Faramarzi, M. A. (2014). Synthesis of functionalized polyethylenimine-grafted mesoporous silica spheres and the effect of side arms on lipase immobilization and application. *Biochemical Engineering Journal, 88*, 131–141.
10. Zucca, P., & Sanjust, E. (2014). Inorganic materials as supports for covalent enzyme immobilization: Methods and mechanisms. *Molecules, 19*, 14139–14194.
11. Min, K., & Yoo, Y. J. (2014). Recent progress in nanobiocatalysis for enzyme immobilization and its application. *Biotechnology and Bioprocess Engineering, 19*, 553–567.
12. Stepankova, V., Bidmanova, S., Koudelakova, T., Prokop, Z., Chaloupkova, R., & Damborsky, J. (2013). Strategies for stabilization of enzymes in organic solvents. *ACS Catalysis, 3*, 2823–2836.
13. Hwang, E. T., & Gu, M. B. (2013). Enzyme stabilization by nano/microsized hybrid materials. *Engineering in Life Science, 13*, 49–61.
14. Gupta, A., Dhakate, S. R., Pahwa, M., Sinha, S., Chand, S., & Mathur, R. B. (2013). Geranyl acetate synthesis catalyzed by *Thermomyces lanuginosus* lipase immobilized on electrospun polyacrylonitrile nanofiber membrane. *Process Biochemistry, 48*, 124–132.
15. Cesar, M., Jose, M. P., Gloria, F. L., Jose, M. G., & Roberto, F. L. (2007). Improvement of enzyme activity, stability and selectivity via immobilization techniques. *Enzyme and Microbial Technology, 40*, 1451–1463.
16. Mohamad, N. R., Buanga, N. A., Mahat, N. A., Lok, Y. Y., Huyop, F., Aboul-Eneinc, H. Y., et al. (2015). A facile enzymatic synthesis of geranyl propionate by physically adsorbed *Candida rugosa* lipase onto multi-walled carbon nanotubes. *Enzyme and Microbial Technology, 72*, 49–55.
17. Brady, D., & Jordan, J. (2009). Advances in enzyme immobilization. *Biotechnology Letters, 31*, 1639–1650.
18. Garcia-Galann, C., Berenguer-Murcia, A., Fernandez-Lafuente, R., & Rodrigues, R. C. (2011). Potential of different enzyme immobilization strategies to improve enzyme performance. *Advanced Synthesis and Catalysis, 353*, 2885–2904.
19. Mogharabi, M., Nassiri-Koopaei, N., Bozorgi-Koushalshahi, M., Nafissi-Varcheh, N., Bagherzadeh, G., & Faramarzi, MA. (2012). Immobilization of laccase in alginate-gelatin mixed gel and decolorization of synthetic dyes. Bioinorganic Chemistry and Applications. 1–6. doi:10.1155/2012/823830
20. Dandvate, V., Keharia, H., & Madamwar, D. (2011). Ester synthesis using *Candida rugosa* lipase immobilized on magnetic nanoparticles. *Biocatalysis and Biotransformation, 29*, 37–45.
21. Raghavendra, T., Basak, A., Manocha, L., Shah, A., & Madamwar, D. (2013). Robust nanobioconjugates of *Candida antarctica* lipase B-multiwalled carbon nanotubes: characterization and application for multiple usages in non-aqueous biocatalysis. *Bioresource Technology, 140*, 103–110.
22. Tiwari, A., Terada, D., Yoshikawa, C., & Kobayashi, H. (2010). An enzyme-free highly glucose-specific assay using self-assembled amino benzene boronic acid upon polyelectrolytes electrospun nanofibers-mat. *Talanta, 82*, 1725–1732.
23. Patel, V., Gajera, H., Gupta, A., Manocha, L., & Madamwar, D. (2015). Synthesis of ethyl caprylate in organic media using *Candida rugosa* lipase immobilized on exfoliated graphene oxide: Process parameters and reusability studies. *Biochemical Engineering Journal, 95*, 62–70.
24. Faramarzi, M. A., & Sadighi, A. (2013). Insights into biogenic and chemical production of inorganic nanomaterials and nanostructures. *Advances in Colloid and Interface Science, 189–190*, 1–20.
25. Wang, R. H., Xin, J. H., & Tao, X. M. (2005). UV-blocking property of dumbbell-shaped ZnO crystallites on cotton fabrics. *Inorganic Chemistry, 44*, 3926–3930.
26. Selvarajan, E., Mohanasrinivasan, V., Subathra, C., & George, P. (2015). Immobilization of *β*-galactosidase from *Lactobacillus plantarum* HF571129 on ZnO nanoparticles: characterization and lactose hydrolysis. *Bioprocess and Biosystems Engineering*. doi:10.1007/s00449-015-1407-6.
27. de Lathouder, K. M., van Benthem, D. T. J., Wallin, S. A., Mateo, C., Fernandez- Lafuente, R., Guisan, J. M., et al. (2008). Polyethyleneimine (PEI) functionalized ceramic monoliths as enzyme carriers: preparation and performance. *Journal of Molecular Catalysis B: Enzymatic, 50*, 20–27.
28. Arica, M. Y., & Bayramoglu, G. (2004). Reversible immobilization of tyrosinase onto polyethyleneimine-grafted and Cu(II) chelated poly(HEMA-co-GMA) reactive membranes. *Journal of Molecular Catalysis B: Enzymatic, 27*, 255–265.
29. Badgujar, K. C., & Bhanage, B. M. (2014). Synthesis of geranyl acetate in non-aqueous media using immobilized *Pseudomonas cepacia* lipase on biodegradable polymer film: Kinetic modelling and chain length effect study. *Process Biochemistry, 49*, 1304–1313.
30. Winkler, U. K., & Stuckmann, M. (1979). Glycogen, hyaluronate and some other polysaccharides greatly enhance the formation of exolipase by *Serratia marcescens*. *Journal of Bacteriology, 138*, 663–670.
31. Lowry, O. H., Rosebrough, N. J., Farr, A. L., & Randall, R. J. (1951). Protein measurement with the folin phenol reagent. *Journal of Biological Chemistry, 193*, 265–275.
32. Nicoletti, G., Cipolatti, E. P., Valerio, A., Carbonera, N. T. G., Soares, N. S., Theilacker, E., et al. (2015). Evaluation of different methods for immobilization of *Candida antarctica* lipase B (CalB lipase) in

polyurethane foam and its application in the production of geranyl propionate. *Bioprocess and Biosystems Engineering, 38*, 1739–1748.
33. Barbosa, O., Ortiz, C., Berenguer-Murcia, A., Torres, R., Rodrigues, R. C., & Fernandez-Lafuente, R. (2014). Glutaraldehyde in bio-catalysts design: a useful crosslinker and a versatile tool in enzyme immobilization. *RSC Advances, 14*, 1583–1600.
34. Hussain, Q., Shakeel, A. A., Fahad, A., & Ameer, A. (2011). Immobilization of *Aspergillus oryzae* β-galactosidase on zinc oxide nanoparticles via simple adsorption mechanism. *International Journal of Biological Macromolecules, 49*, 37–43.
35. Xin, J. Y., Chen, L. L., Zhang, Y. X., Zhang, S., & Xia, C. G. (2011). Lipase-catalyzed transesterification of ethyl ferulate with triolein in solvent-free medium. *Food and Bioproducts Processing, 89*, 457–462.
36. Xiong, J., Huang, Y., Zhang, H., & Hou, L. (2014). Lipase-catalyzed transesterification synthesis of geranyl acetate in organic solvents and its kinetics. *Food Science and Technology Research, 20*, 207–216.
37. Dhake, K. P., Karoyo, A. H., Mohamed, M. H., Wilson, L. D., & Bhanage, B. M. (2013). Enzymatic activity studies of *Pseudomonas cepacia* lipase adsorbed onto copolymer supports containing β-cyclodextrin. *Journal of Molecular Catalysis B: Enzymatic, 87*, 105–112.
38. Ozyilmaz, E., Sayin, S., & Yilmaz, M. (2014). Improving catalytic hydrolysis reaction efficiency of sol–gel-encapsulated *Candida rugosa* lipase with magnetic β-cyclodextrin nanoparticles. *Colloids and Surfaces B: Biointerfaces, 113*, 182–189.
39. Yadav, G. D., & Devendran, S. (2012). Lipase catalyzed synthesis of cinnamyl acetate via transesterification in non-aqueous medium. *Process Biochemistry, 47*, 496–502.
40. Zhang, S., Shang, W., Yang, X., Zhang, X., Huang, Y., Zhang, S., et al. (2014). Immobilization of lipase with alginate hydrogel beads and the lipase-catalyzed kinetic resolution of a-phenylethanol. *Journal of Applied Polymer Science, 131*, 4017–4018.
41. Chua, L. S., & Sarmidi, M. R. (2006). Effect of solvent and initial water content on (*R*, *S*)-1-phenylethanol resolution. *Enzyme and Microbial Technology, 38*, 551–556.
42. Yadav, G. D., & Borkar, I. V. (2008). Kinetic modelling of immobilized lipase catalysis in synthesis of n-butyl levulinate. *Industrial and Engineering Chemistry Research, 47*, 3358–3363.
43. Segel, I. H. (1993). *Enzyme kinetics: behavior and analysis of rapid equilibrium and steady-state enzyme systems*. New York: Wiley.
44. Ferraz, L. I. R., Possebom, G., Alvez, E. V., Cansian, R. L., Paroul, N., de Oliveira, D., et al. (2014). Application of home-made lipase in the production of geranyl propionate by esterification of geraniol and propionic acid in solvent-free system. *Biocatal. Agri. Biotechnol.*. doi:10.1016/j.bcab.2014.07.003i.
45. Paroul, N., Grzegozeski, P. L., Chiaradia, V., Treichel, H., Cansian, R. L., Oliveira, J. V., et al. (2010). Production of geranyl propionate by enzymatic esterification of geraniol and propionic acid in solvent-free system. *Journal of Chemical Technology and Biotechnology, 85*, 1636–1641.
46. Rizzi, M., Stylos, P., Riek, A., & Reuss, M. (1992). A kinetic study of immobilized lipase catalyzing the synthesis of iso-amyl acetate by transesterification in n-hexane. *Enzyme and Microbial Technology, 14*, 709–714.
47. Romero, M. D., Calvo, L., Alba, C., & Daneshfar, A. (2007). A kinetic study of the iso-amyl acetate synthesis by immobilized lipase-catalyzed acetylation in n-hexane. *Journal of Biotechnology, 127*, 269–277.
48. Mohamad, N. R., Mahat, N. A., Huyop, F., Aboul-Enein, H. Y., & Wahab, R. A. (2015). Response surface methodological approach for optimizing production of geranyl propionate catalyzed by carbon nanotubes nanobioconjugates. *Biotechnology and Biotechnological Equipment, 29*, 732–739.
49. Jiang, Y., Guo, C., Xia, H., Mahmood, I., Liu, C., & Liu, H. (2009). Magnetic nanoparticles supported ionic liquids for lipase immobilization: enzyme activity in catalyzing esterification. *Journal of Molecular Catalysis B: Enzymatic, 58*, 103–109.
50. Misiunas, A., Talaikyte, Z., Niaura, G., Razumas, V., & Nylander, T. (2008). Thermomyces lanuginosus lipase in the liquid-crystalline phases of aqueous phytantriol: X-ray diffraction and vibrational spectroscopic studies. *Biophysical Chemistry, 134*, 144–156.
51. Mogharabi, M., & Faramarzi, M. A. (2014). Laccase and laccase-mediated systems in the synthesis of organic compounds. *Advanced Synthesis and Catalysis, 356*, 897–927.
52. Kumar, D., Nagar, S., Bhushan, I., Kumar, L., Parshad, R., & Gupta, V. K. (2013). Covalent immobilization of organic solvent tolerant lipase on aluminum oxide pellets and its potential application in esterification reaction. *Journal of Molecular Catalysis B: Enzymatic, 87*, 51–61.
53. Ozturk, T. K., & Kilinc, A. (2010). Immobilization of lipase in organic solvent in the presence of fatty acid additives. *Journal of Molecular Catalysis B: Enzymatic, 67*, 214–218.
54. Salema, J. H., Humeau, C., Chevalot, I., Harscoat-Schiavoa, C., Vanderessec, R., Blancharda, F., et al. (2010). Effect of acyl donor chain length on isoquercitrin acylation and biological activities of corresponding esters. *Process Biochemistry, 45*, 382–389.

55. Mateo, C., Palomo, J. M., Fernandez-Lorente, G., Guisan, J. M., & Fernandez-Lafuente, R. (2007). Improvement of enzyme activity, stability and selectivity via immobilization techniques. *Enzyme and Microbial Technology, 40*, 1451–1463.
56. Cristina, G. G., Berenguer-Murcia, A., Fernandez-Lafuente, R., & Rodrigues, R. C. (2011). Potential of Different Enzyme Immobilization Strategies to Improve Enzyme Performance. *Advanced Synthesis and Catalysis, 353*, 2885–2904.
57. Kasche, V. (1986). Mechanism and yields in enzyme catalysed equilibrium and kinetically controlled synthesis of β-lactam antibiotics, peptides and other condensation products. *Enzyme and Microbial Technology, 8*, 4–16.

Biocatalysis and Agricultural Biotechnology 10 (2017) 182–188

Contents lists available at ScienceDirect

Biocatalysis and Agricultural Biotechnology

journal homepage: www.elsevier.com/locate/bab

Increasing esterification efficiency by double immobilization of lipase-ZnO bioconjugate into sodium bis (2-ethylhexyl) sulfosuccinate (AOT)- reverse micelles and microemulsion based organogels

Vrutika Patel[a], Milind Deshpande[b], Datta Madamwar[a,*]

[a] PG Department of Biosciences, Satellite Campus, Vadtal Road, Sardar Patel University, Bakrol 388 315, Gujarat, India
[b] Department of Physics, Sardar Patel University, Vallabh Vidyanagar, Anand 388 120, Gujarat, India

ARTICLE INFO

Keywords:
Lipase
Double immobilization
AOT-reverse micelles
Microemulsion based organogels
Polyvinyl alcohol
Esterification

ABSTRACT

In the present study, we developed double immobilization system for entrapment of lipase to increase overall esterification efficiency. Lipase has been attached on functionalized ZnO (zinc oxide) particles. Fabricated lipase-ZnO conjugates were entrapped into sodium bis (2-ethylhexyl) sulfosuccinate (AOT)-reverse micelles. AOT-reverse micelles containing lipase-ZnO conjugate were further entrapped into microemulsion based organogels (MBGs), prepared from polyvinyl alcohol. These immobilization systems were characterized by fourier transform infrared spectroscopy (FTIR) and thermal gravimetric analysis (TGA). Double immobilized lipase (i.e. organogels) showed highest stability and esterification activity. Organogel immobilized lipase was therefore further applied for the synthesis of pentyl valerate and ethyl valerate esters in n-hexane. Successfully, 90% of ethyl valerate and 86% of pentyl valerate were synthesized using prepared double immobilization enzyme. Furthermore, the immobilized biocatalyst shows reusability for 10 cycles with meager loss of activity. The present study revealed a promising perspective to overcome the well-known drawbacks of the chemical-catalyzed route.

1. Introduction

Lipases (EC 3.1.1.3) are the enzymes responsible for the hydrolysis of triglycerides to fatty acids and glycerol (Faber, 2011; Patel and Madamwar, 2015; Lozano, 2010) and are attractive in organic chemistry because of their enantioselectivity, regioselectivity and stereoselectivity. The industrial applications of lipase include fine chemical synthesis, pharmaceutical chemistry, food and dairy industries, also biodiesel production (Faber, 2011; Patel and Madamwar, 2015; Ribeiro et al., 2010; Verma et al., 2013). Despite of all the benefits, the main drawback in carrying out the reaction in apolar organic solvents having tendency to strip away water molecules from the enzyme surface especially from the active site leaving the enzyme inactive (Raghavendra et al., 2014).

To improve lipase activity and stability, many approaches have been explored such as genetic engineering, protein engineering, medium engineering, immobilization and/or process alterations (Hara et al., 2009; Shaotao et al., 2010). “One of the approaches is to use nanostructured materials for enzymatic immobilization processes, although nanoparticles may have some drawbacks, including enzyme exposure to external interfaces, which implies sensitivity to proteolysis etc.” ZnO nanoparticles have been investigated mostly for antibacterial and UV blocking function and in cosmetic and pharmaceutical industries (Wang et al., 2005; Selvarajan et al., 2015). Zn compounds have also been currently listed as GRAS, i.e. generally regarded as safe by the US Food and Drug Administration (21CFRI82.8991). However, ZnO nanoparticles do require some additional functional groups for attachment. There are many reports on the protective effect of polyethyleneimine (PEI), a water soluble cationic polymer with large number of primary amino groups, on the activity of enzymes such as lipases especially in organic media (Khoobi et al., 2014; Garcia-Galann et al., 2011; Patel et al., 2016). PEI grafting onto inert, inorganic supports and then cross-linking with bi-functional agents such as glutaraldehyde (GLU), hexamethylene diisocyanate (HMDI) is an extensively used approach for immobilization of various enzymes, such as lipase (Khoobi et al., 2014; Garcia-Galann et al., 2011; Patel et al., 2016), β-galactosidase (Selvarajan et al., 2015,) and tyrosinase (Arica and Bayramoglu, 2004).

Recently the enzyme-catalyzed biotransformation in non/micro-aqueous solvents has become the exciting field of enzymology (Hara et al., 2009; Klibanov, 2001). Among low water media, water-in-oil (w/o) microemulsions have been widely reviewed as tool for achieving

* Corresponding author.
E-mail addresses: vrutikaptl_19@yahoo.com (V. Patel), datta_madamwar@yahoo.com (D. Madamwar).

http://dx.doi.org/10.1016/j.bcab.2017.03.009
Received 12 September 2016; Received in revised form 9 March 2017; Accepted 9 March 2017
Available online 14 March 2017
1878-8181/

various enzymatic reactions in hydrophobic environment (Biasutti et al., 2008; Pavlidis et al., 2009; Zanetteb et al., 2014). Reverse micelles form thermodynamically stable and optically transparent liquid medium with large interfacial area that provides an aqueous domain where hydrophilic enzymes can be located, an interface where the active site of enzymes can be anchored, and a non-polar organic phase where the hydrophobic substrates or products may be dissolved (Malik and Wani, 2012; Itabaiana et al., 2014; Zoumpanioti et al., 2010a, 2010b). However, practical applications of w/o microemulsions may be limited by the necessity of separating the surfactant from the reaction products. Nevertheless, some microemulsions can be transformed to gels by adding a gelling agent, usually a biopolymer such as gelatin, agar, or a cellulose derivative (Raghavendra et al., 2010; Dandavate and Madamwar, 2007; Wu et al., 2011) to form so-called microemulsion-based organogels (MBGs). MBGs are rigid and stable in various non-polar or relatively polar organic solvents and therefore can be used for several biotransformation in organic media, such as hydrolysis, esterification, and other syntheses (Dandavate and Madamwar, 2007; Wu et al., 2011). The network of the gel is considered to contain a bi-continuous phase that may coexist with conventional w/o microemulsion droplets containing the encapsulated enzyme.

The entrapment of lipases into a film proves to be a simple and efficient method for immobilization as they provide a high surface area for interaction of enzyme with substrate followed by ease of separation and greater enzyme stability with fewer chances of leaching (Wu et al., 2011; Vlierberghe et al., 2011). Eco-friendly polymers have gained a special importance for enzyme immobilization, drug delivery systems and tissue engineering due to their biodegradable nature (Badgujar et al., 2013; Dhake et al., 2011; Grande and Carvalho, 2011). Polyvinyl Alcohol (PVA) is widely known for its biodegradable, biocompatible and eco-friendly biopolymer properties (Grande and Carvalho, 2011). PVA has impressive features like excellent film formation, high interfacial adhesion, flexibility, and emulsification, high tensile strength, non-toxic nature, biodegradable, stabilization of blend and essentially resistant to organic solvent which makes them more ideal for lipase immobilization (Mandal et al., 2014; Hasan-Beikdashti et al., 2012). Dhake et al., 2011 reported immobilization of commercially *Rhizopus oryzae* lipase on a film using a blend of hydroxypropyl methyl cellulose (HPMC) and PVA. Ivaldo developed an efficient catalytic system for immobilizing *Candida antarctica* lipase B (CaLB) on an MBG matrix (MBG_{CaLB}) formed with (hydroxypropyl)methyl cellulose as a gelling agent for synthesis of monoacylglyceride (MAG) under both batch and continuous-flow conditions (Zoumpanioti et al., 2010b). Mandal et al., 2014 reported the development of cationic water-in-oil (w/o) microemulsion doped with newly designed nanocomposite comprising of gold nanoparticle (GNP) decorated single walled carbon nanotube (SWNT).

The present study focuses on the double immobilization of lipase-ZnO conjugate into AOT-reverse micelles, followed by entrapment into gelling matrix of PVA. ZnO nanoparticles were functionalized using PEI and cross linker GLU in order to produce functional groups for enzyme immobilization. Prepared lipase-ZnO bioconjugates were immobilized into AOT-reverse micelles, and these micelles were entrapped into gelling matrix of PVA. Thus in all three different immobilization systems viz: ZnO-E, ZnO-E@RM and ZnO-E-RM@PVA were prepared. Various characterization experiments were carried out which showed the improvement in pH, thermal and storage stability of enzyme after entrapment. In addition, the developed immobilization method for PVA films was further used for biocatalytic transformation of industrially important esters in n-hexane.

2. Materials and methods

2.1. Chemicals and the enzyme

Zinc oxide (ZnO) nanoparticles were synthesized according to the protocol described by Soni et al. (2011). *Candida rugosa* lipase with activity of 875U/g, (3-aminopropyl) triethoxysilane (APTES), polyethyleneimine (PEI), glutraldehyde (GLU) and 4-nitrophenyl palmitate (*p*-NPP) were obtained from Sigma-Aldrich, Germany. Pentyl valerate (≥98%), ethyl valerate (≥98%), 1-pentanol (≥97%) and valeric acid (≥97%) were purchased from Fluka-Chemica (Germany). Ethanol and n-hexane were procured from Spectrochem, India. All organic solvents used were of GC/HPLC grade.

2.2. Fabrication of lipase on ZnO functionalized with PEI

Fabrication of lipase on functionalized ZnO nanoparticles were carried out in two steps. Firstly, Branched polyethyleneimine (1.5 mL) was suspended in a solution containing 10% APTES in ethanol. To this mixture 10 mg of ZnO nanoparticles were added and stirred vigorously to react for 24 h. The obtained composite was purified by centrifugation (10000 × *g* for 15 min) and repeatedly washed with ethanol and milliQ in order to remove excess silane and PEI. Secondly, 10 mg of ZnO-PEI was incubated in 10 mL phosphate buffer solution (50 mM, pH 7.0) containing 1% (w/v) GLU and allowed to react for 10 min. Then, 1 mL of lipase solution (50 mg/mL) was incorporated into the mixture and stirred for overnight. The mixture was centrifuged and washed with phosphate buffer (50 mM) in order to eliminate unbound lipase. The resultant bioconjugant was dried under vacuum (37 °C for 1 h) and characterized as detailed in Section 2.4. The amount of immobilized lipase adsorbed on nanoparticles was determined by measuring the initial concentration and its final concentration in supernatant after immobilization using lipase activity.

2.3. Entrapment of lipase loaded ZnO into AOT/Iso-octane microemulsion and PVA gels

(i) Preparing microemulsions: In 10 mL screw cap vials, 0.1 M sodium bis (2-ethylhexyl) sulfosuccinate (AOT) with $W_o = 60$, 2 mL isooctane and 50 mM phosphate buffer (pH-8.0) were taken to attain the corresponding z([co-surfactant]/[surfactant]) and W_o([water]/[surfactant]) value, respectively. The mixture was vigorously vortexed for 5 min to obtain a clear homogeneous solution of 0.1 M AOT/iso-octane/buffer reverse micelle. Following the similar protocol, suspensions of previously prepared ZnO-E nanocomposite (108 μL) was added to AOT reverse micellar mixture instead of phosphate buffer to obtain the corresponding W_o value. The enzyme entrapped into reverse micelles was designated as ZnO-E@RM. (ii) Preparing gelling matrix: The MBGs were prepared by introducing AOT microemulsion containing ZnO-E to a second solution of 2% PVA dissolved in water. Typically 2 mL of prepared microemulsions was introduced into 2% polymer solution and then moderately stirred to obtain homogenous mixture. Finally, immobilized matrix with entrapped lipase was carefully poured in a Teflon dish and allowed to dry at 40–45 °C for 40 h. A thin film of immobilized lipase was formed, which was then cut into small pieces (1 × 1 cm with 110 ± 10 μm thickness) and stored at 4 °C. Microemulsions prepared with AOT-reverse micelles were designated as ZnO-E-RM@PVA and further characterized as detailed in Section 2.4.

2.4. Lipase activity, Protein content and Immobilization Yield (%) determination

The catalytic activities of free as well as immobilized lipases were assayed using *p*-nitrophenyl palmitate (*p*-NPP) as substrate (Wrinkler and Stuckmaan). The reaction solution was prepared by addition of free or immobilized lipase to p-NPP solution (0.4 mM in 100 mM phosphate

buffer pH 8) and incubated for 10 min at 40 °C, 150 rpm followed by measuring absorbance at 410 nm using UV–Vis spectrophotometer. One unit of enzyme activity is defined as the amount of enzyme that liberates p-nitrophenol at the rate of 1 μmol per min under specified conditions.

The amount of protein was determined by Folin-Lowry method at 595 nm (Lowry et al.) using bovine serum albumin as standard. Percentage Protein loading, specific activity and activity yield was determined by following equations:

% protein loading = amount of protein immobilized ÷ initial amount of protein loaded × 100% activity yield = immobilized lipase activity ÷ - crude lipase activity × 100.

Specific activity = lipase activity ÷ amount of protein used.

2.5. Characterization of immobilized enzymes

2.5.1. Effect of pH on enzyme stability

The effect of pH on enzyme stability was determined after introduction of free as well as immobilized lipases in buffers of citrate (100 mM, pH 5–6), phosphate (100 mM, pH 7–8) and Tris-HCl (100 mM, pH 9–10) for 1 h at 37 °C followed by measuring the relative activity of enzyme. Every hour 1 mL sample was pipette out and then assayed for residual activity, which was expressed as percentage of initial activity (taken as 100%). All the experiments were repeated thrice at each operating condition and the relative standard deviation was within ± 2%.

2.5.2. Effect of temperature on enzyme stability

The thermal stability of free or immobilized lipases was determined by incubating the enzyme in water bath for 1 h at the temperature ranging from 20 to 50 °C followed by measuring the relative activity of enzyme. Every hour 1 mL sample was pipette out and then assayed for residual activity, which was expressed as percentage of initial activity (taken as 100%). All the experiments were repeated thrice at each operating condition and the relative standard deviation was within ± 2%.

2.5.3. Effect of storage on enzyme stability

The storage stability was determined by relative activity measurements of free and immobilized lipase for 20 days at 4 °C. Every hour 1 mL sample was pipette out and then assayed for residual activity, which was expressed as percentage of initial activity (taken as 100%). All the experiments were repeated thrice at each operating condition and the relative standard deviation was within ± 2%.

2.6. Biocatalytic transformation of ethyl and pentyl valerate by free and immobilized lipase

Synthesis of ethyl and pentyl valerate as industrially important esters was studied using free and lipase immobilized on ZnO-E-RM@PVA in n-hexane. The reaction was initiated by addition of free and immobilized lipase in solution consisting of n-hexane (2 mL), with acid/alcohol molar ratios of (2:1. 1:1, 1:2, 1:3, 1:4 and 1:5) followed by incubation at different temperatures (30, 37, 40 and 50 °C), 150 rpm for 0, 2, 4, 6, 8 and 12 h. In parallel, the reaction comprise of ZnO-RM@PVA without lipase was designed for control. The amount of ester produced was analyzed by Gas chromatograph. (PerkinElmer, Model Clarus 500, Germany) equipped with a flame-ionization detector (FID). The column was 30 m Rtx-® – 20 (Crossbond 80% dimethyl-20% diphenyl polysiloxane) capillary column. The temperature of injector and detector were maintained at 250 °C. The carrier gas served as nitrogen with the split flow rate of 90 mL/min. The column temperature was programmed to increase from 40 to 120 °C at the rate of 3 °C/min, from 120 to 200 °C at the rate of 10 °C/min and from 200 to 220 °C at the rate of 2 °C/min. All the aforementioned experiments were done in triplicates and the mean of data obtained was reported. In order to investigate reusability, the immobilized biocatalyst was recovered from the reaction mixture using centrifugation, followed by washing with anhydrous n-hexane after each run. Further immobilized lipase matrix was dried for overnight and implemented with fresh substrates for determination of the esterification percentage. All the experiments were repeated thrice at each operating condition and the relative standard deviation was within ± 2%.

2.7. Characterization study

The chemical modifications was studied by Fourier transform infrared (FT-IR) spectroscopic analysis using Spectrochem GX-IR (Perkin Elmer, USA) in order to confirm binding of lipase on nanoparticles. The vacuum dried samples were mixed with IR grade KBr and finely ground to form homogenous powder under dry conditions for preventing adsorption of water vapour. This mixture was made into pellet and placed inside vacuum concentrator for ensuring total dry conditions. The dried pellets were then fixed in sample holder and analysis was performed in the mid IR region of 400-4000 cm^{-1}. The measurement of mass change during the process was analyzed using TGA/DTA-7200 thermal analyser (Seiko SII-EXSTAR). The system was employed with PtRh furnace capable of operating from 25 °C to 1500 °C, the temperature being measured using type R thermocouple. The measurements are cominducted under controlled atmosphere as the system is vacuum tight. TGA-DSC analysis was performed using 10 mg of samples in alumina crucible without lid, in argon atmosphere. The temperature range was varied from 30 to 1000 °C and with heating rate of 20 °C/min.

2.8. Kinetic parameters

The kinetic parameters for both free and immobilized lipase (ZnO-E-RM@PVA) system were determined by varying substrate molar ratio concentration. The effect of concentrations of valeric acid and pentanol the initial rate of pentyl valerate formation were studied using free and immobilized lipase keeping the initial concentration of one of the substrates, that is, pentanol/valeric acid constant (1 mM), and varying the initial concentration of the other (1 mM, 2 mM, 3 mM, 4 mM, and 5 mM). One unit of enzyme activity was defined as amount of lipase required for synthesis of 1 μmole of pentyl valerate. The K_m and V_{max} values were obtained from Lineweaver–Burk plots.

3. Results

3.1. Characterization studies

3.1.1. Physical appearance of MBGs

The prepared MBGs films were uniform and flexible in nature, having slight transparency with white coloration (Fig. 1a). While lipase entrapped MBGs exhibited somewhat loss in transparency because of nanocomposite (ZnO-E) (Fig. 1b). The control MBGs (without lipase) express thickness values in between 50–65 μm; while the MBGs containing lipase presented thickness values in between 65 and 70 μm (using micrometer screw gauge).

3.1.2. Fourier transform infrared spectroscopy (FTIR)

Fourier transform infrared spectroscopy (FTIR) was performed in order to study the alterations in surface functional groups following functionalization. Although the infrared (IR) spectrum is characteristic of the entire molecule, it is true that certain groups of atom give rise to bands at or near the same frequency regardless of the structure of the rest of the molecule. The FTIR spectral overlay for all the system studied is shown in Fig. 2. FTIR absorption spectrum of lipase (Fig. 2(c)) generally shows three major bands caused by peptide group vibrations in the range of 1800–1300 cm^{-1}. Free and immobilized lipase illustrates a characteristic band of amide II with the maximum of

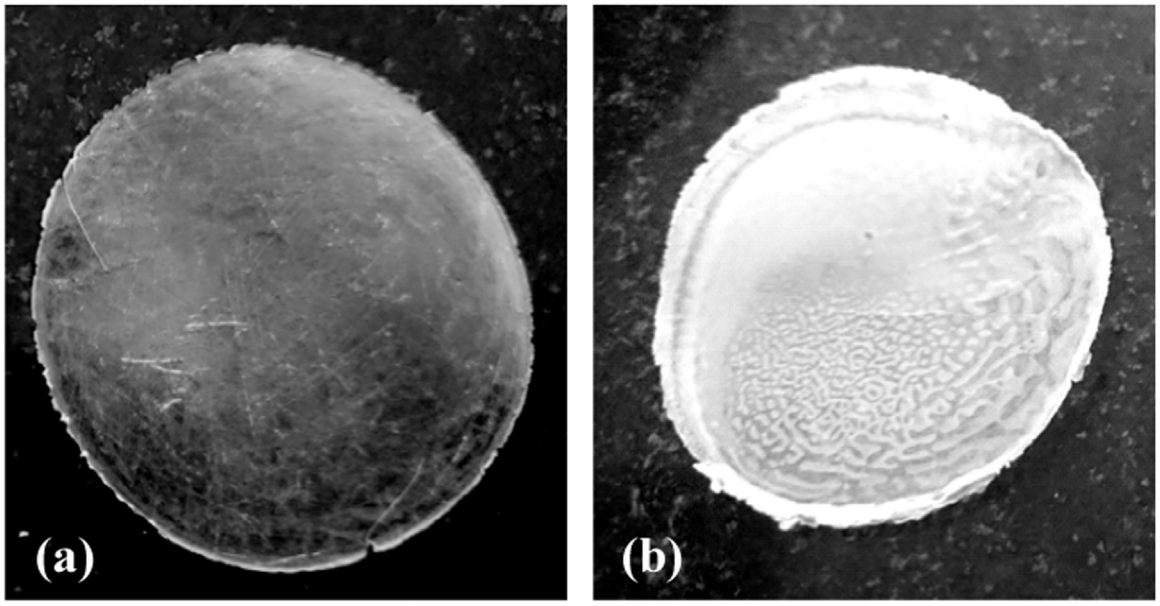

Fig. 1. Physical appearance of prepared PVA gels. (a) Control PVA gel without lipase showing transparency and has thickness of 50–65 μm. (b) Lipase immobilized PVA gel exhibiting somewhat loss in transparency because of nanocomposite (ZnO-E) and showed thickness values in between 65–70 μm.

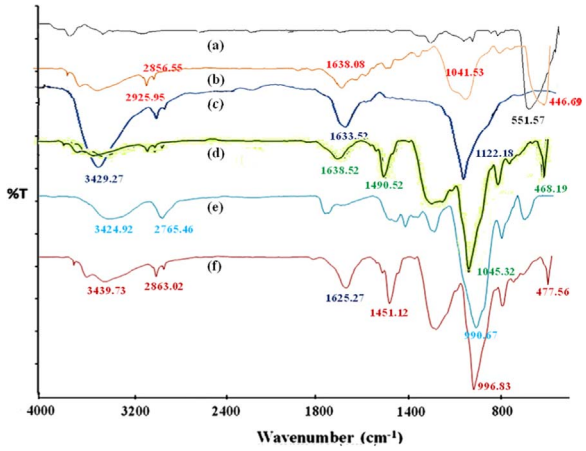

Fig. 2. FTIR spectrum for free as well as all the prepared immobilized lipase systems. (a) pristine ZnO, (b) ZnO-E, (c) Free lipase, (d) ZnO-E@RM, (e) PVA control and (f) ZnO-E-RM@PVA.

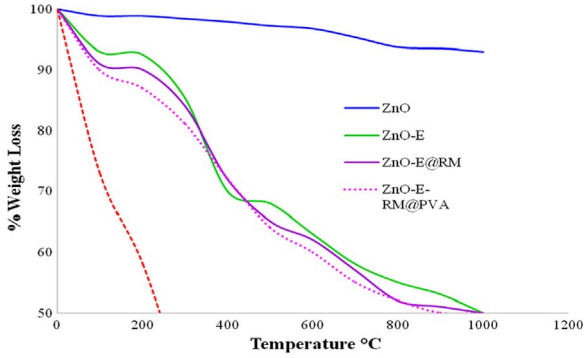

Fig. 3. TGA curves showing % weight loss for the respective free as well as immobilized lipase system at temperature ranging from 0 to 1000 °C.

1490 cm^{-1} due to N-H bending with contribution of C-N stretching vibrations. According to spectra (f), peak at 1451 cm^{-1} indicated C-N stretching of amide bonds hence, showing presence of amide bond formation. This was further supported by peak at 1243 cm^{-1} which can be attributed to the interaction of N-H bending and C-N stretching of amide bond. Furthermore, it is observed that these amide regions are absent in the FT-IR spectrum of ZnO and PVA control (Fig. 2(a) and (e)), respectively addressing strong presence of amide bonds confirming the existence of lipase. Looking at the spectra, it was observed that the immobilization of lipase onto ZnO nanoparticles using reverse micelles as well as organogels proceeded via covalent bonding and not merely physical deposition or adsorption.

3.1.3. Thermal gravimetric analysis (TGA)

The successful functionalization was also reflected in TGA curves performed using *Mettler Toledo*. Fig. 3 shows TGA curves in nitrogen upto 700 °C at heating rate of 20 °C/min. It can be observed from the curve that pristine ZnO showed very small weight loss below 200 °C, but significant weight loss of 2.8% was attained at 550 °C. However, for free lipase gradual decrease in weight loss was observed with increase in the temperature above 100 °C. The gradual decrease in weight is much obvious due to loss of bound water molecule. For all the immobilized enzymes curves (i.e. ZnO-E, ZnO-E@RM and ZnO-E-RM@PVA), nearly 10% of weight loss was observed at around 100 °C and steeply decreasing thereafter with much faster rate above 400 °C. This attributes to thermo-decomposition of lipase indicating successful enzyme immobilization.

3.2. pH, temperature and storage stability

3.2.1. Effect of pH on enzyme stability

Enzyme is very sensitive to pH changes due to alteration in the ionization states of the enzyme and thus affects its selectivity and activity (Patil et al., 2010; Hasan et al., 2015). The effect of pH on relative activity of the free and immobilized lipase using various immobilization matrix as enzyme supports was determined within the range of 5–10 at 37 °C and the results are graphically presented in Fig. 4. The obtained results demonstrate that free as well as immobilized lipase preparations exhibit typical bell-shaped curves with maximum relative activity at pH 8. However, immobilized lipase resulted in maintaining excellent adaptability at a wider pH range with higher relative activity. The lipase entrapped into polymer ZnO-E-RM@PVA represented a higher relative activity of 89% at pH 8 than that of ZnO-E@RM and ZnO-E with 80% and 75%, respectively. Free lipase retained 68% of its initial activity under same condition. The quantized increase in the pH stability profile for all the immobilized lipase preparations

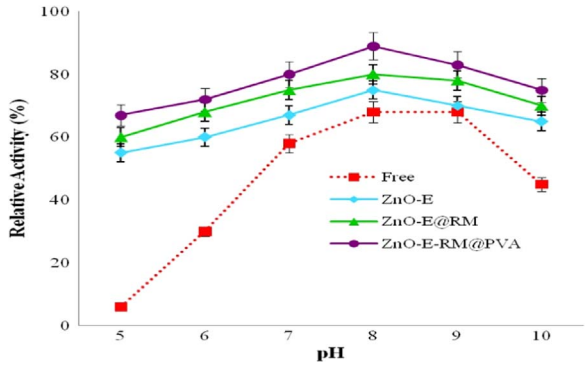

Fig. 4. pH stability curves for free and immobilized lipase preparations. The effect of pH on enzyme stability was determined using different buffers of citrate (100 mM, pH 5–6), phosphate (100 mM, pH 7–8) and Tris-HCl (100 mM, pH 9–10) for 1 h at 37 °C followed by measuring the relative activity of enzyme.

(viz: ZnO-E-RM@PVA > ZnO-E@RM > ZnO-E) can be argued by two reasons. Firstly, immobilization into reverse micelles supplied much more stable biocatalyst against pH which might be ascribed to the restriction in conformational changes following pH change (Raghavendra et al., 2010; Dandavate and Madamwar, 2007). Secondly, the entrapment of such stable enzyme into hydrophilic polymer produces a suitable charge difference by enhancing the electrostatic interaction between enzyme and carrier (Itabaiana et al., 2014, Dandavate and Madamwar, 2007).

3.2.2. Effect of temperature on enzyme stability

Utilization of enzymes in processes often encounters the problem of thermal inactivation. At higher temperature, enzymes undergo partial unfolding by heat-induced destruction of non-covalent interactions (Hwang and Gu, 2013; Garcia-Galann et al., 2011; Sheldon, 2007). In order to assess the thermal stability profile we have measured relative activity of free as well as all the forms of immobilized enzyme by pre-incubating at different temperatures (20–60 °C) for 1 h. The results of temperature stability revealed that lipase entrapped in ZnO-E-RM@PVA matrix is much better than that of the corresponding free enzyme (Fig. 5). ZnO-E-RM@PVA exhibited maximum relative activity of 97% within 40–50 °C higher in comparison to the free lipase which was only 60% under same condition (Fig. 5). However, free enzyme actually decays with temperature at faster rate as compared to immobilized enzyme. Furthermore, the comparison of the relative activities for ZnO-E@RM (85%) and ZnO-E (80%) at higher temperature indicates the better diffusion of substrate and limitation of enzymatic movement after immobilization on applied support.

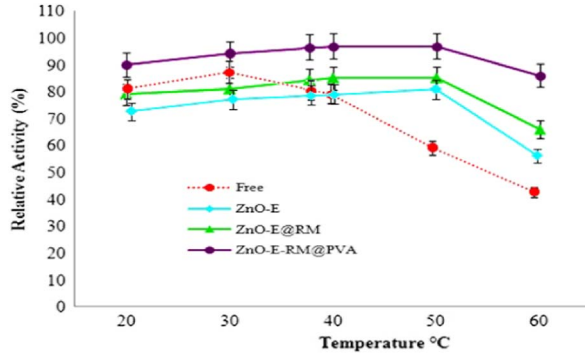

Fig. 5. Temperature stability for free and immobilized lipase preparations. The thermal stability of free or immobilized lipases was determined by incubating the enzyme in water bath for 1 h at the temperature ranging from 20 to 50 °C followed by measuring the relative activity of enzyme.

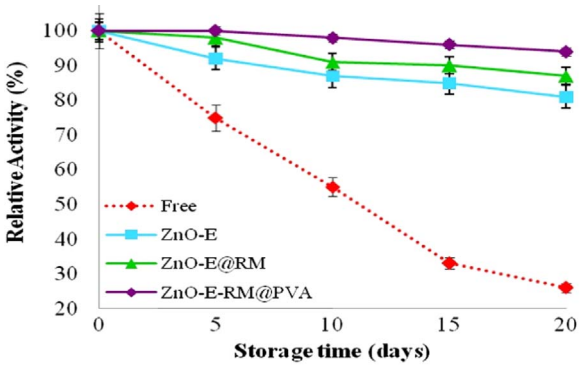

Fig. 6. Storage stability curves for free and immobilized lipase preparations. The storage stability was determined by relative activity measurements of free and immobilized lipase for 15 days at 4 °C.

3.2.3. Effect of storage on enzyme stability

Storage (non-operational) stability of an immobilized enzyme without appreciable loss of enzyme activity is important for the economic viability of a biosynthetic process (Sheldon, 2007). The storage stability of the free and immobilized lipases was investigated for 20 days in phosphate buffers (pH 8) stored at 4 °C. The evaluation of the storage stability for entrapped lipase demonstrated that it increases in the range: ZnO-E-RM@PVA > ZnO-E@RM > ZnO-E > Free lipase. The study revealed that only 26% of the initial activity of free lipase remained after 20 days of incubation at 4 °C, whereas ZnO-E, ZnO-E@RM and ZnO-E-RM@PVA retained 81%, 87% and 94% of their initial activities, respectively (Fig. 6). The study clearly demonstrates that the prepared double immobilization system (i.e. ZnO-E-RM@PVA) exhibits good stability with no significant decrease in activity during storage periods of 20 days at 4 °C. Ample of literatures have stated that enzyme which are entrapped into polymers consist of higher stabilities are most resistant to denaturation effect of organic solvent in biotransformation (Dandavate and Madamwar, 2007; Badgujar et al., 2013; Dhake et al., 2011; Dave and Madamwar, 2006).

3.3. Possible reasons for enhanced stability for ZNO-E-RM@PVA immobilization system

There are three main possible reasons for enhanced lipase activity in prepared double immobilization system (ZnO-E-RM@PVA). (i) In the case of ZnO-E, the spacer arm of glutraldehyde assisted the support to covalently attach lipase via surface residues that boost enzyme loading on the surface of ZnO-E (Garcia-Galann et al., 2011). (ii) The confinement of ZnO-E inside the water pool of AOT-reverse micelles led to the formation of larger sized reverse micelle with higher interfacial area. This augmented interfacial area possibly helped in smooth occupancy of lipase and high local concentration of enzyme and substrate resulting in remarkable improvement in lipase activity. Also the enhanced hydrophobic environment due to incorporation of ZnO-E at the interface might lead to the unfolding of the lid (Asp–Hys–Ser) and provided accessibility of the substrate to the active region of lipase (Mandal et al., 2014; Ghosh et al., 2012; Maiti et al., 2010; Adlercreutz, 2013). (iii) Due to entrapment into microemulsion based organogels, limitation of enzymatic movement after immobilization on support together with better substrate diffusion at a higher temperature improves activity of immobilized lipase (Raghavendra et al., 2010; Dandavate and Madamwar, 2007; Patel et al., 2014).

Thus, the developed double immobilization system of lipase was further used for biocatalytic transformation under organic solvents. The MBG consists of a polymer network in which the enzyme-containing microemulsion is entrapped and is actually a semi solid catalyst was preferred for further study rather than working directly with reversed micelles. This decision was based on the advantages presented by

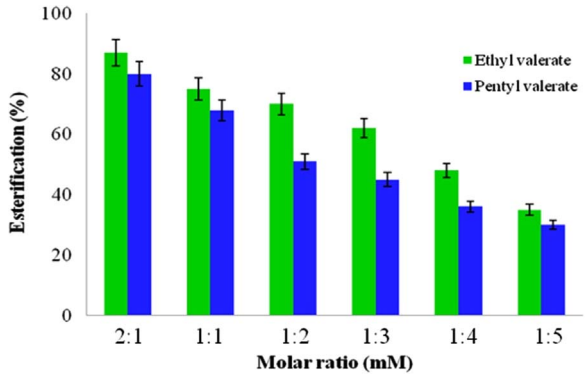

Fig. 7. Influence of acid/alcohol concentration on the efficiency of ester synthesis for lipase immobilized into PVA gel. Reaction conditions: n-hexane (2 mL), 100 mM 1:1 valeric acid/ethanol or valeric acid/1-pentanol separately (acid/alcohol molar ratios of 2:1. 1:1, 1:2, 1:3, 1:4 and 1:5) at 40 °C, 150 rpm.

heterogeneous catalysis over homogeneous one, such as reuse of the catalyst and easier product isolation.

3.4. Biocatalytic transformation of esters

Synthesis of flavors and fragrance esters using immobilized lipase has received immense attention during the last decades. The study was carried out in order to compare potential of free as well as immobilized lipase (ZnO-E-RM@PVA) for synthesis of esters in organic solvents. The results obtained from optimization revealed that the molar ratio of 2:1 for acid/alcohol at 40 °C temperature were the most suitable conditions to get enhanced lipase activity assisted by lipase immobilized on ZnO-E-RM@PVA (Fig. 7). Further it was found that increasing alcohol concentration (than that of optimized) leads to decrease in esterification efficiency. This can be attributed to inhibitory effect of higher alcohol concentration on lipase activity which is illustrated in Fig. 7 (Patel and Madamwar, 2015; Khoobi et al., 2014). Similar inhibitory effects of alcohol on ester synthesis are also reported in various literatures (Patel and Madamwar, 2015; Khoobi et al., 2014; Badgujar and Bhanage, 2014). However, as shown in Fig. 8, using optimized conditions 90% of ethyl valerate and 86% of pentyl valerate was obtained after 8 h of reaction at 40 °C while free lipase attain only 50% of ester synthesis under the same condition. The similar results for enhancing lipase activity after immobilization into polymer was reported by Dhake et al. (2011) showing 2.6-fold increase in synthesis of butyl octanoate using *Pseudomoas cepecia* lipase immobilized into polyurethane copolymers. Dave and Madamwar (2006) immobilized *Candida rugosa* lipase in the polymer of polyvinyl alcohol (PVA), alginate and boric acid. The performance of the immobilized biocatalyst

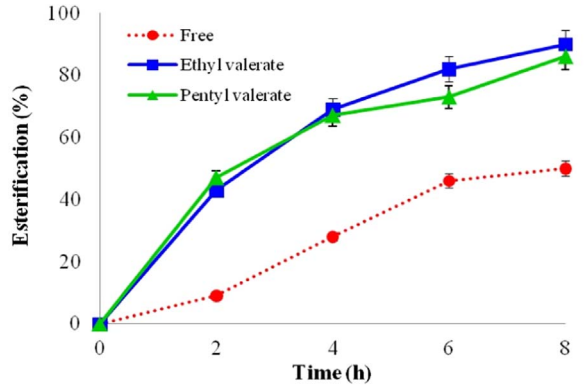

Fig. 8. Time course for the synthesis of ethyl and pentyl valerate by free as well as immobilized lipase (ZnO-E-RM@PVA) using n-hexane as a reaction medium. Reaction conditions: 2:1 acid/alcohol molar ratio, 3 mL n-hexane, pH 8, temperature 40 °C, 150 rpm.

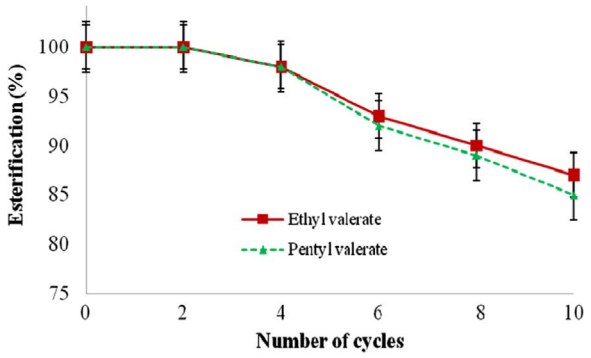

Fig. 9. Reusability study for the synthesis of short chain esters using ZnO-E-RM@PVA entrapment lipase at pH 8 and 40 °C. Reaction conditions: Reaction conditions: 2:1 acid/alcohol molar ratio, 3 mL n-hexane, pH 8, temperature 40 °C, 150 rpm.

was evaluated for the synthesis of ethyl hexanoate in isooctane where the thermal stability of the enzyme increased ten times upon immobilization (Jiang et al., 2009). Itabaiana et al. (2014) reported 99% conversion of MAG using *Candida antarctica* lipase B (CaLB) immobilized cationic reverse micelles into MBG matrix formed with HPMC. Badgujar et al. showed 99% of geranyl acetate synthesis using lipase immobilized into biodegradable polymer blends of HPMC: PVA (Badgujar and Bhanage, 2014).

The results obtained from reusability experiments of the immobilized lipase (ZnO-E-RM@PVA) in n-hexane showed mild decrease in the activity of lipase after 4 cycles, thereafter a gradual decrease in activity was observed upto 10 cycles. However, the immobilized enzyme retained 87% and 85% of its initial activity for synthesis of ethyl valerate and pentyl valerate, respectively after 10 catalytic rounds (Fig. 9). The decrease in catalytic activity may be ascribed to (i) the unfavorable effect of water (released as byproduct during esterification reaction) (Stergiou et al., 2013) and (ii) prolonged exposure to the polar organic solvents (Debnath et al., 2006).

3.5. Reaction kinetics

The study of reaction kinetics was studied for effect of varying substrate concentration for pentyl valerate synthesis. The effect of concentration of pentanol and valeric acid on the initial rate of pentyl valerate synthesis were studied using free and organogels immobilized lipase keeping the initial concentration (1 mM) of one of the substrate, that is pentanol/valeric acid constant, and varying the initial concentration of the other (1 mM, 2 mM, 3 mM, 4 mM and 5 mM). Present results obtained from K_m values suggested that both the forms of enzyme displayed higher affinity towards pentanol $Km_{(free)} = 13.3$ mM and $Km_{(immobilized)} = 7.9$ mM than towards valeric acid $Km_{(free)} = 14.3$ mM and $Km_{(immobilized)} = 7.35$ mM. This indicated that immobilized enzyme showed higher affinity towards both substrates than that of free one. The changes in parameters suggest that immobilization of lipase resulted in an increased affinity for the substrate by improving accessibility of the active site (Das and Chaudhuri, 2000).

4. Conclusion

In particular, a versatile method for double immobilization of *Candida rugosa* lipase was developed successfully on microemulsion based organogels and was well characterized using FTIR and TGA. Thermal and pH stabilities of lipase immobilized on ZnO-E-RM-@PVA were improved in comparison with those of free and other modified analogues. In addition, esterification experiments revealed that ZnO-E-RM@PVA was the best immobilization system for the synthesis of ethyl and pentyl valerate compared with that of free lipase. Reusability study revealed meager loss of initial lipase activity even after 10 cycles. In

nutshell, the facile synthesis procedure is easy to implement and enables the selective separation of enzymes from reaction mixtures.

Acknowledgements

The authors would like to acknowledge University Grants Commission (UGC) grant no. F. 42–167/2013 (SR), New Delhi for financial support. Authors would also like to acknowledge (a) SICART, Vallabh Vidyanagar for FTIR facility and (b) Department of Physics for extending their TGA facility.

References

Arica, M.Y., Bayramoglu, G., 2004. Reversible immobilization of tyrosinase onto polyethyleneimine-grafted and Cu(II) chelated poly(HEMA-co-GMA) reactive membranes. J. Mol. Catal. B: Enzym. 27, 255–265.

Badgujar, K.C., Bhanage, B.M., 2014. Synthesis of geranyl acetate in non-aqueous media using immobilized *Pseudomonas cepacia* lipase on biodegradable polymer film: Kinetic modelling and chain length effect study. Process Biochem. 49, 1304–1313.

Badgujar, K.C., Dhake, K.P., Bhanage, B.M., 2013. Immobilization of *Candida cylindracea* lipase on poly lactic acid, polyvinyl alcohol and chitosan based ternary blend film: characterization, activity, stability and its application for N-acylation reactions. Process Biochem. 48, 1335–1347.

Biasutti, M.A., Abuin, E.B., Silber, J.J., Correa, N.M., Lissi, E.A., 2008. Kinetics of reactions catalyzed by enzymes in solutions of surfactants. Adv. Coll. Interface Sci. 136, 1–24.

Dandavate, V., Madamwar, D., 2007. Novel approach for the synthesis of ethyl isovalerate using surfactant coated *Candida rugosa* lipase immobilized in microemulsion based organogels. Enzym. Microb. Technol. 41 (3), 265–270.

Das, P.K., Chaudhuri, A., 2000. On the origin of unchanged lipase activity profile in cationic reverse micelles. Langmuir 16, 76.

Dave, R., Madamwar, D., 2006. Esterification in organic solvents by lipase immobilized in polymer of PVA–alginate–boric acid. Process Biochem. 41 (4), 951–955.

Debnath, S., Dasgupta, A., Mitra, R.N., Das, P.K., 2006. Effect of counter ions on the activity of lipase in cationic water-in-oil microemulsions. Langmuir 22, 8732.

Dhake, K.P., Tambade, P.J., Qureshi, Z.S., Singhal, R.S., Bhanage, B.M., 2011. HPMC-PVA film immobilized *Rhizopus oryzae* lipase as a biocatalyst for transesterification. ACS Catal. 1, 316–322.

Faber, K., 2011. Biotransformations in Organic Chemistry, 6th ed. Springer Berlin Heidelberg.

Garcia-Galann, C., Berenguer-Murcia, A., Fernandez-Lafuente, R., Rodrigues, R.C., 2011. Potential of different enzyme immobilization strategies to improve enzyme performance. Adv. Synth. Catal. 353, 2885–2904.

Ghosh, M., Maiti, S., Dutta, S., Das, D., Das, P.K., 2012. Covalently functionalized single-walled carbon nanotubes at reverse micellar interface: a strategy to improve lipase activity. Langmuir 28, 1715.

Grande, R., Carvalho, A.J.F., 2011. Compatible ternary blend of chitosan/poly (vinylalcohol)/poly (lactic acid) produced by oil in water emulsion processing. Biomacromolecules 12, 907–914.

Hara, P., Hanefeld, U., Kanerva, L.T., 2009. Immobilized *Burkholderia cepacia* lipase in dry organic solvents and ionic liquids: a comparison. Green Chem. 11, 250–256.

Hasan, N.B., Yie, T.W., Zain, N.A.Z., Suhaimi, M.S., 2015. Immobilization of *Candida rugosa* lipase in PVA-alginate-sulfate beads for waste cooking oil treatment. J. Teknol. 74, 215–222.

Hasan-Beikdashti, M., Forootanfar, H., Safiarian, M.S., Ameri, A., Ghahremani, M.H., Khoshayand, M.R., Faramarzi, M.A., 2012. Optimization of culture conditions for production of lipase by a newly isolated bacterium *Stenotrophomonas maltophilia*. J. Taiwan Inst. Chem. Eng. 43, 670–677.

Hwang, E.T., Gu, M.B., 2013. Enzyme stabilization by nano/microsized hybrid materials. Eng. Life. Sci. 13, 49–61.

Itabaiana, I., Goncalves, K.M., Zoumpanioti, M., Leal, I.C.R., Miranda, S.L.M., Xenakis, A., et al., 2014. Microemulsion-based organogels as an efficient support for lipase-catalyzed reactions under continuous-flow conditions. Org. Process Res. Dev. 18, 1372–1376.

Jiang, Y., Guo, C., Xia, H., Mahmood, I., Liu, C., Liu, H., 2009. Magnetic nanoparticles supported ionic liquids for lipase immobilization: enzyme activity in catalyzing esterification. J. Mol. Catal. B: Enzym. 58, 103–109.

Khoobi, M., Motevalizadeh, S.F., Asadgol, Z., Forootanfarc, H., Shafiee, A., Faramarzi, M.A., 2014. Synthesis of functionalized polyethylenimine-grafted mesoporous silica spheres and the effect of side arms on lipase immobilization and application. Biochem. Eng. J. 88, 131–141.

Klibanov, A.M., 2001. Improving enzymes by using them in organic solvents. Nature 409, 241–246.

Lozano, P., 2010. Enzymes in neoteric solvents: from one phase to multiphase systems. Green Chem. 12, 555–569.

Maiti, S., Das, D., Shome, A., Das, P.K., 2010. Influence of gold nanoparticles of varying size in improving the lipase activity within cationic reverse micelles. Chem. Eur. J. 16, 1941.

Malik, M.A., Wani, M.Y., 2012. Microemulsion method: a novel route to synthesize organic and inorganic nanomaterials: 1st nano update. Arab. J. Chem. 5, 397–417.

Mandal, D., Ghosh, M., Maiti, S., Das, K., Das, P.K., 2014. Water-in-oil microemulsion doped with gold nanoparticle decorated single walled carbon nanotube: scaffold for enhancing lipase activity. Colloids Surf. B 113, 442–449.

Patel, V., Madamwar, D., 2015. Lipase from solvent tolerant *Pseudomonas sp.* DMVR46 strain adsorb on multiwalled carbon nanotubes: application for enzymatic biotransformation in organic solvents. Appl. Biochem. Biotechnol. 6, 1313–1326.

Patel, V., Nambiar, S., Madamwar, D., 2014. An extracellular solvent stable alkaline lipase from *Pseudomonas sp* DMVR46: Partial purification, characterization and application in non-aqueous environment. Process Biochem. 49, 1673–1681.

Patel, V., Shah, C., Deshpande, M., Madamwar, D., 2016. Zinc oxide nanoparticles supported lipase immobilization for biotransformation in organic solvents: a facile synthesis of geranyl acetate, effect of operative variables and kinetic study. Appl. Biochem. Biotechnol. 178, 1630–1651.

Patil, P., Deng, S., Rhodes, I.J., Lammers, R.J., 2010. Conversion of waste cooking oil to biodiesel using ferric sulfate and supercritical methanol processes. Fuel 89 (2), 360–364.

Pavlidis, I.G., Gournis, D., Papadopoulos, G.K., Stamatis, H., 2009. Lipases in water-in-ionic liquid microemulsions: structural and activity studies. J. Mol. Catal. B: Enzym. 60, 50–56.

Raghavendra, T., Sayaniya, D., Shah, A., Madamwar, D., 2010. Synthesis of the 'green apple ester' ethyl valerate in organic solvents by *Candida rugosa* lipase immobilized in MBGs in organic solvents: effects of immobilization and reaction parameters. J. Mol. Catal. B: Enzym 63, 31–38.

Raghavendra, T., Vohra, U., Shah, A.R., Madamwar, D., 2014. Enhanced conjugation of *Canida rugosa* lipase onto multiwalled carbon nanotubes using reverse micelles as attachment medium and application in non-aqueous biocatalysis. Biotech. Prog. 30, 828–836.

Ribeiro, D.S., Henrique, S.M.B., Oliveria, L.S., Macedo, G.A., Fleuri, L.F., 2010. Enzymes in juice processing: a review. Int. J. Food Sci. Technol. 4, 635–641.

Selvarajan, E., Mohanasrinivasan, V., Subathra, C., George, P., 2015. Immobilization of β-galactosidase from Lactobacillus plantarum HF571129 on ZnO nanoparticles: characterization and lactose hydrolysis. Bioprocess Biosyst. Eng. http://dx.doi.org/10.1007/s00449-015-1407-6.

Shaotao, P., Xue, L., Yadong, X., Yuyin, Y., Chong, L., Yunjun, Y., Yun, L., 2010. Esterification activity and conformation studies of *Burkholderia cepacia* lipase in conventional organic solvents, ionic liquids and their co-solvent mixture media. Bioresour. Technol. 101, 9822–9824.

Sheldon, R.A., 2007. Enzyme immobilization: the quest for optimum performance. Adv. Synth. Catal. 349, 1289–1307.

Soni, B.H., Deshpande, M.P., Bhatt, S.V., Chaki, S.H., Kaheria, H., 2011. Study on antimicrobial activity of undoped and Mn doped ZnO nanoparticles synthesized by microwave irradiation. Arch. Appl. Sci. Res. 3 (6), 173–179.

Stergiou, P.Y., Foukis, A., Fillippou, M., Koukouritaki, M., Parapouli, M., Theodorou, L.G., et al., 2013. Advances in lipase catalyzed esterification reactions. Biotechnol. Adv. 31, 1846–1859.

Verma, M.L., Barrow, C.J., Puri, M., 2013. Nanobiotechnology as a novel paradigm for enzyme immobilization and stabilization with potential applications in biodiesel production. Appl. Microbiol. Biotechnol. 97, 23–39.

Vlierberghe, S.V., Dubruel, P., Schacht, E., 2011. Biopolymer based hydrogels as scaffolds for tissue engineering application: a review. Biomacromolecules 12, 1387–1408.

Wang, R.H., Xin, J.H., Tao, X.M., 2005. UV-blocking property of dumbbell-shaped ZnO crystallites on cotton fabrics. Inorg. Chem. 44, 3926–3930.

Wu, S., Liu, X., Yeung, A., Yeung, K.W.K., Kao, R.Y.T., Wu, G., et al., 2011. Plasma-modified biomaterials for self antimicrobial application. ACS Appl. Mater. Interfaces 3, 2851–3286.

Zanetteb, A.F., Zampakidia, I., Sotiroudisa, G.T., Zoumpaniotia, M., Lealc, I.C.R., de Souza, R.O.M.A., et al., 2014. Chemo-enzymatic epoxidation catalyzed by *C. antarctica* lipase immobilized in microemulsion-based organogels. J. Mol. Catal. B: Enzym. 107, 89–94.

Zoumpanioti, M., Merianou, E., Karandreas, T., Stamatis, H., Xenakis, A., 2010a. Esterification of phenolic acids catalyzed by lipases immobilized in organogels. Biotechnol. Lett. 32, 1457–1462.

Zoumpanioti, M., Stamatis, H., Xenakis, A., 2010b. Microemulsion-based organogels as matrices for lipase immobilization. Biotechnol. Adv. 28, 395–406.

Summary and Conclusion of UGC-Major Research Project

"Molecular assessment of bacterial community structures of long term oil contaminated soil and screening of lipase producers for lipase production and their application in ester synthesis in organic solvents"

F. 42-167/2013(SR) (22-03-2013)

- Present study reflects the detection of microbial diversity across oil stress condition favouring *β-proteobacteria* such as *Chromobacterium, Xanthomonas, Pseudomonas, Burkholderia* and *Acinetobacter sp*. The microbial community analysis at the metagenome level gives an insight into the repertoire of species to deal with oil contamination. We also observed, genes corresponding to enzymes involved in a wide variety of reactions and operating in many unrelated biosynthesis pathways collaborates well with the fact that the site of study has long-term oil contamination. In this regard, obtained knowledge will be useful in understanding the pathways for synthesis and metabolism of fatty acids released for oils and the microbial communities dominating in such stress condition.

- An extracellular lipase from solvent tolerant *Pseudomonas* sp. DMVR46 was purified following simple purification procedure with 29.74% recovery. The molecular mass of the lipase was found to be ~32.0 kDa by SDS-PAGE. It exhibited optimum activity at pH 8.5 and 37°C. Among various p-nitrophenyl esters with different chain lengths, the lipase showed maximum activity on p-nitrophenyl palmitate (C16). The enzyme exhibited significant stability in presence of iso-octane and cyclohexane and was activated by Ca^{+2}, Ba^{+2} and Mg^{+2} but SDS and EDTA has negative influence on its activity. The partially purified lipase showed significant esterification activity for synthesis of pentyl valerate and revealed improved catalytic efficiency upon immobilization in microemulsion based organogels.

- Functionalized EGO's were characterized by Transmission Electron Microscopy (TEM), Scanning Electron Microscopy (SEM), Fourier Transform Infrared spectroscopy (FTIR) analysis, Raman spectroscopy and Thermal Gravimetric Analysis (TGA). Modified EGO were employed as a supporting matrix for *Candida rugosa* lipase immobilization and further applied in the synthesis of flavor ester ethyl caprylate. Various conditions were optimized and maximum ester production was obtained at 40°C with caprylic acid/ethanol ratio of 0.15:0.1M using cyclo-octane as a reaction medium. A yield of

85% for ethyl caprylate was observed using lipase immobilized on modified EGO which was higher as compared to that of free lipase.

- Immobilization of lipase onto functionalized CdS nanoparticles provides a simple approach to improve activity, stability and reusability of enzyme for enhanced pentyl valerate synthesis. The kinetics of free and immobilized lipase implies that the enzyme undergoes conformational changes during immobilization which results in lower activation energy requirement. Additionally, the altered specificity of the immobilized lipase exhibited higher esterification activity (84%) in comparison to the free enzyme (50%).

- The results obtained from the present study showed that, among the three prepared nanocomposites, ZnO-PEI-GLU was the best biocatalyst, showing higher ester synthesis (94% after 6h incubation at 40ºC) compared with the other nanostructures containing lipase as well as free lipase. The biocatalytic application evaluates the enhancement of immobilized lipase with 2.23 fold over that of free lipase. Various kinetic parameters were refined by nonlinear regression analysis indicating inhibition effect of geraniol. In addition to this energy of activation was determined showing lower energy requirement for immobilized lipase. Furthermore alkyl ester and alcohol chain length effect was studied to understand the influence of the chain length on immobilized enzyme activity. The reusability of covalently immobilized lipase showed that there is not significant leakage of enzyme during repeated use and 88% activity remains after 20 cycles. This approach proved to be a facile, mild and environmental friendly method for synthesizing flavor ester geranyl acetate.

- In particular, a versatile method for double immobilization of Candida rugosa lipase was developed successfully on microemulsion based organogels and was well characterized using FTIR and TGA. Thermal and pH stabilities of lipase immobilized on ZnO-E-RM-@PVA were improved in comparison with those of free and other modified analogues. In addition, esterification experiments revealed that ZnO-E-RM@PVA was the best immobilization system for the synthesis of ethyl and pentyl valerate compared with that of free lipase. Reusability study revealed meager loss of initial lipase activity even after 10 cycles. In nutshell, the facile synthesis procedure is easy to implement and enables the selective separation of enzymes from reaction mixtures.